MSEL

Materials Science and Engineering Laboratory

CERAMICS

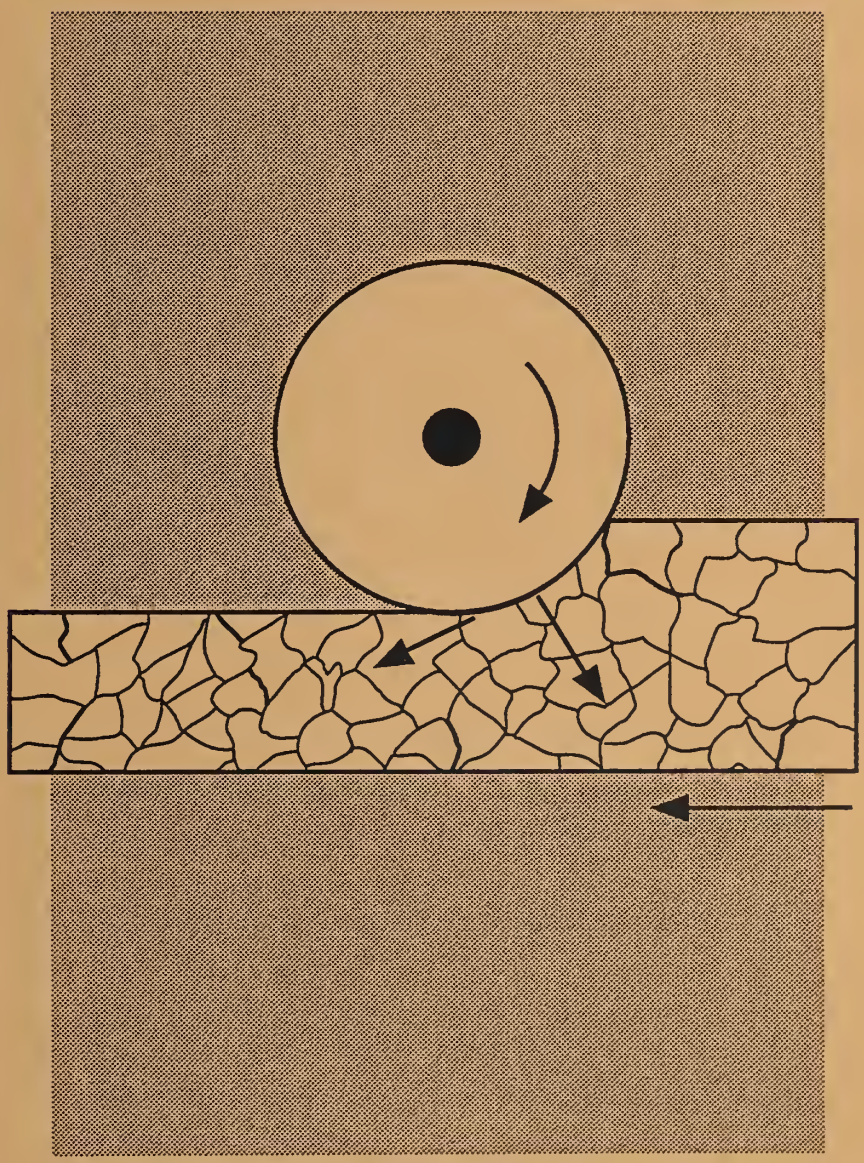

NAS-NRC
Assessment Panel
April 21-22, 1994

NISTIR 5313
U.S. Department of Commerce
Technology Administration
National Institute of Standards
and Technology

Technical Activities 1993

Machining can constitute a significant proportion of of the cost of production of a ceramic component. Diamond wheel grinding, as depicted in the cover schematic drawing, is the most widely used method of surface finishing in the advanced ceramics industry. The Ceramics Division program in grinding addresses the development of both an understanding of the process and a database on the effect of process parameters on material properties. The latter effort is conducted as a NIST/industry/university consortia.

MSEL

Materials Science and Engineering Laboratory

CERAMICS

S. W. Freiman, Chief
S. J. Dapkunas, Deputy

NAS-NRC
Assessment Panel
April 21-22, 1994

NISTIR 5313
U.S. Department of Commerce
Technology Administration
National Institute of Standards
and Technology

Technical Activities 1993

U.S. DEPARTMENT OF COMMERCE
Ronald H. Brown, Secretary

TECHNOLOGY ADMINISTRATION
Mary L. Good, Under Secretary for Technology

NATIONAL INSTITUTE OF STANDARDS AND TECHNOLOGY
Arati Prabhakar, Director

TABLE OF CONTENTS

OVERVIEW

In 1993 the Ceramics Division continued to emphasize a technical program directly relevant to the needs of U.S. industry. This program is made up of tasks which involve standard materials development, construction of evaluated databases, and laboratory research focused on topics that address the dominant issues affecting commercialization of advanced ceramics, namely, processing costs and reliability.

In accord with the strategic plan laid out by the Materials Science and Engineering Laboratory, the Ceramics Division is continuing to expand its direct involvement with industrially related research issues. For example, during this past year a new consortium which will address the intelligent processing of ceramic powders and slurries was formed with six industrial members. The Ceramic Machining Consortium, established in 1992, and consisting of 17 members from industry and academia, is already generating data which will help companies to optimize their manufacturing processes. Other direct programs with industry have been conducted over the past year with Itek Optical Systems, a division of Litton Industries, and one with Norton/Saint Gobain. The Division is also increasing collaborative research activities with other Federal laboratories, e.g., Sandia National Laboratories and the Oak Ridge National Laboratory.

Another important role that the Division continues to play is to bring together U.S. industrial representatives to obtain firsthand knowledge of their research priorities. As examples, workshops were conducted on Measurement Issues in Diamond Films, Lubrication for Advanced Engine Materials, and Machining of Advanced Materials.

The output of the Ceramics Division program is made available to U.S. industry and the ceramics community through a number of avenues including presentations, publications, and direct collaborations with companies and universities. During this past year the research program produced 125 publications, 133 presentations, and three invention disclosures. Five new Cooperative Research and Development Agreements (CRADAS) were signed with companies and universities.

Standard materials and data activities continue to represent an important portion of the Division's program. Three new Standard Reference Materials were developed this year, and an evaluated database on high T_c superconducting materials was begun in collaboration with a Japanese laboratory.

A major effort over the past few years has involved the NIST leadership of the International Energy Agency ceramic powder characterization program. During the past year powder analysis techniques developed on this program were released to standards organizations in the U.S., Japan, and Europe.

The Division's program on high T_c superconducting materials has continued to focus on research relevant to the production of bulk products such as superconducting wires and magnets. We are working closely with the Department of Energy and U.S. companies to develop the data, measurement procedures, and understanding needed for wire development. NIST recently

became a member of the Wire Development Group, a partnership between the Oak Ridge National Laboratory, Argonne National Laboratory, Los Alamos National Laboratories, and the University of Wisconsin to enable the American Superconductor Corporation to commercialize superconducting products.

Work on the use of nanosized materials is being expanded. As examples, research on the development of magnetic nano-composites for use in refrigeration has continued in collaboration with the Metallurgy Division. A study is being carried out on the issues of scale-up of the process for producing silicon nitride from nanosized starting powders. Finally, Division personnel are investigating the preparation of Bi_2Te_3 composites which are of interest as components in thermoelectric refrigerators.

In 1993, both funding and staff levels remained relatively constant. The relatively high percentage of funds from other government agencies continues to be a concern, but we are optimistic about the future support of the NIST laboratory program through the Congressional budget process.

Finally, during the year, Ceramics Division personnel were significantly involved with the NIST Advanced Technology Program (ATP). S. J. Dapkunas and J. A. Carpenter served as members of the ATP Source Evaluation Board for competitions held in 1993, and a large percentage of Division personnel participated in the ATP review and program monitoring processes.

Stephen W. Freiman
Chief, Ceramics Division

TECHNICAL ACTIVITIES*

Certain trade names and company products are mentioned in the text or identified in illustrations in order to adequately specify the experimental procedure and equipment used.

In no case does such identification imply recommendation or endorsement by the National Institute of Standards and Technology, nor does it imply that the products are necessarily the best available for that purpose.

TECHNICAL ACTIVITIES*

I. DATA TECHNOLOGIES GROUP

S. J. Dapkunas

The objective of the Data Technologies Group is to develop and facilitate the use of evaluated data bases for the materials science and engineering communities.

Both research and application directed organizations require readily available evaluated data to take advantage of the large volume of materials information developed on public and privately sponsored programs. This information, particularly numeric data, is available in an ever increasing number of publications published worldwide. The necessity to consolidate and allow rapid comparison of properties for product design and process development underlies the database projects in the Ceramics Division.

The Data Technologies Group activities extend from traditional data compilation to data transfer protocols and the development
of interactive tutorials on the use of materials data.

Specific projects include (1) the traditional Ceramic Phase Equilibria Program conducted in cooperation with the American Ceramic Society; (2) the Structural Ceramics Database developed with support of the Gas Research Institute; (3) the High Temperature Superconductor Database recently initiated in cooperation with the Japanese National Research Institute for Metals; (4) implementation of STEP protocols for international exchange of materials data under the auspices of the ISO 10313 activity and; (5) the development of a phase equilibria tutorial utilizing digital-video-interactive technology.

Significant Accomplishments:

- The Ceramics Division and the Standard Reference Data (SRD) Program completed negotiations with Japan's National Research Institute for Metals to establish a collaborative, international effort to develop a computerized database of evaluated materials properties for high-temperature superconductors (HTSC).

- The Ceramics Division and the SRD Program have initiated a program with the Russian Research Center for Standardization, Information, and Certification of Materials to establish evaluated property data for selected oxide and carbide structural ceramics from worldwide sources. The data will become part of the NIST Structural Ceramics Database which is distributed by the NIST SRD Program.

- An assessment of the corrosion of silicon carbide and silicon nitride ceramics was completed under funding from the Department of Energy's Pittsburgh Energy Technology Center. These materials are candidates for use in coal-fueled heat exchanger applications in which the temperature exceeds 1000 °C and the environments are often complex gaseous and particulate mixtures. Included in the study are atmospheres of dry and moist oxygen, mixtures of hot gaseous vapors, molten salts, molten metals, and complex environments pertaining to coal ashes and slags.

High-Temperature Superconductors

R. G. Munro, and J. R. Rumble, Jr.[1]

[1] NIST Standard Reference Data Program

High-Temperature Superconductors (HTSC) comprise one of the most intensely studied classes of materials currently available. Since their discovery in 1986, more than 35,000 reports on the processing, characterization, and properties of these materials have been published in the open literature. This prolific publication rate is evidence of the intense interest in the potential applications of these materials. Developing commercial applications, however, requires the fabrication of HTSC materials into useful forms such as films on non-HTSC substrates or as wires. The fabrication of such forms is highly dependent on the thermal, mechanical, and chemical properties of these materials because HTSC materials are brittle and often reactive with the relevant substrate materials under processing conditions. While extensive bibliographic databases of titles and abstracts of reports are maintained by several public and private agencies, there has been no systematic compilation, evaluation, and computerization of the numeric data. As a result, there are three major information barriers confronting materials researchers and application designers who would like to use HTSC materials: (1) the quantity of reports; (2) the reliability of the data; and (3) the currency of the results. These barriers are best resolved through the use of evaluated computerized databases.

In 1992, NIST initiated the development of a computerized database of evaluated materials properties for HTSC materials to fulfill this critical need. The project aimed to provide a comprehensive source of information about HTSC materials. Included in the project design were details about processing and measurement methods, chemical composition, crystal structure, a full range of thermal and mechanical properties, and the critical characteristics of high-temperature superconductors.

To ensure the most comprehensive coverage of these rapidly developing results, NIST in the U. S. and the National Research Institute for Metals (NRIM) in Japan established an agreement to collaborate on this effort. NRIM has agreed to provide data not only from Japanese language publications, but also from a special long-term experimental research effort sponsored by Japan's Science and Technology Agency (STA). In the STA project, a master batch of material is prepared by a selected industrial material manufacturer. Samples from the master batch are then sent to numerous laboratories to provide complementary characterization and property measurements. The result is a detailed collection of data from a single batch. At the present time, there does not appear to be any other effort comparable to this STA project anywhere in the world. Under the NIST-NRIM agreement, the STA data will become accessible through the NIST database project.

The first release of the computerized HTSC database is expected to be ready near the end of fiscal year 1994. The program will run on IBM-compatible personal computers under a Windows environment.

Structural Ceramics Database

R. G. Munro, J. R. Rumble, Jr., and S. J. Dapkunas

The potential applications of advanced structural ceramics have been widely appreciated for several decades. Characteristics such as strength retention at high temperature and chemical stability have held forth tantalizing possibilities for more efficient engines, heat exchangers and recuperators, and for more durable chemical processing components. The Structural Ceramics Database (SCD) provides evaluated data for the properties of the primary candidate ceramics for such applications.

The original scope of the database, materials for gas-fueled heat exchangers, has been greatly expanded. Efforts are now underway to include thermal, mechanical, and chemical property data for all types of nominally monolithic structural ceramics. One goal of this new effort is to include data from worldwide sources, especially data that are generally considered by U. S. industries to be inaccessible in practice. Towards that end, an agreement has been established with the Russian Research Center for Standardization, Information, and Certification of Materials. The Russian group will use the NIST SCD Data Entry Software to provide evaluated data for Al_2O_3, B_4C, TiC, and ZrO_2. The data records will include text entries for material processing and specification information, text entries for descriptions of measurement methods, and numeric data for the thermal, mechanical, and chemical properties.

In a special effort, the Ceramics Division has completed a review of the corrosion of two important classes of structural ceramics, silicon carbides and silicon nitrides. When any load-bearing material is used in a corrosive environment, the primary concerns are the survival of the material and the retention of its strength. While the corrosion rates for ceramics can be relatively small, surface pitting and an overall increase in the surface flaw populations generally cause the strength of the material to be decreased and the mechanical lifetime to be reduced. The effects, however, depend significantly on the compositions of the materials, the impinging environment, the exposure history, and the thermal and mechanical characteristics of the application. The NIST review examined the effects of corrosion on material properties, performance, and durability in diverse environments, usually at temperatures of 1000 °C or higher. The environments included dry and moist oxygen, mixtures of hot gaseous vapors, molten salts, molten metals, and complex environments pertaining to coal ashes and slags. The quantitative results from this study will be incorporated into the next version of the Structural Ceramics Database.

Phase Equilibria Information System Incorporating Digital Video Interactive Technology

E. F. Begley and C. G. Lindsay

In materials research, the phase diagram is a critical processing tool describing the relationship between temperature, chemical composition, and gaseous environment to the crystalline phases that should appear. The phase diagram can be considered a "blueprint" for processing materials such as ceramics. The Ceramics Division has initiated the development of innovative, distributable, multimedia software incorporating digital video interactive (DVI) technology to

assist in the understanding and use of these diagrams. This new software will complement phase diagram work that has been part of almost 60 years of cooperation between NIST and the American Ceramic Society.

Two stages have been planned for this project. The first stage will concentrate on developing an application that will enable individuals to learn or review how to interpret and use unary, binary, ternary and quaternary phase equilibria diagrams. This is a necessary precursor to the second stage which will concentrate on the implementation of an application that will provide instruction in developing phase diagrams. The goal of this latter stage is to capture in an expert system the relevant expertise of Dr. R. S. Roth, a nationally recognized scientist with forty years of experience and integrate it with digital video and audio clips of Dr. Roth in action. In this way, the expertise, particularly the laboratory techniques and insights which do not appear in technical publications, would be preserved for future generations and, furthermore, would be widely distributable.

The software will make extensive use of DVI technology which allows motion video and audio signals to be digitally compressed and integrated with traditional software. Motion video and audio allow the user to visualize technical content to an extent not possible with a textbook. this would be particularly helpful in presenting crystallization sequences in ternary systems. Textbook presentations of this principle are often difficult to follow because they necessarily rely on printed words and still pictures to convey the concepts. The ideas are easier to grasp when the sequence is seen to develop in a moving picture accompanied by an audible explanation of what is being shown. As a simple example, a user who does not understand the concept embodied in the term "phase" could ask the software for an explanation. Rather than responding with simple text, the software would show a short video of an expert explaining the concept by actually pointing out the distinct interfaces between phases and demonstrating the separability of two phases.

The target audiences for the software are U.S. industrial scientists and engineers as well as university students in geology, petrology, and materials science programs. Consequently, an essential consideration in selecting and arranging the content of the software is the breadth of occupational and educational levels of the intended audience. Students being exposed to this materials for the first time need to have the full range of pertinent information available for their study, practice, and review. Definitions of terms and concepts must be complete and accurate, but should be incorporated in a way that the main part of the presentation,phase diagram interpretation, does not suffer from too much detail. Professionals reviewing the materials are more likely to want immediate answers to a few questions about phase diagram interpretation without having to wait through extended presentations of supporting concepts. However, in seeking the answers to these few questions, the need occasionally arises to review a supporting concept as well. Therefore, as much detail as practicable will be included and arranged in segments that can be called by the user as desired.

At this point, the components required to develop this software have been acquired and several of the important concepts and definitions have been identified. Video and audio segments have been incorporated into interactive software and the demonstration system was presented to the American Ceramic Society Technical Review Committee in November 1992. We are working

to establish a cooperative relationship with the University of Maryland to develop the academic or classroom perspective needed to identify areas troublesome to students, the knowledge of cognitive issues important to learning, and a testbed of students to check the quality and effectiveness of the tutorial.

STEP Materials

J. A. Carpenter, Jr. and J. R. Rumble, Jr.[2]

[2] NIST Standard Reference Data Program

STEP is the **ST**andard for **E**xchange of **P**roduct Data Model, the now-emerging world standard for computerized exchange of data on manufactured parts. ISO is the International Organization for Standardization and IPO is the IGES/PDES Organization, the organization primarily responsible for the development and promulgation of STEP in the United States.

In this period, J. A. Carpenter, Jr. assumed leadership of the ISO/IPO STEP Materials Committee. That committee refined and issued ISO 10303 Part 45 Materials as a CD (committee Draft), which is currently in ballot by participating ISO countries to determine if it shall advance to a DIS (Draft International Standard).

Meetings were held with staff of the Semiconductor Research Corporation (SRC) and the Microelectronics and Computer Technology Corporation (MCC) resulting in both organizations's serious consideration of adopting STEP in various developmental CAD/CAM projects. These interactions also resulted in identifying the materials-related information needed in those projects.

Additional meetings were held with staff of the Society of Plastic Industries (SPI) and certain of its member companies toward the adoption of STEP in the exchange of data from the testing of materials, the initial focus being on polymers.

CERAMIC PHASE EQUILIBRIA PROGRAM

S. W. Freiman, M. A. Clevinger, T. R. Green[1], K. M. Hill[1],
N. Swanson[1], E. Hayward[1], C. L. Cedeno[1], and H. M. Ondik

[1]American Ceramic Society Research Associates

The Ceramic Phase Equilibria Program continues to provide the ceramics user community with evaluated phase equilibria data covering all non-alloy, inorganic systems. This past year has been the eigth full year of operation of the Ceramics Phase Diagram Data Center under the expansion plan sponsored cooperatively by NIST and the American Ceramic Society (ACerS). Over $2,500,000 was raised by the ACerS from industry and universities for the support of the program.

Examination, evaluation, and digitization of diagrams for inclusion in Volume 10 of Phase Diagrams for Ceramists (now entitled Phase Equilibria Diagrams) has been completed. This topically-oriented hardcover volume contains boride, carbide, and nitride systems of interest to the structural ceramics community. It will be available for distribution in April 1994. Volume 11, focusing on oxides, particularly those of interest for electronic applications will be completed early in 1995.

An updated and expanded database system for use on DOS-based personal computers (PC) will soon be ready for marketing by NIST and the ACerS. The original version has undergone extensive revisions based upon comments received when demonstrated at meetings, and advice from the Standard Reference Data Program staff. The system provides for search and manipulation of both textual and graphics information.

II. POWDER CHARACTERIZATION AND PROCESSING — Subhas G. Malghan

The US advanced structural ceramics industry is continuing to focus on the demonstration of cost-competitive ceramics production. Though several components such as machining have a large influence on total cost, the powders and their processing to green and sintered state is another major factor. In addition, the industry is moving toward the production and application of lower cost materials such as reaction bonded silicon nitride for heat engine applications or 8% Y_2O_3 containing zirconia for thermal barrier applications. Since most of these processes start with fine-size powders as the starting materials, their characterization and processing play a significant role in deciding cost-effective manufacturing. Some issues affecting cost-effective manufacturing are synthesis of novel powders that have tailored properties, repeatability and reproducibility in the measurement of powder properties, procedures in the characterization of secondary properties, and powder-aqueous environment interactions.

Our program on ceramic powders characterization and processing is designed to address some of these significant issues. The primary focus of our program is on improvement of measurement quality in ceramic powders processing. This is accomplished by providing the US ceramics community the ability to control ceramic powder properties so that cost-effective manufacturing can be achieved. The program is continuing to emphasize structural ceramics with applications of silicon nitride to automotive engines and zirconia to coatings for use in aircraft engines. The specific elements of the program are the development of:

- Ceramic powder characterization techniques measurement science, standard methods, and standard reference materials;
- Powder processing science to understand interrelationships between powder characteristics, and their processing environment; and
- Novel synthesis methods as applied to nano-size and ultra-pure powders for processing studies.

The major components of the powders characterization program have been the development of standard procedures, standard reference materials, improving the scientific basis of powder dispersion measurements in slurries, overall improvement in measurement accuracy, and leadership in national and international standardization activities. The powder characteristics of interest include physical and surface chemical properties, and phase composition. In powder processing, our efforts have been focussed around nano-size silicon nitride powders processing, high energy agitation milling of powders, and microstructure modeling as applied to the behavior of particles under stress fields such as in injection molding. The powder synthesis activities are directed toward synthesis of novel precursors and powders for ferrites use as thick films in microwave applications, bismuth telluride-based powders as thermoelectric materials, and magnetic nano-composites for magnetic refrigeration.

Four new efforts were initiated during the year: 1. A joint NIST-industry consortium on intelligent processing of powders and slurries; 2. Extension of international cooperation activity on the development of procedures for secondary properties of powders under the auspices of the International Energy Agency; 3. Characterization of powders used as thermal barrier coatings;

and 4. Modeling and powder-processing interrelationships in injection molding. The consortium, based on our past four years of research, is primarily directed toward developing electroacoustics as a sensor for on-line dispersion monitoring. This effort is expected to be expanded in the future to include other sensors, and models development. The second and third efforts are attempting to develop powders specifications by expanding the range of properties that have relevance to powder response during processing. In the fourth effort, our major activities will be to model the behavior of particles under stress fields as applied to injection molding, and to enhance the characterization of powders and green bodies, as applied to injection molding.

Our future activities are expected to focus on improved understanding of surface chemical interactions between powder and gel-forming chemicals, physical and chemical barriers preventing high green density compaction of nano-powders, near-net-shape forming to decrease the need for machining, and novel methods of coating oxide and non-oxide powders.

Significant Accomplishments:

- The final report on Subtask 6, a powders characterization project under the auspices of the International Energy Agency (IEA), was released to participants. In addition, the report was approved for release to the standards setting bodies in Japan, Europe, and the US. This step is expected to speed up the standardization programs in the participating countries. This is considered to be a significant decision since a number of procedures in this report are ready for standardization, and their unavailability has been a barrier to commercialization in the past.

- A follow-up to the powders characterization project under the IEA program was initiated. The primary emphasis of this project is to focus on secondary properties of powders that potentially have a major influence on the behavior of powder during processing. These procedures are expected to play a significant role in the development of powder specifications. Two additional countries (Norway and Belgium) have joined this activity that brings the total to six, and the number of participants to 44.

- A NIST-industry consortium to address intelligent processing of powders and slurries was initiated. This project, in the initial stages, will focus on the development of electroacoustics for on-line measurement of dispersion during aqueous processing of powders, and on the nuclear magnetic resonance for developing improved understanding of homogeneity in slurries and green ceramic. Six industrial organizations have joined this consortium.

- The data on compaction and pressureless sintering of nano-scale silicon nitride and alumina powders show that the green density has a significant influence on the amount of final densification. Cryogenic compaction of 3 mm diameter samples yielded a maximum random packing which resulted in green densities of 64% and 74% for amorphous silicon nitride and γ-alumina, respectively. Sintering results on these green compacts showed that increased interfacial contact between the particles in silicon nitride are required for improved densification.

- In the development of a silicon nitride standard reference material (SRM) for phase composition analysis, time of flight neutron analysis data has been obtained to enhance the accuracy to the order of 0.1%. The x-ray diffraction for certification of this SRM was carried out by using Rietfeld method. The SRM will contain two powders that have either a high alpha or beta phase composition.

- In a collaborative study with Pennsylvania State University on alumina green compacts, improved capabilities of solid state nuclear magnetic resonance were demonstrated. The distribution of a three component binder was mapped in three dimensions using the measurement of proton nuclear spin-spin relaxation times (T_2) of binders. In addition, a mobile proton species produced during injection molding was detected by the T_2 study.

- Experimental studies involving electroacoustics, adsorption, and dispersion measurement on a number of powders showed that there is a unique way to describe the parameters for dispersion of powders in water. The effective pH at which the particles carry a net zero charge and the pH of dispersion are the most important parameters that define dispersion using polyelectrolytes in aqueous environment. Using this information, one can develop dispersion parameters for most powders of interest to structural ceramics.

- In the electroacoustic analysis of silicon nitride powders, the studies on influence of inorganic salts and organic polyelectrolytes have concluded that the measurement of electrokinetic sonic amplitude (ESA) has the potential to provide data on powders in concentrated suspensions. These studies have formed the basis for the proposed NIST-industry consortium. A workshop was organized at NIST to identify issues in the measurement of surface chemical properties of the powders in aqueous and non-aqueous environments.

International Interlaboratory Comparison of Powders Characterization

S. Malghan and L. Lum

As the structural ceramics industry is progressing toward commercialization, the need for developing commonly acceptable procedures for measurement of powder properties is more important then ever. Some of the reasons for this continuing need are the use of submicrometer powders as the starting materials in the manufacture of ceramic components, and nature of international trade involved in the production and use of fine powders. The powders used in the production of structural ceramics continue to be produced and used in different countries.

This is a continuing project under the auspices of the International Energy Agency (IEA) in which six countries are now participating. The overall goal of the project is to develop pre-standardization procedures for characterization of powders. In 1993, Subtask 6 was completed, and the final report on the project was released to participants. In addition, a highlight of the accomplishments was the decision by the Executive Committee to release the report to the standards setting bodies in the participating countries. As a result, ASTM, CEN, and JSA will be able to use the round-robin data and procedures for developing their standards. Eventually, this effort is expected to speed up the development of international standards. The ASTM C-

28.05 subcommittee has already initiated efforts to draft procedures based on this report.

During the year, a technical plan for Subtask 8, a continuation of Subtask 6 powder characterization project, was developed. Subsequently, the plan was approved by the participants, technical leaders, and the IEA Annex 2 Executive Committee. The overall goal of this project is to develop pre-standardization procedures for characterization of secondary properties of powders such as those for the measurement of slurry pH, green density, and porosity of green ceramic. In addition, several procedures for the measurement of physical, bulk chemical, and surface chemical properties will be examined to improve the quality of data. This is an ambitious project involving a number of very important parameters of powders that have the potential to provide practical guidelines to develop powder specifications. Japan, Germany, Sweden, Norway, Belgium, and the US are participating in this project with the total number of participants at 44. Now, we are developing procedures, collecting powders, and validating the procedures. All three activities require extensive experimental investigations since only a small amount of data are available in the open literature. The samples and procedures are expected to be sent to participants in the next six months.

Standard Reference Materials for X-Ray Diffraction (XRD)

J. P. Cline

Standard Reference Materials (SRMs) for powder diffraction serve to increase the accuracy and precision of measurements by providing a range of materials that exhibit certified or model diffraction properties. SRMs allow the user to trace the results of their measurements to fundamental physical constants, or to values decided through round-robin studies conducted in conjunction with the International Centre for Diffraction Data (ICDD). Quantitative analysis SRM powders are selected for phase purity and freedom from microstructural characteristics that may induce errors in diffraction intensity measurements. A brochure that discusses the range of NIST SRMs for powder diffraction is available from the Office of Standard Reference Materials (OSRM). The following is a brief description of the XRD projects.

We have undertaken a project in collaboration with the Quantum Metrology Division to develop new, high accuracy line position SRMs using an optically-based wavelength/crystal-spacing scale. The fundamental basis is the wavelength of an iodine-stabilized HeNe laser operating near 633 nm that is the most accessible current embodiment of the length standard. The strategies available to us for powder lattice normalization include: continuation of the use of an x-ray line profile as a transfer standard; generation of a effectively narrower profile (likely extracted from a synchrotron radiation continuum) by using a monolithic crystalline monochromator as a transfer standard; or devising a comparator scheme by which a powder spacing may be related to the lattice period of a single crystal. For any of these procedures, we are restricted to parallel beam optics to fit the single crystal characteristics and to gain immunity from penetration effects in the powder specimen.

In parallel with the efforts to assure adequate linkage of the powder spacing scale to basic length standards, another part of this effort is aimed at assuring more optimized and stable materials for distributable line position SRMs. In this aspect, we are examining the effect of crystallite

size on the observed lattice spacings and the stability of the sample d-values with respect to aging and environmental degradation. Of particular significance to this component of the effort is the application of fabrication techniques aimed at producing a narrow range of crystallite sizes and particle morphologies.

A new line profile SRM that displays profiles broadened by crystallite size effects is presently in development. Two methods of pattern deconvolution are being evaluated for use as a certification method. The first consists of the Williamson-Hall approach which requires that the sample broadening be modeled by a specific profile shape function. The second approach involves a Fourier analysis of the diffraction profiles. This method is prone to noise in diffraction data unless analysis excludes the tail region of the diffraction peaks. The four candidate alumina powders considered for use as the material for SRM 676, an alumina SRM certified for quantitative analysis, were analyzed for crystallite size and micro-strain using these techniques. The accurate characterization and modeling of broadening due to the instrument was found to be critical to the accuracy of the results from both methods.

The certification measurements for SRM 656, a quantitative analysis SRM for the two phases of silicon nitride, were completed. The preferred powders for quantitative analysis SRMs consist of phase pure materials of single crystal, isometric particles between 0.5 and 1.0 μm range. The particle size of such powders permits a minimum specific surface area for a material that is free from the effects of extinction. Other factors held constant, the surface of crystal is a region of disorder and, therefore, minimization of surface area will reduce "amorphous" or surface phase contamination. Single crystal particles of isometric morphology would not impart the effects of microabsorption or preferred orientation to subsequent measurement data. The SRM consists of two powders, one containing a large amount of the α phase, while the other is high in β.

The quantification of amorphous content requires a material that is considered to be absolutely phase pure for a baseline and measurements that are free of systematic bias. Such a bias is expected to affect x-ray measurements to a greater extent than the neutron data due to the manifestations of the more complex x-ray optics; neutron measurements have been accurate to within 1% while x-ray measurement errors are typically several times this value. The spectrum of radiation used in neutron time-of-flight (TOF) experiments permits the measurement of extinction effects. Thus, the former of the two approaches may be pursued with x-ray diffraction measurements, while the latter two may be pursued with neutron TOF measurements, with the aid of phase pure standards. Both x-ray powder diffraction and neutron TOF analysis have been used to obtain the accuracy required for analysis of amorphous content to the range of 0.1% for certification of SRM 656.

Particle Size Distribution Standards

J. Kelly, L. Lum, and S. Malghan

The measurement of particle size and particle size distribution of the starting powder as well as powders during processing is important for achieving the desired properties and microstructure from the final product. The ceramic industry produces ceramic components of both non-oxide

and oxide materials. NIST had developed and certified SRM 659 as a silicon nitride powder particle size distribution standard. Subsequently, the need for an oxide SRM was identified. In addition, the ability to measure accurately and reproducibly the size distribution of powdered materials is a critical need of the ceramics and glass industries as well as other industries using powders or granular materials. An important element in achieving this capability in industrial analytical laboratories and quality control programs is the availability of appropriate SRMs of similar composition to those being processed.

The certification of a silicon nitride powder as SRM 659 for x-ray sedimentation type of equipment was completed in 1992. While SRM 659 provides a standard in the one micrometer range, the requirements for standards in larger size ranges are satisfied by several SRMs using spherical glass beads. One of the objectives of this year's effort was to determine the size distribution of two glass bead SRMs that are used for evaluation and calibration of particle size measurement instrumentation. Toward that end we have developed a sample preparation protocol using successive stage riffle-splitting for obtaining representative 6 mg subsamples of the particles from 25 g bottles. The glass beads are imaged by optical and scanning electron microscopy and digital image files created by optical scanning of photographs. A computer program using commercially available software has been written to analyze the digital image files. The computer program calculates the projected area of the glass beads and the equivalent sphere diameter for each of approximately twenty thousand particles taken from several samples of the powder. These data were used to generate the measured size distributions and calculated cumulative weight distributions for SRM certification. The production and certification have been completed for glass bead SRMs 1003b and 1004a.

In another effort, SRM 1978 was developed to provide a standard material in the one micrometer range for use in zirconium oxide powder processing using gravitational sedimentation instruments. This SRM was developed by an interlaboratory comparison study to establish the certified values by four laboratories in the U.S., Japan and Sweden. The experimental procedure developed for this SRM is similar to that for SRM 659. The uncertainty in the certified value at the 50th percentile, 0.98 μm, is 0.04 μm based on all data.

These reference materials are now available through OSRM. Close communication with the industrial end-users of NIST SRMs is maintained through active participation in the ASTM committees relating to ceramics, glass, and particle size standards.

Standards for Mobility Measurements

S. G. Malghan, R. S. Premachandran, and V. A. Hackley

The dispersion characteristics of ceramic powders and other particulate materials depend on the zeta potential of the powder in suspensions. Generally, a high zeta potential or electrokinetic mobility is required for a better dispersion. Though these measurements are carried out in a large number of industries including ceramics, minerals, solid and liquid waste processing, and biological, no standards are available to assure reproducibility and accuracy. Based on an extensive round-robin conducted under a DOE sponsored project during 1988-92, we selected goethite as an ideal material for developing an SRM.

SRM 1980 is being developed by NIST for calibration of electrokinetic mobility measurement instruments that are commonly used. This SRM was produced by synthesizing a goethite, FeO(OH), powder at NIST. The goethite sample is packaged as a 50 mg/L suspension, dispersed in 5 x 10^{-2} M $NaClO_4$ and 100 micromole/g KH_2PO_4. The certification was carried out by a round-robin of five participants. The uncertainty in the certified value for positive electrophoretic mobility, 2.55 $\mu m \cdot cm/V \cdot s$, is 0.12 $\mu m \cdot cm/V \cdot s$, based on all data. At least four different types of instruments were used by the participants which indicated that the data are not affected by the instrument type. A second SRM being certified has a negative mobility in the same range.

Surface Chemistry of Silicon Nitride Powders

V. A. Hackley and S. G. Malghan

With the recent arrival of electroacoustic methods we can now characterize ceramic powder slips containing solid loadings approaching 40% by volume. The measurement of electrokinetic properties is based on the measurement of electrokinetic sonic amplitude (*esa*). The *esa* signal and phase information are used to measure the electrophoretic mobility and zeta potential of the particles. We have applied this technique to investigate the surface chemical reactions of Si_3N_4 powders in aqueous processing of slurries.

The control of reactions at the solid-solution interface is critical in ceramic powder processing. Interfacial electrochemical properties can be significantly affected by the presence of surface impurities or secondary components added to the suspension. For non-oxide materials such as silicon nitride, the presence of oxygen in the surface region is known to modify the electrical double-layer properties in a predictable manner. The isoelectric point (*iep*), or pH of zero electrokinetic charge, of Si_3N_4 decreases linearly with increasing surface oxide thickness. The *iep* is the single most important variable that decides the rheological and dispersion properties of slips. We have examined the role of dissolved ions on the surface chemistry of Si_3N_4 powders, and the implications for the effects of impurities, contaminants and additives in processing. We find that most simple univalent electrolytes behave indifferently toward the Si_3N_4 surface, with the exception of fluoride that specifically adsorbs and may form a strong complex with the surface silicon. Oxy-anions such as sulfate and carbonate adsorb specifically on the Si_3N_4 surface, but the interactions are weaker than previously observed on metal oxides. The alkaline-earth cations, common impurities in commercial powders, exhibit a similar weak specificity over the normal pH range. In the presence of hydrolyzable transition metal cations such as Fe^{+3}, powder surface chemistry is controlled by the adsorption of hydroxy metal complexes and by the solubility of a surface-precipitated metal hydroxide phase. In this case, multiple *iep*'s are possible, and the primary *iep* may be shifted several pH units from the native value. These observations suggest that the so called heterogeneous precipitation could be used as a method for adding inorganic sintering aids and nitriding agents more uniformly and efficiently compared to the use of secondary powder phases.

We have also measured the ionic contributions to the electroacoustic signal for a series of electrolytes. In many cases the electrolyte background signal is significant compared with the powder signal, and must be corrected for in order to avoid serious problems with measurement

artifacts. We have examined the accuracy of applying a simple subtraction procedure to remove background signal, and have generated the necessary data to predict whether a background signal will be significant for a given ion pair in aqueous solution.

Weak-acid polyelectrolytes, such as poly(acrylic acid) (PAA), are added to slips to control particle dispersion and rheology during processing. These polymers impart stability through electrosteric mechanisms that are poorly understood. In the past year, we have begun an investigation of the electrochemical interaction of PAA with Si_3N_4 using electroacoustic analysis coupled with adsorption measurements and potentiometric titration. Preliminary results show a complex interaction mechanism between the polyelectrolyte and Si_3N_4 surface. Electroacoustic measurements correlate with adsorption data as a function of solution pH and polymer concentration. The PAA adsorbs strongly in an acidic medium and reduces the surface potential, as illustrated in Figure 1, that leads to severe agglomeration. In an alkaline medium, the polyelectrolyte is weakly adsorbed as a result of repulsive electrostatic interactions with the particle surface. A range of behaviors is possible between these two extremes, including particle charge reversal. Dispersion properties appear to improve under alkaline conditions, suggesting that *free* polymer may play an important role in the enhancement of slip properties. Some of the major findings in this projects are:

- The role of dissolved ions in the surface chemistry of Si_3N_4 powders was resolved. This work has implications for the effects of impurities, contaminants and additives in aqueous processing of Si_3N_4 powders.

- The contribution of electrolytes to the measured ESA was obtained for a wide range of ion pairs. These data are vital for predicting and evaluating the background signal correction necessary in the electroacoustic analysis of aqueous suspensions.

- The electroacoustic properties of Si_3N_4 slips in the presence of polyacrylic acid dispersants was correlated with polymer adsorption and the degree of ionization as a function of solution pH and molecular weight. The potentially significant role of free polymer in slip dispersion and rheology was identified. The mechanism of interaction and dispersion of these polymeric additives is presently not understood, and yet of critical importance to the powder processing industry.

Consortium on Intelligent Processing of Powders

S. G. Malghan, V. A. Hackley, and P. S. Wang

A NIST-industrial consortium on intelligent processing of ceramic powders and slurries was initiated in September 1993. The participants are from the ceramic powder synthesis and processing industry (Cercom Inc., Eaton Corporation, Kerr-McGee Corporation, Golden Technologies Company, Inc., and St. Gobain/Norton Industrial Advanced Ceramics), and the powder measurement industry (Matec Applied Sciences). This consortium addresses critical powder processing issues identified by industry and builds upon the measurement, characterization and analysis capabilities developed at NIST.

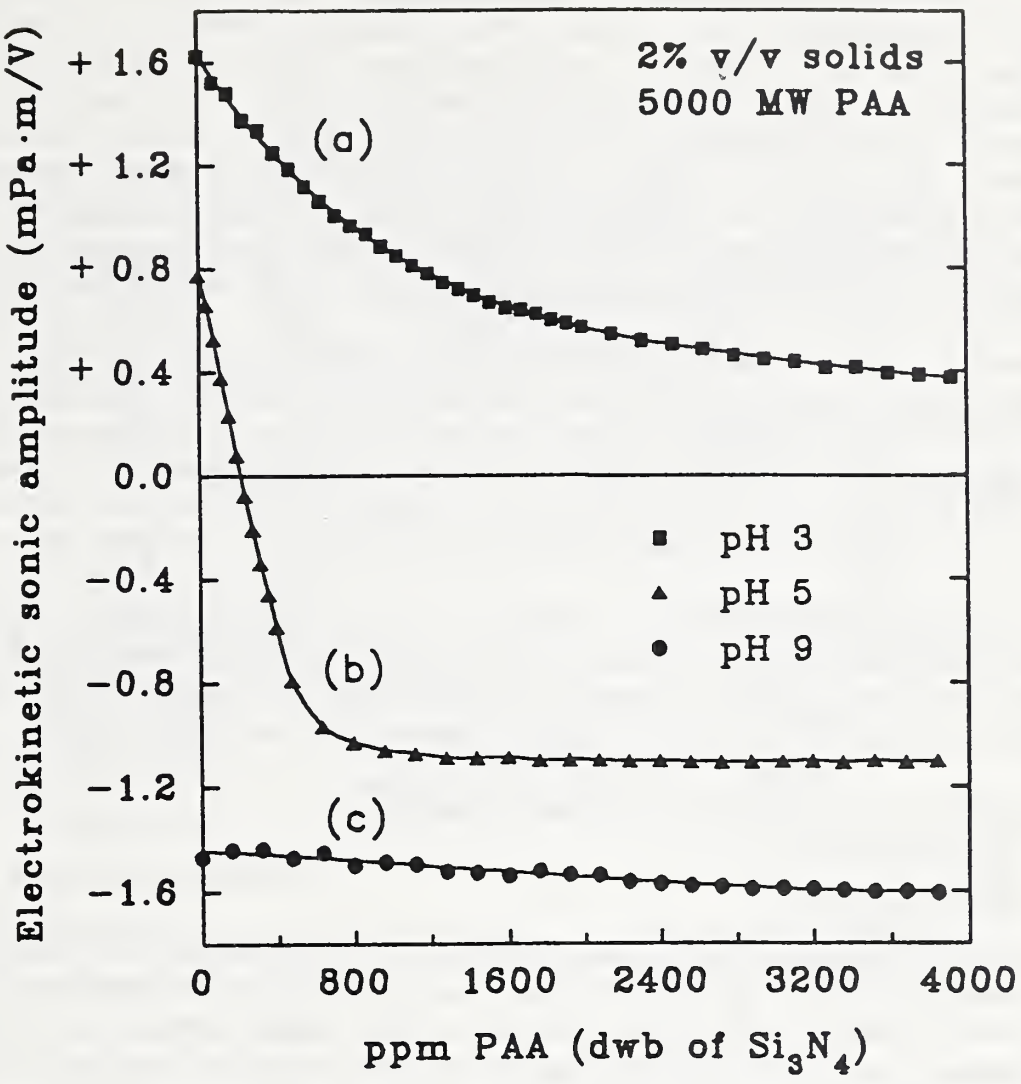

Figure 1. The ESA of silicon nitride powder, SNE-10, in the presence of a 5000 MW polyacrylic acid at three pH values of the suspension.

Reproducible processing is recognized as a vital component in the achievement of cost-effective manufacture and reliable application of advanced ceramics, particularly silicon nitride, for a wide variety of automotive and industrial components. The consensus opinion of a recent workshop held at NIST to identify powder related issues that limit reproducibility of ceramic processing, was that the ability to measure subtle powder characteristics and characterize the behavior of powders in slurries would further the understanding and process control required to improve reproducibility.

Recent advances in electroacoustics and NMR technology have provided a means for improved *in situ* and on-line characterization of slurry processing at various stages from powder to slurry to green body. The application of multiple frequency analysis of the electrokinetic sonic amplitude and phase shift, in conjunction with recent breakthroughs in electroacoustic theory,

allows simultaneous determination of both agglomerate size and particle charge in dense suspensions approaching 40% by volume solids. Using this technique, the electrochemical properties of powders in suspension, and the interaction of slurry components, can be studied and quantified for application in intelligent processing (Figure 2). The distribution of organic in a slurry is a critical parameter in deciding homogeneity of slurry components and agglomerate formation. NMR imaging is a unique diagnostic technique that can provide internal mapping of material distribution. ^{29}Si magic angle spinning NMR spectroscopy is a powerful technique for determination of phase composition of powders. Nuclear spin relaxation times can be used to examine the interaction of polyelectrolyte dispersants with the solid\solution interface.

Our research will focus on Reaction Bonded Silicon Nitride (RBSN) and Sintered Reaction Bonded Silicon Nitride (SRBSN) systems. RBSN/SRBSN routes begin with low-cost metallic silicon powders that are dispersed in an aqueous environment with several secondary components (dispersants, binders, nitridation catalyst and sintering-aids). A green body is produced by a shape forming process such as slip-casting. The shape is then nitrided to form porous silicon nitride with least dimensional change, followed by sintering to an acceptable density.

The objectives of this project are: (1) develop improved surface chemical understanding of aqueous slurry processing of ceramic powders; (2) develop the electroacoustic technique for slurry characterization and on-line measurement applications; (3) develop NMR spectroscopy and imaging techniques for the characterization of powders, slips and green bodies.

Nuclear Relaxation NMR Imaging of Green Ceramics

P. S. Wang

Development of proton nuclear magnetic resonance (^1H NMR) analysis at 400.159972 MHz has been initiated to evaluate the binder in injection molded alumina green compacts. The nuclear spin-spin relaxation times (T_2) of protons in the binder components (paraffin wax, polypropylene, and stearic acid) were measured to allow comparison with those in the injection molded green compacts. ^1H nuclear spin echo signals were observed by a multiple pulse sequence. Block's equations were used to calculate the spin-spin relaxation times from these echo intensities. The T_2 for paraffin wax and polypropylene were in the 30 to 33 μsec range and their intensity decay behaviors were very similar. However, the T_2 value for stearic acid was found to be only 17 μsec and its echo signal intensity decays more rapidly than those for paraffin wax and polypropylene. Injection molded alumina green compacts containing polypropylene/wax/stearic acid from Prof. R. German's laboratory at Pennsylvania State University were examined for binder distribution by proton nuclear magnetic resonance (^1H NMR) imaging. The solid imaging technique of nuclear spin-spin relaxation time (T_2) weighted imaging at 400.159972 MHz was used for this study. Two- and three-dimensional images were constructed from the intensities of these nuclear echo signals.

Binder content variations in three green compacts molded from the same nominal blend composition were detected. The spatially-resolved two-dimensional images obtained by application of the T_2 technique indicated that the green compacts fabricated from the same nominal binder composition did not have the same content as expected. This observation agrees

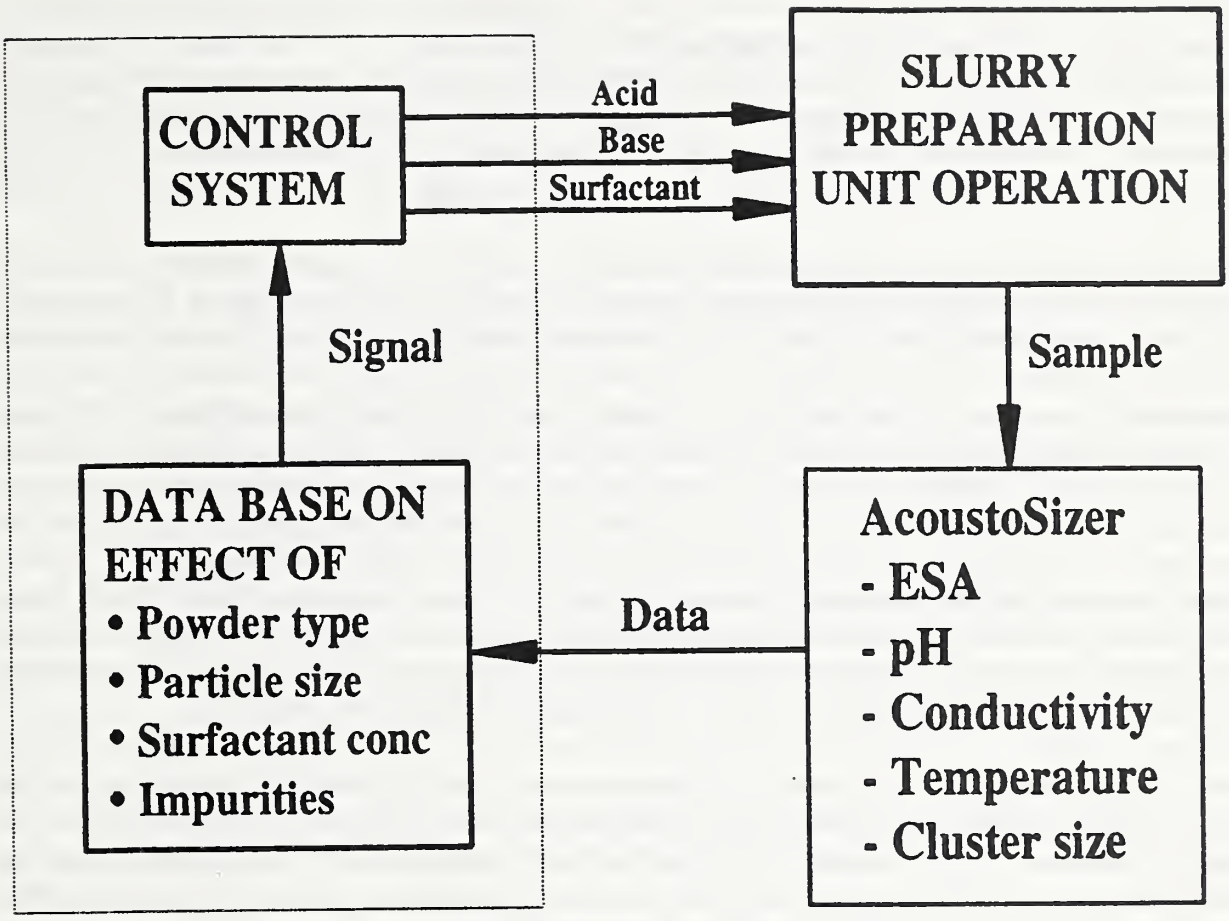

Figure 2. Schematic of (Proposed) On-Line ESA Measurement for Intelligent Processing of slurries. The results obtained in this program will help us design such a system.

well with our previous conclusion drawn from nuclear spin echo studies by Hahn's pulse sequence. A three-dimensional imaging revealed that the binder distribution inhomogeneity and internal imperfection do exist at certain parts of the samples. A binder-rich folding line was also detected in one of these green compacts.

Analysis of the molded compacts also showed the presence of a specie with a T_2 value near 300 μsec. This species may be the result of a reaction during processing or the presence of moisture. The width of RF-pulses used to measure echoes did not have a significant effect on relaxation times, but it should be considered in calculation of echo intensities at equilibrium and hence binder composition. This technique development is expected to allow analysis of both binder content and distribution in molded components with application in process models.

Kinetics of Si_3N_4 Oxidation Using Auger Electron Spectroscopy

P. S. Wang

One of the major technical issues in the processing of silicon nitride ceramic materials is sinterability of silicon nitride starting powders. One piece of relevant data to define the sinterability is to develop data on the formation of oxide layer on the surface of the powder particles at sintering temperatures. Thus, information on oxidation kinetics will be useful in evaluating sinterability. In addition, the oxidation kinetics can define surface reactivity of powders.

Surface techniques such as XPS and/or Bremsstrahlung-excited Auger electron spectroscopy (AES) have been used to measure oxidation kinetics of silicon carbide whiskers, silicon carbide platelets, and silicon nitride powders. With the silicon nitride powders, a difference in activation energy was observed between powders manufactured by direct nitridation and by pyrolysis of silane and ammonia. The silicon nitride powder used in this study was obtained from Union Carbide Coatings Service Corporation. This powder was synthesized by pyrolysis of silane and ammonia. Mean particle size in this powder was 0.2 μm. The powder was vacuum heat-treated to remove chemically-bound hydrogen. The powder prepared by pyrolysis of silane and ammonia was found to contain chemically bound hydrogen. Since this hydrogen is evolved at about the same temperatures that the oxidation begins, this was believed to be the reason for the difference in oxidation kinetics. In the present study, the silicon nitride powder containing chemically bound hydrogen was heat-treated in vacuum to remove hydrogen. The oxidation kinetics of these powders were studied using Bremsstrahlung-excited AES.

The Si KLL peaks for SiO_2 and Si_3N_4 were observed at 1609 and 1612 eV, respectively. This is in good agreement with previously reported results. The increase of SiO_2 component with heating time is a clear indication that surface oxidation increases as a function of heating time and temperature. The average oxide thickness on the surface of the Si_3N_4 particles can be measured from the Si KLL data using the methods developed previously.

The oxide thickness on the vacuum heat-treated Si_3N_4 powder before oxidation was 0.8 nm. Average oxide thickness data for the vacuum heat-treated Si_3N_4 powders as a function of heating time at 850°, 900°, 950°, and 975°C show that at each temperature, the oxidation followed a linear rate law. The activation energy for linear oxidation was measured to be 195 ± 26 kJ/mol (47 ± 6 kcal/mol). This is significantly different from the value of 104 ± 22 kJ/mol measured for the untreated powder. The gas evolution measurements show that more hydrogen is evolved during the oxidation of untreated Si_3N_4 powders than from the treated sample. It is this evolution of hydrogen that apparently has inhibited the oxidation of untreated powders.

Low-Temperature Fabrication of Transparent Silicon Nitride

W. Chen and S. Malghan

The production of nano-size particles has recently enabled the synthesis of a new class of ultrafine-grained materials by using non-conventional compaction and sintering. In the present

research, we are studying the feasibility of producing a nano-phase Si_3N_4 with nanostructure and transparent to visible light without the use of sintering-aids. Our basis for this study has been the use of cryogenic compaction of amorphous silicon nitride powders.

To study the cryogenic or other lubricant compaction process in more detail, we designed and constructed a novel system. The new equipment is capable of producing 3 mm disk-shaped samples under vacuum or in a variety of controlled conditions such as surrounding gaseous or liquid environments, and temperatures in the range from liquid nitrogen to 28°C, and pressures up to 3 GPa. In addition, during powder compaction, continuous measurements of sample volume, applied force, and frictional force between the sample and the die wall are performed.

A maximum random packing density (about 64% of theoretical) for nano-size amorphous Si_3N_4 was achieved by compacting at 2.5 GPa under liquid nitrogen temperature. At room temperature, dry compaction of the same powder at 2.5 GPa resulted in a green density of 57%. These results show that cryogenic compaction is an efficient technique to obtain a high packing density and small-scale porosity. The green body showed transparency under visible light indicating uniform nano-scale porosity. Our attempts to further densify cryogenic-compacted green bodies by sintering and hot-isostatic pressing up to 1500°C have not been successful. We are exploring various alternatives for densification of silicon nitride green compacts.

Because full density may not be obtained without the addition of sintering-aids, we plan to measure the maximum density achievable with the nano-powders with the expectation that the small pore size and associated defects may not drastically reduce mechanical properties. Cryogenic or other lubricant compaction techniques will be used to produce dense compacts (65% or higher density at 2.5 GPa) from amorphous nano-size silicon nitride powder. Following this, the dense compacts will be hot-pressed to increase contact area between particles at 1.0 GPa and 1000°C. Finally, the compact will be pressureless sintered at 1400°C. This process is expected to promote a strong bonding at the contact area due to solid-state surface diffusion. The density of the new microstructure of silicon nitride ceramic with nano-scale porosity and grain size is expected to be between 65 - 80% of theoretical with enhanced optical, electrical, and mechanical properties. These data will not only help develop a new class of materials but also will have broad implications in the development of nano-powders processing technology.

Computational Models of Microstructural Development

W. C. Carter, A. Roosen[1], J. Cahn[2] and J. Taylor[3]
[1] Metallurgy Division, NIST
[2] Metallurgy Division, NIST
[3] Mathematics Department, Rutgers University

A number of issues are being addressed with a common theme of using mathematical tools to develop an improved understanding of particulates behavior in processing and microstructure design. An example is presented on the development of methods and software to calculate the evolution of fully faceted particles for surface and vapor diffusion. This represents the first time such diffusion processes have been exactly analyzed for such faceted crystals that are commonly

found in nature. The results identify visual clues for materials processors and experimentalists to decide which diffusion mechanisms are active during microstructural evolution. This effort also represents the first rigorous approach to calculations of interface evolution in anisotropic systems and will be the cornerstone to future advances in the computational materials science of microstructural development.

Novel mathematical techniques and software were developed to study microstructural development in anisotropic materials and particles. The development of these methods is important in studies of many technological processes including sintering and powder processing. The techniques are also applicable to the study of material behavior at high temperatures and the results are useful to engineers in materials processing design.

Tracking of the evolution of an continuous interface during diffusive transport is a notoriously difficult problem. Modeling interface growth and shape changes is fundamental to the study of microstructural evolution. Methods were recently developed to calculate the time evolution of highly anisotropic two-dimensional interfaces for two cases of diffusive transport; surface diffusion and interface attachment limited vapor diffusion. These two independent diffusive mechanisms are extreme cases of volume conserving flows. In surface diffusion, mass flux is along the interface. In interface attachment limited vapor diffusion, evaporation or growth takes place by attachment of mass at the interface from some ambient (vapor) phase where diffusion is considered to be infinitely fast compared to the attachment kinetics.

Recently developed sharp interface or "crystalline" methods have shown that computations of interface growth can be greatly simplified when the Wulff shape of the underlying crystal is completely faceted. An interface must be completely faceted at any orientation which corresponds to either a facet in the Wulff shape or to missing orientations (edges or corners) in the Wulff shape--in which case the anisotropic analogue to the isotropic mean curvature, called weighted mean curvature (wmc), has a particularly simple form. The average chemical potential along a facet is proportional to wmc (the analogue of Gibbs-Thomsen) and is likewise simple to calculate. The evolution of those interfacial orientations which are not faceted can be approximated in the crystalline method by replacing differentiable Wulff shape with one of many facets. In the case where growth is proportional to the local mean curvature, the crystalline methods appears to converge to isotropic flow, but has not been proven.

The results have practical utility. Typically, scaling laws are applied to some set of stereological measures. Values are plotted on a log-log plot and exponents are used to identify the active diffusive mechanism in the process. Such averaging is open to misinterpretation and conclusions are often equivocal. From visual inspection of our results which show a marked distinction in the interface development depending on the active diffusive mechanism, the dominant diffusive mechanism can be discerned by comparing experimentally observed microstructures to computed results. A video is available and a publication is in progress. Local removal of gradients in wmc is indicative of surface diffusion; long-range coarsening is indicative of interface-limited vapor diffusion. Of course, there are mixed cases where neither process is dominant and calculations of such cases are in progress.

Synthesis of Nanostructured Materials

J. J. Ritter

A new class of materials comprising nano-scale (< 100 nm) particulates is being considered for advanced applications. There are increasing numbers of recent reports that point to the potential for greatly enhanced mechanical, electrical and magnetic properties from these materials. While the field is still embryonic, obvious benefits can be readily appreciated from factors such as reduced flaw size producing substantial increases in strength and special functional properties arising from a high density of interfaces.

The initial task is to identify procedures to generate nano-structured materials in a controlled and reproducible manner. The following are examples of some novel approaches to the synthesis of nanostructured ceramic materials being developed.

Ferrite Materials: These materials are used for miniaturization of microwave communications components. A CRADA has been signed with Trans-Tech, Adamstown MD. Novel chemical syntheses of thick-film microwave ferrite materials will be explored based on the $NiFe_2O_4$, $Y_3Fe_5O_{12}$ and $BaFe_{12}O_{19}$ families of compounds.

Initial studies using modified metal nitrate solutions and a novel sequential dip and cure procedure has shown that good quality, well-adhered $NiFe_2O_4$ films can be deposited on a dielectric substrate. It is hypothesized that the beneficial mechanical properties arise from the controlled deposition of material in 5 nm-thick layers. While this research is in its early stages, the prospects for producing a variety of well-formed magnetic materials in film form is very encouraging.

Thermoelectric Materials: These materials are intended for use for modular thermoelectric refrigeration as an alternative to CFC systems. Chemical synthesis procedures are being developed for Bi_2Ti_3 and related materials that are projected to lead to improved thermoelectric performance. Two routes for chemical synthesis of fine-particulate bismuth telluride-based powders were developed. One of these routes gives plate-like particles that may be amenable to orientation. Procedures for the inclusion of nano-size second phases into these materials have been developed and we have observed that sintered samples compacted between 1.5 and 2.0 GPa show an increased Seebeck coefficient and a lowering of thermal conductivity by a factor of 3 to 5 in these sintered compacts. This latter effect is believed to be due to phonon scattering by nano-porosity generated during sintering. Unfortunately, the processing techniques used to date give samples that exhibit high electrical resistivity. Thus, an improved figure-of-merit has not yet been realized.

Magnetic Nano-composites: These materials are intended for magnetic refrigeration in the 7 to 80 K range. Chemical synthesis of garnet materials of the type $Gd_{1-x}M_xO_{12}$ where M = Fe is being pursued in this project.

Measurements on the GdGaFeO(GGIG) system shows an enhancement in magnetocaloric effect by a factor of about 3.4 over the best currently-used magnetic refrigerant, gadolinium gallium

garnet(GGG), at temperatures around 15K. Moreover, GGIG exceeds the performance of GGG by a significant margin for temperatures in the 10 to 80K range, allowing for the design of magnetic refrigerators that can operate well above the current maximum of 20K. In addition, GGIG does not possess a remanent magnetization and therefore exhibits no hysteresis losses during field cycling, an important factor to be considered in magnetic refrigerant selection. Experimental evidence suggests that the improved magnetocaloric performance of GGIG arises from the presence of nano-sized magnetic regions throughout the material.

High Energy Agitation Milling of Silicon Nitride Powders

D. B. Minor, P. T. Pei and S. G. Malghan

Since most structural ceramics are manufactured from ceramic powders as starting materials that are highly agglomerated due to the van der Waals attractive forces between the primary particles. Shape-forming from fine powders constitutes slurry-based processing and milling is often used to achieve particle size reduction, deagglomeration, and/or homogeneity of the slurry. This project is on the development of high energy agitation milling of silicon nitride powders by the addition of yttria as a sintering-aid. Specifically, we have been studying the factors responsible for repeatability improvement, preparation of high density suspensions, and application of electrokinetic sonic amplitude (ESA) measurement for characterization of milled slurries.

We have carried out a series of experiments under a set of fixed milling conditions to assess factors affecting milling process responses such as particle size distribution, specific surface area, ESA, and the pH at the iso-electric point. Preliminary analysis of these results have shown that variability in the data associated with the measurement error is not a factor. However, material and process variabilities have a strong influence. The material variability is associated not only with batch-to-batch variation as well as microstructural variations due to agglomeration of primary particles and bonding between the particles in as-received powders. In addition, the yttria powder has a strong influence on the variability of milling response. The yttria powders undergo hydrolysis as milling proceeds and interact with the silicon nitride powder. Another significant variability is due to operator influence during milling such as the rate of addition of powder and rate of build-up of solids concentration as milling proceeds in the initial period. These variabilities are being examined so that overall repeatability can be enhanced.

The preparation of high density silicon nitride suspensions is being studied as a collaborative project with the St. Goblin-Norton Company. We have been able to prepare suspensions containing solids loading between 75-79% by weight. These suspensions have been evaluated in both laboratories by slip casting and iso-pressing. In addition, the green bodies have been densified by hot isostatic pressing. The results show that the green densities are considerably higher (about 2.2 g\cm^3) than those obtained by using slurries from vibratory milling. However, the green bodies are brittle since they do not contain binder. Additional hurdles to overcome are green body cracking and decrease of specific surface area of milled powders from 12 to approximately 10 m^2/g.

In a separate study, we are studying the application of ESA measurement techniques to monitor surface chemistry changes in the slurry and to optimize milling conditions. The ESA of milled slurries was found to have a strong correlation with the green density of compacts prepared by slip casting the slurries. This is not surprising since improved dispersion should result in higher green densities due to the presence of larger number of fine particles and their ability to fill interstitial voids.

III. SURFACE PROPERTIES — Stephen Hsu

The ability to control the surface and interface properties of advanced materials such as ceramics, coatings, and composites is a key issue in achieving cost-effective and successful application of these materials.

Surface properties such as elastic modulus, hardness, friction, shear strength, and chemical reactivity control the materials' performance and durability under a variety of environmental conditions. These properties are dependent on the surface texture, microstructure, surface contaminants, defects, and the physical and chemical nature of the molecules at and near the surface. The exact relationship between these parameters and performance is not known.

The objectives of the group are: (1) to develop new measurement techniques to characterize the physical and chemical properties of ceramic surfaces and interfaces under static and dynamic contact conditions; (2) to understand the relationship between microstructure, chemical compositions of the surface and interface, and the micro-mechanical and tribological properties of ceramics and other materials; (3) to develop the science and technology for the control of surface properties by lubrication and surface texture design, and to develop basic design principles for optimum combination of materials and lubricants; (4) to provide data, reference materials, and design guidelines for the introduction of new materials in industrial applications.

Significant Accomplishments:

- A series of wear maps has been updated and published for silicon nitride, silicon carbide, and zirconia as a function of speed and load. These maps provide design guidelines for industrial designers in considering ceramics for applications.

- The chemically assisted machining of ceramics technology has been demonstrated on a surface grinder. A family of chlorinated compounds has been developed that significantly reduce cutting time and at the same time, reduce surface roughness of the as-machined surface, reducing the cost of ceramic components.

- The advanced lubrication technology developed under DOE sponsorship was validated by the Cummins Engines Co. Eight lubricants were selected for testing and only two were able to finish the 200 hour endurance test. One of the two was the technology developed at NIST.

- An industrial workshop on lubrication technology needs for transportation industries was held at Northwestern University, Evanston, IL on Sept. 21-23, 1992. A consensus on research needs and prioritized areas was reached. A report was prepared and has been released by ASME for distribution in 1993. This is the first time that lubricant, automotive, and diesel industries have come together with component suppliers, national laboratories, universities, and government personnel to discuss a single topic and arrive at some consensus.

- We have initiated a joint research program on ceramic valve inserts used in the Caterpillar 3500 series gas engines for cogeneration in conjunction with Caterpillar, GRI, Eaton, Norton, and SWRI. The goal of the project is to develop life prediction methodology for such ceramic components.

- We have demonstrated that silicon nitrides and silicon carbides can be lubricated by a new generation of lubricant chemistries, such as oxygenates and sulfonates. An effective lubricating film can lower the stress intensity at asperity contacts, thus protecting the surface. Successful development of this knowledge could pave the way for wide-spread use of ceramics in engines.

- A new method, the ball on inclined surface, to measure surface quality (surface strength as related to the defects size and population) of as-machined ceramic surfaces has been developed. The location of the first tensile crack in the wear track indicates the stress at which a preexisting crack on the surface propagates to form a tensile crack. The stress level has been demonstrated to correlate with the quality of the surface.

- Nanoindentation and low load instrumented scratching techniques have been applied to measure hardness and scratch properties of copper and molybdenum oxide films with thicknesses in the range 100-600 nm and to nickel/nickel oxide plasma spray deposited coatings. Techniques developed in this research permit determination of mechanical behavior and adhesion of films placed on ceramic and other substrates to improve wear performance.

- A detailed study of the mechanisms of wear of Si-based ceramic over a range of speeds and loads reveals that there are multiple mechanisms at work. Results suggest that wear of ceramics can be classified into three levels: a mild wear region where hardness and surface roughness dominate the process; a severe wear region where fracture dominates; a failure region where fracture and thermal shock combine to cause rapid deterioration and failure.

- A computerized ceramic wear database has been successfully developed. The database contains friction and wear data of ceramics in an user-friendly software package. This and other databases jointly developed between ACTIS Inc. and NIST form the most comprehensive collection of design codes, data bases, and information software in Tribology in the world today.

Wear and Wear Mechanisms for Si-based Ceramics

T. N. Ying[1], Y. S. Wang[1], M. Shen[2], and S. M. Hsu

[1] PhD Candidates, Materials Science, University of Maryland
[2] Post-doctoral Fellow, University of Illinois at Chicago

Advanced ceramics are increasingly being considered for tribological applications such as engine components, bearings, cutting tools, pump seals, etc. However durability is a concern and wear

life and wear mechanisms of Si-based ceramics are not well understood. This research attempts to present a systematic view of how ceramics wear, the dominant mechanisms under which they wear, and the models available to describe the wear processes.

The materials studied included a hot-isostatically-pressed silicon nitride, a hot pressed silicon nitride, and two silicon carbides. The microstructure of the silicon carbide samples is different; one with a duplex structure, one with an equiaxed grain structure. Wear experiments were conducted by using a ball-on-three-flats wear tester. Both the ball and the flats were made out of the same ceramic material.

Wear maps of Si_3N_4 and SiC under dry sliding conditions are shown in Figure 1. The overall wear characteristics of the silicon nitride and silicon carbide shown in the maps are similar in shape with wear transition, defined as a sudden increase in wear due to a small change in either load or speed, observed in both materials. Such transitional behaviors are mainly due to dislocation build up in the grains due to repeated asperity contacts. These eventually lead to intergranular cracking producing large wear particles, which cause gross fracture due to high intensity loading. The location of such transitions as a function of load and speed has an obvious significance in engineering applications. In addition, for a given material pair, the transition location is influenced by the lubrication environment.

Figure 2a which utilizes mean Hertzian pressure to directly compare the materials shows the wear transition boundary, the location at which the wear transition occurs, in Si_3N_4 and SiC under dry sliding and paraffin oil lubricated cases. The existence of the three regions implies that there are different wear mechanisms operating in each of the regions. The diagrams have two key features: the location of the transition boundary and the functional dependence of the transition boundary on speed and pressure.

At low speeds, the transition boundary is shown to be independent of speed, implying that critical stresses for both Si_3N_4 and SiC are responsible for such transitions. As speed increases beyond 0.01 m/s, this boundary starts to bend toward lower contact pressures, suggesting the onset of the temperature influence due to speed increase. The transition boundary between regions B and C represents the wear transitions from severe to ultra-severe wear. The shape of the boundary line indicates that the transition is the result of the combined effect of contact pressure and speed. These results suggest that surface temperatures due to the frictional dissipation of heat play a significant role in the occurrence of wear transitions.

The major effect of adding a lubricant such as the purified paraffinic oil to the wear system is the elimination of high surface temperatures. Under paraffinic oil lubricated condition, as shown in Figure 2b, the wear transition line moves to much higher pressures and speeds. Furthermore, only a mild-to-severe wear transition is present for both Si_3N_4 and SiC. Also, the shape of the transition line is altered suggesting more speed dependence at high pressures and more pressure dependence at high speeds. Both the location and the functional dependence in this case resembles the boundary transition line separating region B and C in Fig. 2a. This similarity is probably due to the flash temperature induced transition.

The mechanism of wear can be examined in terms of the different wear regions. The silicon

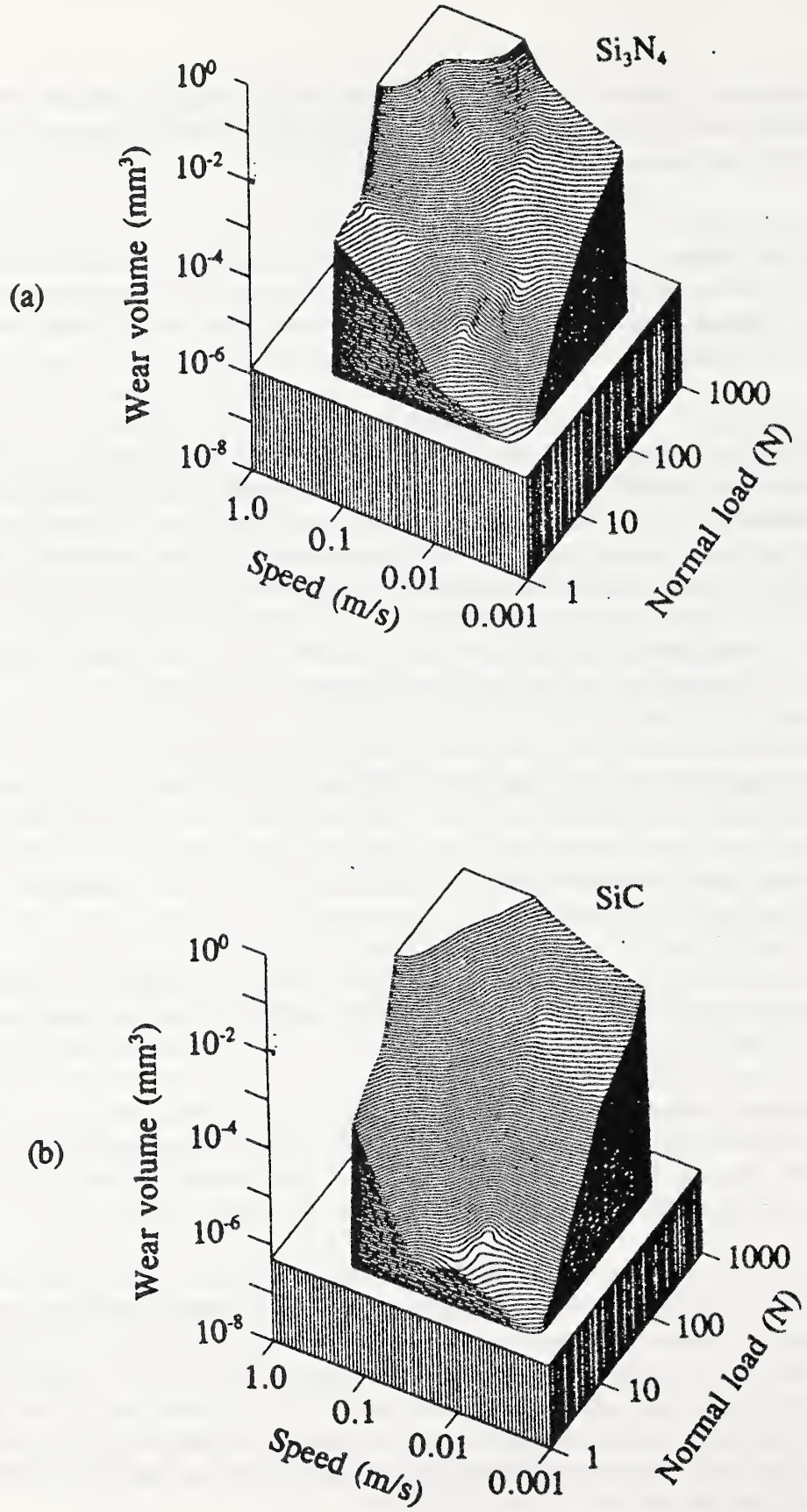

Figure 1. Three-dimensional wear maps of (a) SN1 and (b) SC1 under dry sliding conditions.

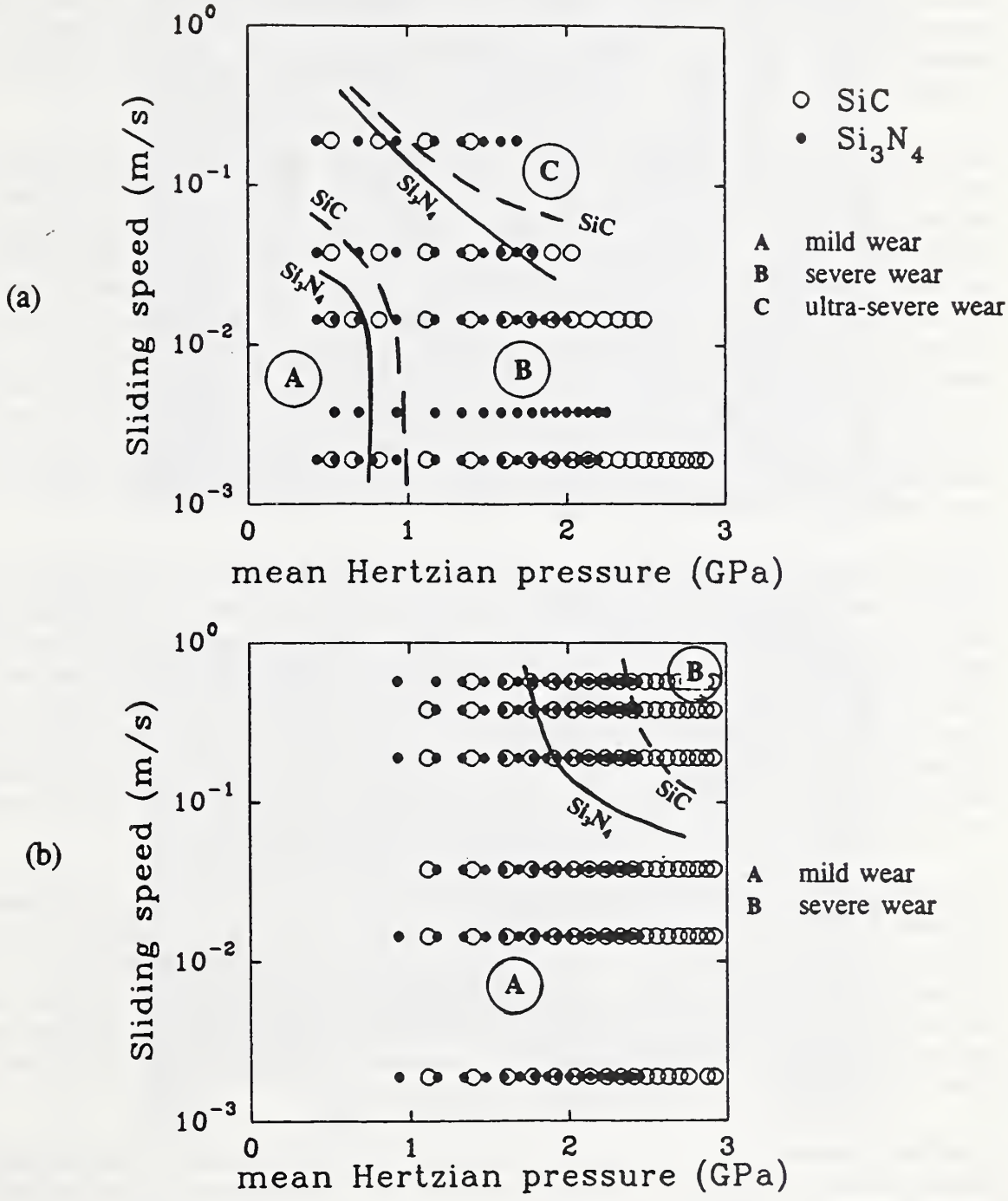

Figure 2. Wear transition diagrams of SN1 and SC1 under (a) dry sliding and (b) paraffin oil lubricated conditions.

nitride surface from region A as shown in Fig. 3a, reveals a polished surface with wear debris in the form of rolls which are perpendicular to the direction of sliding. This is primarily due to the presence of water which reacts with the silicon nitride surface forming silicon hydroxides. The presence of such large particles inside the contact changes the stress distribution which causes the onset of transition. In this region, the pressures at the asperity tips are controlling the wear action. There is not sufficient compressive stress due to normal loading to cause substantial fracture. Therefore, we see abrasion by the asperities and grooves appear on the surface.

The SiC worn surface shown in Fig. 3b displays polished and grooved surface features. The width of the grooves is on the order of 2-3 μm. The micrograph suggests that wear in this region is similar to silicon nitride and is dominated by deformation-controlled processes. After transition to region B in Figure 2a, wear is much more rapid and severe. Brittle fracture has become the predominant wear mechanism in this region after the mild-to-severe wear transitions. Under ultra-severe wear conditions, region C in Fig. 2a, a severely fractured surface covered by large quantity of debris is observed for Si_3N_4, while the worn surface of SiC displays a mostly intragranularly fractured surface. Brittle fracture is still the dominant wear mode in region C. However, the extent of brittle fracture in this region is evidently more severe than in region B. Overall, the dominant wear mechanism for Si_3N_4 and SiC under dry sliding conditions changes from plastic deformation in mild wear regimes to brittle fracture in severe wear regimes.

Under paraffinic oil lubricated condition, there are only two regions, mild and severe wear. For mild wear, polishing is the dominant wear mode. Hence, plastic deformation and asperity abrasion are the dominant wear mechanism. After transition, the surface morphology is rough and full of fracture and grain pull-outs. Observation using transmission electron microscopy (TEM) was conducted showing transgranular dislocations in the sub-surface grains. For SiC, intergranular cracking is present in addition to the dislocation pile-ups. One can conclude that dislocation pile-ups, plastic deformation, and brittle fracture (mostly intergranular cracking) are the predominant wear mechanisms for Si-based ceramics under paraffin oil lubrication conditions.

In addition to the wear mechanisms discussed so far, 3rd-body effects due to the presence of different wear debris are important. The wear level of this case is in region B, i.e., post-transition wear dominated by fracture. The wear scar is found to be covered by a thick layer of loosely bound wear particles. The sizes of these particles are mostly sub-micron. The size and shape of the wear particles are distinctly different from the normal particles where abrasion by the few large particles cause damage. This large amount of submicron particles serves as a form of solid lubrication redistributing the contact stresses.

A series of simple tests was carried out to examine the wear of ceramics from the perspective of the materials' response to stresses. In order to simulate the stress field encountered in the sliding contacts, a ball indenter is used to apply stress on a flat surface. Fig. 4a shows a Si_3N_4 flat sample indented by using a diamond indenter with a spherical tip. The average contact pressure is estimated to be $\sim$ 20 GPa. Hertzian cone crack and radial cracks appear from the circumference of the indentation. Subsurface damage can be observed from the cross-section

(a)

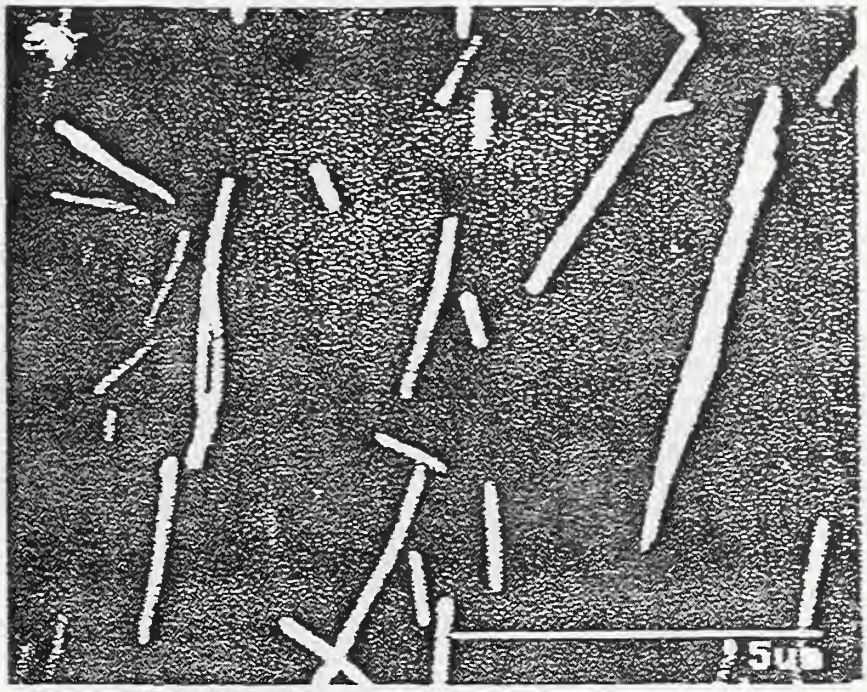

(b)

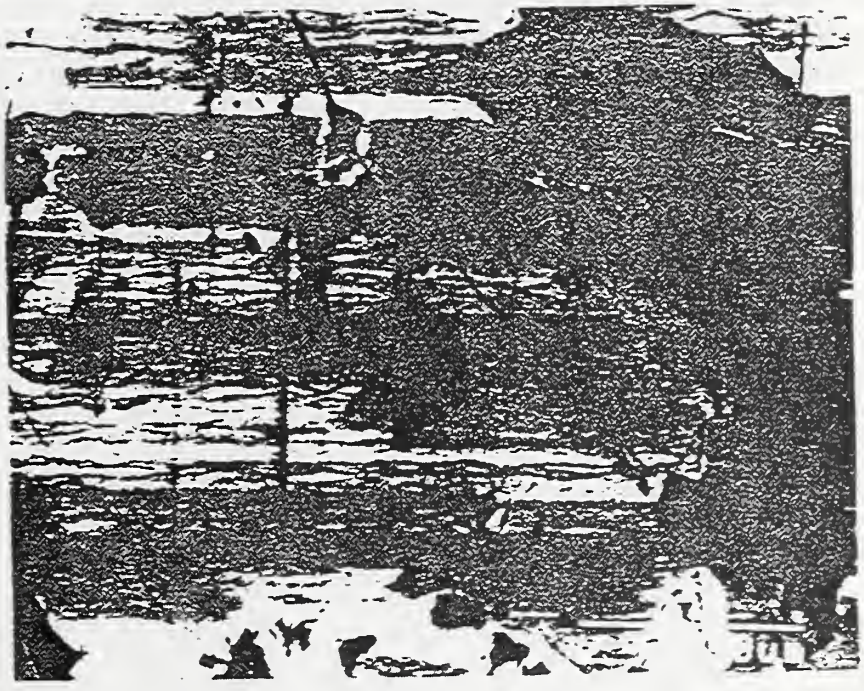

Figure 3. Representative worn surface morphology in mild wear under dry sliding conditions (region A in Fig 2(a)): (a) SN1 and (b) SC1.

shown in Fig. 4b. A lateral crack is observed propagating parallel to the surface. Crack initiation appears at about 10 kg, which corresponds to a mean Hertzian pressure of about 15 GPa. The test results suggest that compressive stress induced tensile cracks are primarily dependant on the mean critical pressure in the contact and the asperity pressure is not a factor here. Very little shear stress is involved in indentation, but the results show considerable compressive stress would be required to initiate damage.

To examine the role of shear force on ceramic damage, a ball-on-inclined plane test was used. The test configuration consists of a ball sliding on an inclined flat plane. The test is designed to measure in a single sliding the various stages of fracture of the ceramic in response to a continuously increasing force. The ball used is a diamond indenter, the flat sample is SN1 silicon nitride, and the incline angle of the flat is 1.1°. The friction coefficient during the scratch test increases from 0.1 at the beginning of the test to 0.4 at the end of the test. Fig. 5 shows the morphology of the wear track. One can see that initially there is a plastically deformed region, followed by tensile crack region, and then the cracks propagate outside the wear track. At the end of the sliding, gross fracture occurs coupled with delamination revealing sheet detachment. Considerably lower pressure is required to cause tensile cracks, 5-8 GPa as compared to 15 GPa estimated from indentation.

To simulate more realistically the contact conditions between two silicon nitride surfaces, a two ball collision test was used to study the deformation and wear processes. The apparatus is the same one used in the ball-on-inclined plane test, except here two silicon nitride balls are collided together and the forces are measured continuously by force transducers. Video pictures are also taken to record the sequence of events. The test was conducted in the absence of any liquid lubricant. The contact configuration dictates an increasing load followed by a decreasing load. A high level of friction, 0.6-0.8, was measured for this test. In Fig. 6, it can be seen that the two surfaces come together and many fine debris are exploding out of the contact zone. This is the first time such event has been recorded in ceramic tribology. When an element of the subsurface volume is under high hydrostatic pressure, a sudden appearance of a crack creates a free surface and the volumetric element breaks into many fine particles and practically explodes out of the contact. Such cracks could be caused by a secondary tensile crack or a shear crack. This explains the mechanism and the source of the sub-micron wear particles discussed previously.

Instrumented Scratch Testing and Nanoindentation

A. W. Ruff and H-J. Shin[1]

[1] Post-doctoral Fellow, University of Maryland

The NIST[2] instrument for controlled load/depth scratching and nanoindentation of materials has been used to characterize the behavior of several ceramic materials. The instrument measures instantaneous load and indenter penetration continuously, with or without simultaneous specimen motion. The data can be used to determine hardness, elastic modulus, ductility, toughness, and resistance to scratching damage. The techniques developed are particularly appropriate for characterizing ceramic coatings, a new NIST technical initiative area for FY94. They are also

(a)

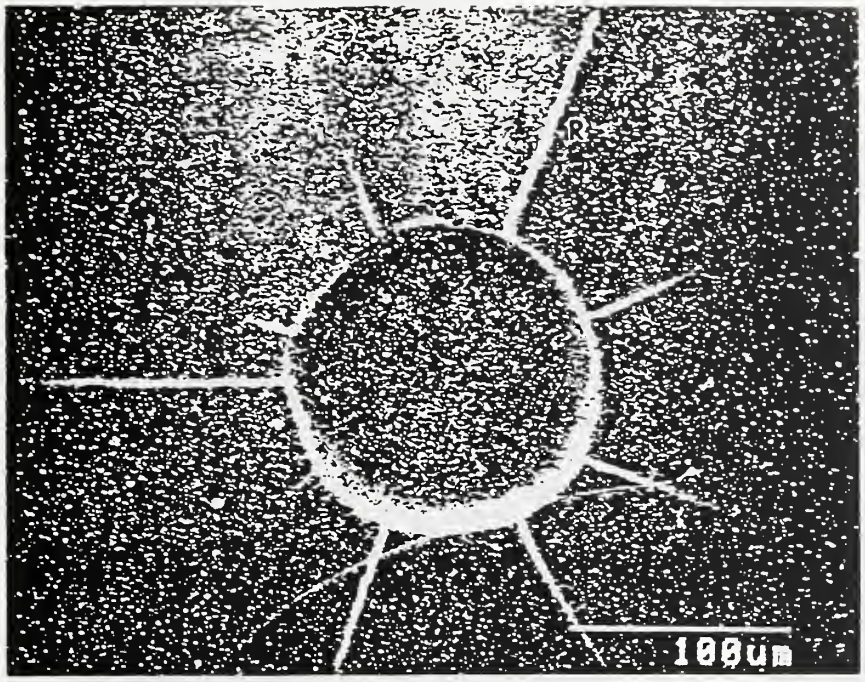

(b)

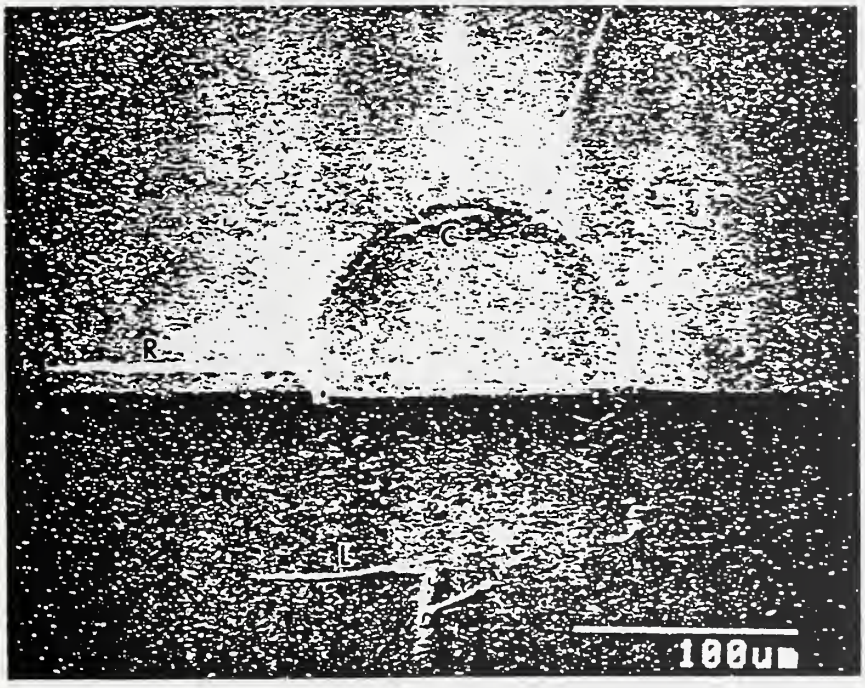

surface

cross-section

Figure 4. Silicon Nitride (SN1) flat sample after indentation by using a diamond indenter (spherical tip radius: 0.2 mm) under 30 kg load and 15 seconds duration: (a) indentation impression, and (b) impression and cross-section. (C=cone crack, R=radial crack, L=lateral crack)

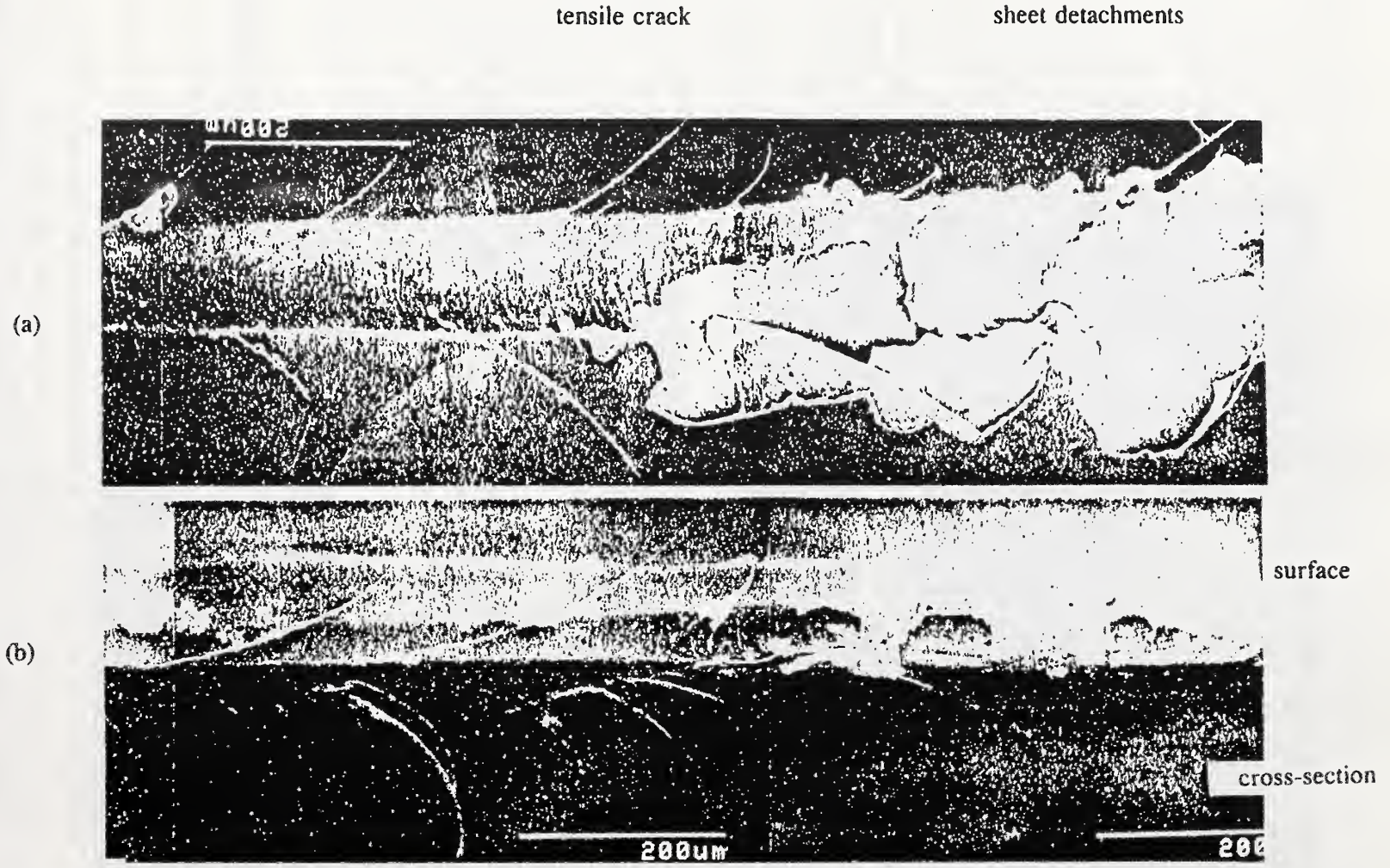

Figure 5. The wear track of a SN1 sample after a ball-on-inclined-plane scratch test: (a) top view of the end of the wear track and (b) cross-section of the wear track.

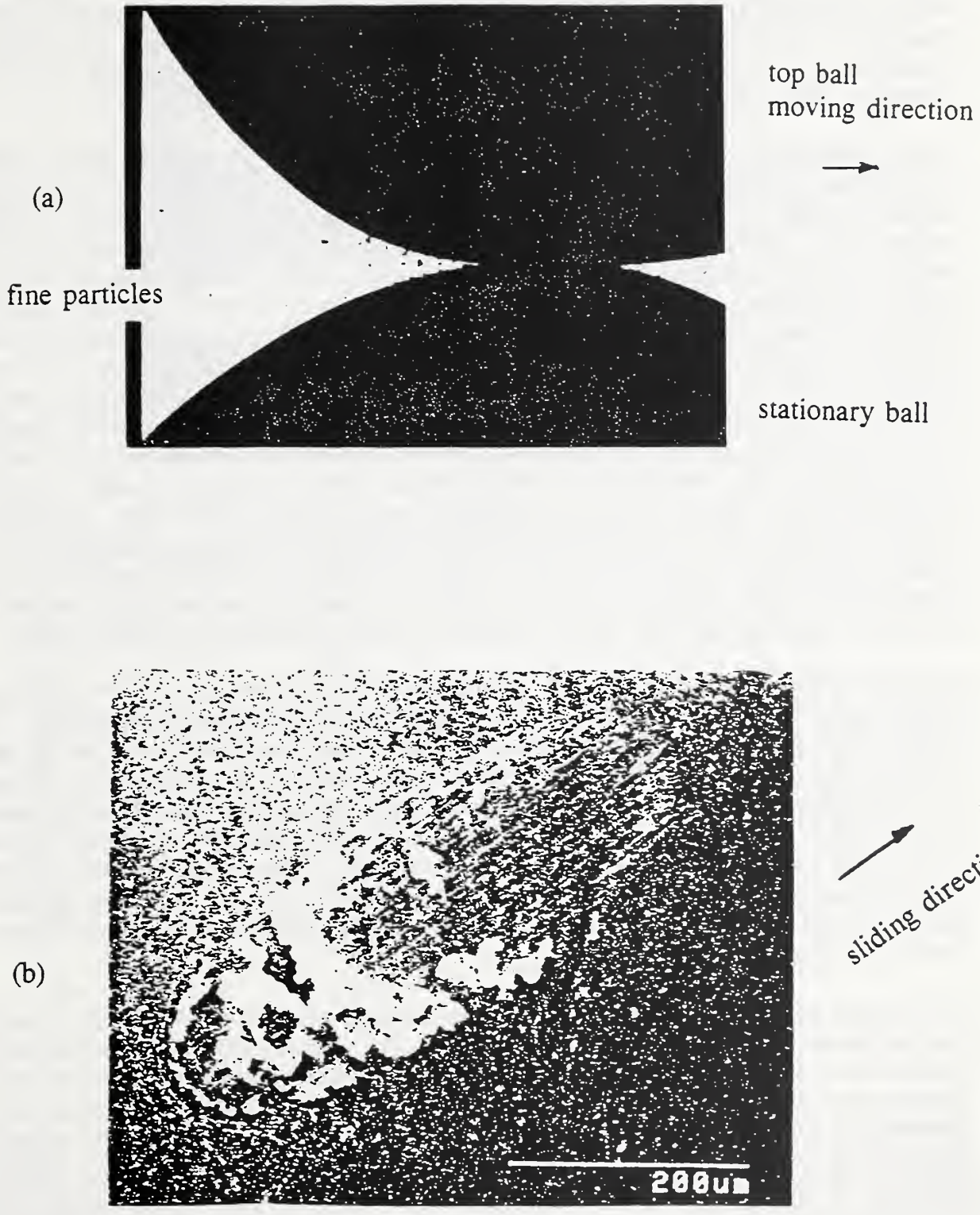

Figure 6. (a) Side-view of a two-ball collision showing numerous fine particles expelled from the contact zone. (b) Wear scar on a ball sample of NS1.

critical to developing an improved understanding of proper surface grinding and finishing methods to be used by industry in preparing ceramic materials for products. This work has been done jointly with staff in the NIST Manufacturing Engineering Laboratory, the Lawrence Livermore Laboratory, the Naval Research Laboratory, the University of Maryland, at a private sector firm, and at the Thermal Spray Laboratory, Stony Brook University (NY).

Controlled scratching and indentation studies were done on CVD silicon carbide, silicon nitride, and a composite alumina-titanium carbide material. Both a diamond pyramid and a single point diamond turning tool were used, in either air or several different fluid environments. Detailed studies of the Al_2O_3-TiC material showed that surface damage caused by scratching was localized within one or two grains distance from the scratch track. Damage consisted of "grain spalls" at the bottom or edge of the scratch (Figure 7a), probably caused by crack growth within the grain boundary regions due to tensile stresses forming behind the indenter during scratching. Observation showed intergranular fracture at spalling sites which is believed to be due to weak grain or interphase boundaries. Another type of damage was "shear cracks" formed perpendicular to the scratching direction inside the scratch track. These shear cracks appeared to be associated with plastic plowing that is atypical for a ceramic material even when confined to local regions. The lateral extent of surface damage from scratching was studied by making two closely spaced parallel scratches in sequence using increasing load values. The second scratch appeared not to be influenced by the first scratch until the distance between the two scratches reduced down to about one half of the scratch width. Once they were close enough to each other, heavy spalling of material between two scratches occurred to an extent not observed in single scratches at even the largest load used in this study on polished surface.

Substantial differences in damage to the material were found by scratching in different fluids. Figure 7b shows results from controlled scratching at loads of 145-172 mN in mineral oil. The changes in the scratch-resisting force curve and in the relative scratch depth curve are the result of severe edge and sub-surface cracking and the associated surface uplifting. This damage occurs sporadically along the scratch and appears to involve some damage accumulation process, possibly elastic strain build-up in the material. The area marked A in (a) that contains considerable scratch edge cracking damage is also marked in (b) with an arrow, where both scratch force and penetration decrease suddenly. Studies are planned to continue to further clarify damage mechanisms, critical load effects, and the importance of different test and material conditions.

Nano-indentation techniques using small spherical diamond tips were also further developed to measure elastic properties of materials and coatings. The method involves low load elastic and plastic indentation of surfaces, while acquiring continuous displacement data. Several models exist for extracting elastic modulus values from those results, although some uncertainty remains concerning the effect of indenter shape on the results. The method can be used for coatings or layers as thin as 100 nm. Results were obtained on nickel/nickel oxide plasma deposited coatings, and showed the effect of coating anisotropy and processing conditions. Techniques developed in this research permits determination of mechanical behavior and adhesion of films placed on ceramic and other substrates to improve wear performance. Such results are needed for development of more durable industrial products, particularly for applications in extreme environments of temperature and chemical reactivity.

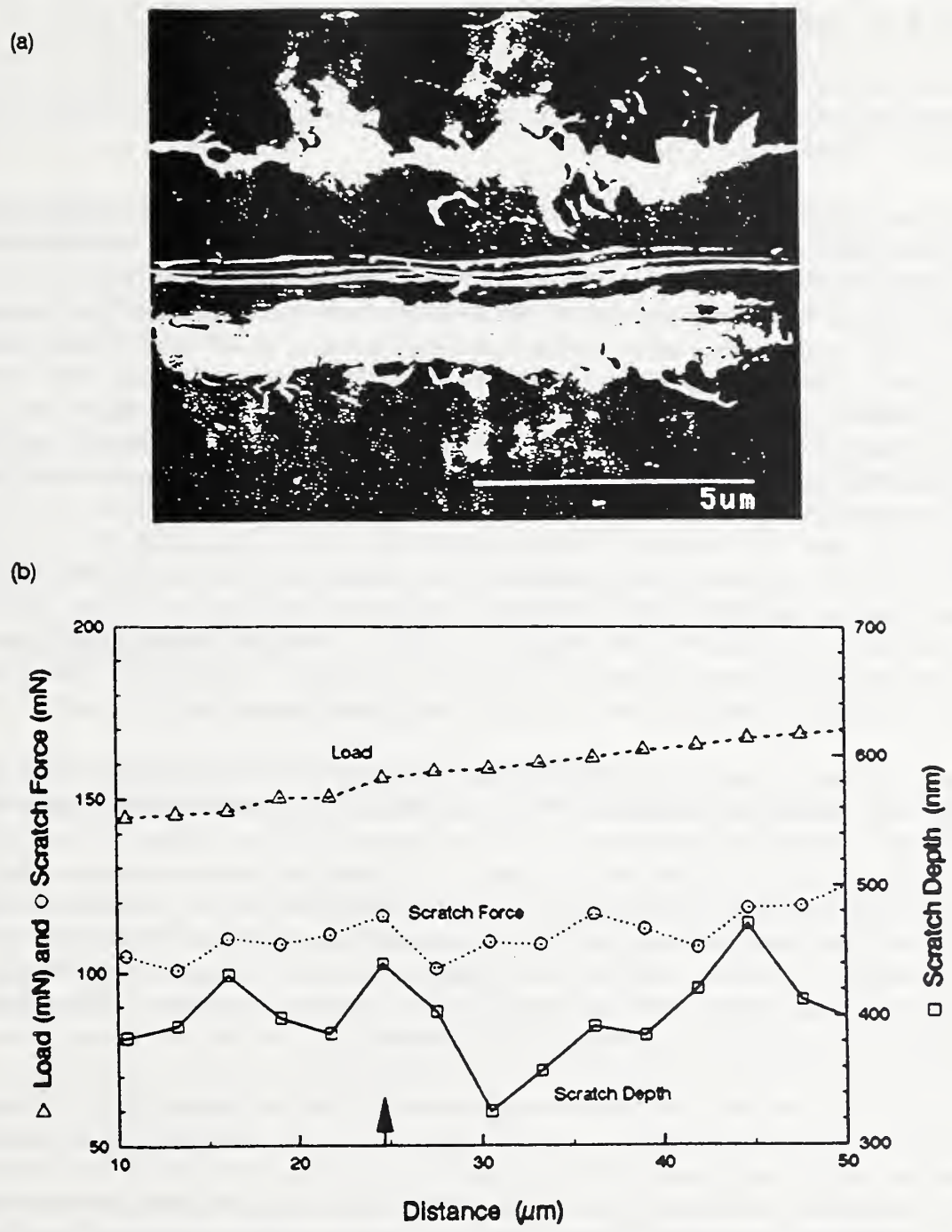

Figure 7. (a) Scanning electron micrograph of scratching damage in alumina-titanium carbide material from a test at loads of 145-172 mN in mineral oil. The area marked A contains considerable edge cracking damage. (b) From the same test, the changes in the scratch (resisting) force curve and in the scratch depth curve are the results of severe sub-surface and edge cracking and the associated surface uplifting. The region marked with an arrow in the graph corresponds to the region marked a in the photograph.

Tribological Films and Coatings

A. W. Ruff, L. K. Ives, H-J. Shin[1], N. Vinod[2], and M. B. Peterson[3]

[1] Post-doctoral Fellow, University of Maryland
[2] Graduate Student, University of Maryland
[3] Guest Scientist, Wear Sciences, Maryland

Friction and wear properties of alloys at high temperatures are controlled by their tribologically generated oxide films, in the absence of other intentional lubrication or surface contamination. However detailed knowledge is lacking on what alloy compositions produce suitable films, and what properties of the oxide films are critical. Studies have been underway at NIST on several pure metals, alloys, and oxides, mainly of copper and molybdenum, in the form of either metal films or powders. These studies have provided valuable information on the process of oxide lubrication in those systems up to temperatures of 800°C, and could also provide insight into improved friction and wear behavior for oxide ceramics. Such information would assist in expanding industrial use of hard, wear resistant ceramics. This research has been done jointly with scientists at the Naval Research Laboratory.

Studies over the past year have been concerned with tribo-chemical solid state reactions of molybdenum, copper, and their oxides. It has been possible to generate low friction films in situ during sliding at temperatures in the range 300 - 800°C. Metal and metal-oxide films and powders have been studied on glass and Al_2O_3 substrates in sliding. Friction coefficients have been as low as 0.3 for copper oxide and 0.2-0.3 for copper-molybdenum oxide.

Some insight has been gained into the mechanisms involved with these thin (up to 500 nm) tribological films. Techniques of nanoindentation and instrumented scratching have been used to measure film hardness and plasticity. Based on numerous sliding tests over a range of temperatures, two general situations seem to occur: in one the film remains continuous during sliding, in the other the film becomes broken into discrete regions or patches. Continuous films with adequate flow and cohesive properties can provide low friction and wear if sufficiently thick compared to surface roughness, and if sufficiently adherent to the substrate. Discrete, patchy films cannot in general provide continuing low friction and wear performance, although they may constitute the final stage of continuous film performance.

In this research, nanoindentation hardness measurements have been made using a 55 deg. trigonal diamond indenter on the copper - copper oxide, molybdenum-molybdenum oxide, and ion-beam mixed copper-molybdenum-oxide films, about 100 to 500 nm thick, formed by vapor deposition on aluminum oxide and glass substrates. Both as deposited/oxidized films and worn/in situ oxidized films were examined. The indentation hardness values actually refer to the film-substrate combination; extracting a film-only hardness value is dependent on correctly adjusting for substrate effects, particularly for very thin films (< 100 nm thick). Results for the copper-oxide films (comparing at loads of 0.02 N, equivalent to depths of 150-200 nm) indicated the presence of a soft film ($H_{.02}$ = 4-6 GPa) on either a glass substrate (where $H_{.02,\ substr.}$ = 7-8 GPa) or an alumina substrate (where $H_{0.2,\ substr.}$ = 15-30 GPa). The as-oxidized copper oxide film structure consisted of small crystallites with considerable porosity. In contrast, the

copper oxide films that were formed during sliding at 600°C showed a smooth, continuous structure and had considerably higher hardness ($H_{.02}$ = 30-45 GPa). It was clear that the film in the wear track was very different in morphology and properties than the unworn films. Studies of actual sliding contacts for the copper oxide films on alumina showed nominal, average pressures of about 0.6 GPa, much less than measured film hardnesses. This indicates that stress concentration within the contact area could be tolerated by these films, up to factors of 10-50 times.

Scratching studies were also conducted on the films and they showed that the copper oxide film adhesion was poor. Scratching at light loads (down to 10 mN) caused complete film detachment. Thus while the copper oxide films showed some cohesion and reasonable hardness (for carrying contact loads), poor substrate adhesion was a serious failing in terms of good wear performance.

By comparison to these results, molybdenum-oxide films showed significantly higher hardnesses; $H_{0.2}$ = 8-10 GPa on glass and $H_{.02}$ = 30-45 GPa on alumina. Further, the ion-beam mixed molybdenum-copper-oxide films also had similar, higher hardnesses. Both of these types of films also exhibited low friction and wear in the 300-600°C range. Preliminary scratching data suggests that adhesion to alumina substrates may also be improved over that of the copper oxide films.

Wear Models for Ceramics

M. C. Shen[1], O. B. Bogatine[2], and S. M. Hsu

[1] Post-doctoral Fellow, University of Illinois at Chicago
[2] Visiting Scholar, Institute of Non-Metallic Materials of Russian Academy of Science at Yakutsk

There are several wear models for ceramics in the literature. Each of the models was developed based on a set of assumptions and fitted with a set of experimental data. In this effort, the wear data available were used to test these models. The first model examined was the lateral crack model. This model was developed for grinding of ceramics and the basis was that materials were primarily removed by lateral cracks. The prerequisites of the lateral crack model are: 1) the applied load is higher than the threshold load for lateral crack initiation; and 2) the material is assumed to be homogeneous. The model neglects the effect of friction and temperature in the material removal process.

The second model examined assumes that the mild-to-severe wear transition is caused by tensile cracking. The effects of microstructure and coefficient of friction are incorporated in the model. Considering the heterogeneous nature of polycrystalline ceramics and the increasing propensity of fracture due to high friction, this model appears to be more realistic for modeling wear of ceramics.

These models were tested against the silicon nitride wear data. Fig. 8 shows the results of the data fit using the lateral crack and the tensile crack models. The experimental wear data are

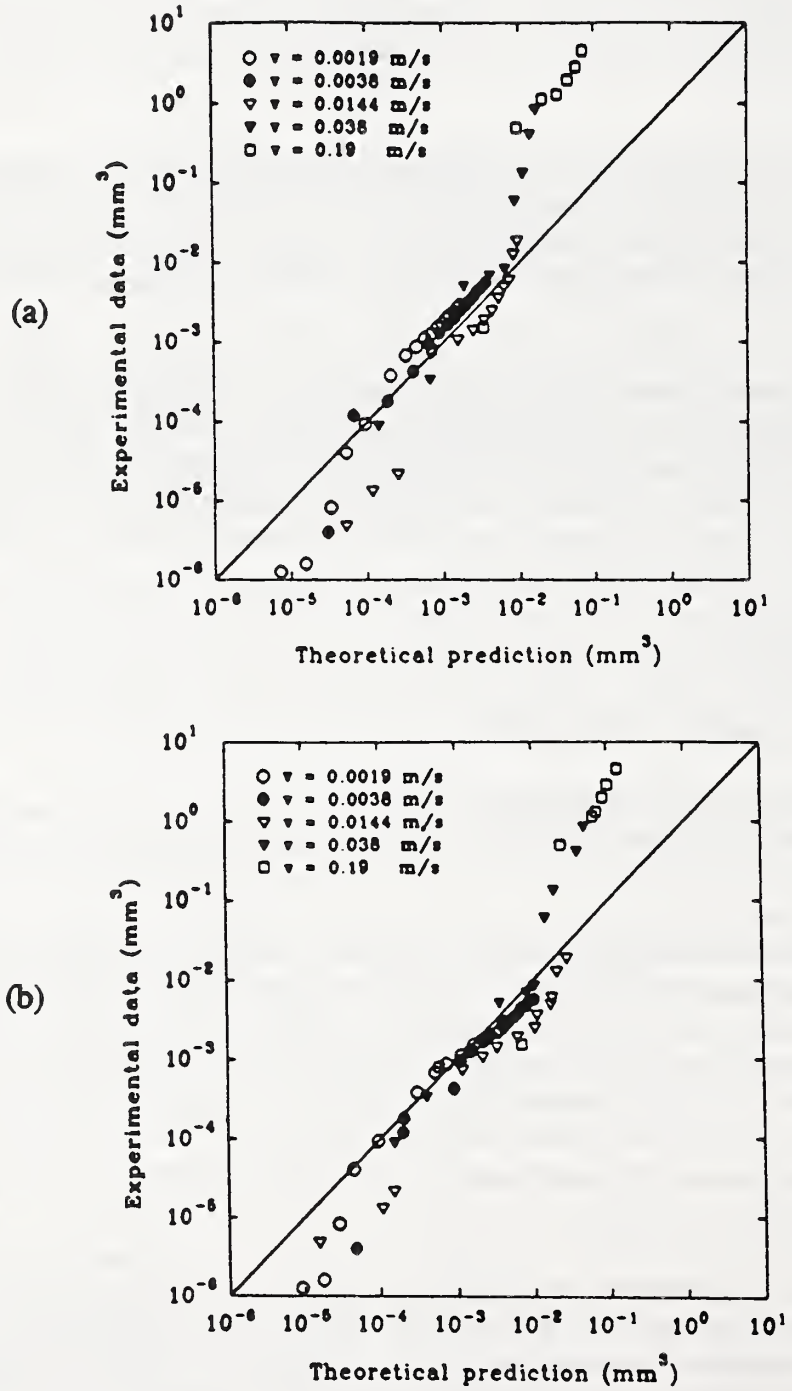

Figure 8. Results of correlation by using (a) lateral crack model and (b) tensile crack model. The experimemtal data were obtained from a Si_3N_4 under dry sliding wear tests of progressive loads and various speeds.

silicon nitride sliding on itself under dry sliding conditions of progressive loads and speeds at room temperature. To use the tensile crack model, the critical damage-induced stress σ_D for this Si_3N_4 was determined experimentally to be ~ 1.4 GPa. The two models predict reasonably well for wear volumes in the range of 10^{-4} to 10^{-2} mm^3. The experimental observations revealed that wear was dominated by brittle fracture in this regime. Brittle fracture was also the predominant wear mechanism in the high wear regime, where wear volumes were beyond 10^{-2} mm^3. Both models underestimate the wear volumes in this high wear regime. Since the wear data collected in the high wear regime were under high speeds, thermal stresses due to frictional heating may present additional stresses causing an ultra-severe wearing condition. The critical velocity model confirms that the criterion of $V > V_{cr}$ is satisfied in this high wear regime. This suggests that thermal shock induced damages are probably responsible for the ultra-severe wear in Si_3N_4. In the mild wear regime, where wear volumes are mostly lower than 10^{-4} mm^3, the two fracture mechanics models provide significant overestimates. Wear in this regime was found experimentally to be dominated by micro-cutting and plastic deformation. The difference in the predominant wear mode seems to explain why the two fracture models fail to correlate with the experimental data in this regime.

The third model examined is pertinent to the thermal shock induced fracture. Due to their relatively poor thermal diffusivity, PSZ materials are prone to suffer thermal shock induced brittle fracture. A critical velocity V_{cr} criterion has been developed to examine the susceptibility to thermal shock induced surface damage in PSZ materials. When the operating velocity V is faster than V_{cr}, i.e., $V > V_{cr}$, thermal shock induced surface damages will occur.

The transitional phenomenon from mild to severe wear in ceramics has been consistently observed experimentally. Although many studies have demonstrated the presence of such phenomena, the mechanism of wear transition is still not well understood. One plausible hypothesis is that wear damages cause changes in surface geometry when two surfaces are in sliding contact. As rubbing continues, changes in surface geometry may increase local stress intensities, which in turn cause further damages. Thus, damages are accumulated and the process repeats itself leading to a wear transition. So far the relationship between the surface geometry changes and damage accumulation process has never been determined. Hence, the purpose of this task is to examine how surface geometry changes are to influence the damage accumulation process.

A mathematical method has been developed to determine the subsurface stress field in the vicinity of a cavity of small depth located inside of a hertzian contact. The defect is assumed to be located at the center of the Hertzian contact. The Hertzian contact has a radius of a, and the defect is a circular hole with a radius of r. Besides the normal load, tangential force is included in the analysis to reflect the effect of friction. Fig. 9 shows the distribution of surface stress σ_{xx} for different defect sizes and a coefficient of friction f = 0.5. The direction of the frictional force is from left to right, and σ_{xx} is the stress component parallel to the direction of frictional force. ere conducted for a wide range of defect sizes, r/a = 0.0005 to 0.6.

Without the defects, the stress component σ_{xx} at the surface is compressive (negative) around the center of the hertzian contact, even under the condition of a friction coefficient of 0.5. The the right edge. The presence of such a sharp maximum compressive σ_{xx} is thought to be

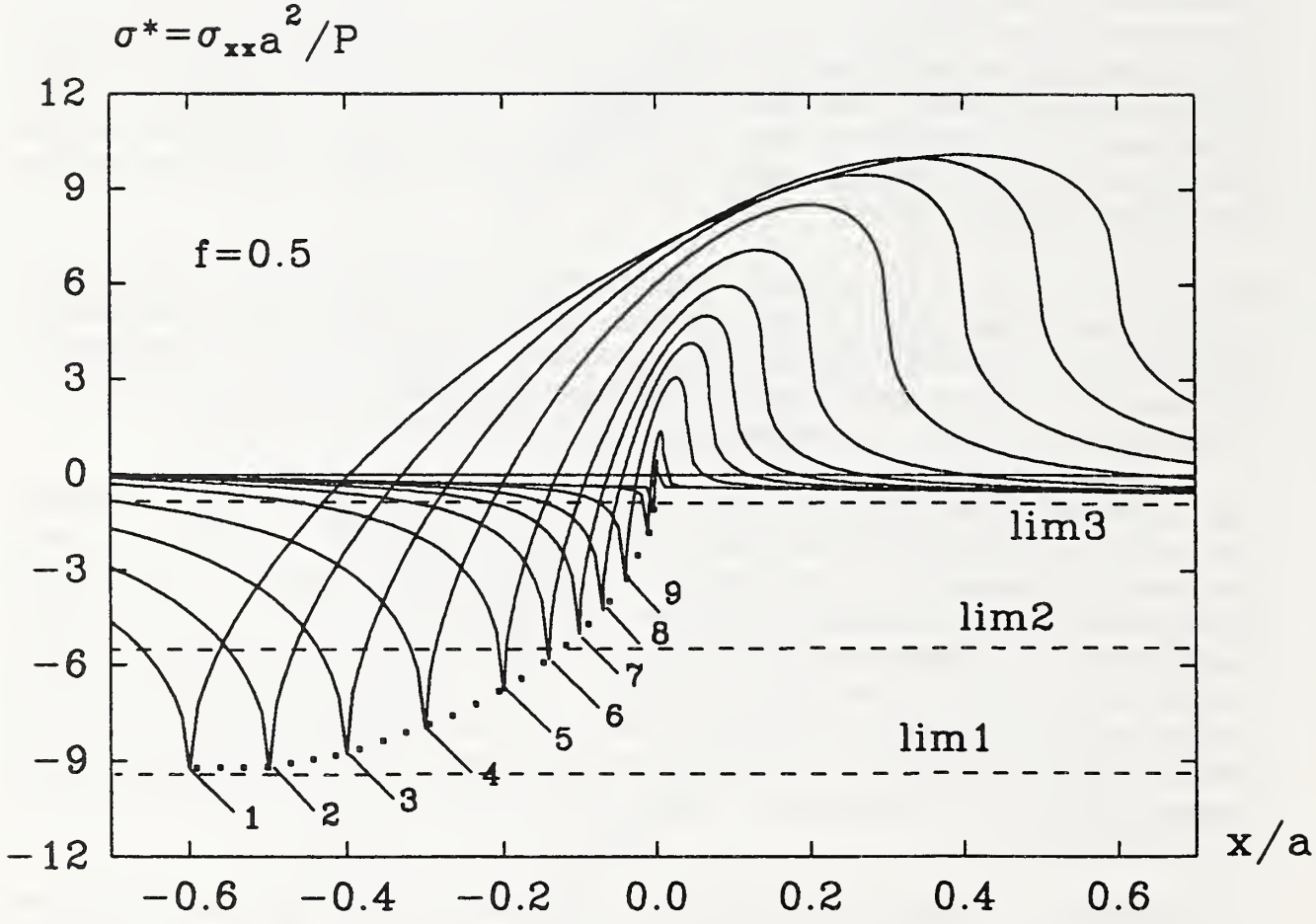

Figure 9. Distribution of the surface stress σ_{xx} in hertzian contact with surface defect of size of r/a = 0.6, 0.5, 0.4, 0.3, 0.2, 0.15, 0.1, 0.07 and 0.04, labeled from 1 through 9. (f=coefficient of friction, P=load, lim 1=limit of the influence form another edge, lim 2=limit of plasticity, lim 3=limit of defect size)

caused by overlapping the negative stress, due to the presence of the left edge of the defect, and positive stress, due to the presence of the right edge. When the defect size is small, the

maximum compressive σ_{xx} at the left edge is relatively small. As shown in Fig. 9, the local maximum compressive σ_{xx} increases with increasing defect size, and may be an order of magnitude greater than the σ_{xx} in an undamaged hertzian contact. The dotted lines in Fig. 9 represent the envelope of those local maxima. This envelope reaches an extreme value somewhere around x/a = 0.6. Consequently, limit 1 in Fig. 9 represents a limit of the influence from the right edge. Because of the substantial increase in the compressive σ_{xx} stress in the vicinity of a defect, even a safe initial contact stress distribution may exceed some dangerous limit such as a limit of plastic yielding or fracture. This kind of limit, shown in Fig. 9 as limit 2, should certainly be considered in estimates of the tendency of direct fracture in a damaged surface. Finally, the limit 3 in Fig. 9 reflects the decrease in σ_{xx} with the decrease in the defect size. Certainly, this limit approaches the value of σ_{xx} of an undamaged surface as the defect size reaches zero.

The results shown in the above clearly suggest that, after a few defects are initiated on the surface, they would act as nucleators to accelerate surface microfracture locally. Further development of such defects seem to follow two possible routes. The first is through an increase in the number of defects and the second follows increases in the size of the defects. Based on the envelope curves shown, the second possibility would eventually prevail.

Numerical Simulation of Sliding Contact Over a Half-Plane

Y.-M.Chen*, L. K. Ives and J. W. Dally[2]

[1] Graduate Student, University of Maryland
[2] Professor, University of Maryland

A number of models have been developed to describe wear processes. Typically, they are largely, if not entirely, empirical in nature. Most often these models determine a wear rate value for a particular exposure condition without identifying an actual mechanism or utilizing relationships based on fundamental materials properties. In this study a two-dimensional finite element analysis code, EPIC II, that had been developed to model the displacement of material resulting from the impact of a projectile with a ductile target was adapted to describe material displacement in a tribological contact. Other finite element analysis approaches have been employed to simulate deformation at sliding contacts, however, they have been limited to strains that are much lower than those known to occur during extended sliding under real contact conditions. The EPIC II code is able to simulate the large deformations, large strains, and high strain rates that can occur in sliding contacts. Experiments were conducted to test the validity of the behavior simulated by the modified EPIC II code and the results were found to be in good agreement.

The experiment consisted of a cylinder with a very large length to diameter ratio loaded against and forced to slide perpendicular to its axis along the flat surface of a thick OFHC copper plate. The symmetry of this geometry permitted an accurate two dimensional simulation. At the completion of the sliding experiment an automated profilometer system was used to map the surface topography of the OFHC copper plate surface.

Utilizing parameters describing the elastic and plastic properties of the OFHC copper material and other conditions of the experiment, the simulation shown in Fig. 10 was obtained.

Future investigations are being considered in which the deformation and flow in a thin ductile film on a hard surface will be simulated in order to model a solid lubricating film.
Such films are important in many tribological applications and currently may have application with respect to reducing the head to disk spacing in hard disk drives, thereby increasing substantially the drive storage capacity.

Microstructural Design of Wear Resistant Silicon Nitride Ceramics

H. Liu[1], V. Nagarajan[2], and S. M. Hsu

[1] Post-doctoral Fellow, University of Illinois at Chicago
[2] Visiting Scientist, Indian Institute of Science, Bangalore, India

The goal of this project is to optimize wear resistance of silicon nitride by tailoring microstructure. Fracture induced wear is controlled by localized stresses at the surface and near surface. Monolithic Si_3N_4 ceramics normally have no effective ways to release stress and energy except fracture. A multilayer architecture is proposed to adsorb strain energy and thus to improve wear resistance. A surface layer with fine grains is preferred because the fine grained structure has high resistance to short cracks. The layer beneath the surface layer is desired to have coarse, equiaxed grains with weak grain boundaries. The weak layers with large grains are likely to adsorb more energy. In order to test this concept, multilayer Si_3N_4 with this structure has been prepared by a tape-casting, lamination and hot-pressing as shown in Fig. 11. Preliminary wear tests suggest that this material has the same wear resistance as that of the best commercial bearing.

Another approach is to introduce surface compressive stress by making a sandwich structure. The surface layer has fine, elongated Si_3N_4 grains, and small amount of SiC particles are added to the bulk Si_3N_4 matrix. Because SiC has higher thermal expansion coefficient than Si_3N_4, compressive stresses build up during cooling after the hot-pressing. Wear of this material is up to 40% lower than that of NBD-100 under high load. This suggests that surface compressive stresses can be effective in reducing wear.

Another approach is to engineer the grain boundary interfaces. The crack arresting/deflecting mechanisms in Si_3N_4 often depend on the ratios of toughness and strength that exists between the grain, grain boundary and the solid solution phases. Hence this approach mainly concentrates on the tailoring of the microstructures through the chemistry at the grain boundaries (such as the nature of secondary phase, thickness of the grain boundary phase, formation of solid solutions). The chemical processing routes adopted in this approach ensure a uniform distribution of the additive glassy phase and hence a uniform microstructure after densification. Our preliminary results on (1) Si_3N_4 (10G1) hot pressed with a novel glass additive (10 wt%) and (2) Si_3N_4 (SNA1) prepared by solution-mixing of the additives are very encouraging. The

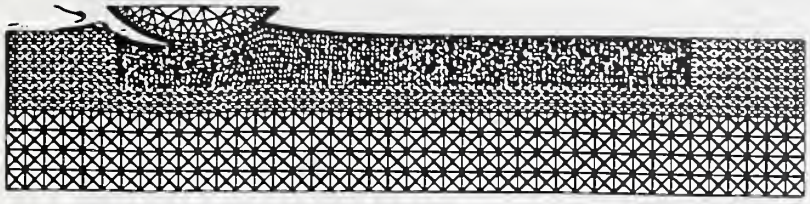

(a) t = 6.0 μs, depth = 52 μm, distance = 120 μm, average velocity = 63.8 m/s

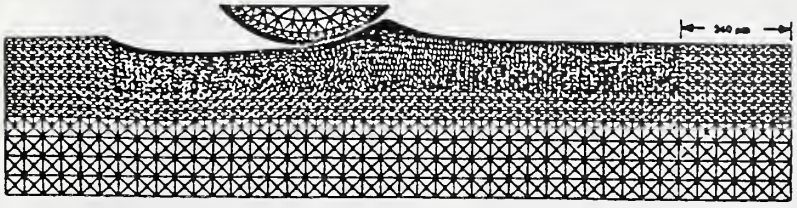

(b) t = 12.0 μs, depth = 18 μm, distance = 614 μm, average velocity = 87.2 m/s

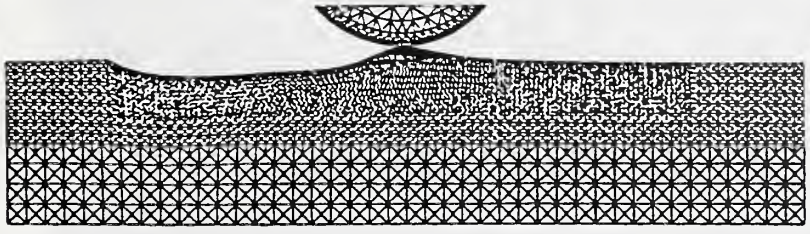

(c) t = 16.0 μs, depth = up 73 μm, distance = 1005 μm, average velocity = 137 m/s

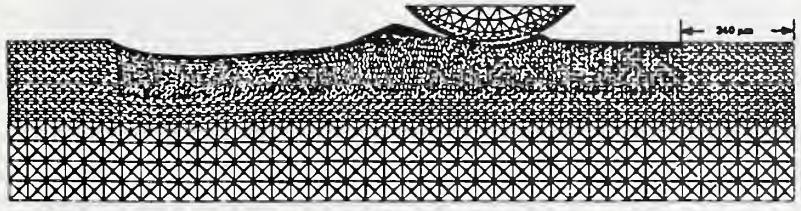

(d) t = 18.2 μs, depth = 8 μm, distance = 1405 μm, average velocity = 221 m/s

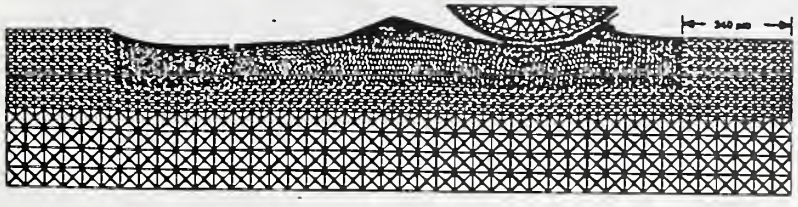

(e) t = 19.0 μs, depth = 32 μm, distance = 1584 μm, average velocity = 227 m/s

Figure 10: Deformations at several times during the sliding contact.

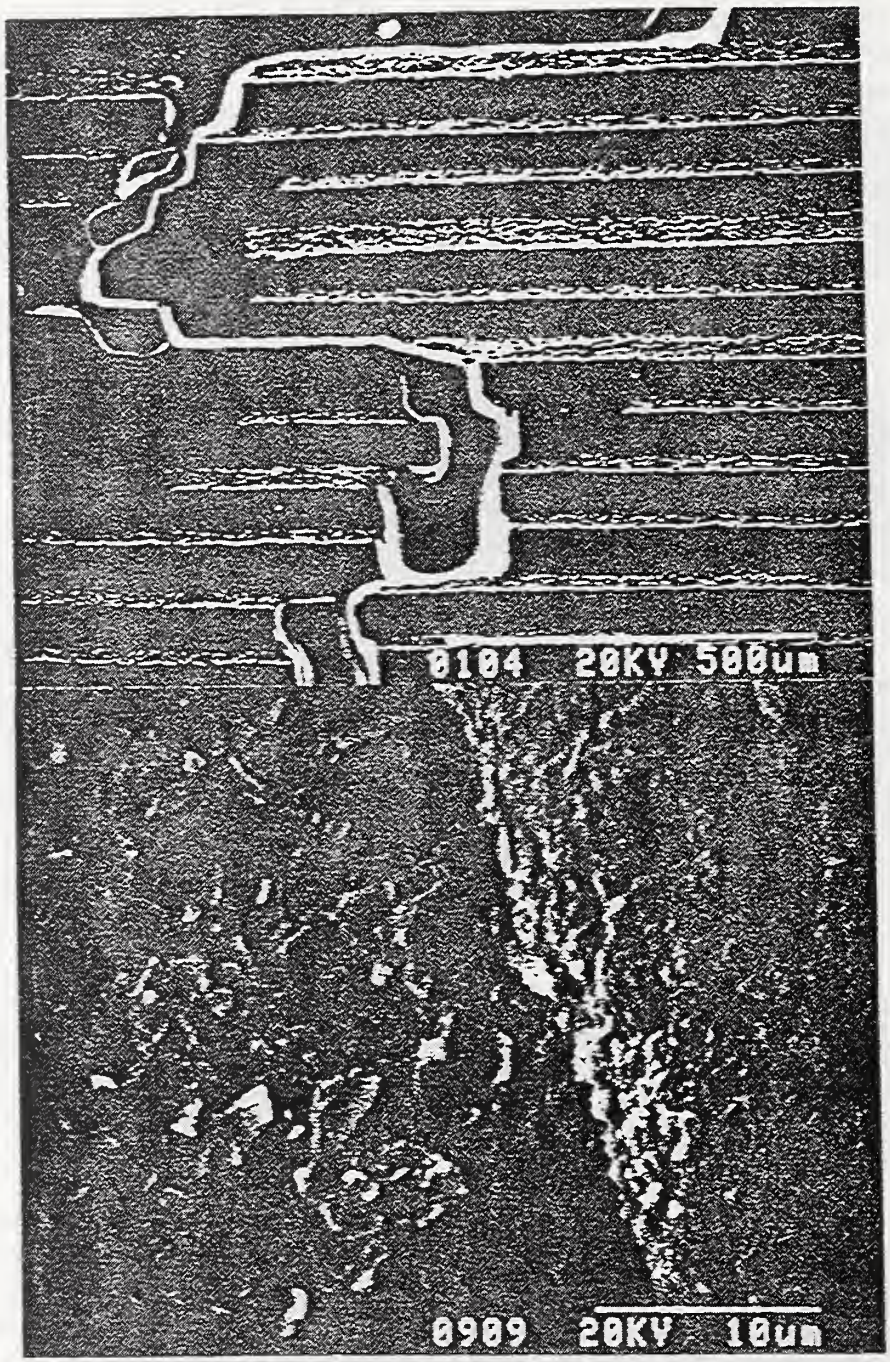

(a)

(b)

Figure 11. SEM micrographs showing (a) side view of a multilayer Si_3N_4 bending bar: crack propagation along weak layers and crack bridging (x 100); (a) top view of scratch damage on a multilayer Si_3N_4: large, equiaxed grained weak layer (left) and fine, elongated grained strong layer (right) (x 3 k).

10G1 material indicates a fine-elongated (grain size < 0.5 microns; Aspect Ratio >7) microstructure which is desirable for reducing the contact damage during wear. The wear volume estimated from the wear scar diameters in 10G1 as a function of load suggests that the designed morphology with appropriate grain boundary engineering can result in high wear resistance. The SNA1 material shows a better wear resistance than the commercial bearing material, NBD 100, at high loads. Furthermore, the crack patterns observed during a Ball-on-Inclined-plane scratch test suggest that the crack-resisting capability of 10G1 and SNA1 may be high. It is expected that further optimization of the microstructure should lead to potential high wear resistance materials.

Effect of Grain Boundary Phase on Wear of Zirconia-alumina composite

Chuan He[1] and S.M. Hsu

[1] Ph. D. candidate, Materials Science Department, University of Maryland

Composition and strength of a grain boundaries play a vital role in the properties of ceramic materials. Although the effect of grain boundary phase on the bending strength has received much attention, the effect of grain boundary phases on wear is often neglected. This project investigates the effect of grain boundary phase in zirconia-alumina composites on wear resistance. The effect of various contents of silica were examined in a ZrO_2-15 v% Al_2O_3 composite.

Three compositions of ZrO_2-Al_2O_3 with different levels of SiO_2 were fabricated: AZS0 (0 v% SiO_2), AZS1 (1 v% SiO_2), and AZS2 (10 v% SiO_2). It should be noted that even in AZS0, a certain amount of SiO_2 is inevitable from contamination. This "intrinsic" SiO_2 is estimated to be 0.1 v%. The composition and microstructural parameters of those materials are listed in Table 1. It can be seen that the major difference among these three materials are the grain boundary glassy phase content. Most of the SiO_2 exists in the grain boundary. However, some of the SiO_2 in AZS2 was found to form mullite ($3Al_2O_3.2SiO_2$). This suggests that not all SiO_2 in AZS2 is in the grain boundary glassy phase and there is certain amount of crystalline mullite in the grain boundary.

The hardness of AZS0, AZS1, and AZS2 were measured from room temperature to 1000°C in vacuum with a Nikkon High Temperature Microhardness Tester. The hardness of the different materials is quite similar below 400°C. This is to be expected because SiO_2 is brittle at low temperatures. When the temperature is above 600°C, the hardness varies among the three materials. AZS2 has the highest hardness while AZS1 has the lowest. The fact that AZS2 has higher hardness than AZS0 at temperatures above 400°C may be explained by the crystallization process of the grain boundary glassy phase in AZS2. The crystallization process occurs during the cooling in the sintering process and during the hardness test. Crystallization of grain boundary glassy phase has been a very successful technique to improve the high temperature properties of Si_3N_4 materials. It should be noted that although crystallization gives AZS2 higher hardness over AZS0, the hardness still decreases rapidly with higher temperatures.

Table 1: Composition and microstructural parameters of AZS0, AZS1, and AZS2

Material		AZS0	AZS1	AZS2
ZrO_2 content, v%		15	15	15
SiO_2 content, v%		0.1	1.1	10.1
Relative density		99%	97%	99%
t/m ZrO_2 ratio		22/78	36/64	23/77
Al_2O_3 grain size	$d_{average}$, μm	1.7	2.0	1.8
	σ_{n-1}, μm	0.8	0.9	0.8
ZrO_2 grain size	$d_{average}$, μm	1.0	1.1	1.0
	σ_{n-1}, μm	0.3	0.4	0.3

Wear transition loads of the composites as a function of SiO_2 content were determined. The transition load has a log-linear relation with SiO_2 content in the range of present study. Based on the present observation, small amounts of SiO_2 in the materials can improve the wear transition resistance. The most reasonable explanation is that the grain boundary glassy phase releases the residual stress during cooling in the sintering process. During the wear test it is possible that the flash temperature reduces the viscosity of the glassy phase which can absorb the strain energy by viscous flow.

There were small spikes in the friction coefficient traces during pretransition sliding wear test suggesting localized surface disruptions during the test resulting from the generation of third body wear particles at the interface due to grain pull-out or localized fracture. The wear of AZS1 and AZS2 are both higher than AZS0. The dominant wear mechanism in the pretransition wear region is primarily plastic deformation with occasional grain pull-out or localized fracture. The difference in pretransition wear resistance between three materials cannot be explained by the difference in hardness alone and may be effected by residual stresses in the materials. For AZS1 the addition of 1% SiO_2 probably reduces the grain boundary residual stress, which would increase the wear resistance. The reason that AZS2 has a higher pretransition wear rate than AZS0 may be that part of the SiO_2 in AZS2 reacts with Al_2O_3 to form mullite ($2SiO_2 \bullet 3Al_2O_3$). It is believed that the crystallization of a grain boundary phase will introduce additional residual stress due to the volume change accompanying the crystallization process.

Chemically Assisted Ceramic Machining

T. Ying[1], J. Gu[2], Y. Wang[1], and S. M. Hsu

[1] Graduate Student, University of Maryland
[2] Post-doctoral Fellow, University of Maryland

This project aims to increase the machining rate of ceramics using chemical reactions at the interface during diamond wheel grinding. The chemical reactions could change the hard ceramic surface into a softer material and hence reduce the contact stresses and damage. The reaction product layer produced could also change the conditions at the interface between the diamond abrasive and the ceramic surface reducing the wear of the diamond thus increasing the machining rate. Si_3N_4 is the main material of focus, but other materials such as SiAlON or SiC will also be examined.

Many halogenated compounds formulated in our laboratory have been proven effective in diamond wheel cutting in that cutting time and surface roughness are reduced compared to water or LECO VC-50. The cutting rate of the new fluids is about five times than that of commercial fluids. Although cutting rates for most of the chemicals examined were found to be about the same initially, the experimental cutting fluids exhibited less decline in rate at longer times.

Data were also generated on a surface grinder which has a constant feed rate control, with forces measured during the grinding by a force transducer. The normal and tangential forces were measured for commercial and experimental fluids. The tangential force (about 25 N) was found to be the same for commercial aqueous and experimental candidate fluids. The normal force increases to about 250 N for the experimental fluid, however. The high normal force during grinding may result in a higher residual compressive stress in the ground parts.

Study will continue in next year to focus on basic mechano-mechanical analysis and technology development in conjunction with an industrial partner.

High Temperature Liquid Lubricant for Advanced Diesel Engine

H. Li[1], Z. Hu[2] and S.M. Hsu

[1] Post-doctoral Fellow, The Pennsylvania State University
[2] Post-doctoral Fellow, University of Maryland

In this project, the important characteristics of high temperature liquid lubricants are explored by comparing the engine test data with laboratory simulating bench test results. The high temperature engine test was conducted at Cummins Engine Co. General phenomena observed in the engine test included excessive sludge formation, heavy deposit build-up in the top ring groove, but few deposits were found on the crownland. Filter plugging and turbocharger failure also have been observed frequently during the engine test. These problem could be mostly attributed to the sludge in the lubricant. Only a few of the specially formulated lubricants were able to finish the 200-Hr engine test.

A sequential thermogravimetric analysis (TGA) procedure was used to examine new and used lubricants from the engine test under both argon and oxygen environments. This method can tell the difference between conventionally formulated lubricants and high temperature liquid lubricants, it also can provide insight on the stability, deposit forming tendency, and oxidative volatility of the lubricants. The impact of engine test on a lubricant also can be detected by the TGA procedure. The TGA combined with engine data suggests that besides thermal and oxidative stability, the oxidative volatility of a lubricant plays a key role in its engine performance.

Lubrication technology for engine particulate control

R. S. Gates and S. M. Hsu

The U.S. Congress has mandated a series of increasingly stringent limits on diesel exhaust emissions effective in 1994 and 1998. The new limits reduce the allowable hydrocarbon (HC), nitrogen oxides (NO_x), and particulate matter emissions from diesel engines. Part of the particulate matter is organic and is derived from the lubricant present in the combustion chamber during operation. As the limit on the particulate level is reduced, the relative importance of the lubricant contribution to particulate increases. It is projected that the percentage lubricant contribution to total particulate will increase from the current 18-25% to about 35-50% for the 1994 engines.

Under the sponsorship of the Department of Energy, Office of Transportation Technologies, the Surface Properties Group has been conducting a research project to reduce the lubricant contribution to diesel particulate. The approach is based on developing an understanding of how lubricants contribute to diesel particulate. This is being accomplished through a combination of analytical method development, bench simulation test development, and examination of the effects of lubricant molecular structure on the formation of particulates. In conjunction with industrial partners, various novel lubricant structures are to be developed to reduce the lubricant contribution to particulates. This is the second year of a three year project.

A rapid analytical technique (simultaneous TGA/DTA) was developed to characterize the organic fractions of the particulate. The lubricant contribution to particulate shows up in this organic fraction and can therefore be quantified. This analysis takes only a few hours resulting in substantial time savings when compared to the usual soxhlet extraction procedure that takes over 24 hours. A recent comparison between supercritical fluid extraction (SFE) and soxhlet extraction of the diesel particulate has revealed that SFE offers several advantages over soxhlet extraction for the analysis of the organic portion of diesel particulate. SFE is more rapid, requiring only 1 hour versus 24 hours for soxhlet extraction. SFE uses carbon dioxide instead of methylene chloride. SFE is less prone to the light end losses attributed to soxhlet extraction. This is especially critical in analyses of diesel particulate with lighter, fuel-derived, organic components.

Bench simulation tests have been developed to study the interaction between lubricants and carbonaceous material (soot) under a variety of conditions. This is important because the adsorption and/or reaction of the polar lubricant degradation products on the soot surface

eventually show up as the organic fractions. Experiments conducted using a commercial lubricant and samples of actual engine soot have indicated that surface reaction and not mere physical adsorption is an important phenomenon in lubricant-soot interactions. The simulation techniques that have been developed give us a means of studying the effect of lubricant structures on the lubricant-soot interaction.

Lubricant solutions are being explored based on novel chemical structures that should have lower contribution to particulate. Much of the characterization, analytical development and engine test verification of being achieved through close collaboration with a variety of industrial and academic contacts.

A Computerized Tribology Information System

A. W. Ruff and S. M. Hsu

The third phase of work on A Computerized Tribology Information System, ACTIS, has been completed. It involved development of a database on advanced ceramic materials of interest for tribological applications. The data sources were NIST research activities, selected published data, and national and international round-robin measurement programs. The database contains about 350 records covering 44 different ceramic materials. It becomes part of the ACTIS data and information system developed at NIST over the past 5 years. The previous materials database in ACTIS, Tribomaterials I, had only 39 records on ceramic materials, and this was felt to be insufficient in view of the high level of interest and need by industry for evaluated ceramic materials data. The new database focuses on ceramics with high industrial importance and for which data availability has been poor. Data areas include wear data, friction data, lubricated sliding data, and mechanical and physical design data. The new database represents the most extensive tribology database on ceramics presently available. Data evaluation was carried out both by NIST and by experts at Stevens Institute of Technology. The user interface was developed by a private sector contractor specializing in PC databases, and is the same as the interface used with the lubricant database in the ACTIS system. The Ceramic Tribomaterials Database can be used separately or as part of the complete ACTIS system.

The ACTIS system now contains twelve different PC modules: the ceramic tribomaterials database, two rolling element bearing design modules, an advanced gear design module, a lubricant database, a lubricant expert system selector module, a numeric database on tribological materials, a design code for contact stress, a design code for lubrication conditions, a simple gear system code, and journal bearing design code, along with an improved central access module. The modules work together within one central PC system.

The overall effort for the ACTIS system, following a plan developed at a workshop held at NIST in 1985, has been supported by NIST, other federal agencies (Department of Energy, Air Force Wright Aeronautical Labs, Army Belvoir Research and Development Center, National Science Foundation), and two professional societies (the Society of Tribologists and Lubrication Engineers, and the American Society of Mechanical Engineers). The ACTIS system is presently being marketed by a not-for-profit corporation, ACTIS, Inc. It is intended for use in the

educational sector for training , and by industrial designers who need the latest data on both new and traditional materials for product development purposes.

Standards and Measurement Activities

A. W. Ruff

This project contributes to new ASTM standards, and involves chairmanship of the Computerization Sub-committee on Wear and Erosion in Committee G2. Two new standards have been completed this year: G-117 on wear data analysis methods, and G-118 on database formats for sliding wear data. The work has been coordinated with ASTM Committees E49 on Computerization of Material Property Data. These standards were developed jointly with representatives from numerous private sector firms, including Eastman Kodak, Carpenter Technology, Deere and Co., IBM, Westinghouse, General Motors, as well as from Oak Ridge National Laboratory, and Iowa State and Tennessee State Universities.

Another on-going task involves the VAMAS Wear Test Method group in an effort to establish a uniform methodology for organizing wear test data. The work involves representatives from 9 countries and over 35 laboratories around the world, and is the first attempt to reach an international consensus on the evaluation and dissemination of wear data.

A task nearing completion concerns preparation of an atlas of worn surfaces. The work involves experts at NIST, Battelle Columbus Labs, and BAM in Germany. The wear atlas will consist of two parts; one a collection of data and micrographs of worn surfaces on a variety of materials under different exposure conditions. The second part will be a computerized database of over 300 records drawn from publications from the International Conference on Wear of materials, over the period 1977-1991. The database will permit searching that literature source for particular tribology data and information.

All of these activities will assist industry in acquiring needed information and data for new and improved product developments, particularly pertaining to applications involving rolling and sliding contacts.

A Catalyst Package for Lubricant Oxidation Evaluation

J. Sun[1] and S. M. Hsu

[1] Post-doctoral Fellow, University of Maryland

A research project was undertaken for the Office of Standard Reference Materials (OSRM) to develop a new lubricant oxidation catalysts package for the sequence III engine test. The old catalyst package was developed for IIID engine test. When the engine test was changed to IIIE, the chemistry and engine test conditions changed significantly that the correlation could not be maintained. The catalyst package was developed under the Recycled Oil Program and was the center-piece of a strategy to monitor the quality of re-refined base oils. The catalyst package since its introduction, has sold all over the world. The new catalyst package will correlate with

the new IIIE engine test (90% correlation coefficient). The new package will be distributed through OSRM.

IV. MECHANICAL PROPERTIES — Stephen W. Freiman (Acting)

The use of ceramics in structural applications such as automotive engines, turbines for power generation, bearings etc. depends upon an ability to control and predict their mechanical reliability. The program of the Mechanical Properties Group has as its broad objectives: (1) the generation of new models and supporting data to elucidate fracture and deformation mechanisms in brittle materials at both ambient and elevated temperatures; (2) the investigation of ceramic microstructures and their relationship to mechanical behavior; (3) the development of standard test methods; and (4) the development of test methodology applicable to obtaining fracture, elastic property, and hardness data for ceramic films and coatings. The advanced ceramics industry's needs for such a program are reflected in their extensive direct participation in NIST programs and the broad agenda and industrial participation in ASTM Committee C28 on Advanced Ceramics.

The projects being conducted by the Mechanical Properties Group are currently focussed in six major areas: 1) Long-term creep and creep rupture of silicon nitride at elevated temperatures, combining creep measurements, detailed microstructural characterization, and small angle x-ray scattering in order to elucidate the mechanisms of creep damage; 2) fracture resistance of silicon nitride with emphasis on understanding mechanisms of self-toughening and microstructural development; 3) Fracture and creep in fiber reinforced ceramic composites involving modeling and measurement development; 4) Machining of ceramics conducted jointly with the Manufacturing Engineering Laboratory and the Ceramic Machining Consortium, including the development of a database for industry as well as increased understanding that could lead to more economical machining methods; 5) Standards development emphasizing development of a standard reference material applicable to ceramic hardness measurements as well as international inter-laboratory efforst to develop a standard technique for fracture toughness; and 6) A new program aimed at understanding the mechanical behavior of films and coatings whose goal is to develop test methods for the hardness, toughness, adhesion, etc. of films and coatings that can be used by U. S. industry.

Significant Accomplishments:

- Mr. George Quinn was elected Chairman of ASTM Committee C28 on Advanced Ceramics. This committee is developing ASTM standards of critical importance to U.S. industry.

- A nano-indentation system was put into operation for use in determining the properties of films and coatings.

- Working with Itek Optical Systems, NIST successfully completed a reliability assessment for large-scale glass aircraft windows using state-of-the-art fracture mechanics and statistical techniques. These are the first non-laminated glass windows approved for aircraft by the Federal Aviation Administration.

- Computer simulations of thermal-expansion-anisotropy induced microcracking in brittle ceramics have been to elucidate the influence of thermal misfit-strain, grain

size, and Poisson's ratio on microcrack density. Results provide insight into the nature of microcrack nucleation and propagation as influenced by microstructural parameters, such as grain-boundary toughness and grain size.

- In joint research with the members of the Ceramic Machining consortium, it was found that under certain conditions grinding rates for silicon nitride can be increased by a factor of 60 over those currently used.

- Two chemical compounds were found to increase the drilling rate of ceramics by more than 50% compared to either pure water or commercial cutting fluids. One of the compound, boric acid was effective in drilling of alumina, a second compound, a silicate, was effective in increasing the drilling rate of silicon, silicon nitride, and silicon carbide.

- Using a newly developed indentation technique, three types of processes were identified for material removal in machining: 1) microfracture and chipping within the grains through crack propagation along the twin/slip boundaries, 2) intergranular fracture and grain dislodgement, and 3) formation of lateral, radial, and median cracks, leading to removal of large pieces.

- A fracture mechanics formalism combined with a non-parametric statistical simulation of the empirical data was developed as a methodology to assess the reliability (i.e., lifetime) of brittle structural components which are subject to failure from time-dependent crack growth. The methodology was applied in a case study to the design of glass aircraft windows in collaboration with ITEK Optical Systems.

- Computer simulations of thermal-expansion-anisotropy induced microcracking in brittle ceramics have been used with simulated, stochastic microstructures to elucidate the influence of thermal misfit-strain, grain size, and Poisson's ratio on microcrack density. Results provide insight into the nature of microcrack nucleation and propagation as influenced by microstructural parameters, such as grain-boundary toughness and grain size.

- To explore experimentally the role of internal residual stresses on the mechanical behavior of ceramic materials with complex and heterogeneous microstructures, one needs material's microstructures with controlled thermal expansion misfit strains. Such microstructures with crystallographic textured were developed in a very anisotropic pseudobrookite material (iron titanate) by slurry processing in a strong magnetic field.

Fracture Behavior of Transformation Toughened Ceramics

L. M. Braun and R. F. Cook*

*IBM T. J. Watson Research Center

Transformation toughened materials possess good thermal shock resistance, high toughness, and moderate strengths. The high toughness values for this class of materials, i.e., zirconia, is a consequence of the tetragonal-to-monoclinic phase transformation induced in metastable grains or precipitates by the enhanced stress field of a propagating crack. The phase transformation is accompanied by volume and shear strains which act to mitigate the tensile field, leading to an increase in fracture resistance or toughness (an R-or T-curve).

The fracture behavior of transformation toughened ceramics is investigated using indentation radial cracking experiments on yttria stabilized tetragonal zirconia polycrystals (Y-TZP) with a range of grain sizes. For all materials investigated, two distinct types of cracks exist. Above a threshold indentation load, short cracks of variable length are observed, "trapped" in a compressive, contact-induced transformation zone. Above a second threshold, longer, "well-developed" cracks of more consistent length form, extend beyond the zone boundary.
A fracture mechanics model for indentation cracking in phase-transforming materials has been developed, based on the competing interaction of the tensile residual-mismatch field and the compressive contact-induced transformation field. In addition to the usual subthreshold and well-developed cracking ranges, the model predicts the trapping of cracks at indentations, within the transformation zone. Therefore, the model explicitly addresses the experimentally observed trapping behavior. Although applied to phase-transforming materials, the principles of the model are generally applicable to systems with short-range, compensating stress fields competing with longer-ranged, dominant fields, leading to two discrete crack populations.

Ceramic Matrix Composites

L. M. Braun

The retention of mechanical strength due to in-service damage is of vital importance in the industrial application of toughened continuous fiber ceramic composites (CFCCs). In order to assess the impact of the toughening achieved in CFCCs on their strengths and flaw tolerance (or damage resistance), it is important to determine the effect of crack size on strength and toughness on a scale comparable to the controlling microstructural features (e.g., fiber spacing). A technique whereby controlled size surface-cracks are introduced by Vickers indentations can be applied to evaluate the effect of crack size on the strength and toughness of CFCCs. Combined with studies of CFCCs with different fiber contents (and matrix microstructures), the application of the indentation-strength technique also allows one to examine the effects of a composites's structure on its mechanical performance. In the present study, dense unreinforced Si_3N_4 and dense Si_3N_4 reinforced with 14 and 29 vol % SCS-6 SiC fibers were evaluated.

The indentation-strength results allow for determination of fracture toughness curves K(c) (resistance curves) as a function of crack size. Fracture toughness curves, as represented by a

shaded band for each individual material, are shown in Figure 1. The fracture toughness curve for the unreinforced Si_3N_4 is indicative of a material with single-valued toughness. A K_0 = 4.8 MPa.$m^{1/2}$ was determined for this hot-pressed Si_3N_4. The toughness for the 14 volume fraction fiber composite increased from the initial K_0 value to 15 -18MPa.$m^{1/2}$; indicative of a material with a sharply rising resistance curve, consistent with the strength response.

In summary, the indentation-strength technique was successfully used to study the mechanical properties of CFCCs. Failure mechanism transitions from catastrophic flaw-sensitive to non-catastrophic flaw-tolerant behavior were observed by increasing both the initial flaw size and the fiber volume fraction. This technique is a powerful tool that can be used to also determine temperature, environmental, and oxidation effects on CFCCs. The technique can also be used to evaluate damage and failure mechanisms in new materials and can be used to compare existing materials.

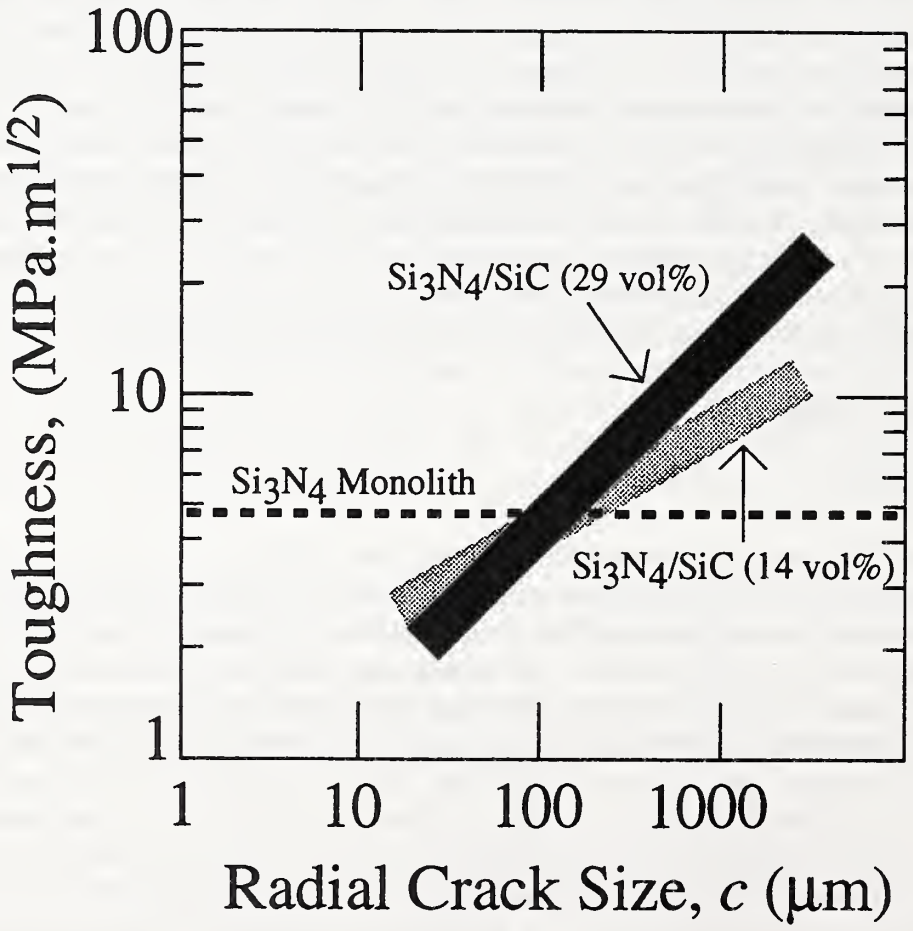

Figure 1. Fracture toughness curves, as represented by a shaded band for each individual material.

Time-dependent Reliability for Silicon Carbide at 1400°C

Tze-jer Chuang and Steve F. Duffy*

*NASA Lewis Research Center, Cleveland, Ohio

Advanced ceramic material systems have several mechanical characteristics which must be considered in the design of structural components. Focussing on laminated CFCMC the most deleterious of these characteristics are low strain tolerance and a large variation in ply failure strength specifically in the direction transverse to the fiber. Analyses of components fabricated from these types of advanced ceramics require a departure from the well-entrenched deterministic design philosophies currently utilized for metal and polymer based composites (i.e., the factor-of-safety approach). Although a diminished size effect in the fiber direction has been reported in the literature, the bulk strength of a unidirectional-reinforced ply will decrease transverse to the fiber direction as the size of the component increases. For this reason the use of a weakest-link reliability theory is advocated in the design of components fabricated from advanced ceramics.

Reliability is defined as the probability that a component performs its required function adequately for a specified period of time under predetermined (design) conditions. Methods of analysis exist that capture the variability in strength of ceramics as it relates to fast fracture. However, creep rupture typically entails the nucleation, growth, and coalescence of voids dispersed along grain boundaries. A method to determine an allowable stress for a given component lifetime and reliability is presented for component service life dominated by creep rupture. This is accomplished by combining Weibull analysis with the principles of continuum damage mechanics.

Fig. 2 depicts several time dependent reliability plots as a function of normalized time. Here normalized time. Here normalized time is defined as the ratio of real time (t) divided by the time to failure (?). In this figure four curves representing different applied stresses are shown. Note that the intercepts along the vertical axis would lie on a fast fracture curve (i.e., the time independent or inert strength curve). In addition as the applied stress is increased, the relative position of the curve shifts downward. For this particular set of material parameters the reliability curves are relatively stable beyond 0.8 normalized time. However, beyond this point reliability drops off rapidly, indicating that the material is becoming unstable.

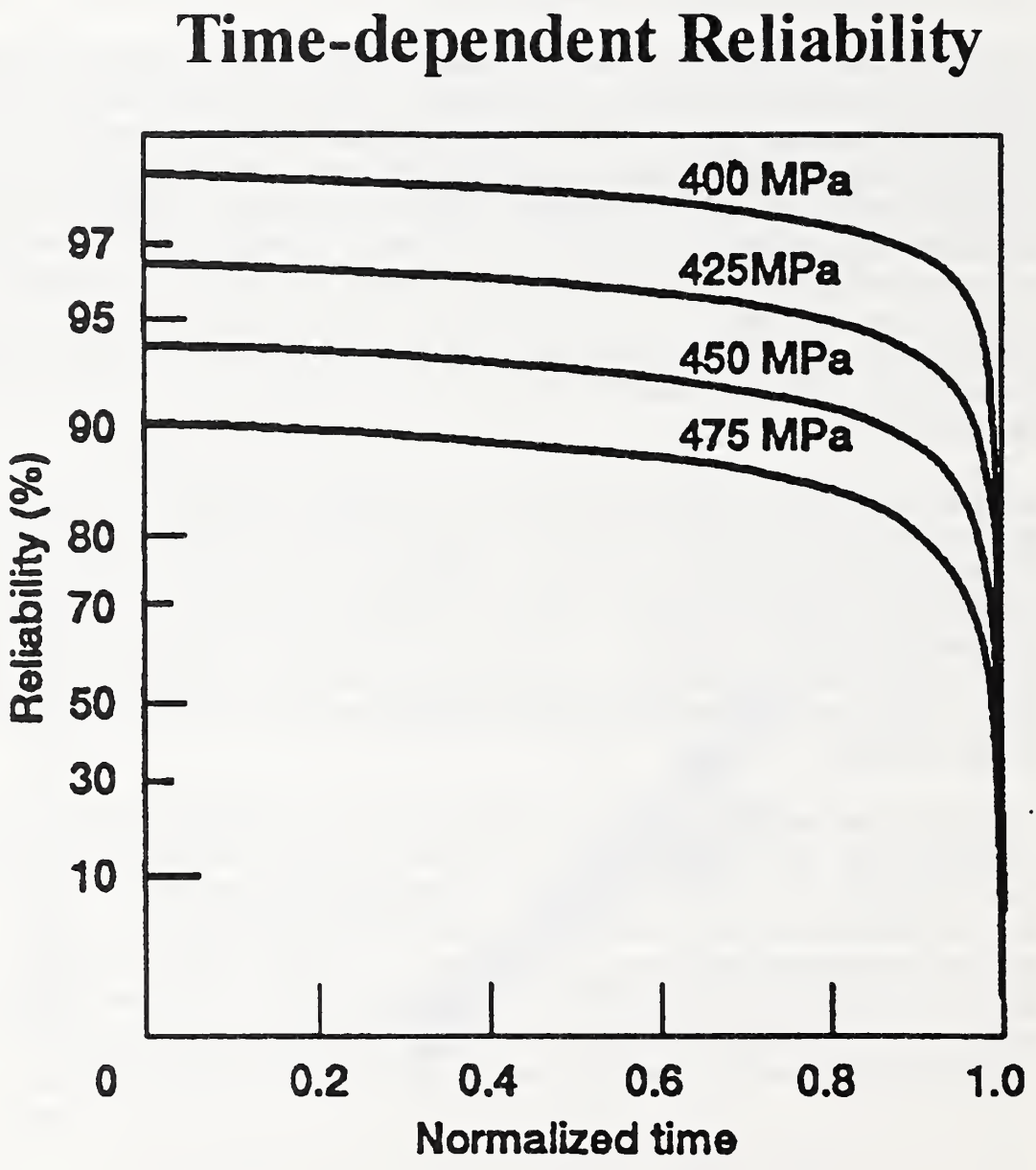

Figure 2. A family of time dependent reliability curves demonstrating the effect of increasing applied stress.

Lifetime Prediction Methodology on Continuous Fiber Reinforced Ceramic Composites

T.-J. Chuang, Ralph Krause and John Blendell

Advanced high propulsion blades made of continuous fiber reinforced ceramic matrix composites to be used in the jet engine of a high speed civil transport vehicle in the 21st century have a target of 18,000 hours in design life under ultra-high temperature and high stress. At issue is how the reliability of the structure or component in question can be assured throughout the entire service life. Development of models for lifetime prediction for these advanced materials under service conditions is required. NIST is conducting a program to develop a methodology for lifetime estimation on these materials under long-term sustained loading conditions. Evidence collected from electron microscopy has indicated that advanced materials behave differently in long-term and short-term responses. For example, the failure mode in a typical elastic (short-term) strength and/or toughness test consists of macrocrack growth with fiber bridging and pull-out; whereas that in a typical (long-term) creep test consists of nucleation, growth and linkage of interfacial microcracks. Thus, enhanced strength/toughness often leads to deteriorated durability. The service life is the sum of times spent in each developmental stage. A time-dependent theory based on mass transport kinetics has been developed which is capable of predicting lifetime if temperature and external loads are given.

A continuum damage mechanics approach is adopted in which constitutive creep laws incorporating damage are constructed based on micromechanical modeling. A model is established to take advantage of the periodic feature of the material. The model which entails two elements (one representing the fiber phase and the other the matrix phase) connected in parallel is subjected to a constant stress applied in the fiber direction. From the requirements of equilibrium and compatibility, a system of simultaneous differential equations was derived for the dependent variables: stress, strain and damage as functions of time, with the initial conditions given by the elastic state of the material. The results suggested that creep life is strongly dependent on applied stress, temperature and volume fraction of the fibers.

Tensile Creep Test Equipment Development

S.M. Wiederhorn, D.E. Roberts, W.E. Luecke and R.F. Krause

During the past five years, an inexpensive tensile creep test was developed in the Mechanical Properties Group. The equipment uses flat dog-bone specimens approximately 50 mm in length, with a gauge section of approximately 14 mm, and a cross section of $\approx$2 mm on a side. Displacements are measured with a commercial laser extensometer. The equipment is stable for test periods in excess of 1000 hr. This equipment is now being used to obtain creep and creep rupture data on ceramics in the temperature range 1000°C to 1500°C. The technique is also being used by six other laboratories nationwide. Many of these laboratories use a commercial version of the apparatus developed and sold by Applied Test Systems. The equipment developed is ideal for laboratory scale tests on experimental materials, and is used primarily to understand mechanisms of failure in structural ceramics at elevated temperatures. During the past two years, methods of measuring displacements were improved through the development of a new flag geometry and a new method of data analysis. This type of test technique is being

considered as part of an ASTM Standard as one of the methods for characterizing creep of ceramic materials.

Creep Cavity Evolution

W.E. Luecke, S.M. Wiederhorn, B.J. Hockey and G.G. Long

Substantial progress has been made in understanding mechanisms of creep in structural ceramics. Cavity formation has been shown to dominate the creep and creep rupture behavior of high temperature structural silicon nitride. Cavity formation was studied on several commercial grades of silicon nitride using transmission electron microscopy, small angle x-ray scattering and precision density measurements. The type of cavity to form depended on both the microstructure and the test temperature. The refractoriness of the vitreous phase that bonds the silicon nitride grains together determined whether isolated lenticular cavities, or crack like cavities are formed at grain boundaries. High temperatures, favored the formation of a third type of cavity, an irregular, non-planar type of cavity that formed at multigrain junctions. Small angle x-ray scattering was used to illustrate the nucleation of small ≈ 100 nm cavities at multigrain junctions, and their growth into much larger $\approx 1\mu$m cavities. The formation and growth of these cavities are believed to account for the difference in creep behavior of silicon nitride in compression and tension. Precision density measurements showed that approximately 85% of the deformation in one grade of silicon nitride (NT154) can be accounted for by cavity formation. Based on the above data, a model of creep deformation is being developed for silicon nitride.

A New Creep Theory based on Cavitation Damage

Tze-jer Chuang

Creep damage in a form of sporadic distribution of cavities at interfaces normal to principal tensile directions is a well-established phenomenon. As a result of cavitation, softening or degradation in stiffness is introduced together with permanent deformation or creep strain. A new creep theory is proposed here based on the assumptions that cavitation is a major contribution to the total creep strain and mass transport (notably surface self-diffusion and interfacial diffusion at the cavity apex) plays an important role in the damage process. The stress dependence on the creep rate is investigated and it was found that in the steady-state creep regime and at lower stresses, the cavity morphology retains equilibrium shapes and creep rate is linearly dependent on the applied stress, the same stress dependence as Coble creep or Nabarro-Herring creep (i.e. stress exponent of unity in the power-law creep equation). However, at higher stress regime, the cavity morphology becomes crack-like, and the dependence of creep rate on the applied stress can be cast in a power-law creep equation with stress exponent n equal to eight (8) or more.

Structural Reliability of Ceramics at Elevated Temperatures

S.M. Wiederhorn, G.D. Quinn and R.F. Krause

Over the past few years, the tensile creep and creep rupture behavior has been characterized in an effort to assemble a data-base to establish the structural reliability of ceramics at elevated temperatures. Our main objective is the construction of fracture mechanism maps, which provide a means of assessing the structural reliability of ceramics at elevated temperatures. They can be used to summarize large quantities of data dealing with effects of load, temperature and environment on component lifetime. They also can be used to generate a design envelopes that defines stress allowables for a given application. During the past year, data was collected on a commercial grade of silicon nitride containing 6 weight percent yttria. Materials of this type will be used as components in high temperature turbines for power generation. The data was used to generate a fracture mechanism map that could be used for structural design, Figure 3. As with other grades of silicon nitride, the map suggests three distinct regions of lifetime control: overload fracture at high stresses and low temperatures; subcritical crack growth at lower stresses and low temperature; and creep rupture at the lowest stresses and highest temperatures. The creep rupture regime involves cavity generation and their effect on crack nucleation and crack growth. Based on this data, a fracture mechanism map was generated and published as part of a recent ASTM proceeding.

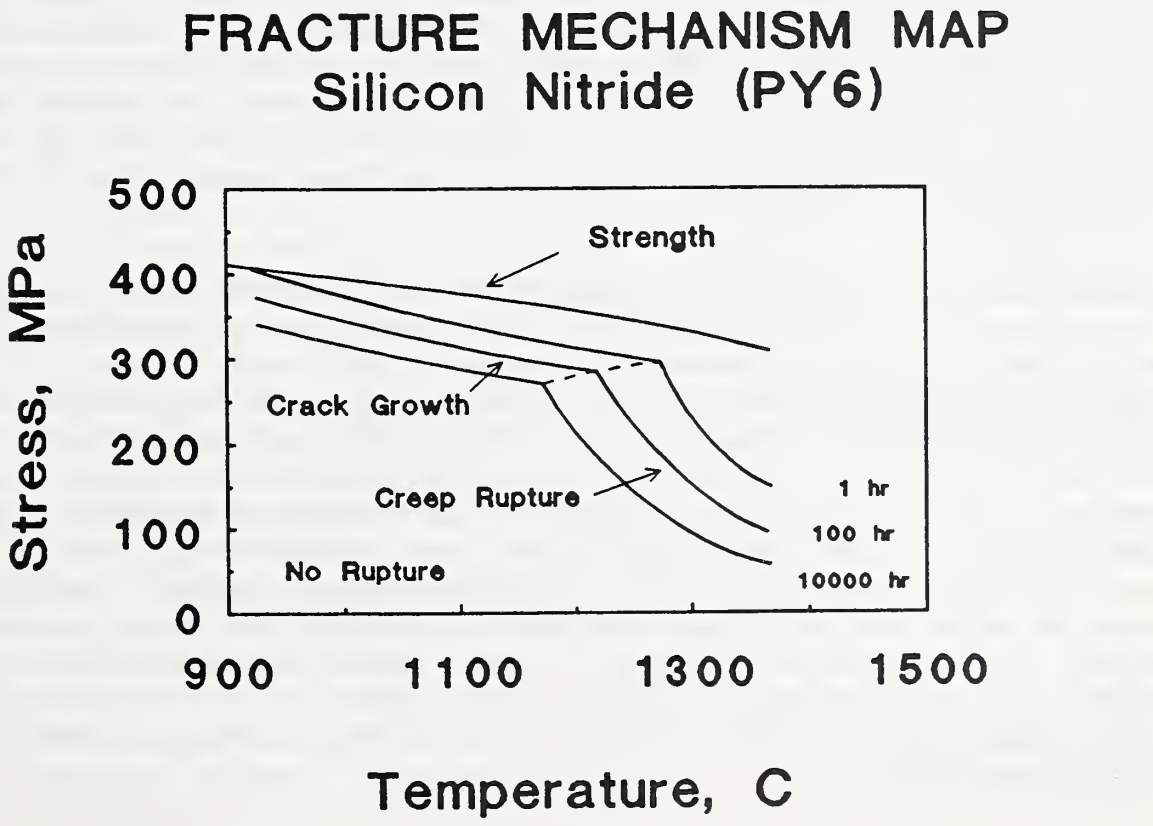

Figure 3. Fracture mechanism map for PY6 in air in tension.

Surface Forces Between Ceramic Materials

D.T. Smith, A. Grabbe and J.-P. Chapel

The surface force apparatus has been used successfully for more than a decade to make fundamental measurements of forces between molecularly smooth mica surfaces in a variety of liquid and vapor environments. Recently at NIST, a method was devised to extend these measurements to silica surfaces. This development greatly extends the range of possible studies that can be made with the apparatus, and in particular it has opened the way to investigating forces between dissimilar materials. Such forces play a vital role in areas such as intergranular fracture, the mechanical properties of composite materials, colloidal processing of mixed powders and composites, and the adhesion of coatings.

In 1993, work on the surface force apparatus was focused primarily on forces between silica surfaces, which are used either as-prepared (using an oxy-hydrogen flame) or after being subjected to a surface treatment that chemically modifies the surface. Forces are measured both in "symmetric" systems, where the two silica surfaces are identical, and in "dissimilar" systems, where opposing silica surfaces have received different treatments.

Work in symmetric systems has been directed at the hydration forces between as-prepared silica surfaces separated by aqueous salt solutions. These forces play a key role in understanding the stability of silica-based colloidal suspensions. It was found that these surfaces almost always display a hydration repulsion, but that the strength and range of the interaction depended both on the cation concentration and its radius (cations investigated included Li^+, Na^+, K^+ and Cs^+). It was also discovered that under very specific circumstances the hydration repulsion was absent. When the force was measured immediately after initial contact with a relatively strong (0.1 M) NaCl solution, several minutes were required for the repulsion to develop, raising interesting questions about the dynamics of the formation of the hydration layer that as yet remain unanswered.

In dissimilar material systems, work has focused primarily on the adhesion between silica and mica and between silica surfaces with different surface treatments. Of particular interest is the phenomenon of charge transfer between the two materials, which results in a strong interfacial adhesion and a strong electric field in the gap as the materials are separated. This field is high enough (approaching 10^9 V/m) that discharges occur across the gap during separation.

Additional work in dissimilar material adhesion has been performed in collaboration with the Eastman Kodak Co. Adhesion and charge transfer between untreated silica surfaces and mica sheets that have received two different surface treatments has been studied. One treatment covers the surface with methyl groups that passivate the surface and reduce adhesion and charging. The other treatment is a coating of a gelatin used in photographic emulsion. This surface shows stronger adhesion and charging than the methyl surface, but not as strong as that seen with bare mica. The goal of the work is to better understand tribocharging effects in film manufacture and handling.

In 1993, several significant improvements to the surface force apparatus were completed. First, it is now possible to slide one surface over the other to study tribocharging, friction and shear behavior on the molecular scale. Second, interferometry is no longer necessary to measure the force between the surfaces, removing the restriction that the surfaces studied be thin and transparent.

Nanoindentation Studies

D.T. Smith

In 1993, a new instrumented indentation facility was established in the Ceramics Division. The facility consists of a Nano Indenter II indentation machine, manufactured by Nano Instruments, Inc., and related computer and optical components, as discussed in the Facilities section of this report. The machine is capable of measuring the hardness and Young's modulus of materials by continuously recording load and displacement information during an indentation cycle. Reliable data can be obtained from surface impressions as shallow as 20 nm, allowing results to be obtained for sample volumes as small as 10^{-17} m^3.

To date, most of the work performed in the new facility has been related to setup, calibration and modification of the equipment to meet the specific research needs of the Division, but several experimental studies have been begun. Of particular interest are studies of ceramic films, coatings and multilayers on a variety of substrates, to understand both the mechanical properties of the films themselves and strength of the film–substrate interface. For example, the hardness of $BaTiO_3$ films prepared for the Electronic Materials group was measured as a function of indentation depth. Films with thicknesses in the 200–300 nm range, and with either (100) or (111) crystallographic orientation relative to the substrate, were deposited on (001) Si with a 25 nm intermediate bond coat of (111) Pt. It was observed that the (100)-oriented $BaTiO_3$ films were twice as hard as (111) films. Other systems currently of interest include Al_2O_3/YSZ ceramic multilayers from Pratt and Whitney, and Al/Cu and Al/Al_2O_3 multilayers prepared by a group at the University of Virginia. A collaboration is also under way with DuPont to study the mechanical properties of individual particles in the 10–50 μm size range, to better understand attrition problems in powder conveyance.

In addition to studying specific systems of technological interest, the facility will also be used to advance standardization within the field of instrumented indentation. There is a need for both standard reference materials and standard data analysis techniques to aid in the comparison of results from different machines and different laboratories.

Microstructural Development *in Situ* Reinforced Silicon Nitride

Jay S. Wallace and James F. Kelly

The extraordinary mechanical properties of *in situ* reinforced silicon nitride materials are related to development of rod-shaped ß-silicon nitride grains during sintering, producing a composite-like, fibrous microstructure. Understanding microstructural development and the role of

microstructure in the mechanical properties has been complicated by the inability to accurately characterize microstructures such as these *in situ* reinforced Si_3N_4 materials with acicular grains.

A unique approach is being taken to analysis of microstructure and the factors controlling microstructural development. First, a technique has been developed for dissolving the oxynitride grain boundary phase without attacking the Si_3N_4 grains. When this grain boundary phase is dissolved, the Si_3N_4 grains are liberated and dispersed for accurate microscopic characterization of size and shape. From these measurements the evolution of populations of grain size and shape are made.

Development of these microstructural analysis techniques allows study of the factors which either promote or inhibit production of the elongated grains which are responsible for the superior mechanical properties of *in situ* reinforced Si_3N_4. Microstructural observations suggest that impingement of growing grains on other grains of similar and larger size restricts further growth. This is supported by measurements of samples for which the volume fraction of Si_3N_4 in the oxynitride phase is varied. Over a wide range of low Si_3N_4 volume fractions, where the growth is not restricted by impingement, the mean size is independent of volume fraction. When the separation between growing Si_3N_4 grains is decreased by increasing the volume fraction of Si_3N_4, their growth is restricted by impingement and the mean size decreases. Microstructural evaluation has shown that impingement limits growth only when the grain inhibiting further growth is nearly the same size or larger than the growing grain; smaller grains are not able to restrict growth of larger grains. This results in the production of multiple grain size populations in a single sample where the largest grains are free to grow while growth of the finer grains is limited by impingement on nearest neighbors. This behavior is contrasted to those samples with low Si_3N_4 volume fractions; where impingement does not occur there is only one grain size population.

These characterization techniques are now being used to determine the effect of microstructure on creep properties of Si_3N_4 materials.

Fracture Toughness Round Robin

George Quinn

An international round robin for fracture toughness testing based on the controlled surface flaw method was successfully concluded. This exercise, which was organized by NIST under the auspices of VAMAS, had twenty four participating labs. Results were surprisingly consistent (Figure 4) despite the need for participants to perform fractographic analysis. Many refinements to the test method were made. A result of this project is that the method will be advanced for standardization in ASTM Committee C-28, Advanced Ceramics.

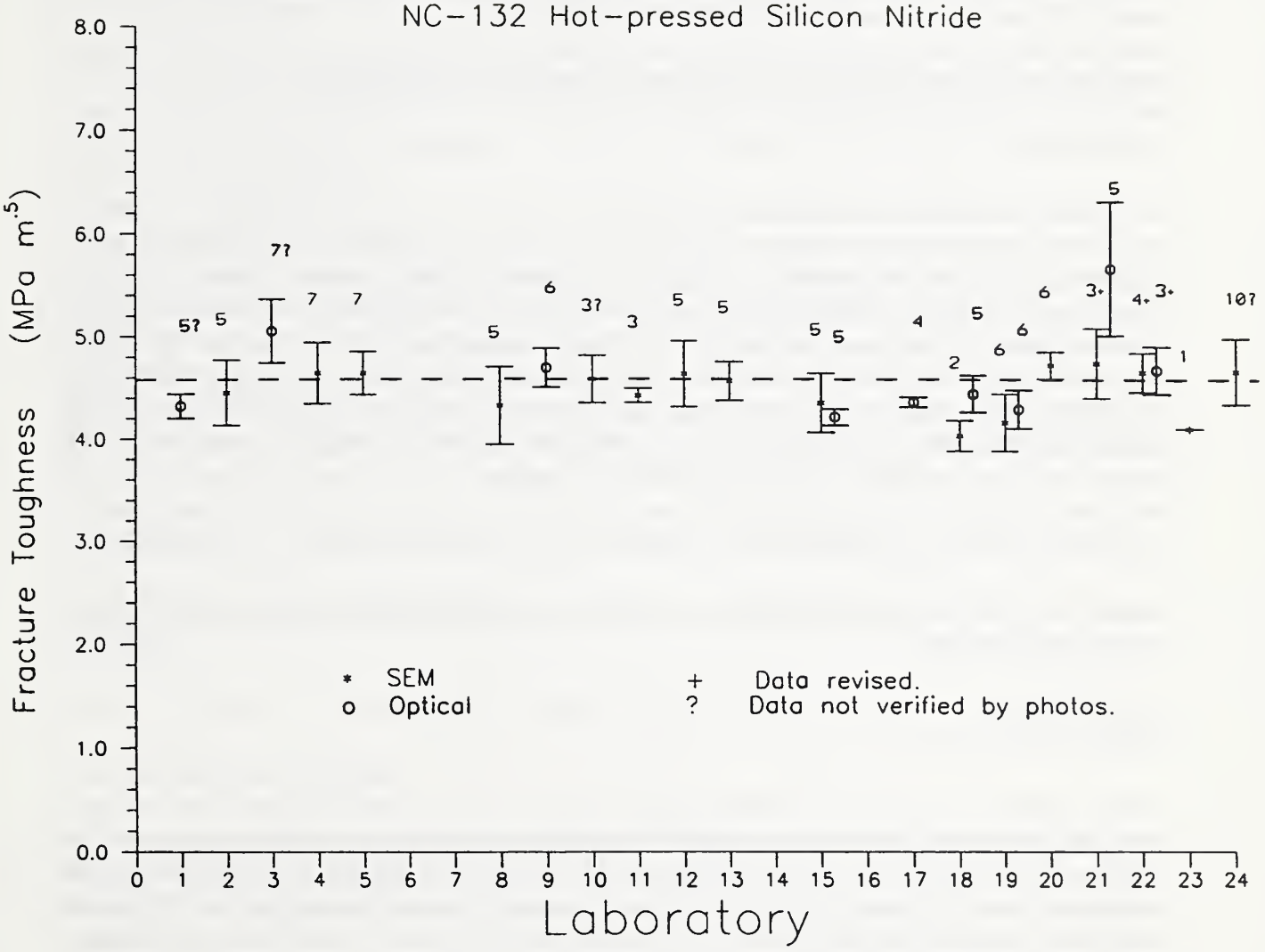

Figure 4. Fracture toughness results for hot pressed silicon nitride as measured by the surface crack in flexure method. Twenty laboratories returned results in this VAMAS round robin. Mean, standard deviation and number of specimen tested are shown for each lab.

Hardness SRM Program

George Quinn

Prototype hardness standard reference materials (SRM's) were prepared to meet a desperate need to improve testing practices for Vickers and Knoop hardness characterization of ceramics. A round robin verified the suitability of the prototypes. Subjectivity in the interpretation of optical images of hardness impressions contributes to very high scatter in hardness readings. NIST is preparing certified SRM's with diagonal measurements made by a calibrated scanning electron microscope. These SRM's will enable users to refine their optical measurement techniques which will improve measurement accuracy and precision.

Coordination of the VAMAS Technical Working Area #3, CERAMICS

George Quinn

Mr. Quinn as chairman managed the activities of TWA #3. In this year three international round robins on advanced ceramics characterization were completed. Mr. Quinn and Mr. Gettings of NIST in cooperation with Mr. J. Kübler of Swiss Federal Research Labs in Switzerland conducted, finished, and documented within one year a twenty four laboratory round robin on fracture toughness testing by the controlled surface flaw method. Mr. Quinn collaborated with Mr. J. Swab of the U.S. Army Research Laboratory to also set up, perform, and finish within one year a fractographic analysis round robin with eighteen labs in North American and Europe. The high-temperature fracture toughness round robin, organized by the Japan Fine Ceramic Center, was also completed this year.

A Fracture Mechanics Approach to the Design of Glass Aircraft Windows: A Case Study

Stephen W. Freiman, Edwin R. Fuller, Jr., George D. Quinn, Janet B. Quinn[1], and W. Craig Carter, and John Pepi[2]

[1]Guest Scientist
[2]ITEK Optical Systems

In the simultaneous presence of tensile stresses and moisture, flaws in glasses and ceramics grow, leading to time-dependent structural failures of components made of these materials. The basic concepts of this phenomenon were developed via a fracture mechanics perspective to assess the reliability (i.e., lifetime) of dual-pane glass aircraft windows. The analysis is based on two principles: (1) a statistical distribution of window strengths; and (2) moisture-assisted, time-dependent growth of defects, or "cracks", under stress.

The strength distribution originates from a distribution of defects on the window surfaces and/or edges, the most severe of which determines the strength of the window. These strength-limiting defects arise from a variety of sources. For a "protected" inner window they typically result from the window preparation procedures, such as grinding and polishing procedures for the center of the pane and similar procedures with subsequent etching for the window edges. The

outer windows additionally can incur various types of in-service "damage", such as, scratches from cleaning and handling, and dust or sand impact damage from environmental or in-flight conditions. Strength distributions for these types of surface conditions were evaluated by rapidly loading biaxial flexure specimens in an inert environment. Data were analyzed as three-parameter Weibull distributions using a maximum likelihood algorithm to determine the estimated Weibull parameters.

When subjected to in-flight stresses from pressure and thermal gradient across a window assembly, defects in the glass pane can grow subcritically due to moisture-assisted crack growth until a critical defect size is reached, and failure occurs. The growth rate depends strongly on the relative humidity. Crack growth parameters for this process were measured with a procedure known as dynamic fatigue, wherein the strength of laboratory specimens are measured as a function of stressing rate. These tests were conducted with idealized, indentation-produced cracks, rather with "natural" flaws, to control the residual stress state associated with the flaws and to reduce experimental variability. As a worst case scenario, these tests were conducted in water at room temperature.

Using a fracture mechanics formalism, the strength and crack growth data can be integrated to obtain an estimate of the window lifetime, or reliability. A question which is not typically considered in such calculations is the confidence level of the prediction. Since this is of utmost importance for a real structural component, and since a previous procedure, developed at NBS in the mid 1970's, was determined to be inappropriate by current understanding, an alternative procedure was developed. In this alternative procedure a simulated distribution of lifetimes is generated from the empirical data via a Monte Carlo technique. This so-called, non-parametric bootstrap procedure was used to estimate the lifetime at a 95% confidence level for survival probabilities of 90% and 99%. Various window configurations and damage types were considered.

Computer Simulations of Thermal Expansion Anisotropy (TEA) Induced Microcracking in Brittle Ceramics

Edwin R. Fuller, Jr., Narayanaswamy Sridhar[1], and David J. Srolovitz[1]

[1]The University of Michigan

Fracture processes in brittle, granular materials, such as fine ceramics, are profoundly influenced by grain-boundary properties and microstructure. Microcracking in single-phase ceramics, resulting from the intrinsic thermal expansion anisotropy (TEA) of the grains, is such a process. Typically, a phenomenon such as this is modelled by an extension of linear-elastic fracture mechanics, either with an idealized micro-mechanics model, i.e., a "regular array" of microstructural features, or from a "continuum perspective." Indeed, such models have contributed to many advances in understanding in recent years. However, an important aspect of the fracture process is ignored by these models, namely, the stochastic nature of the microstructure. Such considerations are crucial to the development of new and improved materials and to structural design with these materials. Knowledge about stochastic aspects is most readily attained from computer simulations: using statistically generated microstructures

and micro-mechanical descriptions of the toughening mechanisms to relate grain-boundary properties and their distributions to processing variables and structural performance. Mimicking physical phenomena with simplistic algorithms, these simulations elucidate the stochastic influence of complex microstructural phenomena, such as thermal-expansion-anisotropy, microcracking, crack deflection and crack bridging, on strength and fracture toughness.

A two-dimensional, micro-mechanics model was developed in collaboration with N. Sridhar and Prof. David Srolovitz of The University of Michigan to simulate TEA-induced microcracking and TEA-influenced crack propagation in microstructural simulations of polycrystalline ceramics. It consists of a two-dimensional, triangular network of springs upon which a polycrystalline microstructure is mapped. The energy of each spring (or bond) has both a bond-stretching and a bond-bending component. The total energy of the system is a sum over all the bonds.

The simulation is periodic in a direction parallel to the applied tensile axis and has free surfaces in the transverse directions. It thus simulates a sample with an effectively infinite gage length. The network is stressed by applying a fixed strain over the gage length and relaxing the node positions with a double-precision conjugate gradient algorithm to minimize the total energy. Bond rupture is affected via a critical bond-strain-energy criterion, and thus mimics a critical strain-energy-release-rate or fracture surface energy criterion for failure. (Bulk and grain-boundary bonds are assumed to have different critical strain energies.) When a bond fractures, the system is re-equilibrated at the existing applied strain, and additional bonds are allowed to fracture, if required, before applying a further strain increment.

Polycrystalline aspects of the ceramic microstructure are introduced into the spring network models by "overlaying" a random, "digitized" ceramic microstructure on the spring network. Accordingly, different spring elements with different constitutive properties and breaking strengths are used to represent various microstructural features, e.g., transgranular versus and intergranular properties.

TEA effects are introduced into the simulation by randomly selecting a high-expansion direction in each grain and initially contracting the network spring in this direction. This contraction was applied gradually, thereby simulating cooling from elevated temperatures. At each (misfit) strain step the system is tested for localized fracture (microcracks).

Initial studies have examined the influence of the size of the misfit strain, the grain size, and Poisson's ratio on microcrack density. Qualitatively, microcracks preferentially form at grain boundaries and propagate either along grain boundaries or into the grains, depending on the relative toughness of the grain boundaries to that of the grain interiors. The influence of TEA-induced microcracking on grain size depends on the damage measure employed. Although microcracking is first initiated in the large-grain microstructures, small-grain microstructures for most of the TEA misfit strain regime have more total microcrack length per area of cracking. Large grain-size microstructures, however, undergo a more detrimental strength degradation as a result of larger microcrack sizes compared to those in small grain samples. Unlike in unconstrained samples, when a sample is constrained during a temperature excursion, the stress created by the overall thermal expansion can directly lead to fracture of the entire sample.

Development of Textured Microstructures with Large Thermal Expansion Anisotropy

S. W. Paulik[1], K. T. Faber[2], and E. R. Fuller, Jr.

[1]Guest Scientist, Northwestern University
[2]Northwestern University

Mechanical properties of single-phase polycrystalline ceramics with large thermal expansion anisotropy have been shown, both experimentally and theoretically, to depend strongly on grain size. This dependence is directly related to the residual stresses, or strains, which are generated in the microstructure during cooling from the fabrication temperature. These stresses are created from the thermal expansion misfit strains that result between neighboring grains with different crystallographic orientations. Crystallographic texture, thereby, provides a means of controlling and tailoring these internal stresses. Our ultimate objective is to examine the role of residual stresses on various toughening mechanism proposed for advanced ceramics with complex and heterogeneous microstructures.

This phenomenon was studied in iron titanate (Fe_2TiO_5), a pseudobrookite material which exhibits a high degree of anisotropy in both its thermal expansion and paramagnetic susceptibility. Anisotropy in the paramagnetic susceptibility allows a crystallographically textured microstructure to be developed by slurry processing in a strong magnetic field. Using a simple measure of crystallographic texture, sintered samples with magnetically-assisted grain alignment have a b-axis alignment approximately three times that of randomly-oriented samples. This texturing reduces the large residual stresses generated from the large thermal expansion anisotropy between the b-axis ($16.3 \times 10^{-6}\ K^{-1}$) and the c-axis ($0.6 \times 10^{-6}\ K^{-1}$), as evidenced by reduced microcracking and morphological texturing of the aligned microstructure.

Contact Damage and Fatigue in Tough Ceramics

Brian R. Lawn, Nitin P. Padture [1], Hongda Cai [2], Fernando Guiberteau [3], Marion Stevens Kalceff [4], Lanhua Wei [5]

[1] Guest Scientist, Lehigh University
[2] Guest Scientist, Lehigh University (now at ORNL)
[3] Guest Scientist, Universidad de Extremadura, Badajoz, Spain
[4] Guest Scientist, University of Technology, Sydney, Australia
[5] Guest Scientist, Wayne State University

Ceramics are limited in their use as practical materials by a low toughness and, correspondingly, a lack of ductility to absorb mechanical energy. Of the various mechanisms that have been advocated for imparting toughness to ceramics, the most widespread and practical is that of "bridging" in which frictional pullout of interlocking grains and second-phase particles retards crack-wall separation. Toughness then becomes a rising function of crack size (so-called resistance-curve behavior). A most important element in enhancing bridging is the controlled introduction of weak interfaces on the microstructural scale, so as to deflect the primary crack and thereby generate a more effective interlocking structure. Bridging is also enhanced by

coarsening and elongating the grain structure and by incorporating internal mismatch stresses. Thus to gain toughness in ceramics one builds in microstructural heterogeneity. However, the toughness is improved only in the "long-crack" region. In the "short-crack" region, built-in weakness can enhance fracture at the microstructural level, reducing laboratory strength and increasing the susceptibility to wear.

In view of this tendency to countervailing interrelations in toughness properties, surprisingly little effort has been made to understand the seemingly deleterious short-crack properties of heterogeneous ceramics. This despite the obvious relevance of these properties to engineering design — in most ceramic components it is the evolution of microstructural-scale flaws that determines the failure characteristics. Our program has adopted a new approach, using an old testing methodology, to determine the essential short-crack properties of tough ceramics.

Our method uses the Hertzian test, in which a hard sphere is loaded onto the specimen surface. The test procedure is uncommonly simple and economical. It samples the test surface over a small area, and generates a relatively high stress. The ensuing damage is controlled and localized, and is readily amenable to examination by a variety of observational techniques. The spherical indenter can be loaded repeatedly, to simulate cyclic fatigue, or translated laterally, to simulate wear damage. We have developed a special specimen configuration, consisting of two polished rectangular half-blocks bonded together with thin adhesive, that allows us to obtain section as well as surface views of the contact damage. Indentations are placed symmetrically across the surface trace of the bonded interface on the top surface. After indentation, the adhesive is dissolved and the half-blocks separated to reveal the subsurface damage. The top and side surfaces of a given half-block are then coated with gold, and viewed in Nomarski illumination.

Several ceramic systems have now been evaluated using this procedure. Our first experiments have been conducted on alumina, the prototypical "model" ceramic. In fine microstructures, a classical Hertzian cone fracture is formed outside the contact circle, typical of ideal homogeneous brittle solids. In coarse alumina, however, the damage is totally different, consisting of a dense zone of intergranular microfractures immediately below the contact. Stress-induced intragrain twins appeared to act as crack precursors in the alumina by concentrating stresses at the weak grain boundaries. The subsurface multiple microfracture damage zone expands dramatically with increasing load, producing a quasistatic "plastic" impression. It also increases with cyclic loading, indicating a pronounced "fatigue" characteristic.

Tests have also been conducted on a machinable mica-containing glass-ceramic from the Corning Company. In this system, the microstructure is readily varied by simple heat treatments, so the influence of microstructure can be studied in a controlled manner. We find a similar "brittle–ductile" transition from classical cone crack to distributed subsurface damage as more second phase mica flakes are crystallized from the glass. The weak mica-glass interfaces provide easy paths for microcracking in the subsurface zone. It is this tendency to enhanced local microcracking that accounts for the machinability of the mica glass-ceramic. A collaborative program with Dr. K. Chyung and Dr. D. Grossman at Corning has been established to continue these studies.

Further work has been conducted on some of the harder ceramics currently used in bearing and machine tool applications, notably silicon carbide and silicon nitride. Recent advances in producing tougher silicon-based ceramics, by growth of elongated grains using in situ processing methodologies, have aroused considerable interest. We find that such microstructural modifications again result in a brittle–ductile transition. Surface and section views of the damage patterns in (A) fine grain and (B) coarse and elongate grain silicon carbide materials are shown in figure 5. The implications concerning prospective damage modes in bearing and wear applications are profound. We are collaborating with Dr. R. Yeckley at Norton/TRW on optimization of silicon nitride microstructures for various applications.

Detailed evaluations are currently being carried out on the subsurface damage. Dr. Lanhua Wei at NIST has used thermal wave imaging to map out the subsurface distributions of microfractures in silicon nitride specimens. This work is of special relevance to the potential use of nondestructive evaluation techniques for evaluating contact and machining damage in bearing materials. In addition, theoretical models, using conventional fracture mechanics and the newest computer simulations are being formulated, in collaboration with Dr. Edwin Fuller and Dr. Craig Carter.

The implications of this work are far reaching. The formation of a single cone crack is highly degrading to strength properties. A distributed subsurface damage zone is less deleterious to strength, but on the other hand enhances wear. The design of ceramics is therefore a matter of compromise: microstructures needs to be tailored according to specific applications.

Machining of Advanced Ceramics

S. Jahanmir, L. K. Ives, T. Strakna*, H. Liang*, H. S. Ahn**, L. Wei***, H. Xu*, T. Hwang*, X. Dong*, G. Zhang*

*Guest Scientist, University of Maryland
**Guest Scientist, Korea Institute of Science and Technology
***Guest Scientist, Wayne State University

The ceramic machining research is being conducted under the auspices of the NIST Ceramic Machining Consortium, which has been established to provide measurement methods, data, and mechanistic information needed by industry to develop innovative cost-effective methods for machining advanced structural ceramics. Currently, the consortium has 17 members: Ceradyne, Cincinnati Milacron, Corning, Dow Chemical, Eaton, Eonic, Ford Motor Company, GE Superabrasives, General Motors, Norton, SAC International, Stevens Institute of Technology, Texas A&M University, Tower Oil and Technology, University of Maryland, W. R. Grace & Company, and West Advanced Ceramics. Current projects include: Grinding Optimization for Advanced Ceramics, Ceramic Machinability Database, Characterization of Machining Damage, Nano-precision Grinding of Silicon Nitride Bearing Materials, Chemomechanical Effects in Drilling and Grinding of Ceramics, and Characterization of Ceramic Grinding Process. Consortium members participate in these projects by providing materials, testing, advice, and other in-kind contributions. Highlights of these projects are described below.

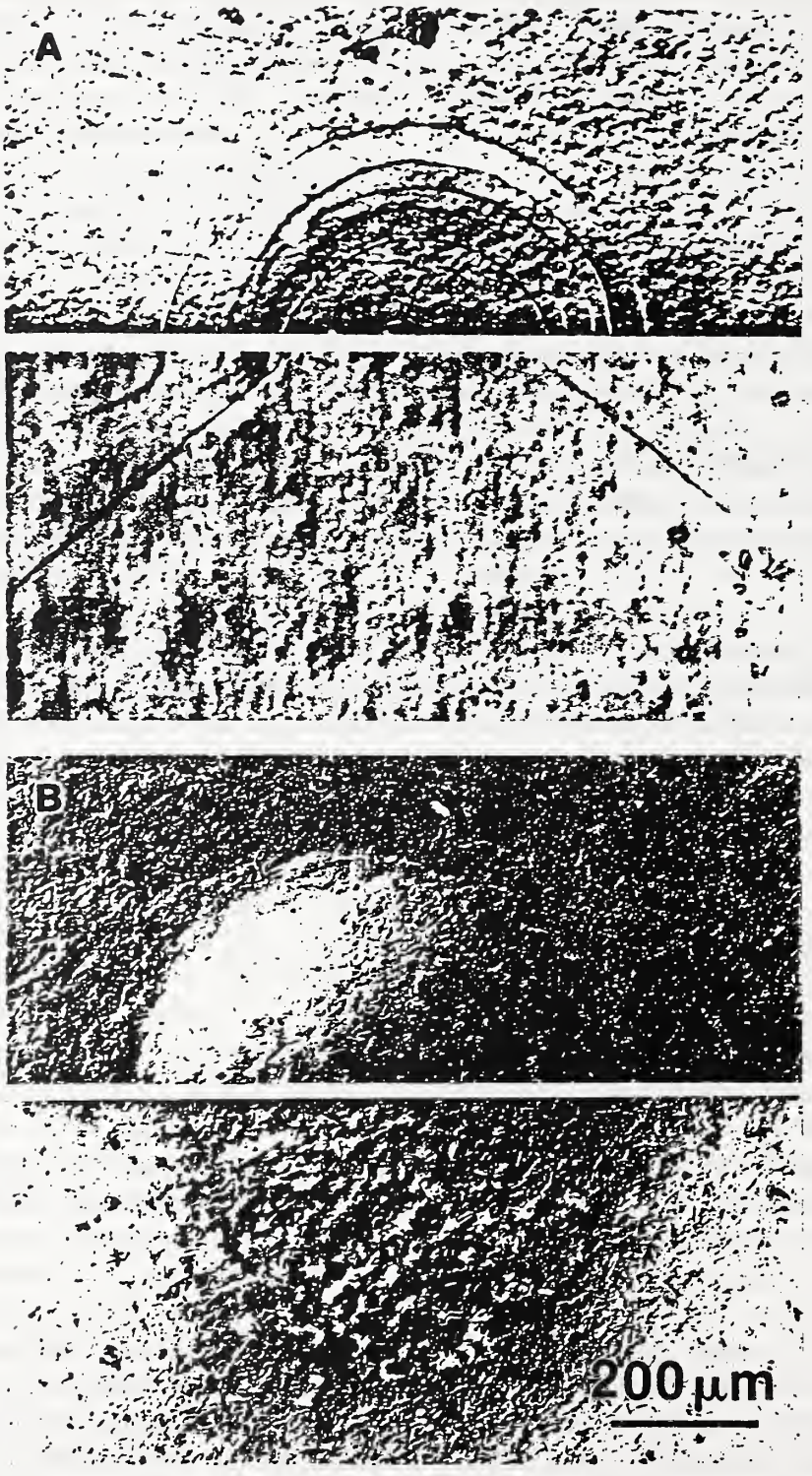

Figure 5. Half-surface (top) and section (bottom) views of Hertzian contact damage in silicon carbide, from a tungsten carbide sphere of radius r=3.18 mm at load P=2000 N: (A) Homogeneous fine-grain form showing well-defined cone crack; (B) Heterogeneous coarse-grain form showing distributed subsurface damage.

Grinding Optimization for Advanced Ceramics

The goal of this project is to produce and collect data on the effects of grinding parameters on properties and performance of ceramics. This project has been planned in two phases. In phase one, the participating consortium members were asked to use their experience in selecting grinding conditions to be used in the study. Each participant machined one set of flexure test bars (28 to 30) of each material, which were then tested and characterized at NIST for surface integrity and fracture strength. The surface roughness was determined by a 3-D stylus surface profilometer; and the surfaces were examined by scanning electron microscopy to evaluate the surface condition. The test bars were subjected to four-point bend tests according to the ASTM Standard C 1161. The fracture strength data were analyzed using Weibull statistics. Two types of silicon nitride materials, reaction-bonded (RBSN) and sintered-reaction-bonded (SRBSN), were used for this study. The results shown in Figure 6 indicate that the grinding conditions used had no effect on the fracture strength of the samples ground in the longitudinal direction; but the fracture strength was reduced when grinding was performed in the transverse direction to the tensile axis of the flexure bars. The extent of strength reduction was somewhat proportional to the material removal rate used in grinding. These results suggest that the material removal rate in grinding can be increased by a factor of 60 over the rate currently used in practice, as long as grinding is performed in a direction parallel to the major tensile stress direction experienced by the component in the intended application.

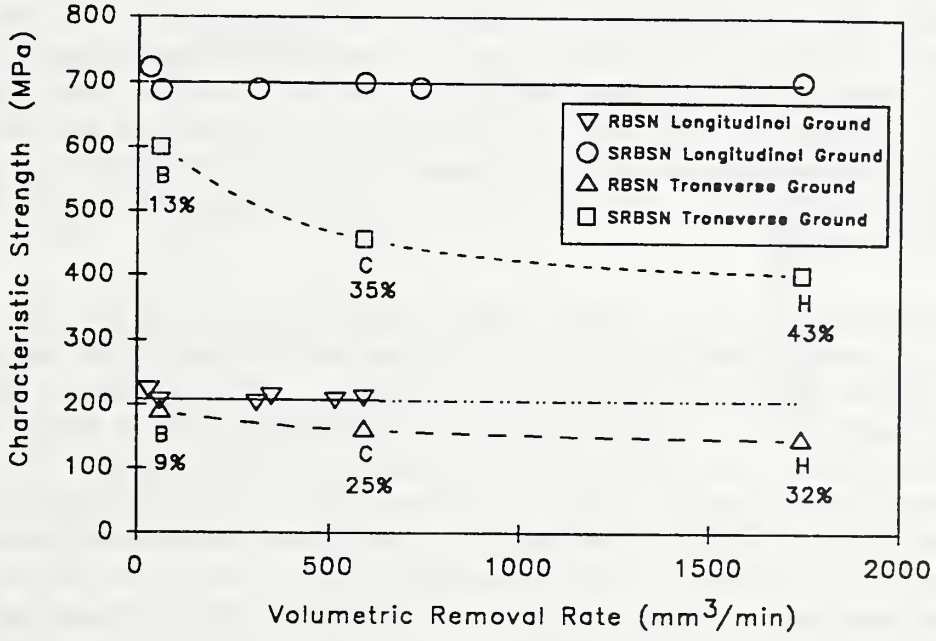

Figure 6. Characteristic fracture strength as a function of removal rate in grinding for two types of silicon nitrides ground in two directions with respect to the tensile axis of the four-point bend bars.

In phase two of this project, a statistical design of experiments is being employed to systematically analyze the effect of various grinding parameters. The aim of this study is to achieve high removal rates while maintaining an acceptable level of surface roughness and strength. It is also planned to identify the material removal mechanisms as a function of grinding parameters, and to use fractography to identify fracture initiation sites. A factorial design of experiments has been developed for this study, which will be performed on three types of silicon nitride materials: reaction-bonded (RBSN), sintered reaction bonded (SRBSN), and sintered silicon nitride (SSN).

Ceramic Machinability Database

The objective of this project is to develop a PC-based database containing evaluated machinability data for ceramics. The Ceramic Machinability Database developed jointly with the Standards Reference Data Program, will provide easy access to machinability data for different types of ceramics and will help users such as manufacturing engineers, tooling managers, and machinists develop machining plans for cost-effective production of ceramic parts. For example, the manufacturing engineer may have already selected the material to be used for the part and the necessary machining operations, but does not know what machining parameters to use. The database will provide this information for the selected material.

Characterization of Machining Damage

The objective of this project is to evaluate and compare thermal wave measurements, ultrasonic methods, and X-ray diffraction for detection and characterization of machining damage in ceramics. In general, microcracks generated in ceramics by grinding can be classified into three types: lateral cracks (parallel to the surface), median and radial cracks (perpendicular to the surface), and small intergranular and transgranular microcracks. In the following experiments, well-defined crack systems were introduced in glass by indentation in order to evaluate the capability of ultrasonic method and thermal wave measurement technique for the detection of each crack system.

The geometry of a pair of Vickers indents on glass is shown in Figure 7 (a). The median\radial cracks emanating from the corners of the indents and the lateral cracks seen as the bright areas are apparent in the optical reflection micrograph. The geometry of the upper indent is schematically shown in Figure 7 (b). The echo-amplitude contour plot of the upper indent is shown in Figure 7 (c). A 50 MHz transducer was used to transmit and receive the normal incident ultrasonic signals using a 30 μm beam width. The sample was moved in 5 μm steps in both x and y directions. The indent geometry is also shown in the contour map in Figure 7 (c) identifying the location of the indent with respect to the echo-amplitude signal. It is noted in the figure that the vertical cracks (i.e., median/radial) with their planes parallel to the incident compressional wave are not discernable. The lateral cracks, however, are detected.

The same indent was evaluated with the thermal wave measurement technique. In order to detect the median/radial cracks emanating from the corners of the indent, the transverse component of the deflected probe beam (parallel to the sample surface) was used, since this component detects the thermal waves with preferential propagation along the surface and

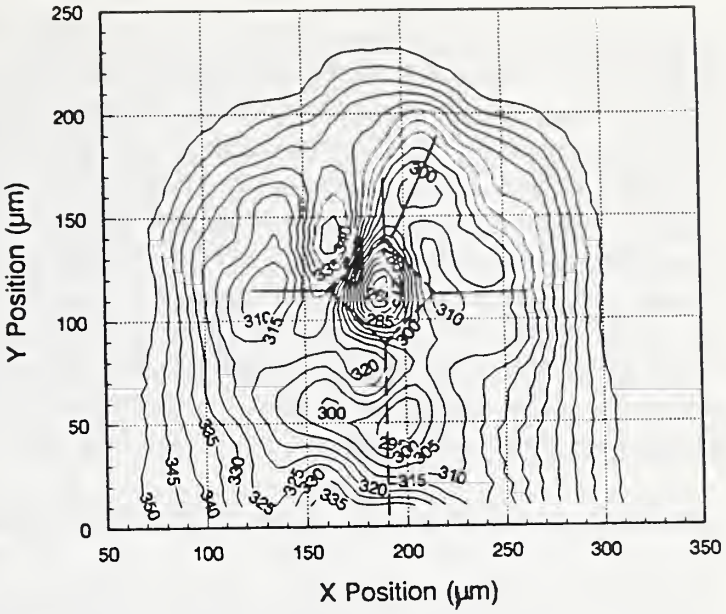

(a)

(c)

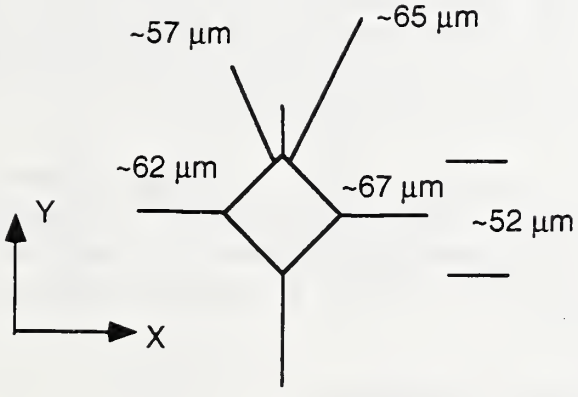

(b)

(d)

Figure 7. (a) Optical reflection micrograph of Vickers indents in a glass specimen, (b) schematic drawing of the upper indent and the vertical cracks, (c) ultrasonic echo-amplitude contour plot of the upper indent, and (d) thermal wave image of the surface using the transverse component of the deflected probe beam (the scan area is 200 x 200 μm).

perpendicular to the vertical crack plane. An image of a raster scan on the specimen is shown in Figure 7 (d), using a step size of 5μm in both x and y direction. The scan area covers a 200 x 200 μm region, giving approximately the same scale as in Figure 7 (b). The modulation frequency used was 20 Hz, corresponding to the thermal diffusion length of 100μm in the material. In the image, the darker areas indicate a lager signal corresponding to higher local temperatures on the specimen. In these high temperature regions, the heat flow is disturbed by the existence of a defect or a crack. The Y-shape of the vertical cracks can be clearly seen in Figure 7 (d). This indicates that the signal corresponds to the median/radial crack system but not to the lateral cracks. Also, the signal is unaffected by the depression of the indent. It is important to note that only the vertical cracks located along the probe beam are sensed by this technique. The cracks along the x direction are located in a plane parallel to the heat propagation direction and do not disturb the heat flow, and therefore are not detected.

Ductile-Regime Grinding of Silicon Nitride Bearing Materials

The objectives of this project are to develop guidelines and recommendations for ductile regime grinding of silicon nitride bearing materials and to identify the effects of grinding parameters and the role of microstructure in obtaining damage-free bearing surfaces. "Ductile regime" grinding is defined as an ultra-precision grinding process where the material is removed from the surface by a plastic deformation process rather than a brittle fracture process. In order to achieve the conditions necessary for ductile regime grinding, a stiff and high-precision grinding machine is used with an extremely small depth of cut in the order of nanometer. The results of this project, which is being carried out jointly with the Precision Machining Research Facility have been very positive, and show that ductile regime grinding can produce a high quality surface with a roughness in the nanometer range. In addition to the fine surface finish obtained by ductile regime grinding, the results show that the fracture strength is increased compared with the strength of flexure bars ground with conventional grinding methods.

Because of the small depth of cut used in ductile regime grinding, the ceramic microstructure is expected to control the material removal process. Recent results obtained on several silicon nitride materials with various microstructures have confirmed this point. The results are being analyzed currently to develop a correlation between mechanical properties and microstructure with the propensity for ductile regime grinding.

Chemomechanical Effects in Drilling and Grinding of Ceramics

The goal of this project is to determine the effects of grinding fluid chemistry on material removal rate in order to selected most promising additives for cutting fluids used with ceramics. Interactions between chemical compounds added to cutting fluids and the workpiece surface in the cutting zone can have pronounced effects on the material removal process during abrasive machining. The influence of chemical compounds in machining is complex and may involve non-stoichiometry reactions accelerated by the mechanical energy involved in machining.

Experiments were conducted on sapphire, polycrystalline alumina, silicon, silicon nitride, silicon carbide, and silica glass to evaluate the chemomechanical effects of several chemical compounds. The tests were performed on a precision drill with metal-bonded diamond core-drills. Following

the experiments, the drilled surfaces, and the diamond particles in the drills were examined by scanning electron microscopy to elucidate the material removal process. Two chemical compounds showed promising results in increasing the drilling rate by more than 50% compared to either pure water or commercial cutting fluids. The following test sequence was used to reduce the experimental uncertainties due to the differences in the condition of the drills, i.e., the number and distribution as well as sharpness of the diamond particles engaged in cutting. First, alumina was drilled for 15 s using distilled water, and the hole depth was measured at the completion of the test cycle. This was followed by a second cycle in which a boric acid solution was substituted for water in drilling the same hole for another 15 s. The hole depth was measured after each cycle. The sequence of drilling alternating between water and the boric acid solution was continued for a total of 180 s. Figure 8 shows the drilling rate against the drilling time for a number of cycles alternating between water and boric acid solution; the drilling rate increases on replacing the distilled water with the boric acid solution. The results indicated an average increase of drilling rate by over 100%. Similar tests on sapphire and silicon based materials provided no significant benefit for the boric acid solution. Based on the results it is postulated that boric acid interacts with the amorphous grain boundary phase in polycrystalline alumina promoting intergranular fracture; thereby, increasing the drilling rate.

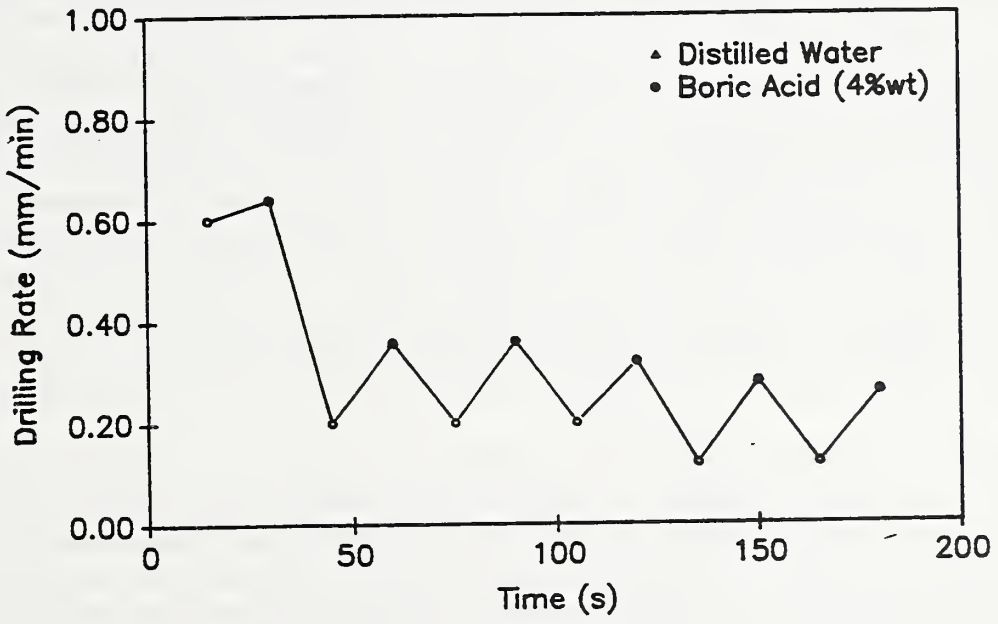

Figure 8. Drilling rate of polycrystalline alumina in alternating test cycles between distilled water and boric acid solution.

A second compound was found that increased the drilling rate of silicon-based ceramics. This compound which is based on a silicate chemistry did not work with glass nor the alumina surfaces. However, it increased the drilling rate of silicon, silicon nitride, and silicon carbide.

Currently, tests are being conducted to evaluate the mechanisms by which the silicate compound interacts with the silicon-based ceramics during drilling.

Characterization of the Ceramic Grinding Process

The objectives of this project are to determine the fundamental mechanisms involved in material removal during ceramic grinding and to explore effects of material properties, grinding fluids, and process parameters. An instrumented surface grinder was used to measure the grinding forces in grinding of several types of silicon nitride. These forces were then used to calculate the specific grinding energy, which is defined as the energy used in removing a unit volume of material from the surface. It was found that the specific grinding energy varies with the grinding parameters and depends on the material type. In a similar experiment with different commercial grinding fluids, it was found that the specific grinding energy also depends on the type of cutting fluid used during grinding. Therefore, the specific grinding energy is not an intrinsic material property, but it is an extrinsic property, since it depends also on the grinding parameters. An attempt was made to correlate the specific grinding energy to the material properties such as hardness and fracture toughness of the silicon nitride materials. It was concluded that the specific grinding energy cannot be correlated with these "bulk" properties. Recent results obtained in scratch testing have shown that the material removal rate is related to the short-crack toughness, as opposed to the long-crack toughness (i.e., a "bulk" property).

V. ELECTRONIC MATERIALS

Grady White

The Electronic Materials Group research during the past year has continued in the three categories which have driven Group efforts in the previous few years: phase equilibria studies of high T_c superconductors, development of measurement techniques, and expansion of modeling capabilities. This year has witnessed, however, an increased number and degree of our interactions with other government agencies and with private industry.

The phase equilibrium program underway has focussed on two aspects of high T_c materials: the Pb-Bi-Sr-Ca-O system and further investigations of the liquidus Ba-Y-Cu-O phase diagram. This work builds upon recent high T_c phase diagram advances made by the Ceramics Division. The significance of this work and of the reputation of NIST for phase equilibria studies is emphasized by the fact that the DoE has chosen NIST as its source for phase diagram expertise in high T_c materials.

The second thrust of the Electronic Materials Group is the continued development of measurement techniques to determine critical materials properties. The Group has experience in measuring mechanical, thermal, and dielectric properties of bulk materials. These capabilities are being extended to include measurements of effects of cyclic loading, interactions between electric field and mechanical loads, thermal properties of films, and thermoelectric power (Seebeck) coefficients. In addition, the ability to measure grain texture, i.e., the degree of grain orientation, has been achieved for both bulk and film geometries. Finally, the capability to measure residual stresses quantifiably over distances of a few micrometers is being developed. While these capabilities are valuable for a wide range of applications and materials, they have been acquired specifically to evaluate ferroelectric actuator materials, which undergo cyclic strains and large electric fields, ferroelectric films, whose properties (electronic or optical) can be enhanced by appropriate texturing of the grains, and bismuth telluride based ceramics for thermoelectric power applications, whose efficiencies depend upon both thermal and electrical conductivities as well as degree of grain alignment. Thermal measurement capabilities have been greatly enhanced with thermal diffusivity measurements being made as a function of microcrack density, machining processes, grain size, and film thickness in a variety of ceramic systems.

The Electronic Materials Group has also expanded capabilities in modeling. First principles calculations are being used to predict phase diagrams in ferroelectric systems. This type of calculations has previously been made only in simpler, non-ceramic systems. Molecular orbital (MO) calculations are being used to evaluate how environments interact with strained ceramic bonds; this effort could result in the ability to predict different ceramics will survive under load in different environments. Finally, surface energy models relating grain growth and faceting to the presence and composition of glassy phases at grain boundaries could have an important impact on the development of processing techniques to design particular textures into ceramic components.

Significant Accomplishments:

- Measurements of Raman peak shifts have demonstrated that internal stresses at specific depths in transparent materials can be detected. In addition, peak shifts in Raman-active coatings have been correlated with the stresses applied to substrate suggesting that stresses applied to materials with no Raman signature might be determined by the application of a Raman-active coating.

- The source of microcracking in cyclically loaded PZT has been traced to the presence of second phases at triple points and along grain boundaries, implying that mechanical properties of PZT might be substantially improved by elimination of second phases.

- The height of the energy barrier to the reaction of water with silica has been determined as a function of strain of the Si-O using ab initio molecular orbital calculations; in addition, a physical interpretation for the decrease of the barrier with strain has been obtained.

- For the first time, First-Principles calculations were used to predict a phase diagram forcomplex oxide system.

- For the first time, phase equilibria studies of the bismuth cuprate superconductors have demonstrated that addition of excess bismuth promotes formation of the "2223" ($T_c \approx$ 110 K) phase. For the lead-containing members, an essentially single phase "2223" region between the approximate limiting compositions $Bi_{1.7}Pb_{0.4}Sr_2Ca_2Cu_3O_z$ and $Bi_{2.3}Pb_{0.4}Sr_2Ca_2Cu_3O_z$ has been located.

PHASE DIAGRAMS

Phase Equilibria and Crystal Chemistry in Ceramic Systems

C. G. Lindsay, S. Bernik[1], and R. S. Roth[1]

[1]Guest Scientist, Institute "Jozef Stefan", The Viper Group

Experimental phase equilibria and solid state chemistry of oxide ceramic systems, a long-standing program at NBS/NIST, continued to concentrate on the $½Bi_2O_3$:SrO:CaO:CuO (BSCCO) system this system is known to contain at least three high-temperature superconducting phases. The system was expanded this year to include extensive examinations in the five component system $½Bi_2O_3$:PbO:SrO:CaO:CuO (BPSCCO). The objective has been to characterize the phase relations involving the phase with highest critical temperature (T_c): nominally $Bi_2Sr_2Ca_2Cu_3O_z$ or $(Bi,Pb)_2Sr_2Ca_2Cu_3O_z$ (2223).

The primary objective in studying the BSCCO and BPSCCO systems is to attempt to find a single-phase 2223 stability region in each system. Part of this objective is to determine whether or not it is possible to form the 2223 phase without Pb. Additionally, we want to determine the phases in equilibrium with 2223 in each system. We have made Pb-free 2223, though not as

a single phase, using excess Bi (starting composition $Bi_{2.5}Sr_{1.9}Ca_{2.1}Cu_3O_z$). Indications of the presence of 2223 by x-ray diffraction (XRD) become stronger (possibly suggesting larger amounts of 2223) with more Bi (starting composition $Bi_{2.75}Sr_{1.9}Ca_{2.1}Cu_3O_z$); but strong XRD indications of CuO are also found. Experiments are now underway in which Bi is increased and Cu decreased in the starting compositions. Excess Bi seems to contribute to the stability of single-phase 2223 in the BPSCCO system as well. When Bi + Pb = 2 in $Bi_xPb_ySr_2Ca_2Cu_3O_z$, at least 10 mol% Bi must be substituted by Pb to obtain any 2223. When Bi + Pb > 2, 2223 can be formed with less than 10 mol% substitution of Pb for Bi. We have obtained single-phase 2223 within XRD detection limits with starting compositions $Bi_xPb_{0.4}Sr_2Ca_2Cu_3O_z$ ($1.7 \leq x \leq 1.9$).

Study of the $\frac{1}{2}La_2O_3$:$\frac{1}{2}Al_2O_3$:$\frac{1}{2}Nb_2O_5$:TiO_2 system, containing microwave dielectric materials, continued this year as well. Lanthanum titanate ($La_{2/3}TiO_3$), has a defect perovskite structure and a dielectric constant nearly invariant with temperature, but is apparently unstable without small amounts of Al. Unfortunately, Al also reduces the dielectric constant. We chose to examine Nb as an alternate dopant based on the isostructuralism between $La_{2/3}TiO_3$ and $La_{1/3}NbO_3$. Our early research in the $\frac{1}{2}La_2O_3$:$\frac{1}{2}Al_2O_3$:$\frac{1}{2}Nb_2O_5$:TiO_2 system showed no $La_{2/3}TiO_3$--$La_{1/3}NbO_3$ solid solution series, but last year, nearly single-phase perovskite-like materials were made with approximate composition $La_{0.63}Ti_{0.90}Nb_{0.10}O_3$ and $La_{0.67}Ti_{0.80}Nb_{0.10}Al_{0.10}O_3$. It is also known that a single perovskite-like $La_{0.67(1+x)}Ti_{(1-x)}Al_xO_3$ phase can be formed for $x \geq 0.10$. The results obtained last year suggest that the $La_{2/3}TiO_3$--$LaAlO_3$ phase field can be extended to at least some degree toward $La_{1/3}NbO_3$. This year, efforts have been directed toward producing large samples of $La_{0.63}Ti_{0.90}Nb_{0.10}O_3$ and $La_{0.67}Ti_{0.80}Nb_{0.10}Al_{0.10}O_3$ for dielectric measurements. It has proven very difficult to obtain $La_{0.63}Ti_{0.90}Nb_{0.10}O_3$ without either monoclinic $LaNbTiO_6$ or $La_2Ti_2O_7$ as a secondary phase. Efforts are continuing both toward obtaining dielectric measurements and toward finding the stability fields for perovskite-like compounds.

Superconducting Ceramic: Crystal Chemistry and Melting Studies of the Ba-Y-Cu-O System

W. Wong-Ng, L. P. Cook and B. Paretzkin[1]

[1]Guest Scientist

In the past year, efforts to study the liquidus phase diagram of the Ba-Y-Cu-O system continued. Since compositional data of the liquid is important for constructing a quantitative phase diagram, we continued to use a procedure designed in our laboratory two years ago which involved a combination of experimental methods to circumvent experimental difficulties. This procedure includes (1) calcination and materials handling in special furnace and dry box assembly, (2) DTA/TGA studies to obtain indication of thermal events, (3) annealing of samples with porous wick materials in order to capture the liquid formed, (4) fast quenching of samples in a liquid nitrogen cooled environment for preserving the oxygen stoichiometry, (5) powder x-ray characterization of solid phases present, (6) SEM studies and x-ray mapping to study the microstructure of the quenched materials, (7) quantitative SEM/EDX analysis of the composition of melts, and (8) hydrogen reduction to obtain the oxygen content.

The main effort in the past year was concentrated on the completion of the quantitative liquidus diagram of the BaO-$\frac{1}{2}Y_2O_3$-CuO system near the high T_c phase $Ba_2YCu_3O_{6+x}$ in air as well as determination of the effect of oxygen partial pressure on the minimum melting of the system. The resulting liquidus diagram indicates that the primary phase field of $Ba_2YCu_3O_{6+x}$ is narrow, with $<$ 1 mole% $\frac{1}{2}Y_2O_3$; therefore stoichiometry must be precisely controlled to maximize yield of $Ba_2YCu_3O_{6+x}$ by single crystal growth technique. Low temperature melts have low yttrium, indicating the growth rate and the size of single crystals may be restricted. Loss of oxygen accompanies melting, indicating the melt needs adequate oxygen during crystallization, and as a result, P_{O2} can be used as a control variable during melt processing.

A pressure-temperature phase diagram for the composition $Ba_{27.8}Y_{5.5}Cu_{66.7}O_x$ was constructed. It was found that, as the oxygen partial pressure decreases, the eutectic melting temperature decreases. The eutectic melting reactions in the oxygen partial pressure region $0.0015 < P_{O2} < 1$ atm and at the more reduced region of $0.0009 < P < 0.0015$ atm, were found to be

$$Ba_2YCu_3O_{6+x} + CuO + BaCuO_{2+x} \text{ ---> } L$$

$$Ba_2YCu_3O_{6+x} + Cu_2O + BaCu_2O_2 \text{ ---> } L$$

respectively. Also, depending on the composition used and oxygen partial pressure, the topological sequence of reaction at higher temperature is different. The Y content of the melt decreases as the oxygen partial pressure decreases (ie. from $\approx$ 0.45% in 1 atm to 0.08% in 0.0015 atm O_2), but there is not a substantial difference between that in air and in oxygen. These results imply that there will probably not be a substantial increase of the Y content or the expansion of the primary phase field of $Ba_2YCu_3O_{6+x}$ at 1 atm oxygen partial pressure. Figure 1 is the pressure temperature dependence of the phase equilibria of the eutectic composition of the Ba-Y-Cu-O system.

Research in the A-R-Cu-O systems, where R=lanthanides and yttrium, and A=Ba, Sr and Ca continued. For example, the effects on compound formation of two important factors, the progressively decreasing size of the lanthanides and different oxidation state stability of these elements, continued to be studied. Collaborative efforts were conducted with the International Center of diffraction Center (ICDD) towards the preparation of powder x-ray patterns of compounds in these systems in order to provide standards for the high T_c community.

In addition to the above activities, two reviews have been completed, one on the crystal chemistry and crystallography of the Ba-Cu-O system and another one on the Sr-Nd-Cu-O system. These two systems are of interest to researchers in the high T_c area. The crystal chemistry of the Ba-Cu-O system provides an essential basis for study of the complex barium- and copper-containing high T_c phases such as $Ba_2RCu_3O_{6+x}$, $Ba_2Tl_2Ca_{n-1}CuO_x$, and $Ba_2TlCa_{n-1}Cu_nO_x$. The crystal chemistry of the compounds in the Sr-Nd-Cu-O system, which contains the high T_c superconductor phase $Sr_{1-x}Nd_xCuO_2$, was found to be very complicated. An understanding of the non-stoichiometry of oxygen which leads to different possible distributions of anionic vacancies in the pervoskite layers provides further understanding of the possible role oxygen plays in the superconductors.

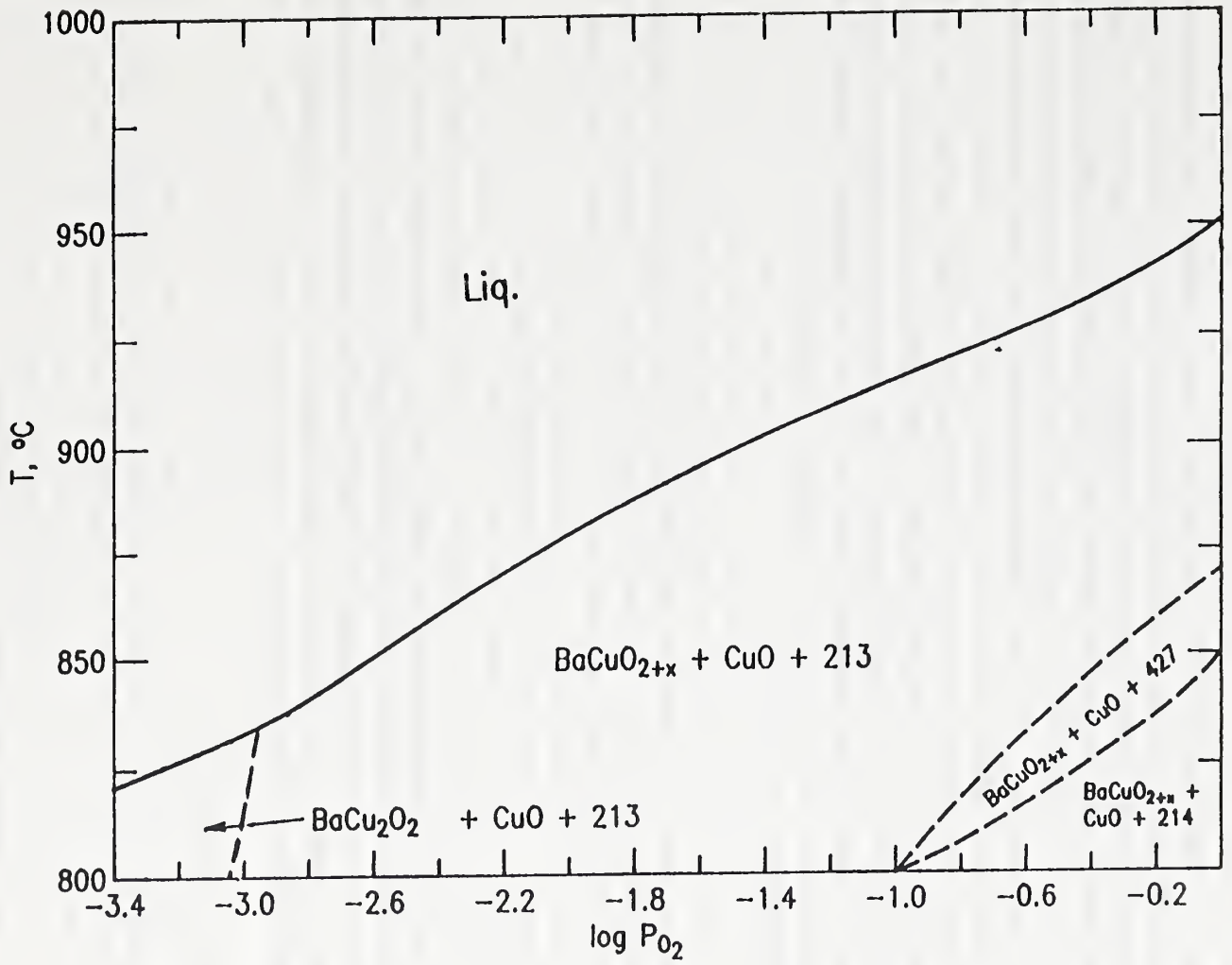

Figure 1. Pressure-temperature dependence of the phase equilibria of the eutectic composition; unit of oxygen partial pressure used in 10^{-5} Pa.

Single Crystal X-ray diffraction Studies

W. Wong-Ng and R. S. Roth[1], Y. S. Dai[1], and, M. Mathew[2]

[1]Guest Scientists, The Viper Group, Smithsonian Institute
[2]Polymer Division

Crystallographic structural characterization has been shown to be essential for understanding phase equilibria. During the research of potential microwave materials, it was found that recent devices on the international market utilize ZnO as an additive to counter balance the negative dielectric temperature coefficient of barium titanates $BaTi_4O_9$ and $Ba_2Ti_9O_{20}$. Phase equilibrium and single crystal study of the Ba-Zn-Ti-O system is therefore important to understand the effect of Zn on the crystal chemistry of barium titanate compounds. Last year, we reported the structures of three new ternary oxides with formulas $Ba_4ZnTi_{11}O_{27}$, $BaZn_2Ti_4O_{11}$ and $Ba_2ZnTi_5O_{13}$. We have continued our effort to determine the crystal structure of a related fluoride, $Ba_2Zn_{7-x}Ti_xF_{18-y}O_y$ by using single crystal X-ray diffraction method. Most crystals were found to be twinned. The twinning direction has been determined. Similar to the three oxides mentioned above, this compound consists of a 3-dimensional corner-shared interconnecting network of octahedral $(Zn,Ti)O_6$ groups. Substitution of Zn by Ti and F by O was found in some sites.

In the area of structural characterization of high T_c superconductors, collaboration has been extended to outside research laboratories with Bai-Hao Chen of IBM, Bryan Eichgorn of University of Maryland and Phillip E. Fanwick of Purdue University. Structures of two more members of a newly discovered series of compounds of $Ba_{n+1}A_nS_{3n+1}$, where A = Hf and Zr have been determined. Ruddlesden-Popper type structures play an important role in high T_c superconductor series, i.e. in the Bi and Tl containing compounds of $(Tl,Bi)_m(Ba,Sr)_2Ca_{n-1}Cu_nO_{2n+m+2}$, where m=1 or 2 for the Tl system and m=2 for the Bi system. To our knowledge, only compounds with $n \leq 3$ have been reported and well characterized. In this new series of compound of $Ba_{n+1}A_nS_{3n+1}$, n has been observed as high as 5. Our collaborative results also showed a progression of symmetry of these compounds from tetragonal to more distorted orthorhombic as n increases. The reason of the absence of superconductivity in these compounds and the possibility of inducing superconductivity by doping is currently under investigation.

MEASUREMENT TECHNIQUES

Cyclic Loading of PZT

M. D. Hill, G. S. White, C-S. Hwang[1]

[1]Guest Scientist, Seoul National University

The effect of mechanical cycling (four point bend) and electrical cycling (ac excitation at the longitudinal resonance frequency) on the degradation of the mechanical properties of PZT bars was examined.

TEM of cycled specimens revealed microcracks which originated from second phase material located at triple junctions. EDX showed that this second phase material contained Pb, Ti and Fe but no detectable Zr.

High intergranular microcrack densities were observed for mechanically cycled samples and samples electrically cycled at temperatures $\leq$ 80 °C. Electrically cycled samples allowed to heat, via internal friction to a steady state temperature of 180 °C showed much lower crack densities. d_{33} measurements revealed that depolarization occurs in the 180 °C electrically cycled samples but not in mechanically cycled material nor in the 80 °C electrically cycled material. Also, samples heated in a furnace to 180 °C in the absence of external stress showed no evidence of depolarization. It appears that at lower temperatures ($\leq$ 80 °C), electrical and mechanical cycling leads to microcracking while at elevated temperatures ($\approx$180 °C), domain reorientation competes with microcrack formation.

An S-N Curve for indented PZT specimens was generated by mechanical cycling in four point bending at different stress amplitudes. Theoretical S-N curves were derived by numerical integration techniques assuming that slow crack growth is the sole mechanism for crack extension and, ultimately, sample failure. These theoretical models took into account the effects of the residual stress field from the indentation The slope of the theoretical S-N curves were different from that of the experimental S-N curve, suggesting that a mechanism other than slow crack growth is responsible for the behavior observed for mechanically cycled PZT.

Thermal Wave Measurements in Ceramic Systems

L. Wei[1] and G. S. White

[1]Guest Scientist, Wayne State University

Through our contract with Wayne State University, both the hardware and software of the thermal wave system at NIST were upgraded to the current state-of-the-art. The hardware improvements now allow measurements to be made at $\approx$100 KHz, which improves the depth resolution of the system by almost x10. This improvement makes it possible to investigate the thermal diffusivity of ceramic films less than a micrometer thick. The software improvements allow much more precise determinations of thermal diffusivity to be obtained, due to the improved 3-D model of heat flow incorporated into the programs.

The improved thermal wave system has been used to detect damage resulting from machining of Si_3N_4 (in collaboration with Said Jahanmir, Mechanical Properties Group) and from cyclic (ball on flat) loading of alumina (in collaboration with Brian Lawn, Laboratory Scientist). In the latter case, damage attributed to microcracks was clearly seen in thermal wave images. The system has also been used to measure thermal diffusivity in the oxide layers on Si as a function of film thickness. In all cases, experiments are continuing and models describing the heat flow in terms of the specimen characteristics, i.e., microcrack density and film thickness and adherence, are being developed.

Intergranular Wetting in Al_2O_3

J-H. Choi[1], B. J. Hockey[2], C. A. Handwerker[3], S. M. Wiederhorn[4], J. E. Blendell

[1]Guest Scientist, Seoul National University
[2]Mechanical Properties Group
[3]Metallurgy Division
[4]MSEL

Many of the properties of advanced ceramics are critically dependent on the nature and distribution of thin intergranular films. The idea that a second phase will either completely wet or be completely isolated is based on the assumption that the interfacial energy between the two phases is isotropic. It is known that ceramics exhibit pronounced surface energy anisotropy as exhibited by the faceted crystal faces commonly observed. Thus it is expected that wetting of grain boundaries by a second phase will depend both on the anisotropy of the solid-liquid energy and on the anisotropy of the grain boundary energy.

Low-angle tilt boundaries (7° about $<10\bar{1}0>$) were produced by annealing a layer sample containing tape-cast Al_2O_3 between two near basal (0001) plane sapphire crystals. The Al_2O_3 tapes contained 4% anorthite glass. As the sapphire grew and consumed the polycrystalline tapes, a liquid layer was formed at the boundary. At long times a low-angle tilt boundary was formed. It was found that boundary structures containing both wetted and non-wetted regions were stable, in contrast to the isotropic model where it is assumed that the glass either completely wets the surfaces or a dry grain-boundary is formed. The orientation of the boundary relative to the sapphire crystal structure determined what type of boundary was stable. Based on these observations, we have developed a method for determining the shape of a partially wetted interface. Using the equilibrium shape of a crystal in contact with the liquid (the Wulff shape), the shape of a fully wetted interface can be determined. The shape of the fully wetted interface can be combined with the Wulff shape of the grain boundary (which can be calculated for low-angle boundaries) to give the shape of the partially-wetted interface. This shape can then be used to predict when wetting will occur and to what degree.

However, the Wulff shape for anorthite glass-filled pores in Al_2O_3 is not known with enough accuracy for a determination of the wetting conditions. We have attempted to measure the Wulff shape by examining the shape of glass inclusion formed by infiltrating cracks. Cracks were formed either by thermal shock or by indentation. The cracks were then infiltrated by anorthite glass and allowed to heal during a high temperature anneal, resulting in glass pockets at different crystallographic orientations completely inside single crystalline Al_2O_3 . Pores of various sizes formed; the shapes were measured as a function of time and size to determine when the equilibrium shape was reached.

The implications for improving the properties of advanced ceramics are clear, in that using the shape of a partially wetted grain boundary, the degree of texture needed to either prevent or to allow wetting is known. Thus, some of the properties of ceramics can be tailored by controlling the orientation of the boundaries in the samples. Also, this technique has allowed us to determine the surface tension of Al_2O_3 in a direct method, with the only assumption being the

ratio of the surface energy of the basal plane to the rhombohedral plane surface energy. Based on observations of when the boundaries are fully dewetted and knowledge of the Wulff shape of the crystals, the surface tension can be determined. For the basal plane of Al_2O_3 in contact with anorthite, the surface energy was found to be $0.9J/m^2$ (assuming that the ratio was 1.4). This is in good agreement with the estimates of the surface energy from a variety of other studies. The determination of the exact Wulff shape for this system will allow a better measurement of the surface energy of Al_2O_3 .

Thermoelectric Refrigeration using Thermogenic Materials

J. J. Ritter and C. K. Chiang

Theoretical projections indicate that an improved thermoelectric figure-of-merit, Z, for bismuth telluride-based thermogenic materials could be achieved through a decrease in thermal conductivity in these materials. This effect becomes apparent from an inspection of the expression for the figure-of-merit, $Z = S^2/\rho K$, where S is the thermopower (Seebeck coefficient), ρ, the electrical resistivity and K, the thermal conductivity. It is believed that the introduction of nanoporosity or a nanosized second phase, being of the order of the wavelength of phonons, could serve as phonon scattering sites, and thus decrease thermal conductivity. Two chemical synthetic procedures amenable to the production of bismuth telluride-based materials with nano-inclusions as a second phase have been developed.

The first of these procedures involves the coprecipitation of bismuth and tellurium oxides. The mixed-oxides are chemically reduced to give equiaxed particulates approximately 25nm in size. Thermoelectric measurements on sintered specimens compacted at 1GPa or less exhibit very low Seebeck coefficients. When compaction pressures are raised to 1.5GPa and higher, sintered specimens exhibit substantially increased Seebeck coefficients as well as a reduction in thermal conductivity by factors of 3 to 5. The latter effect may arise from phonon scattering by nanoporosity generated as a second phase during sintering. Unfortunately, these samples concomitantly exhibit low electrical conductivities. As a result, an improved figure-of-merit has not yet been realized.

An alternative chemistry for bismuth telluride synthesis involves the complexation of bismuth and tellurium ions with a polyfunctional organic acid. The resultant metal-organo complexes are thermally processed to a mixed-oxide precursor. Hydrogen reduction of the precursor gives plate-like particles of bismuth telluride. Thus, an important option for processing this polycrystalline material arises from the particle morphology. It may be possible to texture bismuth telluride platelets to take maximum advantage of the anisotropic nature of their thermoelectric properties with respect to the crystallite axes.

Both approaches allow the introduction of second phases as nanosized inclusions in bismuth telluride. Second phases successfully introduced to date include Fe, Ni, SiO_2, and C. The metal-organo route readily permits the synthesis of bismuth telluride alloy systems such as Bi-Sb-Se-Te. Evaluations of the thermoelectric properties of these more complex materials are pending.

Ferroelectric Thin Films by Pulsed Laser Deposition

L. P. Cook, B. W. Lee[1], C. K. Chiang, W. Wong-Ng, P. K. Schenck[2], C-S. Hwang[1], P. S. Brody[3] and K. W. Bennett[3]

[1]Guest Scientist, Hanyang University, Seoul National University
[2]Metallurgy Division
[3]Army Research Laboratory, Adelphi, Maryland

During the year, work on pulsed laser-deposited thin films was completed in three principal areas: 1) crystallization of amorphous $BaTiO_3$; 2) preparation and characterization of $PbTiO_3$ - $Pb(Mg_{0.5}W_{0.5})O_3$; and 3) preparation and characterization of Nb-doped PZT.

Barium titanate films are of interest because of their high dielectric constant, giving it potential application as thin film capacitors at a great saving in space for a given charge storage capacity. Studies of the crystallization of amorphous laser deposited $BaTiO_3$ concentrated on microstructural investigation of the crystallization process and the relation of the microstructure to the crystallization kinetics. TEM examination of the amorphous as-deposited material indicated that the films had columnar structure and confirmed their lack of crystallinity. In spite of the columnar nature of the initially amorphous deposits, post-depositional isothermal crystallization resulted in essentially random orientation of crystallites $\sim$5 nm in diameter. Crystallization was essentially complete at 650 °C, with no detectable second phases. The $BaTiO_3$ crystallization kinetics are consistent with a simple model involving rapid, dense nucleation, followed by unimpeded growth, with a change in growth kinetics occurring at the point where the growing crystals unpinge upon one another. A major challenge in processing the amorphous $BaTiO_3$ is the elimination of voids associated with shrinkage produced during the crystallization process. The shrinkage voids tend to reflect the columnar structure by forming channels parallel to the columns. Unfortunately these voids have prevented measurement of the dielectric constant. Another issue important in the crystallization of $BaTiO_3$ is related to the apparent cubic nature of this material. To investigate this, an estimate of residual stress was obtained by x-ray line profile analysis. The stresses estimated on this basis may be sufficient to cause substantial change in the temperature of the ferroelectric phase transition, possibly explaining why no tetragonality was observed in these materials.

(Mg,W)- doped $PbTiO_3$ is of interest because of possible applications in imaging and image storage. The advantage of this material over pure $PbTiO_3$ is that it is less tetragonal, and hence the material can be cooled through the ferroelectric phase transition without microcracking. During the year, efforts were concentrated on preparing single phase perovskite and minimizing the troublesome occurrence of the pyrochlore phase. A processing diagram indicating the regions of optimum film growth in terms of background oxygen pressure and substrate temperature was developed. The crystallographic orientation of these films, if crystallized during deposition (rather than by post annealing amorphous films) is strongly controlled by preferred orientations in the underlying Pt substrates. It has not proved possible to control the orientation of the deposited film independently of texturing in the substrate. The crystallographic orientation of the film has a marked effect on the ferroelectric properties. To optimize the remanent polarization on (100)-oriented Pt substrates, a random orientation of the film was

successfully produced by a novel two-stage deposition process in which a thin layer of amorphous material was deposited on Pt, then crystallized, with the remaining material deposited at a higher temperature. These films had the highest remanent polarizations.

Degradation of ferroelectric properties with time (fatigue) has been a longstanding issue in the development of ferroelectric thin film memory devices. However it was noted that PZT films with Nb seemed to undergo much less fatigue. To investigate this possibility further, PZT targets containing 0.5, 1.0 and 1.5 wt% Nb were prepared, films were deposited, and fatigue properties were measured. Results to date indicate that Nb doped samples show substantially less fatigue out to at least 10^{12} cycles than non-doped material.

Until recently, much of our effort was devoted to preparing ferroelectric thin films of nominal phase purity. However, for practical application in which laser deposition of ferroelectric thin films is integrated with device manufacturing procedures, it will be necessary to produce, not only ferroelectric properties, but also quality surface smoothness with freedom from particulates, pinholes, and other flaws. Experiments to date have shown that the background pressure during deposition has a large effect on surface smoothness; generally films deposited at higher oxygen pressures (e.g. PO_2 = 40 Pa) are characterized by higher surface roughnesses. Substrate temperature may also play a role, with geometrical factors and the nature of the laser target surface also having an effect. A major challenge in the further development of these materials is the improvement of surface smoothness and the elimination of pinhole and particulate defects.

Stress Measurements Using Micro-Raman Spectroscopy

G. S. White, L. M. Braun[1], G. J. Piermarini, M. R. Gallas[2], and Y. Chu[2]

[1] Mechanical Properties Group
[2] Guest Scientist, Instituto de Fisica da Ufrgs, Howard University

The ability to measure stress on a local scale has important implications for the design of modern materials and, because of the catastrophic fracture characteristics of brittle materials, particularly for ceramics. The capability to determine residual stresses resulting from processing techniques as well as the potential ability to map out stress distributions resulting from the presence of defects, e.g., cracks, pores, or inclusions, or from material modifications, e.g., reinforcing fibers or electrode layers, would permit the generation of models which could, in turn, optimize design and manufacturing procedures for enhanced material applications. With these goals in mind, we have continued our investigation of using the micro-Raman technique to determine stresses in ceramic materials.

Measurements of stresses in polycrystalline alumina and in single crystal sapphire have been made during the past year by correlating shifts in the sapphire peaks with a known applied load. The loads were generated in a biaxial fixture described last year which produced a uniform tensile load on one side of disk shaped specimens and a uniform compressive load on the other side. In situ measurements demonstrated that stresses approximately 10% of the strength of the material could be detected reliably. In addition, measurements of transparent material (sapphire) showed that the signal for the Raman spectrum is predominately controlled by the material at the focal plane of the microscope in the micro-Raman system.

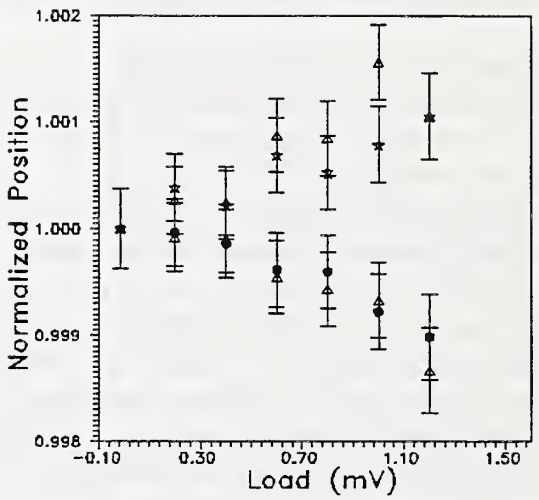

Figure 2 Peak position, formalized by initial position as a function of applied load for the top surface (bottom curves) and the bottom surface of a sapphire disk.

Figure 2 is a plot of the shift in an alumina peak position as a function of applied load for a sapphire specimen. The surface of the sapphire was originally in a state of uniform compression, due to the sawing and polishing associated with the sample preparation. The data in the figure which are shifted to lower wavelengths with externally applied load represent the fact that the residual compressive stress on the top surface of the specimen is decreasing. In contrast, the remaining data were taken by focussing the microscope at the bottom of the specimen and represent the increasing compressive stress at that point of the specimen. This figure demonstrates that: 1) stresses well below the strength of the material can be determined by this technique 2) both tensile and compressive stresses can be measured, and 3) the technique is sensitive to the focal plane of the measurement and is insensitive to the remaining optical path through the material.

Experiments made on polycrystalline alumina have demonstrated that measurements within individual grains can be made; due to the focal spot size of the laser, the grain size has to be on the order of several micrometers.

In addition, the calibration of the pressure dependence of the Raman scattering peaks for α-alumina has been accomplished with the aid of a diamond anvil high pressure cell (DAC) specially modified with low fluorescence diamond anvils coupled with the ruby fluorescence method of pressure measurement. The calibration was made to 1750 MPa, exceeding the maximum strength of α-alumina crystals (1000 MPa) by a wide margin. From a least-squares linear fit to the data, the wavenumber shift with pressure was calculated to be $0.0022 \pm 6.9 \times 10^{-5}$ $cm^{-1}MPa^{-1}$ for α-alumina. In the case of α-alumina, residual stresses on the order of 500 to a maximum of 1000 MPa are expected before cracking occurs.

Lifetime Predictions in InP

G. S. White, L. M. Braun[1], W. C. Carter[2], and E. R. Fuller, Jr.[3]

[1]Mechanical Properties Group
[2]Powder Characterization and Processing Group
[3]Division Scientist, Ceramics Division

Lifetime predictions have been made for single crystal InP. InP has important applications as a connector for optical fiber cables; therefore its reliability, particularly in inaccessible locations, is a matter of substantial industrial significance. The key points of concern were: 1) what is the susceptibility of InP to environmentally enhanced crack growth (i.e., the susceptibility of InP to crack growth for loads less than the ideal strength of the material as a result of attack of the stressed crack tip bonds by water molecules) and 2) once the susceptibility of water was determined, what could the lifetime be expected to be for a range of applied static loads?

In addition to strength measurements made on the as-received material, dynamic fatigue measurements (measurements of breaking strength as a function of loading rate) were made on indented specimens in liquid water and in Ar gas at 50% relative humidity (RH). The dynamic fatigue measurements covered 5 orders of magnitude in velocities. InP is so insensitive to water enhanced crack growth, however, that even with this range of velocities, no precise measure of N (a parameter related to the efficacy of an environment at enhancing crack growth; the larger N, the less the tendency for environmentally enhanced fracture to occur) could be obtained. The best fit to the dynamic fatigue data resulted in N-values of 269 for the 50% RH environment and of 958 for liquid water. While these values could easily be off by a large amount, they do indicate that InP is not very susceptible to slow crack growth in either water or humid gas. Resultant lifetime predictions indicate that, if the material does not break immediately upon the application of a load, it will probably last for many years. This information suggests that, from a mechanical reliability standpoint, InP will function well as a fiber optic coupler.

The large uncertainty remains a problem from a scientific standpoint, however. InP has the same structure as GaAs, which has been shown not to be susceptible to water-vapor enhanced fracture but to be susceptible to liquid water. The uncertainty in N does not let us draw any conclusions for InP. Therefore, we plan to conduct crack growth measurements of InP using a double cantilever beam geometry.

$BaTiO_3$ Films on Pt Substrates

M. D. Vaudin, C-S. Hwang[1] , P. K. Schenck[2]

[1]Guest Scientist, Seoul National University
[2]Metallurgy Division

Pulsed laser deposition (PLD)

Fine-grained (<20 nm) thin films (100 to 500 nm thick) of $BaTiO_3$ have been deposited on self-heated Pt/Ti/SiO_2/Si substrates using PLD. Observation of the films indicated that faceted hillocks of Pt formed on the surface of the substrate and the $BaTiO_3$ film followed the Pt surface morphology and was itself rough; for current device applications of high dielectric thin films, particularly in the area of advanced DRAMs (≥256 Mb), the surface of the film must remain planar to ±20 nm. To reduce the thermal processing time of the substrates and thus the Pt hillock formation, the method of heating the substrate has been changed from resistive self-heating (passing a current through the substrate) to a small BN resistive heater.

The formation of the faceted hillocks (or "mesas") of Pt has been studied by annealing substrates at temperatures from 500 °C to 750 °C under various oxygen partial pressures for times up to 15 minutes. The substrates were then observed with SEM, TEM and atomic force microscopy (AFM). Figure 3 is a bright-field cross-section TEM micrograph of a substrate which was annealed for 1.5 h at 750 °C in flowing N_2 with 20 ppm residual O_2. The micrograph shows a Pt mesa, 100 nm high and 500 nm across, with a $\{111\}_{Pt}$ top surface.

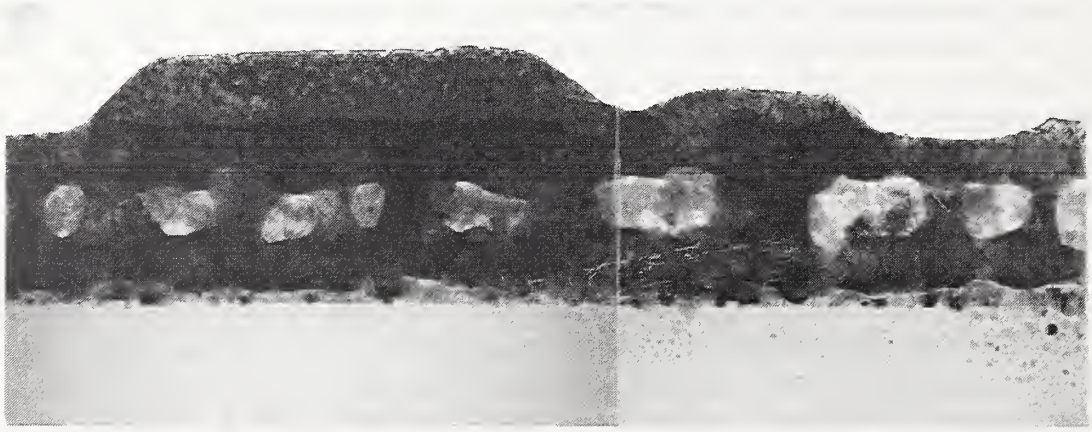

Figure 3 Bright-Field cross-section TEM micrograph of Pt/Ti/SiO_2/Si substrate annealed 1.5 h at 750 °C in 20 ppm O_2. The Pt film thickness is 200 nm. The micrograph shows a Pt "mesa", 100 nm high and 500 nm across, with a $(111)_{Pt}$ top surface, and TiO_2 grains in the center of the Pt film.

The light contrast regions in the center of the Pt film which are TiO_2 grains that forms when Ti diffusing from the interlayer along Pt grain boundaries to the surface reacts with oxygen diffusing down grain boundaries from the surface. This oxide formation results in a volume increase which is the driving force for mesa production. Before annealing, the substrates had been characterized by powder x-ray diffraction and the degree of $<111>$ preferred orientation had been determined. After annealing, the crystallographic orientation of a number of mesas in selected samples was determined using backscattered electron Kikuchi patterns (BEKP) which showed that the mesas had a more pronounced $<111>$ texture than the as-received substrate. Since TiO_2 production causes significant surface roughening, we plan to anneal substrates with a thinner Ti interlayer to investigate whether there is a critical Ti thickness below which this phenomenon does not occur.

Nanosize Powder Processing

G. J. Piermarini, M. R. Gallas[1], A. Pechenik[2], B. J. Hockey[3]

[1]Guest Worker, Instituto de Fisica da Ufrgs
[2]Guest Worker, Air Force Office of Scientific Research
[3]Mechancial Properties

A fundamentally new approach to the fabrication of ceramic materials is currently being studied at NIST. The method involves the production of nanometer size ceramics using cryogenic (liquid nitrogen) compaction of nanosize particles followed by pressureless heat treatments. Materials which are intrinsically transparent can be made into transparent green-state compacts by this process because the material does not scatter visible light. Transparent greenware produced by this method permits easy flaw detection during fabrication, hereby augmenting quality control. Required sintering temperatures are significantly lower than those used for more coarse-grained ceramics. Transparent ceramic compacts of cubic materials such as γ-alumina and silicon nitride have been made by this process without requiring the addition of sintering aids. Transparent, bulk γ-alumina ceramic with hardnesses in the 10 GPa range have been made for the first time.

Innovative Processing of Sol Gel Derived Nanosize Powders

G. J. Piermarini, M. R. Gallas[1], J. J. Ritter[2], B. J. Hockey[3]

[1]Guest Scientist, Instituto de Fisica da Ufrgs
[2]Powder Characterization and Processing Group
[3]Mechanical Properties Group

Gel shrinkage and crack formation during drying are problems encountered in the early stages of the processing of sol-gel nanosize particulates. In fact, these problems have prevented the sol-gels from being utilized in commercial ceramic processing methods. NIST is studying methods to minimize shrinkage and crack-formation by a novel approach of subjecting semi-cured gels to a series of controlled cyclic compactions to extrude and eliminate unwanted solvents, while simultaneously achieving a high-density green-state without cracking. Subsequent heat treatment

under a program of controlled pressure/temperature/environments to produce sintered bodies is then carried out. The compacts are evaluated for optical clarity, microstructure, microhardness, and fracture toughness.

Amorphous silica was fabricated from the sol-gel material by the application of pressures up to 3000 MPa at room temperature and also under liquid nitrogen. Heat treatments of the green bodies were carried out at both 400 and 800 °C for various time periods. The starting material is amorphous and in the form of a viscous gel. The gel cures into a very porous glass over a period of 7-10 days during which time it undergoes enormous shrinkage (about 50%) usually accompanied with cracking and an increase in viscosity (ultimately exceeding the glass transition, 10^{13} Poise). In our experiments, samples of the silica-gel were removed for processing each day during the cure period to determine if an optimum cure condition was relevant to the processing procedure employed. Indeed, this was found to be the case as our results show that the best compacts can be made starting with gel taken in the 4^{th}-to-7^{th} day of cure, pressing it to clarity using only 3000-4000 MPa and sintering for 4 hr at 600 °C. Optically clear, dense, crack-free amorphous compacts were made with hardness values in the 10 GPa range. This value of hardness is significantly larger than the typical silica glass hardness of 6-to-8 GPa. In fact, 10 GPa is typical for crystalline silica.

MODELLING

Molecular Orbital Calculation

W. Wong-Ng, G. S. White, S. W. Freiman, and C. G. Lindsay

Efforts continued to investigate the interaction of environmental species such as water with silicon and with vitreous silica. Experimentally, it has been observed that water enhances the crack growth of silica but not silicon under externally applied strain. In the past year, ab initio molecular orbital calculations (MO) have been performed on both systems. Factors such as the size of crack tip (crack-wall), net charge on the crack-tip atoms as a function of strain were investigated for both systems.

Si:
Our results show that the unstrained crack tip opening is too small to accommodate environmental molecules; strain is necessary both to widen the crack tip and to attract and to orient the molecule. As tensile strain was applied along the Si-Si crack-tip bond, the net charge on both Si atoms increased (more positive) regardless of the manner the strain was applied (ie. with or without angle distortion, and whether the strain was distributed evenly in the neighborhood of the crack-tip bonds). This is different from the situation of silica in which when the crack-tip Si-O bond is strained, the net charge of Si becomes more positive and O becomes more negative, which enhances the interaction with an environmental molecule containing atoms which both donate and accept electrons.

The absence of chemical reaction in Si with environmental molecules is also demonstrated from the geometry optimization calculations of the system $Si_8H_{18}O+H_2O$. In the absence of strain, the water molecule is always about 5Å from the crack-tip Si [$O(H_2O)$...Si], whereas under 15%

strain (15% elongation of the Si-Si bond), the molecule is able to move closer towards the crack-tip (still at a relatively great distance of 2.9Å, which is slightly less than the sum of the Van der Waal's radii of Si (1.7Å) and O(1.4Å)). This separation suggests that no chemical reaction takes place. Therefore, despite strain widening the size of the crack-tip, the result of charge redistribution at the crack-tip does not favor chemical reaction.

Silica:
Reaction calculations between silica and water show that without the application of strain, the activation energy (difference in energy between reactants and transition complex) is $\approx$45 Kcal/mole, and the reaction is slightly endothermic. With strain applied, this energy decreases to $\approx$22 Kcal/mole, due to the raise of the reactant energy, and the reaction becomes exothermic. The increase in the reactant energy was determined to be due to distortion of the silica tetrahedra and is insensitive to the specific environmental molecule present.

First Principles Phase Diagram Calculations

B. P. Burton, A. Pasturel[1], G. Ceder[2], S. Greiner[3], and R. E. Cohen[4]

[1]CNRS, Grenoble France
[2]Massachusetts Institute of Technology
[3]Allied Signal Research, Des Plaines Il.
[4]The Geophysical Laboratory, Carnegie Institute of Washington, D.C.

Relaxor ferroelectrics are a technologically important class of solid solution materials in which the ferroelectric properties are sensitive functions of composition and quenched in cation order. The results of a first principles calculation of order-disorder phenomena in $Pb(Sc_{1/2}Sc_{1/2})O_3$ (PST) were reported at the Eighth International Meeting on Ferroelectrics and at the Calculation of Phase Diagrams (CALPHAD XXII) meeting. In addition, work continues on a first-principles phase diagram (FPPD) calculation for the relaxor solid solution system $(1-x)Pb(Sc_{1/2}Sc_{1/2})O_3 - xPbTiO_3$.

In collaboration with Gerbrand Ceder and his student Patrick Tepish, we have done three different FPPD calculations for the system CaO-MgO. This was done to assess the relative merits of the three different techniques for calculating the formation energies of ceramic compounds with large unit cells. From these we obtained model Hamiltonians that were used as input for FPPD calculations.

FPPD calculations were used to study stable and metastable bcc based ordering in the systems Fe-Be and Mg-Li. These calculations combine full potential electronic structure calculations (to obtain a model Hamiltonian) with a cluster variation method phase diagram calculations. In the Fe-Be system, both chemical and magnetic ordering were considered and it was demonstrated that: 1) Magnetic ordering is responsible for the observed B2 (CsCl structure) ordering in metastable bcc solutions (without magnetism B32 ordering would occur); 2) The energetic cost of mixing atoms of very different sizes is responsible for observed spinodal ordering/phase separation in metastable bcc solutions; 3) The DO_3 structure Fe_3Be phase is predicted to be less stable than a mixture of ferromagnetic BCC Fe plus ferromagnetic B2.

VI. OPTICAL MATERIALS

Albert Feldman

The objectives of the Optical Materials Group are to provide data and their evaluation, measurement methods, standards and reference materials, concepts, and technical information on the fundamental aspects of processing, structure, properties, and performance of optical and photonic materials. The program supports generic technologies in crystalline, glassy, and thin film inorganic optical and photonic materials in order to foster their safe, efficient and economical use. Research in the group addresses the science base underlying advanced optical and photonic materials technologies together with associated measurement methodology.

The principal activity of the Optical Materials Group is being directed toward materials for photonic technology related to data processing, storage, and display. Three aspects of this technology to be addressed are modulator materials, storage media materials, and material for compact short-wavelength radiation sources to increase storage density. In the area of modulator materials, we are evaluating new processing methods that would result in thin film materials with superior properties such as enhanced electro-optic modulator characteristics. In the area of storage media materials we are addressing the development of thin film photorefractive materials, in which the storage method involves modification of the refractive and absorptive properties upon exposure to optical radiation. Ferro-electric oxides (more specifically barium titanate) are the materials we are studying in the latter two aspects because they possess large electro-optic coefficients and a large photorefractive effect.

In the area of materials for short wavelength sources, our studies are being directed toward crystalline materials with large band gaps. This is because a large bandgap is required if a material is to emit radiation at short wavelengths. We have been studying diamond, a wide band-gap material; we are extending this work to other wide band-gap materials that hold greater promise as optical sources, such as gallium-nitride, aluminum-nitride, zinc-selenide, and in the future, quantum well structures of these materials. Diamond possesses numerous superior properties make it an excellent material for a variety of photonic applications. In addition to its optical transparency, it has the highest thermal conductivity of any material at room temperature making it an excellent substrate material for solid-state semiconductor laser sources.

Work on gallium-nitride and zinc-selenide is just beginning. A key issue in the research will be the characterization of defects to very low concentration levels (less than 10^{15} cm^{-3}). Collaborations have been established for the purpose providing data that will allow manufacturers to improve the quality of the materials. Specimens of gallium nitride are being provided by Johns Hopkins Applied Physics Laboratory and specimens of zinc-selenide are being provided by Eagle Picher. NIST will be characterizing the defects in the material; feedback between processors and NIST may allow the producers to improve the quality of their materials to the point where viable, compact short wavelength laser sources can be produced.

Significant Accomplishments:

- Electro-optic thin film ceramics proposed for use in future photonic information technology systems must have great microstructural and compositional uniformity and yet must be fabricated by practical methods, such as metalorganic chemical vapor deposition

(MOCVD). Our MOCVD facility has been modified to improve the through-thickness uniformity of polycrystalline barium titanate ($BaTiO_3$) films. Films prepared in the modified system have shown improved microstructural and compositional uniformity as determined by cross-sectional transmission electron microscopy and by secondary-ion mass-spectroscopy (SIMS) depth profiling.

- Raman spectroscopy has been used to characterize the structure of MOCVD-grown $BaTiO_3$ films. The films were grown at NIST and at Advanced Technology Materials (ATM). The spectra showed features due to crystalline and amorphous phases suggesting the presence of material other than $BaTiO_3$. The intensity of the impurity-phase features in the spectra varied from film to film. Lines due to tetragonal $BaTiO_3$, the phase required for photonic applications of the material, were identified in the spectra of the films with lowest impurity-phase content. The results demonstrate the usefulness of Raman spectroscopy for characterizing of the structure of $BaTiO_3$ films, complementing other techniques such as X-ray diffraction and electron diffraction.

- High-power high-speed electronics is projected to be an important application of chemical vapor deposited (CVD) diamond and doping with boron to produce p-type material would be a major component of this technology. A set of boron-doped diamond films grown by filament-assisted chemical vapor deposition was characterized by Raman spectroscopy. The peak of the diamond Raman line was observed to shift to lower wavenumber with increasing boron concentration and, in the most heavily doped films, to broaden in an asymmetric manner toward lower wavenumber shift. Our results indicate that Raman spectroscopy is a useful method for evaluating the effect of boron doping on the diamond microstructure and on the charged carrier density.

- Diamond cannot be used at temperatures significantly greater than 500 °C because it oxidizes in air. Reducing the oxidation rate might make it usuable at these high temperatures. We have found that the oxidation rate of CVD dimond in pure flowing oxygen at 700 °C can be significantly lowered if it is doped with boron. The oxidation rate, as measured by thermogravimetric analysis, of a CVD diamond film doped with 0.6 % boron was one tenth the oxidation reate of undoped CVD diamond.

- Grain boundaries in high temperature superconductors can severely degrade critical current densities, J_c, thereby preventing the use of these materials in high-power commercial applications such as motors and power-transmission systems. Understanding how grain boundaries affect the dynamics of flux penetration may allow us to develop materials with high J_c. A high-resolution magneto-optical imaging system has allowed us to quantitatively measure the flow of flux across grain boundaries in $YBa_2Cu_3O_{7-x}$ (YBCO) polycrystals. This is the first time such measurements have been made. Flux penetration of all high-angle grain boundaries (misorientation angle greater than 10°) occured at very low applied fields (1-2.5 mT). Flux penetration of small-angle grain boundaries (misorientation angle less than 10°) required higher applied fields; the smaller the misorientation angle, the higher the applied field required for flux penetration.

FERROELECTRIC OXIDE THIN FILMS FOR PHOTONICS

Photonic devices made of ferroelectric oxide films that have large electro-optic coefficients are expected to have a major role in future information technology systems. U.S. dominance in these advanced technologies will be important for maintaining the future economic health of the nation. Pioneering new methods of materials fabrication and characterizing the materials produced is an important means of promoting U.S. dominance in these technologies.

Metalorganic Chemical Vapor Deposition of Barium Titanate

D.L. Kaiser, M.D. Vaudin, C.-S. Hwang, L.D. Rotter, L.H. Robins and G. Gillen[1]

[1]Surface and Microanalysis Science Division

The ferroelectric oxide barium titanate ($BaTiO_3$) has excellent electro-optic properties that make it potentially very useful for many photonic applications such as electro-optic modulation and switching, holographic imaging and data storage, and frequency doubling to produce blue/green light. Commercialization of these processes for future information technology systems requires that high-quality, single crystal films be fabricated reproducibly by a practical processing technique such as metalorganic chemical vapor deposition (MOCVD). Furthermore, the preparation of films with optimal electro-optical properties can only be achieved through detailed studies of how defects affect critical properties and how defect concentrations and distributions can be controlled by processing.

Our research has focused on the growth and microstructural characterization of polycrystalline films of $BaTiO_3$. Films were deposited at 600°C on fused quartz substrates in a research-scale MOCVD system with the precursors titanium isopropoxide (TIP) and barium B-diketonate [$Ba(thd)_2$]. The microstructures of the films were characterized by several techniques. Crystalline phases were identified by x-ray powder diffraction (XRD) techniques and the presence of tetragonal $BaTiO_3$ was detected by Raman spectroscopy. Compositional homogeneity through the film thickness was determined by secondary ion mass spectroscopy (SIMS) depth profiling and structural uniformity was determined by cross-sectional transmission electron microscopy (TEM). Energy dispersive x-ray spectroscopy measurements revealed that the films contained approximately 2 mole % strontium.

Initially, films that had appeared to be pure $BaTiO_3$ by XRD had been found to be structurally and compositionally nonuniform through the film thickness. The titanium concentration was found to vary through the thickness and transition layers at the film/substrate interface had compositions that varied from film to film. To improve uniformity, the MOCVD system was modified by installation of: 1) an elevated pressure TIP bubbler to stabilize the TIP concentration in the process gas; and 2) a process-gas bypass apparatus to allow the gas composition to stabilize before deposition. A film prepared in the modified system was pure $BaTiO_3$ with a slight $<100>$ texture as determined by XRD. (See Fig. 1.) The SIMS depth profiles, seen in Fig. 2, indicated good uniformity of the barium, strontium and titanium concentrations from the surface of the film (depth = 0) to the film/substrate interface (depth $\approx$ 1.2 μm). The high ion counts at the surface of the film were an artifact of the SIMS

measurement; the gradual decrease in the silicon ion counts from the film/substrate interface into the film may indicate silicon diffusion into the film. A cross-sectional TEM image, seen in Fig. 3, revealed a uniform, columnar microstructure with grain widths in the range 0.1 to 0.2 μm. Lattice imaging studies showed that the white streaks between the grains in Fig. 3 were amorphous material. Raman spectroscopy measurements revealed that the films contained tetragonal $BaTiO_3$, the phase required for use of the material in photonic devices.

The next phase of this project will be devoted to the goal of epitaxial growth of $BaTiO_3$ on lattice-matched substrates, such as MgO and $KTaO_3$. The microstructures of these films will be characterized by the above techniques and by small angle neutron scattering. In addition, electrical, optical and electro-optical properties of the films will be measured and correlated with the defect structures. Results of these characterization studies will provide input for modifying the deposition process to further improve the quality of the films.

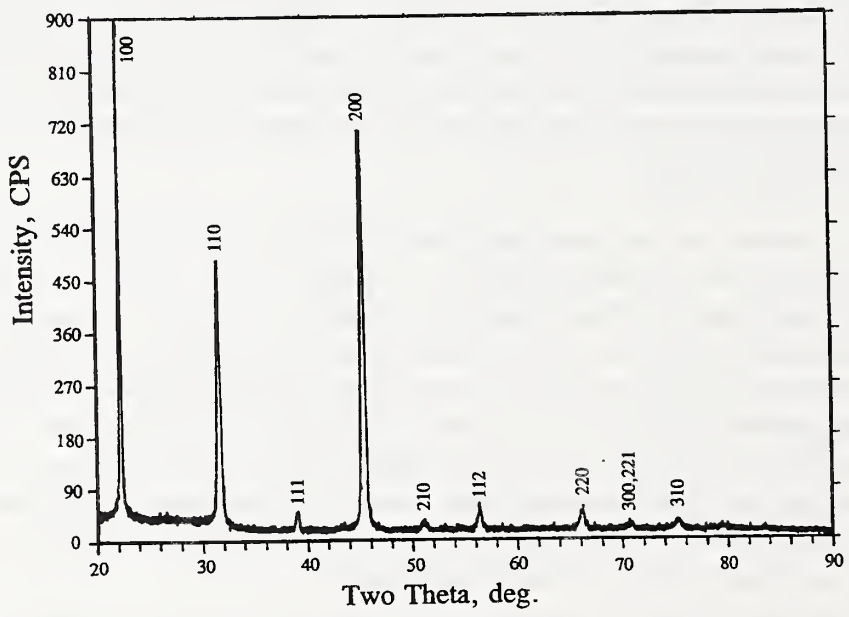

Figure. 1. Conventional θ-2θ XRD pattern for the film deposited in the modified MOCVD system. $BaTiO_3$ peaks are indexed with the indices of the cubic phase.

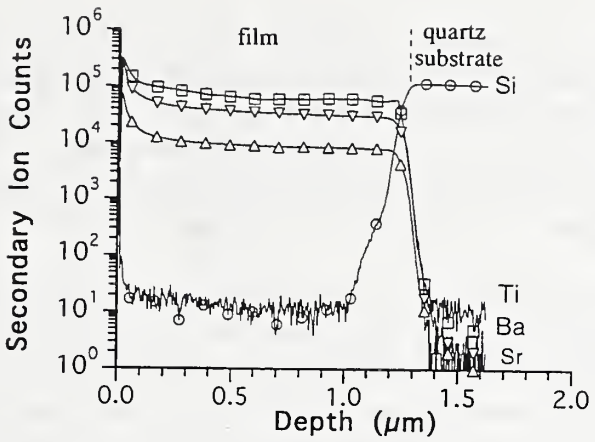

Figure 2. SIMS depth profile data on the film deposited in the modified MOCVD system.

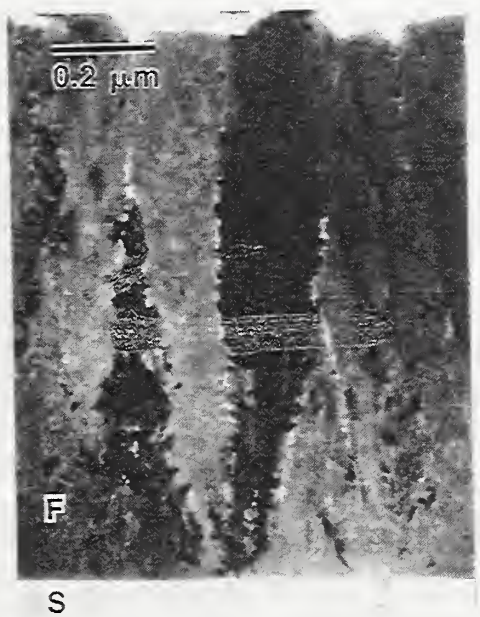

Figure 3. Cross-sectional TEM micrograph of film deposited in the modified MOCVD system showing the substrate (S) and the $BaTiO_3$ film (F).

Structure and electro-optic properties of barium titanate thin films

L. H. Robins, L. D. Rotter, and D. Kaiser

For use in practical photonic applications, films of $BaTiO_3$ will have to be of the tetragonal phase with negilible contamination by impurities and other structural phases. It is expected that single-crystal films, or highly oriented and poled polycrystalline films, will be needed to minimize optical scatter and maximize the strength of the electro-optic effect. Characterization methods that provide detailed information about the structure and compostion of the films are thus needed to provide feedback for improving the deposition process.

Raman spectroscopy can provide structural information that is difficult to obtain by other methods even though it does not directly determine the crystal structure, such as is done by X-ray or electron diffraction. For example, the tetragonal axis in $BaTiO_3$, the c-axis, is difficult to distinguish from the other principal axes by diffraction methods because of the small anisotropy in lattice spacing. However, Raman spectroscopy is very sensitive to the orientation of the c-axis in single-crystal $BaTiO_3$ because of the coupling of the Raman phonons to the electric dipole moment, which is parallel to the c-axis.

Raman spectra were obtained from a number of $BaTiO_3$ films grown by metal-organic chemical vapor deposition (MOCVD). These films had been grown at NIST and at Advanced Technology Materials (ATM). For comparison, the Raman spectra of a large single crystal and of a bulk ceramic specimen were recorded under conditions similar to those used to obtain the thin-film spectra. All the MOCVD specimens showed spectral features due to phases other than $BaTiO_3$. The intensity of the non-$BaTiO_3$ features differed significantly from film to film, and the most intense non-$BaTiO_3$ features in the ATM films differed from those in the NIST films. The Raman spectra of five specimens are shown in Fig. 4. From top to bottom, these are a NIST film with high impurity-phase content, designated N35, a NIST film with low impurity-phase content, designated N36, an ATM film with high impurity-phase content, designated A46, an ATM film with low impurity-phase content, designated A40, and the bulk ceramic specimen.

Lines attributed specifically to the tetragonal phase occur in the spectra of the ceramic specimen and the films with lowest impurity-phase content: specifically, the narrow line at 305 cm^{-1} and the relatively narrow line at 710 cm^{-1} to 720 cm^{-1}. Unlike some of the broad Raman lines, these narrow lines have been shown to vanish at temperatures above the tetragonal-to-cubic phase transition in single-crystal $BaTiO_3$, which occurs at about 135°C. The presence of the narrow lines in the spectra of the purer $BaTiO_3$ films strongly suggests that the crystal structure of these films at room temperature is tetragonal rather than cubic. Additional measurements of the Raman spectra are planned to investigate the dependence of the various spectral features on temperature.

Optically polarized Raman spectra from the large single crystal were found to be strongly dependent on the orientation of the crystal axes. The observed orientation dependence is in good agreement with previous results for single-crystal $BaTiO_3$. The results suggest that Raman spectroscopy should be useful in determining the orientation of the crystal axes in epitaxial single-crystal or highly oriented polycrystalline films.

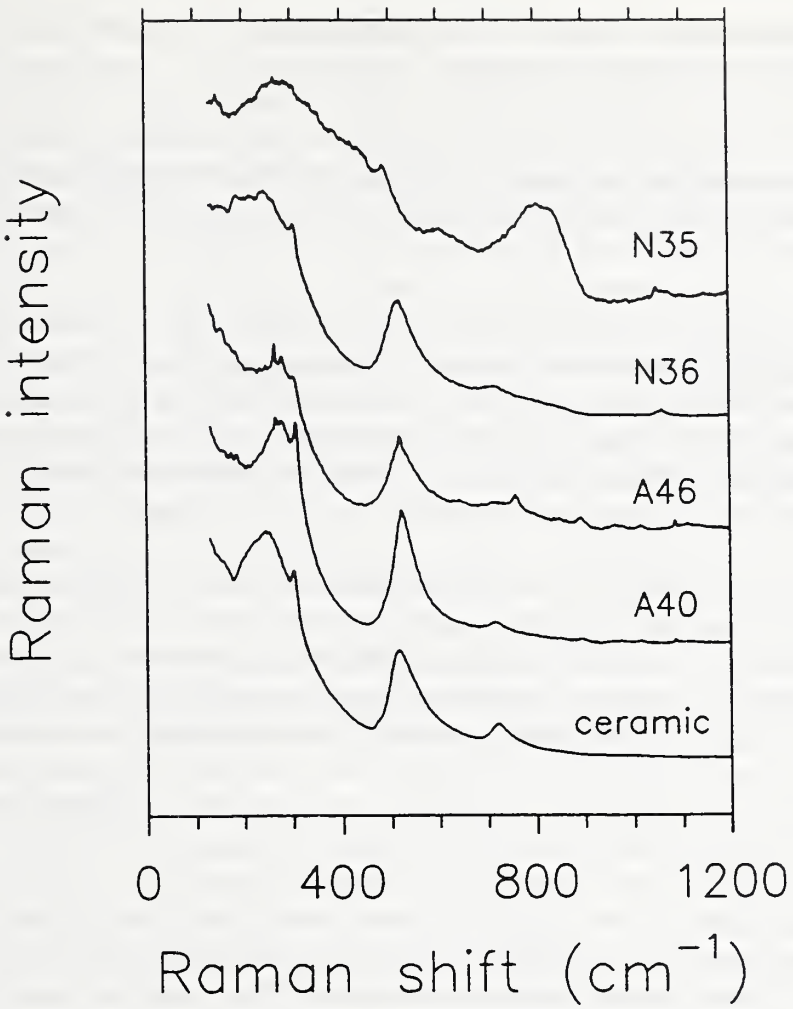

Figure 4. Raman spectra of five $BaTiO_3$ specimens. The top four spectra are from MOCVD-grown films: N35, grown at NIST, high impurity-phase content; N36, grown at NIST, low impurity-phase content; A46, grown at ATM, high impurity-phase content; and A40, grown at ATM, low impurity-phase content. The bottom spectrum is from a bulk ceramic specimen. The narrow lines at 305 cm^{-1} and 710-720 cm^{-1}, in the spectra of N36, A40, and the ceramic, are attributed to tetragonal-phase $BaTiO_3$.

Polarimetric Investigation of Barium Titanate Films

L.D. Rotter, D.L. Kaiser, A. Feldman, L.H. Robins, M.D. Vaudin, C.S. Hwang

The purpose of this project is to develop techniques to characterize currently grown $BaTiO_3$ films. The films under investigation were grown by MOCVD at NIST and at Advanced Technology Materials (ATM).

Most applications of $BaTiO_3$ thin films will require poled epitaxial films of the material in which the optic axis lies either in the plane of the film or perpendicular to it. This orientation allows us to make use of the largest electro-optic coefficient in the material, r_{42}, for modulator

applications and to achieve maximum photorefractive gain. In a periodically poled film one can realize efficient second harmonic generation.

However, truly epitaxial films of $BaTiO_3$ are not yet available. The films tend to be polycrystalline with randomly oriented or partially oriented crystallites and the phases present are not entirely of the desired tetragonal phase; cubic and amorphous phases are usually present as well.

We are developing optical techniques which, in conjunction with x-ray scattering and TEM, are expected to quantitatively determine the ratio of the tetragonal phase to the cubic plus amorphous phase volume ratio in thin films of $BaTiO_3$. The techniques employ polarimetry to investigate the linear birefringence (LB) and effective linear electro-optic coefficient (r_{eff}). Both LB and r_{eff} are signatures of the tetragonal phase; in cubic and amorphous phases, LB and r_{eff} would both be zero. In the following, we discuss LB; r_{eff} will be treated in the future.

The specimen and a photoelastic modulator (PEM) are placed between crossed polarizers and the throughput intensity of HeNe laser radiation (wavelength, 632.8 nm) is measured. The modulation frequency of the PEM is 50 KHz. If the beam possesses a large cross-sectional area, LB is found to be zero. However, by focussing the beam to a 2.6 μm diameter gaussian spot size, we obtain a signal indicating LB is present. If the specimen is translated across the beam, we find that the LB varies rapidly on the scale of the spot size. The peak throughput measured, however, is orders of magnitude smaller than what would be obtained for a single crystal specimen. It is found that the peak intensity values decrease as the spot size increases.

It is known from TEM that the crystallite size in these films is about 10 to 100 nm. The film thickness as determined by a number of methods is usually in the range of 300 nm to 1.5 μm. X-ray scattering shows random orientation in some films, partial orientation in others, and equivalent cubic $<100>$ orientation (i.e., cubic $<100>$, or tetragonal $<100>$ or $<001>$ oriented) in others. However, the orientation of the optic axis is not known even in the $<100>$ oriented films. Raman scattering shows some tetragonal phase exists, but not how much.

We therefore arrived at the following hypothesis: The optic axis is randomly distributed among the equivalent cubic $<100>$ directions. When the spot size is large the experiment averages over so many randomly oriented crystallites that the film looks isotropic, and the LB averages to zero. When the spot is decreased to several microns the number of crystallites over which the experiment averages becomes sufficiently small so that fluctuations from the mean value of zero become apparent. The smaller the spot size, the fewer the crystallites, and the larger the fluctuations.

To test this hypothesis we have modelled the film as a dense array of stacks of linear retardation plates, each plate representing a single crystallite. If a plate represents a cubic crystallite or amorphous section of the film, the retardation of a plate is zero. The probability, P, that a plate will be cubic or amorphous is the volume fraction of the cubic plus amorphous phases. If a plate represents a tetragonal crystallite, the retardation is calculated from a random distribution of crystallite sizes and orientations. The objective then is to determine P. We note that a stack of linear retardation plates is equivalent to a single elliptical half-wave plate (i.e., a half-wave

plate where the eigenpolarizations are elliptical). We have written a computer program to simulate the LB experiment. It uses the Jones calculus to compute the equivalent elliptical waveplate of each stack and the ellipticity of the eigenpolarizations, and collects the values in an array representing the plane view of the film. It convolutes this array with a gaussian profile representing the laser beam power distribution. The probability distribution functions (PDFs) for orientation of the optic axis are obtained by considering the ratio of peak heights in the x-ray spectra. The PDF for the crystallite size can be estimated from TEM pictures. Preliminary simulated LB measurements qualitatively reproduce the experimental data.

We are in the process of increasing the speed of the calculation which will allow us to examine the effect of different PDFs for the crystallite orientation and size, and different values of P on the LB. We will then be able to determine with what accuracy changes in P can be distinguished from changes in the PDFs. We will also examine the interplay between the spot size, the PDFs, and P to determine if we can estimate the crystallite size PDF in the absence of TEM data by collecting data with different spot sizes. Simultaneously, we are examining a number of films with different crystallite sizes and degrees of orientation.

The technique developed here should be applicable to any film in which a single birefringent phase is mixed with isotropic phases. Thus, it should be a useful diagnostic tool for most ferroelectric oxides, as well as other anisotropic polycrystalline films.

DIAMOND THIN FILMS

Chemical vapor deposition of diamond will have a significant economic impact in the near future on a range of commercial products including durable cutting tools and heat dissipating substrates for electronics and opto-electronics. Diamond is an enabling technology because its economic impact will be greater than the market for the material itself, creating markets that might not otherwise develop. Thus, CVD diamond research at NIST is important for helping U.S. industry obtain a competitive edge. In addition to research on materials characterization methods, NIST has been making an significant impact by organizing standards related workshops at which representatives of U.S. companies come together to decide on generic issues important to diamond technology.

Characterization of Boron-Doped CVD Diamond Films

L. H. Robins, E. N. Farabaugh, and A. Feldman

Raman spectroscopy is commonly used to characterize the crystalline quality of CVD diamond films. The first-order Raman spectrum of crystalline diamond consists of a single narrow line at 1333 cm^{-1}. In undoped CVD diamond specimens, extra broad lines in the Raman spectrum indicate the presence of nondiamond carbon phases. The linewidth and change in peak position of the diamond line provides information about strain and disorder within the crystalline diamond phase.

A set of boron-doped diamond films has been characterized by Raman spectroscopy. The boron concentrations, which were determined by secondary ion mass spectroscopy (SIMS), ranged

from 200 to 6300 ppm. Within the set of boron-doped films examined here, the boron concentration was found to have a strong effect on the form of the Raman spectrum. The peak of the diamond Raman line shifted to lower wavenumber with increasing boron concentration. In the most heavily doped films, the diamond line also broadened in an asymmetric manner. The width of the line on the low-wavenumber side of the Raman peak was greater than the width of the line on the high-wavenumber side of the Raman peak. The intensity of the broad nondiamond carbon lines at first decreased as the boron concentration increased, up to 1300 ppm, but then increased with further increases in boron concentration. The Raman spectra of the boron-doped films are shown in Fig. 5. The peak position of the diamond line is plotted as a function of boron concentration in Fig. 6.

Several factors may contribute to the dependence of the Raman spectrum on the boron concentration. The behavior of the broad nondiamond lines suggests that boron doping tends to suppress the growth of nondiamond carbon phases at low concentration, but enhances the growth of nondiamond carbon at high concentration (above 1300 ppm). The most interesting effect is the shift and broadening of the crystalline diamond line. One possible explanation for such a shift would be an increase in the average C-C bond length with increasing boron concentration; this would act to lower the frequencies of all of the lattice vibrations. However, X-ray diffraction results do not show an observable increase in the mean lattice constant with boron doping. We believe that the shift and broadening of the diamond line is due primarily to the interaction between the Raman-active phonon and the charge carriers (holes) introduced by the boron doping. Similar effects have been observed previously in heavily doped silicon and germanium. According to these researchers, the deformation of the lattice by the Raman-active phonon causes an energy splitting at the top of the valence band. Dynamic redistribution of carriers between the deformation-split bands causes a softening of the lattice and, hence, a downward shift of the Raman frequency[1].

Another effect occurs when the spin-orbit splitting between different valence bands is smaller than the optical phonon frequency, as in silicon and diamond. In this case, intervalence-band transitions can give rise to electronic Raman scattering. This scattering occurs in the same frequency range as the conventional Raman scattering due to optical phonons. Interference between these two types of Raman scattering can causes an asymmetric broadening the observed Raman line. This effect was observed by Cardona and co-workers in silicon that had been heavily doped with acceptor impurities.

More work is needed to quantify these effects. In particular, measurements of both carrier concentration and boron concentration are needed to investigate whether it is only the charge carriers (holes) or whether it is the total impurity atom content that correlates with the shift and broadening of the diamond Raman line. Our results suggest it might be possible to use Raman spectroscopy to measure the carrier concentration in heavily boron-doped diamond.

Raman spectroscopy may prove useful as an *in situ* noncontact nondestructive method of measuring the extrinsic carrier concentration during deposition of boron-doped films. This is because in diamond, the carrier concentration due to doping has been found to be larger than the intrinsic carrier concentration even at the temperatures necessary for CVD growth ($\sim 800°C$).

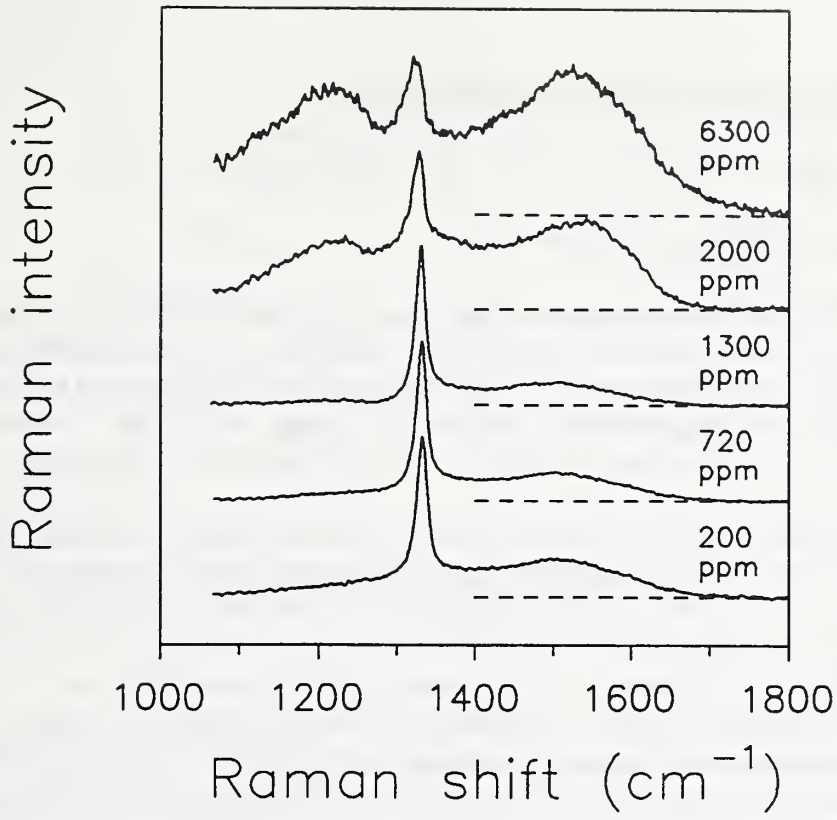

Figure 5. Raman spectra of boron-doped diamond films grown by filament-assisted CVD. The boron concentration in parts per million, as measured by SIMS, is shown for each film. Spectra are rescaled and offset to best display the lineshape variation.

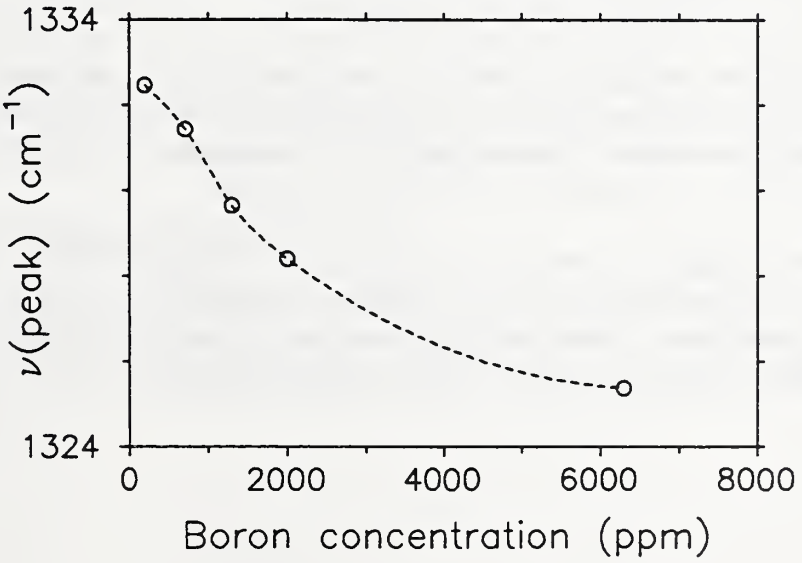

Figure 6. Peak shift of the diamond Raman line as a function of boron concentration in heavily boron-doped diamond films. Peak positions were obtained from the spectra shown in Fig. 5. The dashed line that connects the data points is purely empirical.

OXIDATION OF BORON DOPED DIAMOND FILMS

E.N. Farabaugh and E. Johnson[1]

[1]Naval Air Warfare Center, China Lake, CA

Diamond cannot be used at temperatures significatantly greater than 500 °C because it oxidizes in air. Reducing the oxidation rate might make it usuable at these high temperatures. We have conducted oxidation rate experiments on chemical vapor deposited diamond to ascertain whether the oxidation rated can be significantly reduced by doping with boron. Previous studies had shown a reduced in oxidation rate of single crystal diamond doped with boron.

Boron doped diamond films have been produced by the hot filament chemical vapor deposition (HFCVD) process by bubbling argon through a solution of B_2O_3 in ethanol. This solution furnished both the carbon for the diamond film growth and the boron for doping. The argon gas was then mixed with hydrogen. This mixture served as the feed gas for doped diamond film growth. The highest growth rate for these boron doped diamond films was 0.7 $\mu m \cdot h^{-1}$. The boron concentration in the films was controlled by changing the concentration of B_2O_3 in the ethanol. The highest doping level, as measured by secondary ion mass spectrometry (SIMS), was 6300 ppm atomic. Raman spectroscopy and x-ray diffraction both confirmed the presence of diamond films.

The oxidation rate of doped and undoped diamond films was measured by thermogravimetric analysis (TGA) at 700 °C in flowing high purity oxygen. The results the TGA work are shown in Table 1. We see a general trend of reduced oxidation rate with increasing boron concentration. The oxidation rate of a film with 0.6 % boron is 0.1 the oxidation rate of the undoped film.

Auger analysis of these samples after oxidation was carried out to investigate the mechanism responsible for the reduced oxidation rate with doping. The spectra indicate that partially oxidized diamond films contain a layer of B_2O_3 on the surface. It would seem that the B_2O_3 layer acts as a barrier to oxidation of the underlying diamond.

The utility of boron doping in lowering the oxidation rate will depend on the intended use of the diamond. Thus, applications that are not deleteriously affected by the presence boron might benefit. On the other hand, optical applications and applications that require the material to be electrical insulating would not be able to use the doped material.

Table 1. Rate of weight loss of boron doped CVD diamond due to oxidation in flowing oxygen at 700 °C.

Boron atomic fraction ppm	Rate of weight loss per cent/min
0.	1.1
200.*	0.65
6300.*	0.11

* Measured by SIMS

WORKSHOP ON CHARACTERIZING DIAMOND FILMS

A. Feldman

The second in a series of workshops was held at NIST on February 24th and 25th to discuss the characterization of diamond films and the need for standards in diamond technology. The audience targeted for this workshop were the producers and potential users of CVD diamond technology in the United States. Three technical topics that have relevance to applications of chemical vapor deposited (CVD) diamond were discussed: characterization of optical absorption and scattering for optical applications; characterization of electrical properties and electrical contacts for electronic applications; and, standardization of thermal conductivity measurement for heat spreading applications. A particular accomplishment of the workshop was the formation of a working group to evaluate methods of measuring the thermal conductivity or thermal diffusivity of CVD diamond. A round-robin has been organized to compare different measurement techniques. A set of specimens prepared voluntarily by producers of CVD diamond have been circulated among experts in the measurement methodologies. NIST is coordinating the circulation of the specimens among the measurement laboratories and will collate the results of the measurements for presentation at the next working group meeting.

HIGH T_c SUPERCONDUCTING CRYSTALS

Large scale commercial applications of high temperature superconductions will depend our ability to to produce material that can sustain high critical current densities (J_c). Our ability to control a prime factor in promoting high J_c, flux pinning, is the motivation of the research discussed below.

Magnetization of $YBa_2Cu_3O_{7-x}$ Polycrystals

D.L. Kaiser, M. Turchinskaya[1], F.W. Gayle[2], A. Shapiro[2], A. Roytburd[3], A.A. Polyanskii[4], V.K. Vlasko-Vlasov[4], L.A. Dorosinskii[4], and V.I. Nikitenko[4]

[1]Consultant
[2]Metallurgy Division
[3]University of Maryland
[4]Institute for Solid State Physics, Russian Academy of Sciences

Many grain boundaries in high temperature superconductors act as weak links or regions of poor superconductivity, thereby lowering the critical current density (J_c) and preventing the use of these materials in high-power electrical applications such as superconducting motors and power transmission systems. Understanding the underlying microstructural causes of this weak link behavior is critical to achieving high J_c values. Although the role of grain boundaries in electrical transport in the high temperature superconductor $YBa_2Cu_3O_{7-x}$ (YBCO) has been studied extensively, there have been no detailed investigations of the effect of grain boundaries on microscopic flux flow during magnetization. In this study, we have used a high-resolution magneto-optical method to directly observe real-time flux flow in bulk-scale YBCO polycrystals containing [001] tilt grain boundaries of known misorientation angle, Θ.

The magneto-optical technique utilizes an yttrium-iron-garnet indicator film, having in-plane magnetic anisotropy, placed over the specimen. After cooling the specimen with liquid helium in zero magnetic field, an external field (H_a) in the range of 0 to $\pm$ 65 mT is applied parallel to the common [001] axes of the grains in the specimen. Real-time dynamics of the magnetic flux as a function of temperature (7 to 50 K) and H_a are viewed and recorded by means of a video system. Calibration of the indicator films allows the resulting images to be converted to quantitative magnetic induction maps.

Flux flow was studied in polycrystals containing both high-angle grain boundaries (HAGB, $\Theta > 10°$) and low-angle grain boundaries (LAGB, $\Theta < 10°$). At low temperatures (7 to 20 K), with increasing field, flux penetrated first along HAGBs, then along LAGBs, and finally into grains along the direction of twin boundaries. At higher temperatures (30-50 K), intergranular penetration occurred at lower fields than those required for penetration of LAGBs. The field required for initial penetration (H_{a1}) of a boundary was strongly correlated with misorientation angle as shown in Fig. 7. For LAGBs, H_{a1} increased strongly with decreasing Θ, whereas for all HAGBs, H_{a1} was in the range of 1-2.5 mT. While flux penetrated instantaneously along the entire length of each HAGB at its H_{a1} value, the distance of penetration along LAGBs increased gradually with increasing fields above H_{a1}.

In the final stage of flux penetration, flux flowed into grains from HAGBs, from LAGBs and from the edges of the specimen. Flux flow always proceeded along the direction of twin boundaries. In general, the depth of flux penetration into a grain from a grain boundary was greatest when the twin boundaries in the grain were normal to the grain boundary. The penetration depth decreased with increasing angle between the grain boundary normal and the twin boundary.

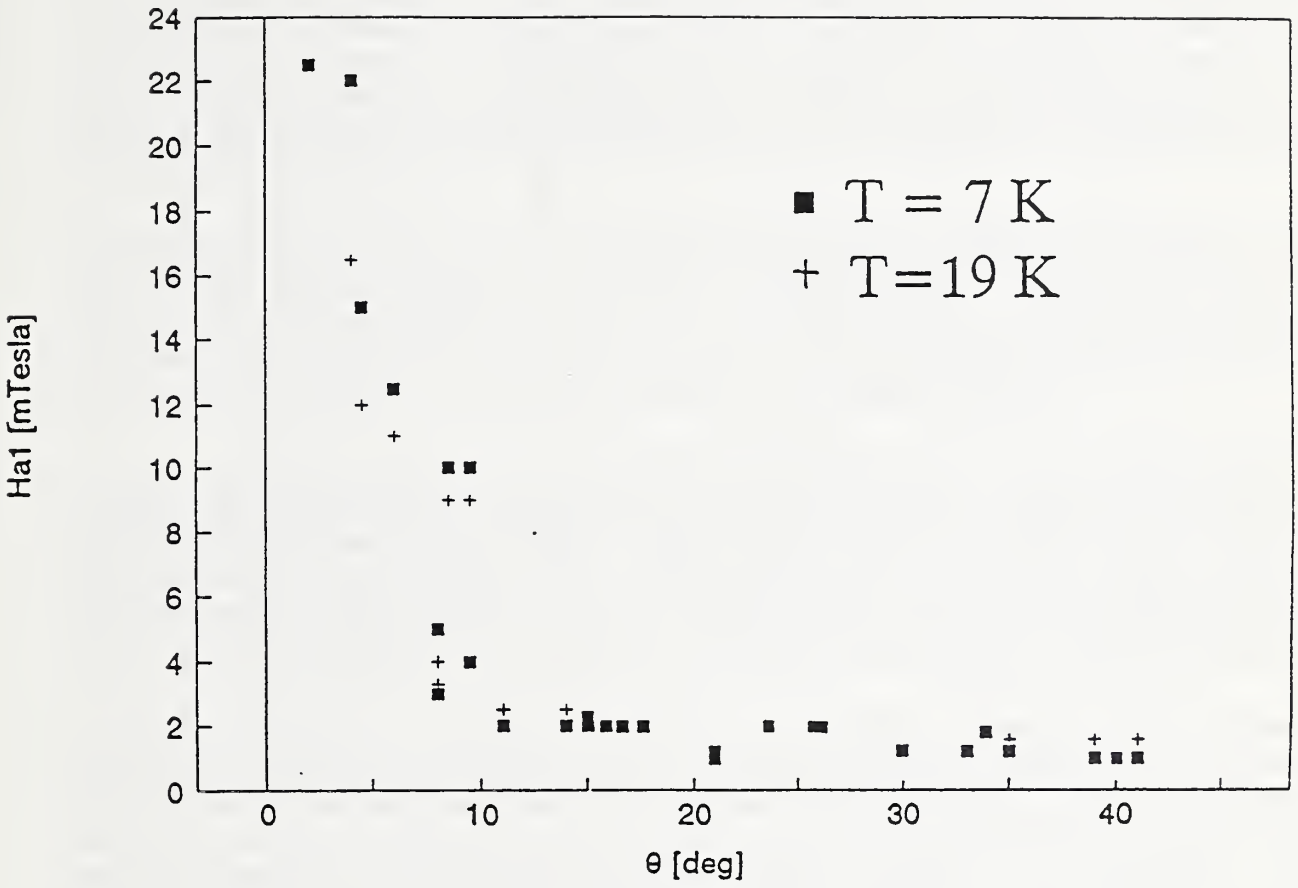

Figure 7. Dependence of the field required for initial flux penetration (H_{a1}) on misorientation angle (Θ) in YBCO polycrystals at temperatures of 7 and 19 K. H_{a1} is strongly dependent upon Θ for LAGBs; for all HAGBs, H_{a1} is in the range of 1-2.5 mT.

In summary, flux motion in YBCO polycrystals in an increasing external magnetic field is highly nonuniform, and highly anisotropic due to the presence of grain boundaries and twin boundaries. The extent of flux penetration depends on the misorientation angle of the adjacent twin crystallites and the angular relationship between twin boundaries and grain boundaries.

VII. MATERIALS MICROSTRUCTURE CHARACTERIZATION — Gabrielle Long

The Materials Microstructural Characterization Group in the Ceramics Division operates two x-ray experimental beamports at the National Synchrotron Light Source, where researchers from NIST, industry, academia and other government laboratories carry out state-of-the-art measurements on ceramic, semiconductor, photonic, metallurgical, polymeric, and other materials of high scientific or technological interest. Measurement capabilities include ultra-small-angle x-ray scattering, x-ray topography, x-ray diffraction-imaging microscopy, x-ray absorption fine structure spectroscopy, standing-wave x-ray scattering, and reaction-kinetic surface science measurements.

Another major area for this Group is a processing/microstructure program in ceramics at the Cold Neutron Research Facility at the NIST Research Reactor. This year, we have commissioned a ceramics furnace which fits onto the small-angle neutron scattering (SANS) instruments. The microstructure evolution of ceramics during sintering can now be examined quantitatively and without interruption as a function of processing variables.

The range of scientific problems which have been addressed over the past year include sintering of commercial alumina powders, processing of nanophase ceramics, research on microwave-assisted reaction-bonded silicon nitride, icosahedral-phase AlPdMn, characterization of man-made and natural diamond, strain effects in homoepitaxial films on diamond, creep cavitation of silicon nitride, strain sensitivity in high-Tc superconducting tapes, and the determination of atomic-scale and molecular-scale structures at technologically-important surfaces and interfaces.

In addition, as part of a national facility, time on the NIST instruments at the National Synchrotron Light Source is made available to qualified researchers based on peer-reviewed proposals. In the past year, researchers from chemical, aerospace, energy, materials production industries as well as from NIST laboratories, other government laboratories and universities have completed experiments that could not have been performed elsewhere in the United States. The long term goal of research at these facilities is to enable researchers to address basic issues so that U.S. manufacturers can provide superior materials based on structural information not available elsewhere.

Significant Accomplishments:

- A ceramics furnace, which fits into the small-angle neutron scattering instruments, has been commissioned. The new instrument permits *in-situ* measurements on materials during heat treatment. We have been able to investigate, non-interruptively, and for the first time, the effects of sintering parameters on microstructure during densification.

- Small-angle neutron scattering has revealed how grain microstructure development in nanophase ceramics can be engineered by control of processing parameters. In particular, we have explored the influence of sintering temperature and environment in controlling grain growth, and the role of additives in suppressing potentially deleterious phase transitions.

- An extended formulation for analysis and interpretation of multiple small angle scattering studies of advanced ceramics has been developed. The new formulation permits coarse plate-like or ribbon-like microstructures to be quantitatively characterized. The improved method provides a powerful new tool for probing the late stages of sintering in ceramics, and for detecting the onset of incipient microcracking during processing.

- Studies of the microstructure development of silicon nitride during sintering has revealed significant morphological changes during the late sintering stages. As more sintering variables are probed, a generalized model for grain-pore evolution is emerging.

- The defect microstructure of thick homoepitaxial diamond films has been studied by x-ray diffraction imaging. For the first time, nearly-perfect man-made diamond was used as a substrate. The low defect density and the very low residual strain in man-made diamond allowed us to observe and measure changes caused by the deposited film. The surprising result was that the film induces a large strain in the substrate, with the film in tension and the substrate in compression.

- The successful application of ZnSe as a wide band-gap material depends critically on the availability of large high-quality crystals. X-ray diffraction imaging has been applied to the problem of characterizing defects in this material as a function of growth conditions in an effort to determine the parameters that suppress defect generation. Our studies of the subsurface microstructure of substrate wafers has led to the modification of wafer processing proceedures in the industry.

- X-ray transmission topographs of partially-twinned $Ba_2YCu_3O_{7-x}$ crystals and of thermomechanically-detwinned $Ba_2YCu_3O_{7-x}$ crystals reveal that the detwinning process leaves significant residual strain.

- Fluorescence-yield near-edge x-ray absorption measurements of a buried metal/polymer interface were used to determine the orientation of polymer aromatic ring planes in the interface region. This type of information is critical for predicting and optimizing adhesion at these technologically-important interfaces.

- Standing-wave x-ray data on the Bi-Si(111) interface were used to determine directly the position of the Bi atoms. The surface was proven to be a honeycomb array of Bi atoms, each located above a first-layer Si atom with no lateral reconstruction. This result resolves conflicting reports in the literature from STM studies, which variously found the structure to be monomer, trimer, and honeycomb reconstructions. The standing-wave data are supported by Rutherford backscattering results which determine the absolute coverage of Bi to be 2/3 monolayer.

- Crystal lattice deformation associated with optical fanning in photorefractive barium titanate has been observed directly for the first time. High resolution x-ray diffraction images display the strain pattern induced by laser beam fanning in a highly perfect barium titanate crystal. The observation provides a basis for refining models for fanning

and thus for improvement of photonic devices that utilize photorefraction for ultra high capacity parallel information processing, such as self-pumped phase conjugate mirrors.

- The first high resolution x-ray diffraction images of epitaxial bismuth germanium oxide layers on sapphire substrates have been obtained. Diffraction was observed simultaneously over a large fraction of the layer-substrate surface indicating a high degree of orientation over a large area. The degree of epitaxy thus displayed suggests that this economical approach to photorefractive oxide layer formation is technically promising for electrooptic elements for high capacity information processing.

- Changes in the formation of periodic irregularities in strontium barium niobate that can be correlated with specific changes in growth procedures have been observed for the first time. These irregularities affect the uniformity of photorefractive response in photorefractive devices for high capacity information processing. On the basis of this study we anticipate that more effective control of the growth process can be exercised, leading to practical options for more rapid information processing.

- Initial results of a study of the one of the boules of cadmium zinc telluride grown on space shuttle USML-1 indicate that the microstructure of the material grown in microgravity is substantially changed from that of similar material terrestrially grown. Whether this results in superior performance of infrared detectors made from these crystals remains to be determined.

Microstructure Control in Nanophase Zirconia

A. J. Allen, S. Krueger[1], G. Skandan[2], J. Parker[3] and G. G. Long

[1]Reactor Radiation Division
[2]Rutgers Univeristy
[3]Nanophase Technology Inc.

Nanophase ceramic oxides, having grain sizes in the range 5 - 50 nm, are of technological interest because they enable the sintering of small grained, fully dense samples at substantially reduced temperatures (less than 1000° C). The resultant materials exhibit novel properties including plastic deformation by creep processes at low temperature. However, they also offer the prospect for combining advanced mechanical properties (e.g. high strength and wear resistance) with good formability during processing into components. In practice, however, it is difficult to obtain high density material without coarsening of the pore/grain microstructure. Therefore, we seek to obtain a better understanding of how the microstructure develops during sintering, and of how sintering parameters and additives can be used to improve the final microstructure.

We have carried out an extensive characterization of nanophase zirconia, n-ZrO_2, for which small samples have been fabricated using a cold-finger gas-condensation technique, or alternatively a commercial continuous-flow technique. Specimens 0.5 - 1 mm thick and 5 - 10 mm in diameter have been used in absolute-calibrated small-angle neutron scattering

experiments. Indeed, we are the first to carry out a completely quantitative non-destructive SANS characterization of the microstructure changes during sintering under different conditions. We have studied the effects of sintering temperature, pressure and time, air *vs.* vacuum conditions, and the use of yttria to stabilize the a-b transformation during sintering. Our measurements have established that, for samples less than 100% dense, the characteristic scattering of nanophase materials arises from the grain/pore interfaces, not from a supposed low-density disordered grain-boundary phase, as proposed in earlier studies.

Figure 1 shows the radially-summed absolute-calibrated SANS data for n-ZrO_2 in the as-compressed state and after sintering in air for 20 minutes at 800° C. These data exhibit the characteristic hallmarks for SANS from nanophase materials: the coarsening of the grain size during sintering, as measured by the narrower profile, and the interparticle interference peak which develops during early densification. The fitted lines are based on a grain/pore microstructure model developed for nanophase ceramic systems. The primary scattering features are slightly oblate pores between the grains. In the as-compressed state, the excess scattering at low scattering wavevectors, Q (where $Q=(4\pi/\lambda)\sin(\phi_s/2)$, λ is the neutron wavelength and ϕ_s is the angle of scatter), is attributed to the presence of some coarser pores. Such coarser porses are probably associated with a small amount of grain agglomeration. The interparticle interference peak appears as soon as the sintering has imposed some ordering in the grain/pore morphology, and is caused by the relatively monodispersed grains separating discrete nearest-neighbor pores while there is still a high number density of such pores present in the system. The peak moves to lower Q and eventually disappears as full density is approached.

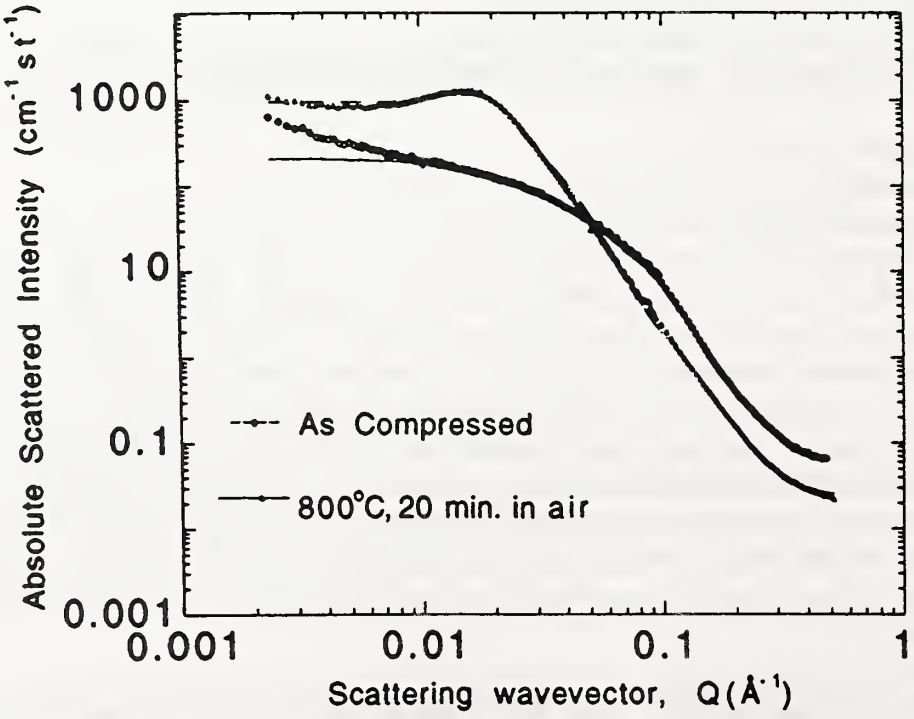

Figure 1. Absolute-calibrated SANS data for n-ZrO_2 in the as-compressed state (open circles) and after sintering in air for 20 minutes at 800 °C (solid triangles).

From our model a number of nanophase microstructure parameters can be quantified and followed through the sintering process: grain size and polydispersity, grain/pore surface area, porosity and coarse pore volume fraction, and the fractional closure and disappearance of pores along the grain boundaries. We have found that the most important microstructure-determining material variable is the relative density. Figure 2 illustrates this point by showing how the inferred grain diameter varies with the relative density of the material. Control of the grain size and ensuring cohesion of the grain boundaries as full density is approached are the major challenges for future work.

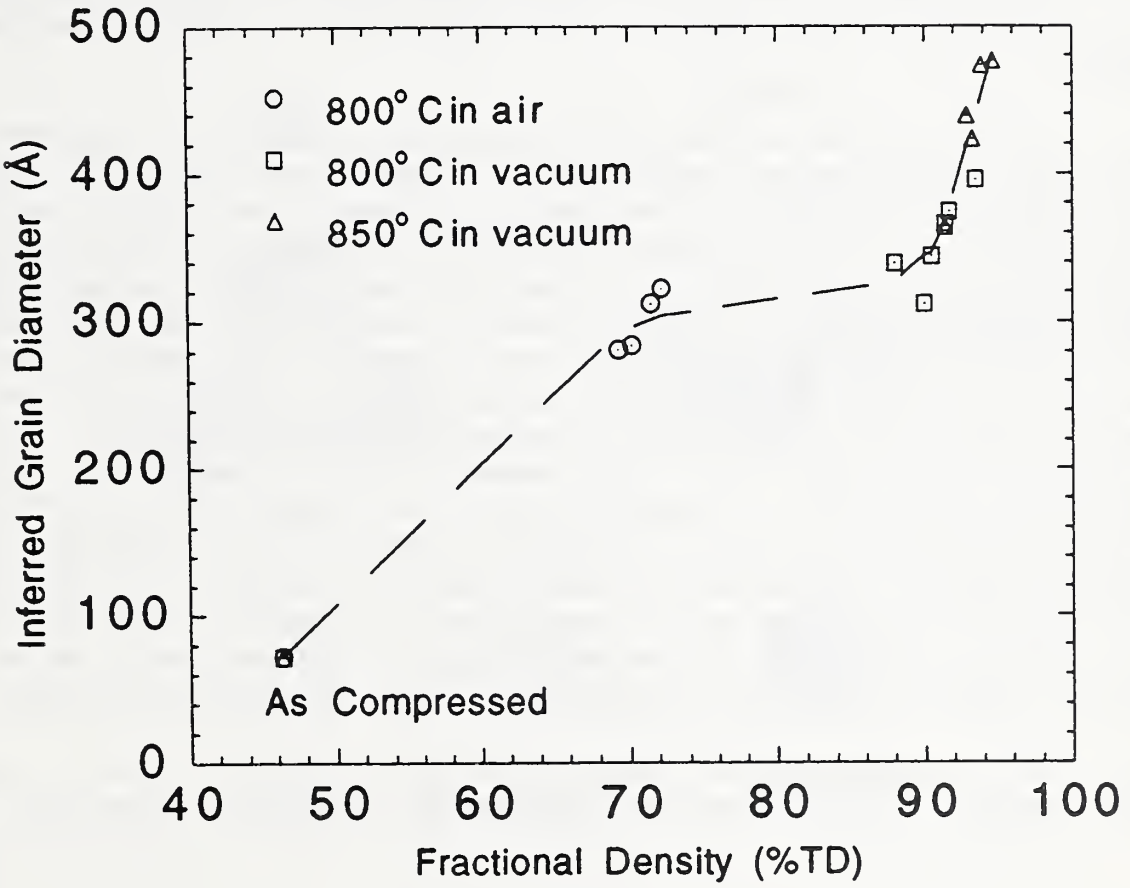

Figure 2. Grain diameter of the nanoparticles as a function of the achieved density of the ceramic body.

Surface Sensitive X-ray Standing Wave Studies of Relaxation at Metal-Silicon Interfaces

J.C. Woicik, T. Kendelewicz[1], A. Herrera-Gomez[1], K.E. Miyano[2], P.L. Cowan[3], C.E. Bouldin, P. Pianetta[4], and W.E. Spicer[1]

[1]Stanford Electronics Laboratory
[2]Brooklyn College
[3]Argonne National Laboratory
[4]Stanford Synchrotron Radiation Laboratory

Combining the surface sensitivity of low-energy electron yield with the position sensitivity of the x-ray standing-wave technique, we have developed a new method for determining the position of surface atoms at clean semiconductor surfaces. Our structural determination for the clean InP(110) surface now stands as a model test system for new diffraction techniques such as low-energy positron diffraction and chemical-shift low-energy photoelectron diffraction.

Recent work has extended our studies to the examination of the degree of relaxation of semiconductor surfaces beneath metal overlayers. Although precise knowledge of these atomic positions is paramount for the testing of theoretical modelling of order at semiconductor surfaces, the prior amount of experimental knowledge relevent to subsurface distortion was scant; it had typically been assumed in the analysis of structural data that the substrate assumes its ideal bulk structure beneath the overlayer. For the In-terminated Si(111) surface, however, there is a large body of theoretical work predicting that this interface is relaxed by as much as 0.3 @. Our study of the In-terminated Si(111) surface has found that the In bonds to an ideal *unreconstructed* top layer of Si atoms. Further examination of this system with surface extended x-ray absorption fine structure spectroscopy, which measures the adatom-to-substrate near-neighbor bond lengths directly, confirms the standing-wave results and demonstrates that, in systems which deviate from tetrahedral geometry, large deviations in bond lengths from the simple sums of covalent radii can also be present. This data have corrected the long existing misconception that the stability of this geometry results from substrate relaxation; it has also revealed the limited accuracy of theory in predicting near-neighbor bond lengths at surfaces and interfaces.

Figure 3 shows our structural determination for the Si(111) à3xà3-In interface. The In atoms are bonded 1.71 @ above the top layer of an ideal, unrelated, Si double layer.

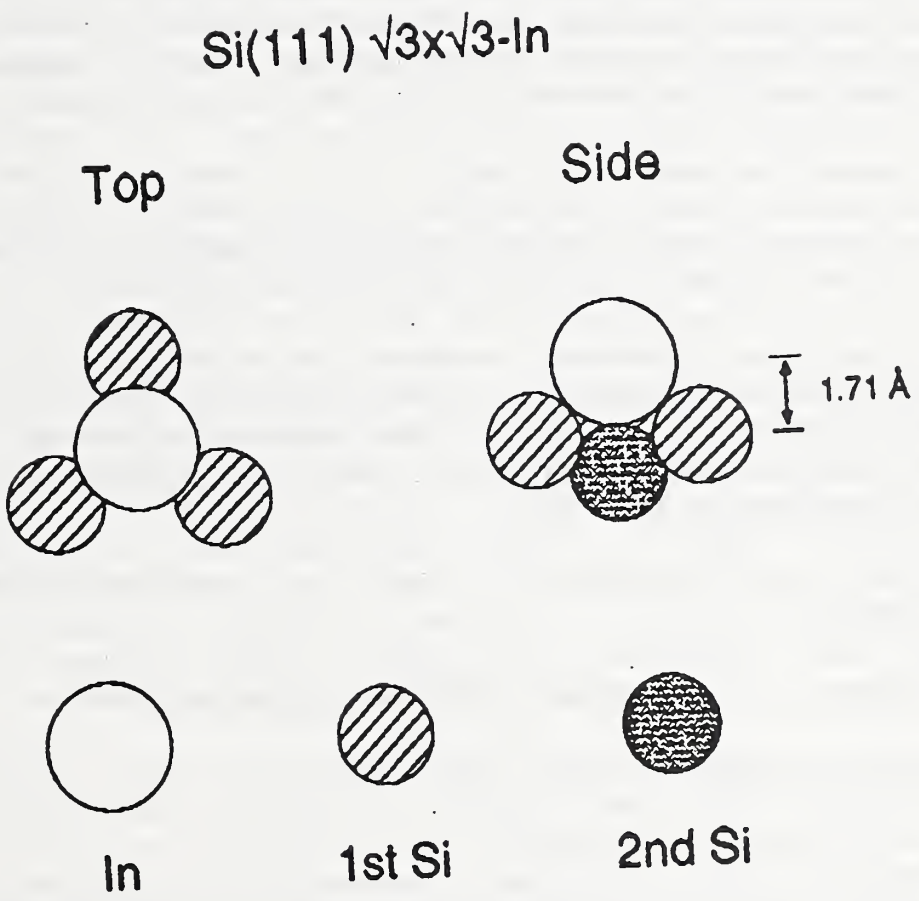

Figure 3. Structural model of the determined Si(111) $\sqrt{3}$x$\sqrt{3}$-In interface.

Fluorescence-Yield Near-Edge X-ray Absorption Fine Structure of a Buried Metal/Polymer Interface

D.A. Fischer, B.M. DeKoven[1], and G.A. Mitchell[1]

[1]Dow Chemical Corporation

DVS bis-BCB (divinyl siloxane bis-benzocyclobutene) is used for dielectric layers in new-generation multilayer interconnect devices (multichip modules) [1]. For this application, it is important to understand the nature of the bonding and complexing which occurs as the metal/polymer interface. The depth sensitivity of about 200 nm, and the nondestructive nature of fluorescence yield, make it particularly useful in studying the buried interface between DVS bis-BCB coated with 10 to 100 nm of aluminum. In contrast, the relatively small depth sensitivity of traditional electron yield makes it useless as a probe of the buried interface since it would only measure within the outer 5 nm of the aluminum overlayer.

We have measured fluorescence-yield carbon K near-edge spectra for the bare polymer, and for 50 nm aluminum on 50 nm DVS bis-BCB. Figure 4 shows the normalized spectra for normal and glancing-incident x-rays. To enhance the metal/polymer interface sensitivity, each panel shows a difference plot (coated polymer minus bare polymer). The C-C π^* peak (at 286 eV) of the aromatic ring of DVS bis-BCB in the difference plots undergoes a dramatic enhancement in polarization dependence after the formation of the metal/polymer interface. This polarization enhancement at the interface region indicates that the aromatic ring planes of DVS bis-BCB are highly oriented towards the surface normal. This type of fluorescense-yield soft-x-ray data is extremely useful for the prediction and optimization of adhesion at metal/polymer interfaces.

[1] T.M. Stokich, Jr., W.M. Lee and R.A. Peters, Proc. of the Materials Research Society **227**, 103 (1991).

Microradiography of *In-situ* Strained High Tc Superconductor Tapes

R.D. Spal, C. K. Chiang, G. N. Riley, and A. Otto[1]

[1]American Superconductor Corporation

Given the brittle nature of high temperature superconductors, it is difficult to fabricate them into wire which can tolerate strain and maintain high critical current. To understand critical current degradation with strain, and to improve strain tolerance, it is desirable to study the evolution of wire microstructure with strain. Toward these ends, NIST and American Superconductor Corporation (ASC) are collaborating in an x-ray microradiographic study of Bi2223/Ag metal matrix composite wire subjected to tensile strain. The wire, in the form of thin (typically 175 μm) tape containing multiple superconductor filaments, is fabricated by ASC using either oxide-powder-in-tube (OPIT) or metallic precursor methods. The microradiography is carried out with synchrotron radiation, monochromated to 24 keV to give reasonable (about 10%) transmission, at NIST beamline X23A3 at NSLS, using a

asymmetric Bragg diffraction microscope developed and recently patented by NIST. This study is intended to complement optical and electron microscope studies carried out by ASC. Since microradiography is non-destructive, the evolution of microstructure with applied stress can be followed. Areas of a few mm^2 can be examined at a spatial resolution of about 1 μm, thereby obtaining both macroscopic and microscopic views.

A preliminary experiment on pre-strained 19 filament OPIT tapes showed many high visibility cracks at 3 and 10% strain, one at 0.7%, and none at 0%. A second experiment concentrated on low strain, applied in-situ to a 19 filament OPIT tape. Digital images of a 0.5 mm long section of tape, covering nearly its entire 2.5 mm width, were taken at five strains from 0 to 1.34%. Cracks appear between 0.55 and 0.80% strain, but their visibility is low, partly due to overlapping of filaments. The images are being analyzed to obtain crack dimensions and strain maps. There are many instances of dark spots of various shapes which appear at some strain levels but not others. They are believed to be extinctions by individual crystal grains which accidently satisfy the Bragg condition. While currently a nuisance, in the future they could provide valuable information on crystal orientation.

Defect Characterization of ZnSe by X-ray Diffraction Imaging

D.R. Black and H.E. Burdette

The successful commercial application of ZnSe as a wide band-gap material depends on the ability to grow large, high-quality single crystals. To improve crystal perfection and the yield of device material, the relationships between the growth conditions and defect generation are under intense investigation. X-ray diffraction imaging, which is highly sensitive to lattice defects, is being used in a critical characterization program on the bulk ($\sim$0.5 μm thick) and near-surface regions of substrate crystals, with spatial resolution of order one micrometer. The technique is sensitive to defects that change the local atomic spacing or the local crystallographic orientation such as: stacking faults, dislocations, voids, inclusions, inhomogeneous strain and the presence of additional phases.

We have performed studies on several wafer-sized crystals as well on as-grown material. Long-range inhomogeneous strain, residual subsurface damage, and a complex dislocation network have been observed. In addition, a critical examination of the near-surface regions of substrates has revealed otherwise unobservable damage from cutting and polishing. This observation has led the crystal grower to modify the surface preparation techniques.

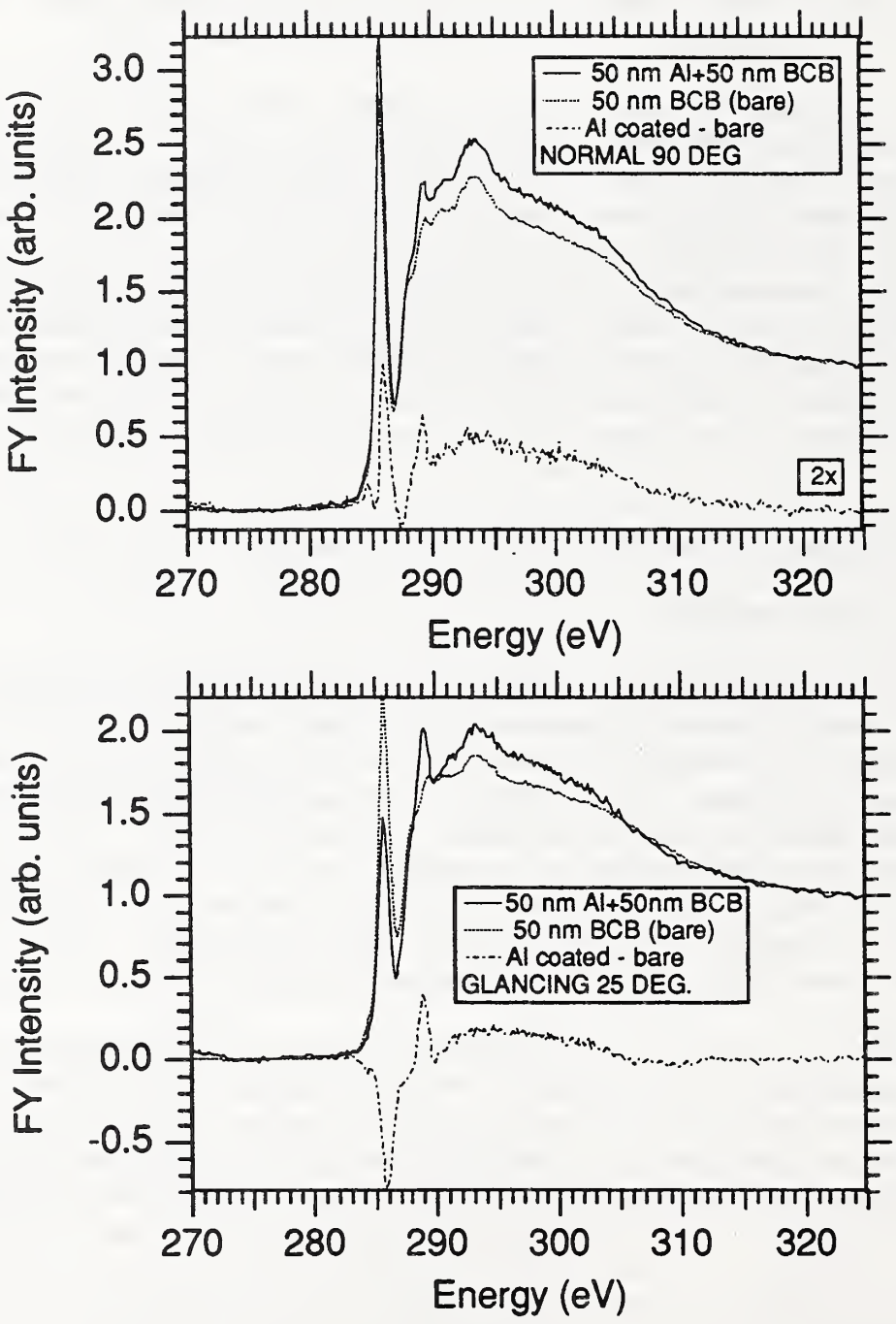

Figure 4. FY carbon K near edge spectra for evaporated aluminum coated (50 nm thick) DCVS bis-BCB (50 nm thick) as well as the identical bare polymer, upper and lower paneslshow spectra for normal and glancing incident x-rays respectively. In order to enhance the metal/polymer interface sensitivity each panel shows a difference plot (coated polymer minus bare polymer).

In Situ X-Ray Diffraction Imaging of Optical Interactions in Photorefractive Crystals

Bruce Steiner, Mark Cronin-Golomb,[1] Gerard Fogarty,[1] John Martin,[2] and Robert Uhrin[2]

[1]Electro-Optics Technology Center, Tufts University
[2]Deltronic Crystal Industries, Inc.

Increased signal processing capacity and speed may be facilitated by the development of optical approaches, which incorporate parallelism with relative ease. One promising technique for processing optical signals uses photorefractive crystals; however this is complicated by amplified optical scattering (fanning) in some materials such as barium titanate and by periodic irregularities identified as striations in other materials such as strontium barium niobate. In each case, the irregularities in signal processing response are traceable to crystalline disorder. The relative importance of various specific crystal irregularities is not yet known; nor are the role that they play in the crystal optics and their specific origins during growth understood. The development of a satisfactory understanding of these defects should lead to improvement in optical signal processing through growth of more satisfactory photorefractive crystals. We thus set out three years ago to address these issues through direct, *in situ*, observation of photorefractive crystals and optical interactions in them.

This past year we succeeded for the first time in imaging the lattice deformation due to photorefractive fanning in barium titanate. The images obtained showed conclusively that the fanning is due to internal scattering and not to surface interactions. We have shown also that the sources of this scattering are smaller than one micrometer in dimension. Further progress in this direction would be facilitated by improvement in spatial resolution in these experiments.

Moreover, we have now observed changes in the periodic irregularity observed in strontium barium niobate. These striations interfere in the establishment and reading of photorefractive gratings. The diffraction images can be correlated with recorded changes in growth conditions and thus are expected to lead to substantial improvement in the crystals grown and thus ultimately in the feasibility of high capacity photorefractive image processing.

This work was made possible by funding from ARPA and from the NIST Advanced Technology Program.

Irregularities in Crystals Grown in Microgravity and Related Terrestrial Crystals: their Nature, Genesis, and Effects on Electro-Optical Device Performance

Bruce Steiner, Lodewijk van den Berg,[1] Heribert Wiedemeier,[2] Yu Ru Ge,[2] Ravindra Lal,[3] and David Larson[4]

[1]EG&G Energy Systems
[2]Rensselaer Polytechnic Institute
[3]Alabama A&M University
[4]Grumman Corporation

Crystals grown in microgravity have previously been found to have properties superior to those of directly comparable terrestrial crystals. For example, the charge carrier mobility of x- and gamma-ray mercuric iodide detectors made from space-grown crystals was a least six times higher than for similar detectors made from ground-grown crystals. This superiority has naturally led to substantial interest in crystal growth in space. Neither the structural nature of the differences nor their origins in crystal growth had been determined prior to the initiation of the current program. Since both issues are important to the space crystal growth program and indeed to improvement in the effectiveness of crystal growth in general, we have established a collaborative program with commercial and academic crystal growers in NASA's Microgravity Sciences and Applications Program.

We have focussed this year on the two materials grown on space shuttle IML 1 in February 1992: vapor-grown mercuric iodide and solution-grown triglycine sulfate; and on the observation of two of the four materials grown on space shuttle USML 1 in April 1993: mercury cadmium telluride layers grown by vapor transport on cadmium telluride substrates, and Bridgman-grown cadmium zinc telluride.

In the initial ground-grown mercuric iodide crystals observed in high resolution diffraction imaging, more than one phase in the form of arrays of non diffracting inclusions was observed. These appeared to stiffen the lattice, imparting long range regularity to it. With the suppression of these inclusions, either through growth in microgravity or through the use of more highly purified starting material, the lattice was appreciably weakened.

It has been unclear whether the long range changes in lattice orientation observed were characteristic of the growth process, or simply a result of the slicing and polishing process for what was now a very soft material. This past year we showed conclusively that the lower level of inclusions in superior material softens the resulting crystals, leading to the necessity for the development of new techniques for crystal handling in order to realize the superior long range order inherent in recent improvements in processing whether in microgravity or on the ground. The required new sophisticated crystal handling techniques have now been successfully developed and demonstrated to be effective in superior diffraction images. We anticipate that the result of these advances will be radiation detectors with substantially improved properties.

Through the immediate application of these new crystal handling techniques, we found that the mercuric iodide crystal vapor-grown on IML-1 had long range uniformity in lattice orientation a factor of 15 higher than that of comparable terrestrially grown material. Uniformity in intermediate range lattice orientation, *i.e.* on a scale comparable to the 1 mm thickness of the crystal slice, was found to be a factor 10 - 20 higher than a comparable crystal grown on the ground.

This increased uniformity in the orientation of the lattice in the space-grown IML-1 crystal on a scale comparable to the charge carrier travel distance fulfills the principal expectations for this space crystal growth experiment. Mercuric iodide is extremely soft at crystal growth temperature and thus particularly susceptible to hydrostatic loading by gravity. Reduction of this loading by growth on IML-1 resulted as expected in more uniform lattice orientation than that achieved with comparable material on the ground. The expected improvement in the electrical parameters of radiation detectors made from other slices of these crystals, which are expected to be particularly sensitive to lattice regularity over the distance travelled by charge carriers, has been achieved. The superior electrical properties of these crystals result, in turn, in an increase in energy resolution for the detectors made from them. Moreover, these improved crystal handling techniques made possible the following observations, which themselves are expected to result in still further improvement in this technology.

Single crystals of mercuric iodide recently grown on the ground from newly available more highly purified source material have demonstrated precipitation hardening in those regions that grew in the [110] direction, and its absence in those that grew in the [001] direction. This observation may lead to the terrestrial growth of superior crystals for radiation detectors as well.

Anomalous x-ray diffraction through a mercuric iodide crystal in Laue geometry at 11 keV has been observed this year for the first time. The new level of crystalline order thus demonstrated is expected to lead both to understanding of the genesis of the inclusions and to further increases in the electrical properties of high energy radiation detectors made from this material.

A triglycine sulfate crystal grown on IML-1 has been examined with high resolution diffraction imaging in order detect the interface between the terrestrially grown seed, which had been deliberately dissolved back in the early parts of the space-growth experiments, and that part of the crystal grown in microgravity. The precise location of this interface is important because it determines the regions of the crystal to be compared after their fabrication into infrared detectors.

The layers of mercury cadmium telluride grown on cadmium telluride grown on USML-1 provided preliminary evidence for a higher degree of long range order than that found in comparable terrestrial systems. Initial results of a study of the one of the boules of cadmium zinc telluride grown on USML-1 indicate that the microstructure of the material grown in microgravity is substantially changed from that of similar material terrestrially

grown. Whether these results lead to superior detector device performance remains to be determined.

This work was funded by the NASA Microgravity Sciences and Applications Division.

Defects in Epitaxially Layered Systems: Their Genesis and Effects on Semiconductor Device Performance

Bruce Steiner, Joseph Pelegrino[1] and Larry Sorenson[2]

[1]NIST Electronics and Electrical Engineering Laboratory
[2]University of Washington

Commercially available semi-insulating gallium arsenide and indium phosphide wafers, used in photonic device fabrication, have a very high density of severely strain-inducing crystallographic irregularities such as dislocations, anti-phase boundaries, low angle grain boundaries, stacking faults, etc. ($>10^3$ cm^{-2} etch pit density). Epitaxial layers grown on the surfaces of these substrates contain defects, some of which propagate from the underlying wafers into the layers grown on them and *vice versa*. Moreover, other crystal defects are introduced by device fabrication and processing. We are examining the various factors that influence the generation of disorder in these layers. The diffraction imaging of layered semiconducting crystals over the past three years has resulted in the development of criteria for the nucleation and propagation of irregularities in layered systems.

This past year we have focused on the influence of layer thickness around the critical thickness, *i.e.* the thickness above which pseudomorphic growth of a lattice-mismatched layer cannot be sustained. Our studies have addressed strained indium gallium arsenide layers on gallium arsenide substrates. High resolution x-ray diffraction also was performed to determine the lattice constant of the strained films. Initial results find the layers to be pseudomorphic and uniform below the critical thickness; however, above the critical thickness the layers are found to relax through a network of misfit dislocations, which propagate into the substrate. The density of these defects is found to be directly related to the thickness of the layer and hence to its degree of relaxation. These defects are found to have preferred nucleation around pre-existing defects in the substrate.

Growth-Related Factors in the Optical Performance of KDP

Bruce Steiner, James DeYoreo,[1] and Chris Ebbers[1]

[1]Lawrence Livermore Laboratory

Growth related factors are believed to limit the performance of potassium dihydrogen phosphate crystals in high performance systems for laser fusion. Therefore, we have initiated an exploratory program to observe whether the disorder visible in high resolution x-ray diffraction imaging is relevant, and, if so, how. Initial results are extremely

encouraging. We have observed strong evidence for strains associated with clearly visible faceted growth.

Irregularities in Quartz Resonator Structures

Bruce Steiner, Robert R. Whitlock,[1] and Michael I. Bell[1]

[1]Naval Research Laboratory

The frequency stability of quartz resonators is believed to be determined by crystalline irregularities that are induced either during crystal growth or subsequent complex machining into delicate devices that are designed to vibrate independently of their attachment. We have initiated a study of the irregularities in devices and in the material from which they are made. Initial imaging proved successful in spite of the challenging suspension of these devices, which is an intrinsic part of their structure.

RESEARCH STAFF

DATA TECHNOLOGIES

Begley, Edwin F.	• Database management methods • Engineering database structures • Digital video interactive technology
Carpenter, Joseph A., Jr.	• Functional ceramics applications • Technical assessments • Industrial liaisons
Cellarosi, Mario	• Glass Standards
Clevinger, Mary A.	• Phase diagrams for ceramists • Computerized data
Dapkunas, Stanley J.	• Structural ceramics applications • Technical assessments
Munro, Ronald G.	• Materials properties of advanced ceramics • Data evaluation and validation • Analysis of data relations

POWDER CHARACTERIZATION AND PROCESSING

Carter, Craig W.	• Materials thermodynamics • Advanced mathematical and computational techniques • Computation of materials processes
Cline, James P.	• Standard reference materials • High-temperature x-ray diffraction • Microstructural effects in x-ray diffraction • Rietveld Refinement of XRD data
Kelly, James F.	• Quantitative scanning electron microscopy • Image analysis • Microstructure analysis • Powder standards
Lum, Lin-Sien H.	• Powder characterization • Instrumental analysis
Malghan, Subhas G.	• Powder and dense slurry characterization • Colloidal processing and forming • Interfacial and surface chemistry of powders

	• Standards development
Minor, Dennis B.	• Analytical SEM of ceramics and particulates • Powder test sample preparation • Powder characterization
Pei, Patrick T.	• Spectroscopic and thermal characterization • Chemical coating • Powders characterization
Ritter, Joseph J.	• Chemistry of powders synthesis • Specialty powders synthesis • Powder preparation and compositional evaluation
Wallace, Jay S.	• Processing and microstructure • Silicon nitride densification • Thermal analysis
Wang, Pu Sen	• Solid state NMR • Surface characterization by x-ray photoelectron and Auger electron spectroscopy

SURFACE PROPERTIES

Gates, Richard S.	• Tribo-chemistry • Surface chemical properties of ceramics • Machining of ceramics
Hsu, Stephen M.	• Ceramic wear mechanisms • Engineered ceramic surfaces • Lubrication and machining of ceramics
Ives, Lewis K.	• Wear of materials • Transmission electron microscopy • Mechanical properties
Ruff, Arthur W.	• Wear of materials • Microstructure effects • Mechanical behavior

MECHANICAL PROPERTIES

Braun, Linda	• Raman stress measurements

	• Ceramic matrix composites • Toughening mechanisms
Chuang, Tze-Jer	• Creep/creep rupture • Fracture mechanics • Finite-element modeling • Lifetime predictions
Cranmer, David C.	• Ceramic and glass composite fabrication • Composite test development • Ceramic composite properties • Glass viscosity • Properties of glass
Hockey, Bernard J.	• Electron microscopy • High-temperature creep
Jahanmir, Said	• Ceramic Machining Research • Machining Data
Kauffman, Dale A.	• Glass melting
Krause, Ralph F., Jr.	• Creep in flexure and tension • Fracture mechanics • Hot pressing • Chemical thermodynamics
Quinn, George	• Mechanical Property Test Standards • Standard Reference Materials • Creep Testing
Smith, Douglas T.	• Surface forces • Charge transfer at interfaces • Adhesion and friction • Colloidal processing

ELECTRONIC MATERIALS

Blendell, John E.	• Ceramic processing and clean-room processing • Sintering and diffusion controlled processes • Processing high T_c ceramic superconductors

	• Activation chemical analysis
Burton, Benjamin P.	• Calculated phase diagrams • Ferroelectric ceramics
Chiang, Chwan K.	• Electronic ceramics • Thermoelectric power measurements • Electrical measurements
Cook, Lawrence P.	• High temperature chemistry • Phase equilibria
Hill, Michael D.	• Mechanical properties of PZT • Ceramic processing
Lindsay, Curtis G.	• Phase equilibria of high dielectric ceramics • Phase equilibria of high T_c ceramics • MO calculations of environmentally enhanced fracture
Piermarini, Gasper J.	• Ceramic processing and high pressure sintering • Pressure-induced transformation toughening • High pressure physical properties and structures • High pressure X-ray diffraction and spectroscopy
Vaudin, Mark D.	• Electron microscopy of ceramic superconductors and of ceramic-ceramic and ceramic-metal composites • Microscopy and diffraction studies of interfaces • Computer modelling of grain boundary phenomena • Dielectric Films
White, Grady S.	• Thin films • Nondestructive evaluation • Subcritical crack growth • Stress measurements • Cyclic fatigue
Wong-Ng, Winnie	• X-ray analysis • X-ray standards • Molecular orbital calculations

OPTICAL MATERIALS

Farabaugh, Edward N.	• Chemical vapor deposition of diamond • Structure and morphology analysis • Scanning electron microscopy • X-ray diffraction • Thin film deposition • Surface analysis
Feldman, Albert	• Chemical vapor deposition of diamond • Thermal properties • Modelling thermal wave propagation • Thin film optical properties
Kaiser, Debra L.	• Bulk single crystal growth • Phase equilibria • Physical properties and structures of high temperature superconductors • Interfaces in high temperature superconductors • Chemical vapor deposition of ferroelectric oxide thin films
Robins, Lawrence H.	• Defect identification and distribution in CVD diamond • Stress in ceramics • Cathodoluminescence imaging and spectroscopy • Photoluminescence spectroscopy • Optical properties • Raman spectroscopy • Scanning electron microscopy
Rotter, Lawrence D.	• Measurement of electro-optic coefficients • Photorefractive effect • Optical spectroscopy of thin films

MATERIALS MICROSTRUCTURE CHARACTERIZATION

Black, David R.	• Defect microstructure in diamond • Polycrystalline diffraction imaging • X-ray imaging of photonic materials
Bouldin, Charles E.	• X-ray absorption spectroscopy • Diffraction anomalous fine structure • GeSi heterojunction bipolar transistors

Burdette, Harold E.	• X-ray optics • X-ray diffraction imaging • Crystal growth • Instrumentation
Fischer, Daniel A.	• X-ray absorption fine structure • X-ray scattering • Surface science
Long, Gabrielle G.	• Small-angle x-ray and neutron scattering • Ceramic microstructure evolution as a function of processing • X-ray optics
Spal, Richard D.	• X-ray optics • Diffraction physics • X-ray scattering
Woicik, Joseph C.	• UV photoemission • X-ray standing waves • Surface and interface science

DIVISION OFFICE

Freiman, Stephen W.	• Electronic ceramics • Mechanical properties • Superconductivity
Fuller, Edwin, R., Jr.	• Influence of microstructure on fracture and other physical properties of materials • Toughening mechanisms in ceramics and ceramic composites, and their relations to processing • Interfacial fracture and toughening mechanisms in reinforced ceramic composites • Processing/property relations and phase equilibria of high T_C ceramic superconductors
Steiner, Bruce W.	• High resolution diffraction imaging • Nature, genesis, distribution, and effects of irregularities in monolithic crystals and multilayers • Non linear optical processes

GUEST SCIENTISTS AND GRADUATE STUDENTS

Allen, Andrew	University of Maryland
Bell, Michael I.	Naval Research Laboratory
Bernik, Slavko	University of Ljubljana
Blackburn, Douglas	Consultant
Block, Stanley	Consultant
Brower, Daniel	Optex Corporation
Bogatin, Oleg	Institute of Nonmetallic Materials
Butler, Elizabeth	Rutgers University
Cedeno, Christina	American Ceramic Society
Chapel, Jean-Paul	Ecole Normale Superieure, Paris
Chen, Yung-Mien	University of Maryland
Chen, Wei	Alfred University
Dai, Yongshan	Smithsonian Institute
Dally, James	University of Maryland
Domingues, Louis	Trans-Tech, Inc.
Dong, Xiaoyuan	University of Maryland
Frederikske, Hans	Consultant
Gallas, Marcia	Instituto de Fisica da Ufrgs
Green, Thomas	American Ceramic Society
Grabbe, Alexis	Postdoc (ex - University of North Carolina at Chapel Hill)
Gu, Jia-Ming	University of Maryland

Hackley, Vince	University of Wisconsin
Haller, Wolfgang	Abbott Laboratories
Harmer, Martin	Lehigh University
He, Chuan	University of Maryland
Hill, Kimberly	American Ceramic Society
Hong, William	Institute for Defense Analysis
Hwang, CheolSeong	Seoul National University
Hu, Zu-Shao	East China University
Jemian, Peter	Illinois Institute of Technology
Kerch, Helen	Johns Hopkins University
Krebs, Lorrie	Johns Hopkins University
Kruger, Jerome	Johns Hopkins University
Laor, Uri	Nuclear Research Center of the Negev
Larsen-Basse, Jorn	National Science Foundation
Lee, Byeong	Hanyang University
Lee, Hsien-Ming	University of Maryland
Lee, Soo Wohn	University of Illinois
Liang, Hong	University of Maryland
Liu, Hanyan	Northwestern University
McMurdie, Howard	Joint Center for Powder Diffraction Studies
Messina, Carla	American Ceramic Society
Ondik, Helen	American Ceramic Society
Pan, Yi-Ming	Southwest Research Institute

Paretzkin, Boris	Joint Center for Powder Diffraction Studies
Paulik, Steven	Northwestern University
Pechenik, Alex	Air Force Office of Scientific Research
Perez, Joseph	Department of Energy
Peterson, Marshall	Wear Sciences
Premachandran, Ramannair Sarasamma	Indian Institute of Technology, Madras
Roth, Robert	Consultant
Russell, Thomas	Naval Surface Warfare Center
Sater, Janet	Institute for Defense Analysis
Shechtman, Dan	Johns Hopkins University
Shen, Ming	University of Illinois
Shin, Hung Hyangjae	University of Maryland
Smith, Wallace	Office of Naval Research
Sponner, Stephen	Oak ridge National Laboratory
Strakna, Timothy	University of Maryland
Sun, Jian-Xia	Shanghai University of Science and Technology
Swanson, Nils	American Ceramic Society
Vandiver, Pamela	Smithsonian Institute
Vinod, Natarajan	University of Maryland
Wang, Yushu	University of Maryland
Wei, Lanhua	Wayne State University
Xu, Huakun	University of Maryland

Ying, Tsi-Neng	University of Maryland
Zhang, Guangming	University of Maryland
Zimmerman, Michael	Northwestern University

OUTPUTS AND INTERACTIONS

TECHNICAL PUBLICATIONS

DATA TECHNOLOGIES

R. G. Munro and S. J. Dapkunas, Corrosion Characteristics of Silicon Carbide and Silicon Nitride, J. Res. NIST 98 (5) 607-631 (1993).

R. G. Munro and S. J. Dapkunas, Corrosion of Ceramics in Coal-Combustion Applications, Proceedings of the Ninth Annual Coal Preparation, Utilization, and Environmental Control Contractors Conference, pp. 202-209 (1993).

R. G. Munro, submitted to ASTM, The Role of Corrosion in a Material Selector Expert System for Advanced Structural Ceramics.

Begley, E.F. and Lindsay, C.G., "A Multimedia Tutorial on Phase Equilibria Diagrams," American Ceramic Society Bulletin, Volume 72, No. 12, pp. 103-104, 1993.

John Rumble, Jr. and Joseph Carpenter, Jr., "Materials 'STEP' into the Future," Advanced Materials and Processes, vol. 142, No. 4, October 1992, pages 23-27.

POWDER CHARACTERIZATION AND PROCESSING

Cline J. P., "Powder Diffraction SRMs", Brochure available from the SRMP office, January 1994.

Rosetti G. A., Cross E., and Cline J. P., "Structural Characteristics and Ferroelectric Phase Transition Behavior of Lanthanum-Substituted Lead Titanate" submitted to Journal of Materials Science, 1993.

Kreider K. G., Tarlov M. J., and Cline J. P., "Sputtered Thin Film pH Electrodes of Platinum, Palladium, Ruthenium and Iridium Oxides" submitted to Sensors and Actuators, 1993.

Kalceff W., Cline J. P., and Von Dreele R. B., "Size/Strain Broadening Analysis of SRM 676 Candidate Materials", submitted to Advances in X-ray Analysis, vol 37, 1993.

Cline J. P., Handwerker C. A., Vaudin M. D., and Blendell J. E., "Texture Measurement of Sintered Alumina Using the March-Dollase Function" submitted to Advances in X-ray Analysis, vol 37, 1993.

Cline J. P., "An Overview of NIST Powder Diffraction Standard Reference Materials," submitted to the Proceedings of The Third European Powder Diffraction Conference, 1993.

Wang P. S., Malghan, S. G., Dapkunas, S. J., Hens, K. F., Raman, R., "NMR Characterization of Injection Molded Alumina Green Compacts: I. Nuclear Spin-Spin Relaxation," submitted to the Journal of Materials Science, 1993.

Wang P. S., Malghan S. G., Dapkunas S. J., Hens K. F., Raman R., "NMR Characterization of Injection Molded Alumina Green Compacts: II. T_2-Weighted Proton Imaging," submitted to the Journal of Materials Science, 1993.

Wang P. S., Malghan S. G., Hsu S. M., Wittberg T. N., "An X-Ray Induced AES Study of the Effect of Chemically Bound Hydrogen on the Oxidation Kinetics of a Si_3N_4 Powder," submitted to the Surface and Interface Analysis, 1993.

Hackley V. A. and Malghan, S. G., "Polyelectrolytes as Dispersants in Colloidal Processing of Silicon Nitride Ceramics," *Polymer Preprints*, **34**, 1024 (1993).

Hackley V. A. and Malghan S. G., "Investigation of Parameters and Secondary Components Affecting the Electroacoustic Analysis of Silicon Nitride Powders," in *Electroacoustics for Characterization of Particulates and Suspensions*, *NIST Special Publication 856*, S.G. Malghan, Ed. (U.S. Department of Commerce, Technology Administration 1993) p 161.

Hackley V. A., Wang P. S. and Malghan S. G., "Effects of Soxhlet Extraction on the Surface Oxide Layer of Silicon Nitride Powders," *Mat. Chem. Phys.*, **36**, 112 (1993).

Hackley V. A. and Malghan, S. G., "The Surface Chemistry of Silicon Nitride Powder in the Presence of Dissolved Ions," submitted to *J. Mat. Sci.* (1993).

Shull R. D., McMichael R. D., Ritter J. J., Swartzendruber L. J. and Bennett L. H., "Nanocomposite Magnetic Refrigerants," Proc. 7th International Cryocooler Conference, Santa Fe, NM, Nov. 1992.
Shull R. D., McMichael R. D., Ritter J. J. and Bennett L. H., "Nanocomposites for Magnetic Refrigeration," Proc. MRS Conf., Dec 3, 1992, Boston MA.

Ritter J. J., "A Chemical Synthesis of Bismuth Telluride and Bismuth Telluride Composite Thermoelectric Refrigerants," submitted to Chemistry of Materials.

Shull R. D., Kerch H. M. and Ritter J. J., "Magnetic Properties of Colloidal Silica: Potassium Silicate Gel/Iron Nanocomposites," J. App'd Phys., 38th Conf. on Magnetism and Magnetic Matl's, Minneapolis MN, Nov. 15-19, 1993.

McMichael R. D., Ritter J. J. and Shull R. D., "Enhanced Magnetocaloric Effect in $Gd_3Ga_{5-x}Fe_xO_{12}$," J.App'd Phys., 73, 6946-6948, (1993).

Shull R. D., McMichael R. D., and Ritter J. J., "Magnetic Nanocomposites for Magnetic Refrigeration," Nanostructured Materials, 2, (1993), 205-211. Oct. 1992.

Deb K. K., Hill M. D. and Kelly J. F., "Pyroelectric Characteristics of Modified Barium Titanate Ceramics," Journal of Materials Research Vol. 7, No. 12, Dec. 1992.

Chen W., Pechenik A., Dapkunas, S. J., Piermarini G. J., and Malghan S. G., "Novel Equipment for the Study of the Compaction of Fine Powders," accepted for publication by J. American Ceramic Society, October 1993.

Cox B. N., Carter W. C., and Fleck N. A., "A Binary Model for Failure of Textile Composites," submitted to Acta Met., December 1993.

Malghan S. G., Premachandran R. S., and Pei P. T., "Mechanistic Understanding of Silicon Nitride Dispersion Using Cationic and Anionic Polyelectrolytes," accepted for publication by Powder Technology, September 1993.

Premachandran R. S. and Malghan S. G., "Dispersion Characteristics of Ceramic Powders in the Application of Cationic and Anionic Polyacrylates," accepted for publication by Powders Technology, October 1993.

Wang, P. S., Malghan, S. G., Hsu, S. M., and Wittberg, T. N., "Oxidation of Surface-Treated α-SiC Platelets Studied by XPS and Bremsstrahlung-Excited AES," Surface and Interface Analysis., 20, 105-110, 1993.

MECHANICAL PROPERTIES

Lawn, B. R., Padture, N. P., Braun, L. M., and Bennison, S. J., "Model for Toughness-Curves in Two-Phase Ceramics: I. Basic Fracture Mechanics," J. Am. Ceram. Soc., 76 [9] 2235-40 (1993).

Padture, N. P., Runyan, J. L., Braun, L. M., Bennison, S. J., Lawn, B. R., "Model for Toughness-Curves in Two-Phase Ceramics: II. Microstructural Variables," J. Am. Ceram. Soc., 76[9] 2241-47 (1993).

Braun, L. M. and Cook, R. F., "Effect of Stress on Trapped Cracks in Y-TZP," Science and Technology of Zirconia V, S.P.S. Badwal, M. J. Bannister, and R.H. J. Hannink eds., Technomic Publishing Company, Inc., Lancaster, PA 1993.

"A Methodology to Predict Creep Life for Advanced Ceramics Using Continuum Damage Mechanics Concepts" T.-J. Chuang and S. F. Duffy to be published in ASTM STP 1201, 1993.

Chuang, T.-J., Chu, J.-L. and Lee, S., "High Temperature Crack Growth in Dissimilar Media," Proc. 8th International Conference on Fracture, Keiv, Ukraine, June 8-14, 1993.

Krause, R.F. Jr., "Flat and Rising R-Curves for Elliptical Surface Cracks from Indentation and Superposed Flexure," (in press) J. Am. Ceram. Soc., 77 (1994).

Krause, R.F. Jr., and Wiederhorn, S.M., "Tensile Creep of a Silicon Nitride Ceramic," Silicon Nitride 93, Proceedings of the International Conference on Silicon Nitride-Based Ceramics, Stuttgart, Germany, Oct 1993, Trans Tech Publications Ltd., Switzerland, 1994, pp 619-624.

Luecke, W.E., Wiederhorn, S.M., Hockey, B.J. and Long, G.G., "Cavity Evolution during Tensile Creep of Si_3N_4," Mat. Res. Soc. Symp. Proc. **287** 467-472 (1993).

Luecke, W.E. and Wiederhorn, S.M., "Tension/Compression Creep Asymmetry in Si_3N_4," Silicon Nitride 93, Proceedings of the International Conference on Silicon NItride-Based Ceramics, Stuttgart, Germany, Oct 1993, Trans Tech Publications Ltd., Switzerland, 1994, pp 587-592.

Romero, J.C., Arsenault, R.J., and Krause, R.F. Jr., "Microstructural Changes During Creep of a SiC/$A\ell_2O_3$ Composite," Mater. Sci. and Eng. A., (1994).

Wiederhorn, S.M., Quinn, G.D., and Krause, R.F. Jr., "Fracture Mechanism Maps: Their Applicability to Silicon Nitride," Life Prediction Methodologies and Data for Ceramic Materials, ASTM STP 1201, C.R. Brinkman and S.F. Duffy, Editors, American Society for Testing and Materials, Philadelphia, 1993.

Wiederhorn, S.M., Quinn, G.C., and Krause, R.F. Jr., "High Temperature Structural Reliability of Silicon Nitride," Silicon Nitride 93, Proceedings of the International Conference on Silicon Nitride-Based Ceramics, Stuttgart, Germany, Oct 1993, Trans Tech Publications Ltd., Switzerland, 1994, pp 575-580.

Horn, R.G., Smith, D.T., and Grabbe, A., *Nature* **366**, 442-443 (1993).

Jahanmir, S., and Fischer, T. E., "Friction and Wear of Advanced Ceramics," Tribology Handbook, Vol 3, in press.

Gangopadhyay, A., and Jahanmir, S., "Self-lubricating Ceramic Matrix Composites," Friction and Wear of Advanced Ceramics, S. Jahanmir (Ed.) Marcel Dekker, New York, NY, (1993) 163-198.

Dong, X., and Jahanmir, S., "Wear Transition Diagram for Silicon Nitride," Wear, 165 (1993) 169-180.

Jahanmir, S., "Advanced Ceramics in Tribological Applications," Friction and Wear of AdvancedCeramics, S. Jahanmir (Ed.) Marcel Dekker, New York, NY, (1993) 3-13.

Jahanmir, S. and Dong, X., "Wear Mechanisms of Aluminum Oxide Ceramics," Friction and Wear ofAdvanced Ceramics, S. Jahanmir (Ed.) Marcel Dekker, New York, NY, (1993) 15-50.

Alexeyev, N. and Jahanmir, S., "Mechanics of Friction in Self-lubricating Composite Materials, Part 1. Mechanics of Second Phase Deformation and Motion," Wear 166 (1993) 41-48.

Alexeyev, N. and Jahanmir, S., "Mechanics of Friction in Self-lubricating Composite Materials, Part 2. Deformation of the Interfacial Film," Wear 166 (1993) 49-54.

Jahanmir, S. and Dong, X., "Wear Transition Diagrams for Ceramics," Proceedings of the 1st International Symposium on Tribology, Y. S. Jin (Ed.), International Academic Publishers, Beijing, PRC, (1993) 362-371.

Jahanmir, S. (Ed.), Friction and Wear of Ceramics, Marcel Dekker, New York, NY (1993).

Jahanmir, S. (Ed.), Machining of Advanced Materials, Proceedings of the International Conference on Machining of Advanced Materials, National Institute of Standards and Technology, Special Publication 847, Government Printing Office, Washington, DC (1993).

Cai, Hongda, Faber, Katherine T., and Fuller, Edwin R. Jr., "Crack Bridging by Inclined Fibers/Whiskers in Ceramic Composites" J. Am. Ceram. Soc., **75** [11], 3111-3117 (November 1992).

Paulik, S. W., Faber, K. T., and Fuller, E. R. Jr., "Development of Textured Microstructures in Ceramics with Large Thermal Expansion Anisotropy," J. Am. Ceram. Soc., **77** [2], (1994).

SURFACE PROPERTIES

He, C., Wang, Y. S., Wallace, J. S., and Hsu, S. M., "The Effect of Microstructure on the Wear Transition of Zirconia Toughened Alumina," Wear, 162-164, p. 314-321, 1993.

Ying, T. N., and Hsu, S. M., "Asperity-Asperity contact mechanisms simulated by a Two-ball Collision Apparatus," To appear in Wear in 1993.

Wang, J. C., and Hsu, S. M., "Chemically Assisted Machining of Ceramics," accepted for publication in J. of Tribology.

Lee, S. C., Hsu, S. M., and Shen, M. S., "Ceramic Wear Maps: Zirconia," Journal of the ACerS, 76, [8], 1937-47, 1993.

Zhang, P. Y., and Hsu, S. M., "Inhibition Mechanisms of Some Antioxidants in Lubricant Oxidation Using a Chemiluminescence Technique," submitted to J. of Lub. Sci.

Hsu, S. M., Shen, M., Klaus, E. E., Cheng, H. S., and Lacey, P., "A Mechano-Chemical Model: Reaction Temperatures in a Concentrated Contact," submitted to Wear.

Ruff, A. W., "Multilayer Coatings for Tribological Applications," A. W. Ruff, Proceedings of a DOE Workshop on Coatings for Advanced Heat Engines, Monterey, CA, 1993, pp. IV-45 to 54.

Ruff, A. W., and Peterson, M. B., "Wear of Self-lubricating Composite Materials vs. MoS_2 Films," Wear 162-164, 492-497, 1993. (also in Wear of Materials-1993, pp. 492-497).

"Standard on Calculating and Reporting Measure of Precision Using Data From Interlaboratory Wear or Erosion Tests," ASTM G-117 (93) (author: A. W. Ruff).

"Standard Data Format for Computerization of Wear Test Data," ASTM G-118 (93) (author: A. W. Ruff)

Ruff, A. W., and Bayer, R. G., Wear Test Selection for Design and Application, eds., ASTM STP 1199, Philadelphia, PA, 1993.

Ruff, A. W., Shin, H., and Evans, C. J.,"Chemo-mechanical Damage During Diamond Tool Scratching of CVD Silicon Carbide," Proc. ASME Symposium on Contact Problems and Surface Interactions in Manufacturing and Tribological Systems, ASME, 1993.

Chen, Y-M., Ruff, A. W., and Dally, J. W., "Numerical Simulation of the Micro-indentation Process," Proc. ASME Symposium on Contact Problems and Surface Interactions in Manufacturing and Tribological Systems, ASME, 1993.

Chen, Y-M., Ruff, A. W., and Dally, J. W., "A Method for Determining Material Properties from Instrumented Micro-indentation Experiments," Y. M. Chen, A. W. Ruff, and J. W. Dally, J. Matls. Research, 1993, in press.

Armstrong, R. W., Shin, H., and Ruff, A. W., "Elastic/Plastic Effects During Low-load Hardness Testing of Copper," submitted to Acta Met. 1993.

ELECTRONIC MATERIALS

Rawn, C. J., Roth, R. S., Burton, B. P., Hill, M. D., "Phase Equilibria and Crystal Chemistry in Portions of the System SrO-CaO-$\frac{1}{2}Bi_2O_3$-CuO, Part V The System SrO-CaO-$\frac{1}{2}Bi_2O_3$, accepted, Journal of the American Ceramic Society.

Wong-Ng, W., Cook, L. P., Paretzkin, B., Hill, M. D., Stalick, J. K., "Crystal Chemistry and Phase Equilibrium Studies of the BaO-$\frac{1}{2}R_2O_3$-CuO_x System in Air. VI. R-Neodymium"; in press Journal Less Common Metals.

Wong-Ng, W., Cook, L. P., "Eutectic Minimum Melting in the System BaO-$\frac{1}{2}Y_2O_3$-CuO_x in Air"; in press Journal of the American Ceramic Soc.

Burton, B. P., Pasture, A., "LMTO/CVM Calculations of BCC Based Phase Ordering in the System Fe-Be"; Proceedings of the NATO/ASI Statics & Dynamics on ordering in Alloys, 6/21/92-7/3/92, Rhodes, Greece, in press.

Rhine, W. E., Hallock, R. B., Davis, W. M., and Wong-Ng, W., "Synthesis and Crystal Structure of Barium Titanyl Oxalate, $BaTi(O)C_2O_4)_2 \cdot 5H_2O$: A Molecular Precursor for $BaTiO_3$. Chemistry of Materials, 4, 1208, 1993.

Hill, M. D., Blendell, J. E., Vaudin, M. D., and Chiang, C. K., "Effect of Processing Conditions on the Microstructure and Superconducting Properites of Sintered $YBa_2Cu_3O_{6+x}$ Superconductors; Journal of the American Ceramic Society, in press.

Burton, B. P., Rawn, C. J., Roth, R. S., and Hwang, N. M., "Phase Equilibria and Crystal Chemistry in Portions of the System SrO-CaO-Bi_2O_3-CuO, Part IV - The System CaO-Bi_2O_3-CuO; J. NIST, 98, 469-516, (1993).

Smilgys, R. V., Hsieh, T. J., Robey, S. W., and Chiang, C.K., "Reactive Coevaporation of DyBaCuO Superconducting Films on MgO (100): The Effect of Substrate Annealing; J. Vac. Sci. & Tech. A 11(4), 1993.

Freiman, S. W., and Hill, M. D., "Mechanical Reliability of High Tc Superconductors, Proc. of Fifth US-Japan Workshop on High Tc Materials.

Wong-Ng, W., Mighell, A., and Karen, V., "Materials Research Society, Short Course on Crystallographic Databases for Chemical and Materials Analysis; Boston, Ma., Nov. 1992.

Wiederhorn, S. M., Hockey, B. J., Handwerker, C. A., and Blendell, J. E., "On the Wetting of Grain Boundaries in Aluminum Oxide", Journal of the American Ceramic Soc., in press.

Sora, I. N., Wong-Ng, W., Roth, R. S., Rawn, C.J., and Burton, B. P.,"X-Ray and Neutron Diffraction Study of $CaBi_2O_4$," J. Chem. Mater., in press.

Wong-Ng, W., "Structures and X-Ray Patterns of Compounds in the Sr-Nd-Cu-O System", to be published in the Powder Diffraction Journal.

Lee. H. M., Chuang, T. J., Chiang, C. K., Cook, L. P., and Scheck, P. K., "Crack Development in Pulsed Laser-Deposited PZT Thin Films, MRS Symposium Proceedings on Laser Deposition, eds. B. Braren, J. Dubowski, and D. Norton, J. Mat'ls. Soc., v. 285, 409-413, 1993.

Lee, B. W., Lee, H. M., Cook, L. P., Schenck, P. K., Paul, A., Wong-Ng, W., Chiang, C. K., Brody, P. S., Rod, B. J. and Bennett, K. W., "Preparation of $PbTiO_3Pb(Mg_{0.5}W_{0.5})O_3$ Thin Films Using Pulsed Laser Deposition, MRS, Symposium Proceedings on Laser Deposition.

Lindsay, C. G., Rawn, C. J., Roth, R. S., "Powder X-Ray Diffraction Data for $Ba_4ZnTiu_{11}O_{27}$ and $Ba_2ZnTi_5O_{13}$," Journal: Powder Diffraction, in press.

Carpenter, J. A. Jr., Piermarini, G. J., Dickens, B., Manning, J. R., Read, D. T., Mattis, K. G., Kreider, K. G., Mattis, R. L., Evans, R.,"NIST/NCMS Program on Electronic Packaging: First Update", to be published in the proceedings of the Symposium on Microelectronic and Optoelectronic Packaging, American Ceramic Society, San Franciso, CA Nov. 1-4, 1992.

Russell, T. P., Miller, P. J., Piermarini, G. J., and Block, S., "Pressure/Temperature/Reaction Phase Diagrams for Several Nitramine Compounds", to be published in the Journal Proceedings of MRS Vol. 296, 119 (1993).

Handwerker, C. A., Blendell, J. E., Interrante, C. G., and Ahn, T. M., "The Potential Role of Diffusion-Induced Grain-Boundary Migration in Extended Life Prediction", Proceedings MRS Mtg, Nov. 92.

Gallas, M. R., and Piermarini, G. J., "The Bulk Modulus and Young's Modulus of Nanocrystalline -γ-Alumina", submitted to Journal of the American Ceramic Society.

Lindsay, C. G., White, G. S., Freiman, S. W., and Wong-Ng, W.,"A Molecular Orbital Study of the Environmentally-Enhanced Crack Growth Process in Silica," submitted to Journal of Amer. Ceram. Soc. 1993.

Pechenik, A., Piermarini, G. J., and Danforth, S. C., "Low Temperature Densification of Silicon Nitride Nanoglass, " Proc. of 2nd International Conference on Nanostructured Materials, Cancun, New Mexico, Sept. 23, 1992.

Chen, Bai-Hao, Wong-Ng, W., and Eichhorn, B., " Structural Reinvestigation of $Ba_3Zr_2S_7$ by Single Crystal X-Ray Diffraction".

Wong-Ng, W., Roth, R. S., Sunshine, S., and Rawn, C. J., "Refined Crystal Structure of Willemite, $Zn_2[SiO_4]$."

Wong-Ng, W., "X-Ray Diffraction Patterns for BaR_2PdO_5."

Mathew, M. and Wong-Ng, W., "Crystal Structure of a New Monoclinic Form of Potassium Diyhydrogren Phosphate Containing Orthophosphacidium Ion, $(H_4PO_4)^+$, Journal of Solid State Chemistry, in press.

Meng, W. G., Vaudin, M. D., Bartholemeusz, M. F., and Wert, J. A., "Experimental Assessment of Crack Tip Dislocation Emission Models for an Ald67Crd8Tid25 Intermetallic Alloy," to be published in Met Trans A.

Bennett, K. W., Brody, P. S., Rod, B. J., Cook, L. P., Schenck, P. K., and Dey, S., "Dielectric Constant and Hysteresis Loop Remanent Polarization From 100 Hz to 2 MHz for Thin Ferroelectric Films," Ferroelectric Thin Films II, A. I. Kingon, ed., v. 243, 507-512, 1993.

OPTICAL MATERIALS

Kaiser, D.L., Vaudin, M.D., Gillen, G., Hwang, C.-S., Robins, L.H. and Rotter, L.D., "Growth and Characterization of Barium Titanate Thin Films by Metalorganic Chemical Vapor Deposition (MOCVD)," J. Crystal Growth, in press.

Kaiser, D.L., Vaudin, M.D., Gillen, G., Hwang, C.-S., Robins, L.H. and Rotter, L.D., "Growth of $BaTiO_3$ Thin Films by MOCVD," MRS Proceedings, Symposium on Metal-Organic CHemical Vapor Deposition of Electronic Ceramics, Fall, 1993, in press.

Robins, L.H., Farabaugh, E.N. and Feldman, A., "Cathodoluminescence Spectroscopy of Free and Bound Excitons in Chemical-Vapor-Deposited Diamond" Physical Review B, in press.

Robins, L.H. and Black, D.R. "Defect Mapping of a Synthetic Diamond Single Crystal by Cathodoluminescence Spectroscopy", Journal of Materials Research, in press.

Jin, S., Fanciulli, M., Moustakas, T.D. and Robins, L.H., "Electronic Characterization of Diamond Films Prepared by Electron Cyclotron Resonance Microwave Plasma", in Diamond Films '93, Proceedings of the Fourth European Conference on Diamond, Diamond-like and Related Coatings, in press.

Shechtman, D., Hutchinson, J.L., Robins, L.H., Farabaugh, E.N. and Feldman, A., "Growth Defects in Diamond Films", J. Mater. Res. 8 (3), 473-479, (1993).

Shechtman, D., Feldman, A., Vaudin, M.D. and Hutchison, J.L., "Moire-Fringe Images of Twin Boundaries in Chemical Vapor Deposited Diamond", Appl. Phys. Letters **62**, 487-489 (1993).

Feldman, A., Beetz, C.P., Klocek, P. and Lu G., "Workshop on Characterizing Diamond Films II", NISTIR 5198, May 1993.

Feldman, A., Beetz, C.P., Klocek, P. and Lu, G., "Workshop on Characterizing Diamond Films II", Conference Report, J. of Res. NIST, **98**, 375-381 (1993).

Feldman, A. and Frederikse, H.P.R., "Measuring the Thermal Diffusivity of Chemical Vapor Deposited Diamond" in Proceedings of the Applied Diamond Conference 1993, the Second International Conference on the Applications of Diamond Films and Related Materials, (MYU, Tokyo, 1993) pp. 261-268.

Turchinskaya, M., Kaiser, D.L., Gayle, F.W., Shapiro, A.J., Roytburd, A., Vlasko-Vlasov, V., Polyanskii, A. and Nikitenko, V., "Direct Observation of Anisotropic Flux Penetration in Twinned $YBa_2Cu_3O_{7-x}$ Single and Polycrystals," Physica C **216**, 205-210 (1993).

Turchinskaya, M., Kaiser, D.L., Gayle, F.W., Shapiro, A.J., Roytburd, A., Dorosinskii, L.A., Nikitenko, V.I., Polyanskii, A.A. and Vlasko-Vlasov, V.K., "Real-Time Observation of the Effect of Grain Boundaries on Magnetization of $YBa_2Cu_3O_{7-x}$ Polycrystals," Physica C, in press.

MATERIALS MICROSTRUCTURE CHARACTERIZAITON

Allen, A. J., and Jemian, P. R., "The Effect of the Shape Function of Small Angle Scattering Analysis by Maximum Entropy Method," J. of Applied Crystallography, (1993).

Allen, A. J., and Berk, N. F., "Analysis of SAS Data Dominated by Multiple Scattering for Systems Containing Eccentrically-Shaped Particles or Pores, J. of Applied Crystallography, (1993).

Black, D. R., Larson, D. L., Silberstein, R. P., DiMarzio, D., Carlson, F. C., Gillies, D., Long, G., Dudley, M., and Wu, J., "Compositional, Strain-Contour, and Property Mapping of CdZnTe Boules and Wafers," Semiconductor Science and Technology, (1993).

Black, D. R., Kycia, S. W., Goldman, A. I., Lograsso, T. A., Delaney, D. W., Sutton, M., Dufresne, E., Bruning, R., and Rodricks, B., "Dynamical X-ray Diffraction from an Icosahedral Quasicrystal," Physical Review Letters, (1993).

Black, D. R., and Robins, L. H., "Defect mapping in synthetic single-crystal diamond by cathodoluminescence spectroscopy," J. of Materials Research, (1993).

Bouldin, C. E., Tan, Z., Heald, S. M., Rapposch, M., and Woicik, J. C., "Gold-Induced Germanium Crystallization," Physical Review B, (1993).

Fischer, D. A., Moodenbaugh, A. R., and Xu, Y., "Oxygen K Near-Edge X-Ray Absorption Spectroscopy of $La_{2-x}M_xCu0_4$(M=Ca, Sr, and Ba): x Dependence of Hole State Density," Physical Review B (1993).

Fischer, D. A., Srivatsa, A. R., Borra, R. T., and Skotheim, T. A., "A Near Edge X-ray Absorption Study of Diamond-Like Nanocomposites," Proceedings of the Third International Symposium on Diamond Materials, Honolulu, HI, May 16-21, 1993.

Fischer, D. A., Purdie, D., Muryn, C. A., Crook, S., Wincott, P. L., and Thornton, G., "Potassium bond site in ZnO(0001)p(2x2)K," Surface Science Letters, (1993).

Fischer, D. A., Davis, S. M., Meitzner, G. D., and Gland, J., "Studies of Fluorine in Catalysts with Ultra-Soft X-ray Absorption Spectroscopy," J. of Catalysis, (1993).

Fischer, D. A., Mitchell, G. E., DeKoven, B. M., Yeh, A. T., Gland, J. L., and Moodenbaugh, A. R., "Ultra-soft X-ray Absorption Spectrocopy: A Bulk and Surface Probe of Materials," MRS Proceedings "Applications of Synchrotron Radiation Techniques to Materials Science" MRS Spring Mtg, San Francisco, CA, April 12-16, 1993.

Fischer, D. A., Huang, S. X., and Gland, J. L., "Aniline Hydrogenolysis on the Pt(111) Single Crystal Surface: Mechanisms for C-N Bond Activation," ACS Symposium on "Mechanism of HDS/HDN Reactions" Chicago, IL, August 22-27, 1993.

Fischer, D. A., Hastie, G. P., Roberts, K. J., Adams, D., and Meitzner, G., "Investigating the Structural Chemistry at the Interface Formed Between Zinc Dialkyldithiophosphate (ZDDP) and Mild Steel Using Ultra-Soft X-ray Absorption Spectroscopy," Japanese J. Applied Physics, Proceedings 7th International Conference on X-ray Absorption Fine Structure, Kobe, Japan, (1993).

Long, G. G., Jemian, P. R., and Weertman, J. R., "A Gradient Method for Anomalous Small-Angle X-ray Scattering," Journal of Applied Crystallography, (1993).

Long, G. G., Krebs, L. A., Kruger, J., Ankner, J. F., Satija, S. K., Wiesler, D. G., and Majkrzak, C. F., "Neutron Reflectivity Studies of the Passive Film on Iron," Proceedings of Symposium on "Oxide Films on Metals and Alloys," ed. by Barry MacDougall. The Electrochemical Society, Toronto, October 11-16, 1992.

Long, G. G., Krebs, L. A., Kruger, J., Wiesler, D. G., Ankner, J. F., Majkrzak, C. F., and Satija, S. K., "Passive Film Studies Using Neutron Reflectivity," Proceedings of the 12th International Congress on Corrosion, Houston, TX, September 19-24, 1993.

Long, G. G., Luecke, W., Wiederhorn, S. M., and Hockey, B. J., "Cavity Evolution During Tensile Creep of Si_3N_4," Materials Research Society Symposium Proceedings, Boston, MA, **287**, 467-472 (1993).

Woicik, J. C., Kendelewicz, T., Miyano, K. E., Herrera-Gomez, A., Cowan, P. L., Karlin, B. A., Bouldin, C. E., Pianetta, P., and Spicer, W. E., "Structural Study of Sb Monolayers on Ga As(110) with the X-ray Standing-wave Technique," Physical Review B, (1993).

Woicik, J. C., Kendelewicz, T., Herrera-Gomez, A., Andrews, A. B., Kim Boong Soo, Cowan, P. L., Miyano, K. E., Bouldin, C. E., Karlin, B. A., Herman, G. S., Erskine, J. L., Pianetta, P., and Spicer, W. E., "Adatom Location on the Si(111) 7x7 and Si(111) $\sqrt{3}$x$\sqrt{3}$-In Surfaces by the X-ray Standing Wave and Photoemission Techniques," J. of Vac. Science and Tech., (1993).

Woicik, J. C., Herrera-Gomez, A., Kendelewicz, T., Miyano, K. E., Pianetta, P., Southworth, S., Cowan, P. L., Karlin, B. A., and Spicer, W. E., "Determination of the Geometrical Configuration of Bi on GaAs(110) by X-ray Standing Wave Triangulation," J. of Vac. Science and Tech. A, (1993).

Woicik, J. C., Kendelewicz, T., Herrera-Gomez, A., Miyano, K. E., Cowan, P. L., Karlin, B. A., Pianetta, P., and Spicer, W. E., "X-ray Standing Wave Study of the Sb/GaAs(110) Interface Structure," J. Vac. Science & Tech. A, (1993).

Woicik, J. C., Kendelewicz, T., Herrera-Gomez, A., Miyano, K. E., Cowan, P. L., Bouldin, C. E., Pianetta, P., and Spicer, W. E., "The Si(111)$\sqrt{3}$x$\sqrt{3}$-In Interface: An Unrelaxed T_4 Geometry," Physical Review B, (1993).

Woicik, J. C., Kendelewicz, T., Miyano, K. E., Herrera-Gomez, A., Cowan, P. L., Pianetta, P., and Spicer, W. E., "Structure of Sb Monolayers on Ge(111)2x1: A Combined Study Using Core Level Photoemission, X-ray Standing Waves, and Surface Extended X-ray Absorption Fine Structure," Physical Review B (1993).

Steiner, Bruce, Tseng, Wen, Comas, James, Laor, Uri, Dobbyn, Ronald C., and Rajan, Krishna, "Defect Formation in Semiconductor Layers during Epitaxial Growth," J. Crystal Growth, **128**, 543-549 (1993)

Steiner, Bruce, Comas, James, Tseng, Wen, and Laor, Uri, "The influence of lattice mismatch on indium phosphide based high electron mobility transistor (HEMT) structures observed in high resolution monochromatic synchrotron x-radiation diffraction imaging," Proc. Mat. Res. Soc. **281**, 127-132 (1993)

Steiner, Bruce, Comas, James, Tseng, Wen, Laor, Uri, and Dobbyn, Ronald C., "Defects in III-V Materials and the Accommodation of Strain in Layered Semiconductors," J. Elect. Mat. **22**, 725-738 (1993)

CERAMICS DIVISION PATENTS

1993

Oxygen-Containing Organic Compounds as Boundary Lubricants for Silicon Nitride Ceramics (D)	R. S. Gates S. M. Hsu
A Method of Obtaining High Green Density from Ceramic Powders (D)	S. G. Malghan R. S. Premachandran.
Method of Producing a Smooth Plate of Diamond (I)	A. Feldman E. N. Farabaugh
Asymmetric Bragg diffraction microscope (I)	R. Spal
Method for Fabrication of Dense Compacts from Nanosize Particles Using High pressures and Cryogenic Temperatures (P)	A. Pechenik G. J.Piermarini

1992

Novel Method of Bonding Materials Together - "Nanoglue" (P)	D. T. Smith R. G. Horn, A. Grabbe
Coprecipitation Synthesis of Precursors to Bismuth-Containing Superconductors (I)	J. Ritter
A Super Stable High-Temperature Liquid Lubricant Containing a Unique Antioxidant and Additive Solulubilizing Ternary System (D)	J. Perez, C. Ku, Y. M. Zhang
A Chemical Assisted Process for Rapid Machining of Tough Ceramics (D)	J. Wang, S. M. Hsu
A Cutting Fluid Additive for Machining of Ceramics (P)	S. Jahanmir, G. Zhang
Hydroxyl Containing Organic Compounds as Boundary Lubricants for Silicon Nitride Ceramics (D)	R. S. Gates, S. M. Hsu
A Process to Lubricate Titanium with Chlorinated Hydrocarbons (D)	J. Wang, S. M. Hsu
A Process to Machine Titanium Using Chlorinated Hydrocarbons (D)	J. Wang, S. M. Hsu

Methods of Reducing Wear on SiC Ceramic Surfaces (P)	D. E. Deckman S. M. Hsu
Detergent and Dispersant Type Organic Compounds as Boundary Lubricants for Silicon Nitride Ceramics (D)	R. S. Gates S. M. Hsu

1991

Diamond Coated Laminates and Methods of Producing Same (D)	A. Feldman E. N. Farabaugh
High Resolution X-Ray Microtomographic Detector (P)	R. D. Spal R. C. Dobbyn M. Kuriyama
A Colloidal Processing Method for Coating Ceramic Reinforcing Agents (I)	S. Malghan C. Ostertag
U.S. Patent No. 5,039,550, August 1991	
Process for the Fabrication of Ceramic Monoliths by Laser-Assisted Chemical Vapor Infiltration (I)	J. Ritter
A Method for Making Translucent High Purity Transparent Silicon Nitride (P)	A. Pechenik G. Piermarini S. Block S. Danforth

1990

Novel Synergistic Additive Packages Containing High Molecular Weight Antioxidants for High Temperature Lubricants (P)	S. Hsu J. Perez C. Ku Y. Zhang
Low Energy (Thermal) Neutron Absorbing Glass (A)	D. Blackburn (Retired) C. Stone D. Cranmer D. Kauffman J. Grudl
Process for Elimination of Twins in Perovskite-Type Superconducting Single Crystals (D)	D. Kaiser F. Gayle

A Method for Fabrication of Materials from Nano-Sized Particles Using High Pressure and Cryogenic Temperatures (I)	A. Pechenik G. Piermarini
Aluminum Hydroxides as Solid Lubricants U.S. Patent 4919829, issued April 24, 1990	R. Gates S. Hsu

1989

Ultraviolet Transmitting Glass for 308mm Ring Dye Laser (D)	D. Blackburn D. Cranmer D. Kauffman
Buffered Cell for Sintering of High T_c Thallium Containing Ceramics (D)	L. Cook
Polished Plates of Chemical Vapor Deposited Diamond (A)	A. Feldman E. Farabaugh
Additive Packages Containing High Molecular Weight Antioxidants for High Temp Lubricant (D)	S. Hsu J. Perez C. Ku
A Novel Fluid to Solubilize High Temperature Liquid Lubricant Antioxidants (D)	J. Perez C. Ku S. Hsu
A Process for the Controlled Preparation of a Composite of Ultra-Fine Magnetic Particles Homogeneously Dispersed in a Dielectric Matrix (P)	J. Ritter R. Shull
Optical Sensor: Molecular Orientation and Viscosity of Polymeric Materials (D)	A. Bur R. Lowry R. Roth
Elimination of Twins in Perovskite-Type Superconducting Single Crystals (D)	F. Gayle D. Kaiser

1988

Stress-Free Sintering of Fiber-Reinforced Ceramic Composites (D)	C. Ostertag
Electrode Array for Analysis of Particles in Slurries (D)	A. Dragoo

Quantitative & Qualitative Technique for Assessing Stresses During Densification (D)	C. Ostertag
Process for the Preparation of Fiber-Reinforced Ceramic Matrix Composites (A)	W. Haller U. Deshmukh
A Process for the Chemical Synthesis and Forming of BiPbSrCaCuO and BiSrCaCuO High Temperature Superconductors Materials (D)	J. Ritter
Low Temperature Chemical Synthesis of Precursors to $BiCaSrCuO_x$ High Temperature Superconductor Powders (D)	J. Ritter
High Pressure Process for Producing Transformation Toughened Ceramics (I)	S. Block G. Piermarini
Superconductor-Polymer Composite (D)	A. DeReggi C. Chiang G. David

(D) = INVENTION DISCLOSURE
(P) = PENDING DECISION BY PATENT OFFICE
(A) = INVENTION ALLOWED BY PATENT OFFICE
(I) = PATENT ISSUED

CONFERENCES AND WORKSHOPS SPONSORED

A workshop was organized by S. G. Malghan on electroacoustics for characterization of powders and slurries. The workshop addressed recent developments in measurements, theory and application of the technique to inorganic and organic systems.

Silicon Nitride 93: International Conference on Silicon Nitride-Based Ceramics University of Stuttgart, Stuttgart, Germany, October 4-6, 1993. E.R. Fuller Member, International Advisory Committee

NISS-NIST Workshop on Statistics and Materials Science: Microstructure - Property - Performance Relations, NIST, Gaithersburg, MD, July 26-28, 1993. Co-Organized by Alan Karr, NISS, and E. R. Fuller, Jr., NIST

Workshop on Crystallographic Data Bases, International Union of Crystallographic Congress Co-Organizer-Winnie Wong-Ng and Alan D. Mighells, Bejing, China, August 1993.

Workshop on Characterizing Diamond Films II, A. Feldman, Organizer and Chairman, February 24, 25 (1993). A NIST sponsored workshop for U.S. companies covering in depth issues related to applications of diamond and the need for standards.

First meeting of the Technical Advisory Meeting Consortium for Commercial Crystal Growth organized by G. Long, May 20-21, 1993, at the National Institute of Standards and Technology.

STANDARD REFERENCE MATERIALS

The Division provides science, industries, and government a central course of well characterized materials certified for chemical composition of physical or chemical properties. These materials are issued with a certification and are used to calibrate instruments, to evaluate analytical methods, or to produce scientific data which can be referred to a common base.

DESCRIPTION	SRM NUMBER
Abrasive Wear	1857
Alumina Elasticity	718
Alumina Glass Anneal Point	714
Alumina Glass Anneal Point	715
Alumina Melting Point	742
Aluminum Magnetic Susceptibility	763-1
Aluminum Magnetic Susceptibility	763-2
Aluminum Magnetic Susceptibility	763-3
Barium Glass Anneal Point	713
Borosilicate Glass Composition	93(A)
Borosilicate Glass Thermal Expansion	731L1
Borosilicate Glass Thermal Expansion	731L2
Borosilicate Glass Thermal Expansion	731L3
Cadmium Vapor Pressure	746
Calibrated Glass Beads	1003*
Calibrated Glass Beads	1004a*
Catalyst Package for Engine Simulation (IIID)	1817
Catalyst Package for Engine Simulation (IIID)	1817b
Catalyst Package for Engine Simulation (IIIE)	8500
Catalyst Package for Engine Simulation (IIIE)	8501
Catalyst Package for Engine Simulation (IIIE)	8500a
Chlorine in Base Oil	1818
Container Glass Composition	621
Container Glass Leaching	622
Container Glass Leaching	623
Copper Thermal Expansion	736L1
Fused Silica Thermal Expansion	739L1
Fused Silica Thermal Expansion	739L2
Fused Silica Thermal Expansion	739L3
Glass Analytical Standard	1835
Glass Dielectric Constant	774
Glass Electrical Resistance	624
Glass Fluorescence Source	477

Total Nitrogen in Oils	1836
Wear Metals in Oil	1084a
Wear Metals in Oil	1085a
X-Ray Diffraction Instrument Sensitivity	1976
X-Ray Diffraction Intensity	676
X-Ray Diffraction Intensity Set	674a

*New in FY-1993

SELECTED TECHNICAL/PROFESSIONAL COMMITTEE LEADERSHIP

American Association for the Advancement of Science

- Physics Section
  - B. Steiner, Representative of the Optical Society of America

American Association for Crystal Growth
- D.L. Kaiser, Trustee

American Ceramic Society

- Program and Meetings Committee
  - S. Freiman, Chairman
- Glass Division
  - Committee on Glass Standards Classification and Nomenclature
    - M. Cellarosi, Chairman
  - Editorial Committee
    - S. Wiederhorn, Subchairman
- Basic Science Division
  - E. Fuller, Vice-Chair
  - Editorial Committee
    - B. Lawn, Chairman

ASM International
- Energy Division
  - S. Dapkunas, Past Chairman, Division Council Member
- Journal of Materials Engineering and Performance
  - S. Dapkunas, Editorial Board
- Journal of Thermal Spray Technology
  - S. Dapkunas, Editorial Board
- Washington D.C. Chapter Education Committee
  - J. A. Carpenter, Jr., Chairman

American Society for Engineering Education
- Postdoctoral Review Committee
  - A. Feldman, Member

American Society for Testing and Materials
- C14: Glass and Glass Product
  - M. Cellarosi, Chairman
- C14.01: Nomenclature of Glass and Glass Products
  - M. Cellarosi, Chairman

C28. Advanced Ceramics
G. D. Quinn, Vice-Chairman
C28.05: Powder Characterization
S. Malghan, Working Group Chairman
C28.07: Ceramic Matrix Composites
D. C. Cranmer, Chairman
D2: Petroleum Products and Lubricants
E24.07: Fracture Toughness of Brittle Nanmetallic Materials
G. D. Quinn, Member
E29.01: Advanced Ceramics, Organizational Meeting
M. Cellarosi
E42: Surface Science
G. G. Long, Member
E49: Computerization of Material and Chemical Property Data
R. G. Munro, E. F. Begley, Members
Fl:02: Lasers
A. Feldman, Subcommittee Editor
G2.2.02: Solid Particle Erosion
A. Ruff, Task Group Leader
G2.4.04: Pin-on-Disk
A. Ruff, Chairman
G2.12: Computerization in Wear and Erosion,
A. Ruff, Chairman

American Society of Mechanical Engineers

Journal of Tribology
S. Jahanmir, Associate Editor
Research Committee on Tribology
S. Jahanmir, Member
S. Hsu, Member
Wear of Materials Conference Steering Committee
A. Ruff, Member

Applied Diamond Conference
A. Feldman, Executive Committee

Diamond Films and Technology
Editorial Advisory Board
A. Feldman, Member

IEEE Lasers and Electrooptics Society
Washington-Northern Virginia Chapter
B. Steiner, Treasurer

International Center for Diffraction Data
High Tech Materials Task Group
W. Wong-Ng, Chairman

International Energy Agency
Task II - International Standards
S. Hsu, Overall Task Leader on Powder Characterization
Subtask 6 Powder Characterization Subgroup
S. Malghan, U. S. Task Leader

International Union of Crystallography (IUCr)
Commission on Crystallographic Studies at Controlled Pressures and Temperatures
G. Piermarini, Chairman

Minerals and Metallurgical Processing Journal
Editorial Board
S. G. Malghan, Member

National Materials Advisory Board, National Academy of Sciences
Committee on Superhard Materials
A. Feldman, Member
Committee on High Temperature Coatings
S. J. Dapkunas, Member

National Synchrotron Light Source
Housing Committee
C. E. Bouldin, Member
User Executive Committee
G. G. Long, Member
EXAFS Special Interest Group
C. E. Bouldin, Chairman
Proposal Study Panel
D. A. Fischer, Chairman
B. Steiner, Member
Housekeeping Committee
J. C. Woicik, Member

NIST Cold Neutron Research Facility
G. G. Long, Program Advisory Committee Member

Optical Society of America
Archie Mehan Prize Committee
B. Steiner, member

Powder and Bulk Engineering Journal
S. Malghan, Member Editorial Advisory Board

Powder X-Ray Diffraction Data
W. Wong-Ng, Consulting Editor

Society of Photooptical Instrumentation Engineers
Kingslake Award Committee
B. Steiner, Past Chairman

Society of Tribologists and Lubrication Engineers
Annual Meeting Program Committee
S. Jahanmir, Member
Board of Directors
S. Hsu, Director
Ceramics and Composite Committee
S. Jahanmir, Chairman

Strategic Defense Initiative Organization Technology Applications Office (SDIO/TA)
Materials and Electronics Panel
J. A. Carpenter, Jr., Member

Superconductor Applications Association
E. Fuller, Jr., Member of Advisory Board

U. S. Department of Energy, Office of Program Analysis
Peer-Review Panel for Office of Basic Energy Sciences, "Structural Ceramics and Mechanical Behavior of Ceramics: Emphasis on Mechanical Behavior"
E. Fuller, Jr., Chairman

Versailles Project on Advanced Materials and Standards (VAMAS)
Technical Working Area on Ceramics
G. D. Quinn, U. S. Representative and International Chairman

Technical Working Area on Wear Test Methods
S. Jahanmir, U. S. Representative and International Leader

INDUSTRIAL

ACTIS, Inc.

An agreement has been signed between NIST and ACTIS, Inc. for a joint research and development activity related to comprehensive computerized tribology databases. These databases will be evaluated by NIST and marketed by ACTIS, Inc. Other participants in the program are DOE, U.S. Army, U.S. Air Force, ASME and STLE.

Advanced Technology Materials

Dave Black (NIST) and Dr. Nik Buchan of ATM are studying defects in 6H-SiC wafers.

Advanced Technology Materials (G. Stauf and P. Van Buskirk) is collaborating with NIST (C.-S. Hwang, L. H. Robins, L. D. Rotter, M. D. Vaudin and D. L. Kaiser) to study the processing/structure/property relationships in $BaTiO_3$ thin films deposited by MOCVD. Films grown at ATM under various processing conditions have been characterized at NIST by transmission electron microscopy, Raman spectroscopy, x-ray diffraction and electro-optical measurements. These specimens are being compared with specimens prepared by NIST (D. Kaiser). The specimens are allowing us to develop methods of analyzing the defect structure of MOCVD ferroelectric oxide films.

Specimens of silicon carbide single crystal provided by Advanced Technology Materials have been examined for defect content by cathodoluminescence (L. Robins) and X-ray diffraction imaging (D. Black).

As part of the development of the thin film program in the Ceramics Division, several collaborations with ATM have been established. In this group, Cheol Seong Hwang is doing TEM characterization (planar and cross section) of thin films of $BaTiO_3$ and $Ba_{1-x}Sr_xTiO_3$ on single crystal MgO and Pt-based substrates. ATM has agreed to perform electrical characterization of thin films made at NIST. (Mark Vaudin)

AKZO Chemical Co.

A Cooperative Research and Development Program continues to utilize the NIST technology (S. M. Hsu, NIST; T. Marolewski, AKZO) in development of a high temperature liquid lubricant for evaluation in low heat rejection engines.

Allied Signal Corporation

A joint research program is underway to determine the role of impurities in superconducting ceramic powders on limiting the critical current density in the final product. Allied (A. Trivedi) is supplying superconducting powders containing various quantities of carbon and other

impurities. NIST (S. Freiman) is processing these powders and determining critical current densities. The work will be published as a joint paper.

S. G. Malghan is conducting collaborative studies with B. Busovne and J. Pollinger of Garrett Ceramic Components (an Allied subsidiary) on the interactions of powder-binder-sintering aid in the processing of silicon nitride powders. Garrett intends to utilize the results developed at NIST.

A collaborative effort between NIST (Benjamin Burton) and S. P. Greiner, Allied Signal has begun to conduct first principles phase diagram calculations of BCC based ordering in Ca-Mg-Li alloys.

American Superconductor

The preferred crystallographic orientation of 2223 BSSCO superconductor in Ag-swaged "wires" is being investigated using x-ray diffraction techniques (see above report). This is part of a project to investigate correlations between the mechanical and electrical properties of the BSSCO wire and the texture induced in the wire by the fabrication method. (Mark Vaudin).

Study the effect of mechanical strain on the electrical properties of silver-sheathed bismuth superconductor (BSCCO-2223) tapes. (C.K. Chiang)

American Xtal Technology, Inc.

Collaboration in the characterization of gallium arsenide substrates grown with a greatly increased degree of regularity by a new commercial process: vertical gradient freeze is being carried out by Bruce Steiner, NIST, and Morris Young, President, AXT, Inc.

Argonne National Laboratory

Dr. Paul Cowan of ANL and Joe Woicik (NIST) are collaborating on the study of novel semiconductor structures and bulk semiconductor impurities.

AT&T Bell Laboratories

Dr. Clifford King of Bell Labs and Joe Woicik (NIST) are collaborating on the growth, characterization and the consequences of strain in SiGe and other group IV semiconductor quantum structures.

Dr. Jim Patel of Bell Labs and Joe Woicik (NIST) are collaborating on standing-wave x-ray studies of Pb on Ge.

In collaboration with AT&T, lifetime predictions for InP in water and in 50% RH were made. The results indicated that optical couplers made with InP would survive the chemical environment in which they were placed (G.S. White, L.M. Braun, W.C. Carter, and E.R. Fuller, Jr.).

Battelle Columbus Laboratories

A joint activity is underway to prepare a wear atlas from selected literature and research findings at Battelle Columbus Laboratories, NIST, and the West German Bundesanstalt fur Materialprufung. Battelle (W. Glaeser) and NIST (A. W. Ruff) are evaluating publications in wear and friction to select authoritative findings that relate wear and friction with materials properties and surface morphology.

Buffalo Medical Center

Dr. George Detitta of Buffalo Medical Center is the co-investigator of the development of a standard reference material for the alignment of single crystal x-ray diffractometers. NIST (Winnie Wong-Ng).

Catalyst Research Corp.

D. Schrodt (CRC) has obtained laboratory procedures from J. Ritter for designing tests for Li-batteries.

Caterpillar Company

The Surface Properties Group at NIST is working with Caterpillar Company in several areas. F. Kelly is working with S. M. Hsu in the area of advanced lubrication, diesel particulate reduction and engine simulations. He is also working with A. W. Ruff to improve the wear resistance of tractor under-carriage linkage. S. M. Hsu is also working with K. Bruk, B. Hockman, and R. Nevinger on the design of ceramic valve seat inserts.

As part of the DOE sponsored study on diesel particulates formation, S. M. Hsu and R. S. Gates at NIST is working with the CRC study group to jointly evaluate the effects of fuel type, engine design and service duty on diesel particulate formation. The study group consists of the major oil companies, engine manufacturers and component suppliers. Various particulate samples were received from the study group who is currently conducting various engine tests and full-scale field tests of different engine and fuel combinations.

Crystacomm

Characterization of defects in 7.62 mm (3 inch) diameter InP wafers is carried out in a collaboration between George Antypas of Crystacomm and Dave Black (NIST).

Crystallume

Dr. Mary Anne Plano of Crystallume is collaborating with Dave Black (NIST) in the characterization of strain and defect generation in thick CVD-grown homoepitaxial diamond films.

Cummins Engine Company

S. M. Hsu is working with J. Wang, M. Naylor, and T. Gallant of Cummins Engine on the lubrication of new materials, evaluation of chemistries and development of advanced lubrication concepts for future engines. In conjunction with Akzo Chemicals Company under a DOE contract, new chemistries are being developed and these chemistries are being evaluated in prototype engines by Cummins.

Deere and Company

A collaborative research project is in progress between Deere and Company (P. A. Swanson) and NIST (L. K. Ives) to determine the influence of crystal structure on galling resistance of nitrided 4140 steel.

Delco Products (Division of General Motors)

Dr. V. Ananthanarayanan, Delco Products, has collaborated with S. Malghan in developing test procedures for evaluating the dispersion of strontium ferrite in aqueous environment. Two scientists spent two months at NIST to conduct experimental research. Based on these results, a development program is being carried out at the Delco Products production facility.

Deltronic Crystal Industries

Collaboration in the characterization of barium titanate and strontium barium niobate and correlation of the results with specific changes in crystal growth procedures are being carried out by Bruce Steiner, NIST, John martin and Robert Uhrin, Deltronic Crystal Industries, as well as by Mark Cronin-Golomb and Gerard Fogarty, Tufts University.

DOW Chemical Company

Gary Mitchell and Ben Dekoven of the Dow Chemical Company have begun a research collaboration with Dan Fischer (NIST) to study polymer surfaces and metal polymer interfaces using ultra soft x-ray absorption spectroscopy. The concentrations and orientations of functional groups have been characterized at and near the surface for a series of model polymeric materials. The materials studied include poly(acrylic acid), poly(butyl methacrylate), polystyrene, polycarbonate, poly(ethylene terephthalate), and model acrylic coatings.

Eagle-Picher

A collaboration has been initiated between Eagle-Picher Research Laboratory (G. Cantwell) and NIST (L. Robins and D. Black) to characterize defects and dopant impurities in zinc selenide single crystals. These crystals are being developed as substrates for laser/LED devices. Eagle-Picher currently has an ATP grant for this work.

EG&G Energy Systems

Collaboration in diffraction imaging of irregularities in terrestrial and space-grown mercuric iodide crystals, used or high energy radiation detectors, is underway by Bruce Steiner, NIST, and Lodewijk van de Berg, EG&G.

Exxon Research and Engineering

George Meitzner and John Sinfelt of Exxon are collaborating with Dan Fischer (NIST) to study the electronic structure of adsorbed carbon monoxide and hydrocarbons on platinum-supported catalysts using near-edge spectroscopy above the carbon K-edge.

Eaton

S. M. Hsu is working with J. Edler and M. Leydet of Eaton to jointly evaluate ceramic material for gas-fuelled co-generation engines. NIST conducts wear tests and mechanistic studies and provides feedback to Eaton. This is part of the study sponsored by GRI.

Eastman Kodak Company

D. T. Smith (NIST) has been collaborating informally with Ravi Sharma of Kodak's Polymer Research Laboratory to study the surface charging properties of thin insulating films of potential industrial interest in Kodak.

E. I. DuPont de Nemours & Co.

NIST (L. P. Cook) is collaborating with DuPont on their ATP thallium high T_c research on problems in processing and characterization, especially as related to the phase equilibria of these materials and their interaction with ferroelectrics in thin film devices.

DuPont (D. Roach) has provided alumina and alumina-zirconia fibers to C. Ostertag for incorporation into ceramic, ceramic-metal, and glass matrix composites.

C. Torardi of AT&T Bell Laboratories has assisted R. Roth and C. Rawn of NIST in determining crystal structures of calcium bismuth oxides that occur in the Bi-Sr-Ca-Cu oxide system. This system is currently of major interest as it contains important high-temperature superconducting materials.

Edge Technology Inc.

Artificial diamonds to be used as machine tools were supplied to D. R. Black. Topographic examination of these crystals was correlated to optically observed defects for quality control.

Ford Motor Company

Ford Motor Company (K. Carduner and M. Rokosz) have been active in the application of

NMR spectroscopy and imaging to characterize ceramic materials. Collaborative effort with P. S. Wang involves data exchange of Si-29 CP/MAS NMR for phase composition determination of silicon nitride and carbide powders. In the future, we plan to exchange imaging capabilities.

Gas Research Institute and Center for Advanced Materials, Pennsylvania State University

The Structural Ceramics Database project was funded in part by the Gas Research Institute through the Center for Advanced Materials at Pennsylvania State University, as an important step towards the use of advanced ceramics in heat exchangers and gas-fueled engines.

General Electric

NIST has been collaborating with General Electric (W. Banholzer) to evaluate a single-crystal diamond wafer by spatially resolved CL spectroscopy (L. Robins) and X-ray diffraction imaging (D. Black).

GE Corporate Research Center

Dr. Donna Hurley of GE and Dave Black (NIST) are performing defect characterization on isotopically-controlled man-made diamond crystals. They are studying the relationship of defects to ultrasonic measurements on these materials.

Geophysical Laboratory, Carnegie Institute of Washington, DC

NIST (Benjamin Burton) has been working with R. E. Cohen, The Geophysical Laboratory, Carnegie Institute of Washington, D.C. on a first principles study of cation ordering in the relaxor ferroelectric system $Pb(Sc_{1/2}Ta_{1/2})O_3$-$PbTiO_3$.

Grumman Corporate Research

Dave Black (NIST), Hal Burdette (NIST) and G. Long (NIST) are collaborating with Dr. Dave Larson of Grumman on the characterization of earth-grown and space-grown CdZnTe crystals.

GTE Laboratories, Inc.

GTE (J. Baldoni) has provided whisker-reinforced and whisker-free silicon nitrides to S. Wiederhorn and D. Cranmer for evaluation of creep and creep rupture, and changes in microstructure as a result of creep.

Collaboration in diffraction imaging on irregularities in gallium arsenide. (Bruce Steiner, NIST, and David Matthiesen and Brian Ditchek, GTE)

Hughes Research Laboratories

Collaboration in the crystal growth of barium titanate. (Bruce Steiner, NIST, Mark Cronin-

Golomb and Gerard Fogarty, Tufts University, and Barry Wechsler, Hughes)

IBM, Almaden Research Laboratory

Interactions between NIST (W. Wong-Ng) and IBM (T.C. Huang) focused on the investigation of the X-ray property of PZT and $BaTiO_3$ thin films which were prepared at NIST using the laser deposition technique.

Illinois Superconductor

NIST (John Blendell) has collaborated with ISC in support of their ATP project. This has involved determining the reaction path form forming $YBa_2Cu_3O_{6+x}$ in different atmospheres.

International Centre for Diffraction Data (ICDD)

As the Chairperson (W. Wong-Ng, NIST) of the Ceramics Subcommittee, efforts have been initiated to organize the inorganic materials of the X-ray Powder Diffraction File (PDF) into minifiles according to their functions, properties or structure. W. Wong-Ng also serves as a consulting editor for the PDF.

ITEK Optical Systems

A joint research program with ITEK Optical Systems was undertaken to assess the reliability of dual-pane glass aircraft windows. ITEK provided as-polished glass specimens from which both strength and crack growth properties were evaluated at NIST. These data were combined with a finite-element stress analysis by ITEK and a fracture-mechanics and statistically based methodology, developed at NIST, to determine pane lifetimes under various conditions at a 90% survival probability to a 95% confidence level.

Johns Hopkins University Applied Physics Laboratory (JHUAPL)

Dennis Wickenden of the JHUAPL is collaborating with NIST (L. Robins) in a project for characterizing defects and dopant impurities in thin films of gallium nitride and $Al_xGa_{1-x}N$ by spatially resolved CL. These materials are being developed for short-wavelength laser and LED devices. The specimens, grown at JHUAPL, are being characterized at NIST.

Kennemetal Inc.

S. M. Hsu is cooperating with the machining group at Kennemetal (R. F. Upholster) on jointly developing chemically assisted technology of ceramics. Samples were exchanged and many discussions were held. Some of the more promising chemistries may be tested at their facility. Kennemetal is the largest US manufacturer of ceramic wear inserts.

Kobe Steel Electronic Research Center

Characterization of defects in natural diamond substrates and in doped homoepitaxial

diamond films is currently the subject of a collaboration between Dave Black (NIST) and Dr. Brad Fox of Kobe Steel.

Lawrence Livermore Laboratories

As part of a study with Pat Johnson of Lawrence Livermore Laboratories, of the cohesive strength of grain boundaries in Ni_3Al as a function of grain boundary misorientation and symmetry, alloy stoichiometry and boron concentration, grain orientations in test bars have been measured at NIST (Mark Vaudin) prior to mechanical testing.

Collaboration on the crystal growth of potassium dihydrogen phosphate for high power lasers is being carried out by Bruce Steiner, NIST, and James DeYoreo and Chris Ebbers, LLL.

Matec Applied Sciences

This cooperative research is related to the development of electrokinetic sonic amplitude measurement for dispersion of powders in dense slurries. Research at NIST under the direction of S. Malghan will be utilizing hardware and software developed by Matec Applied Sciences for on-line measurement of dispersion.

Morgan-Matroc

In collaboration with Morgan-Matroc, damage in PZT-8 due to cyclic loading has been investigated. Morgan-Matroc supplied the specimens and information regarding their piezoelectric properties and NIST (G.S. White, M. Hill, C. Seong) provided information on the mechanical response to loading.

Nanophase Technology Inc.

Dr. John Parker of Nanophase Technology is collaborating with G. Long (NIST) and S. Krueger (NIST) in the investigation of microstructure evolution during densification of nanophase ceramics.

NASA Consortium for Commercial Development

Cooperative research is aimed at understanding fundamentals of zeolite nucleation, growth of CdTe single crystals and strain development during growth of GaAs. G. G. Long, D. R. Black, H. E. Burdette, and S. Krueger (Reactor Radiation Division) are working with E. Coker, H. Wiedemeier and D. Larson on this research.

National Institute of Statistical Sciences (NISS)

A collaboration between NISS, the Ceramics Division, and the Statistical Engineering Division has explored cross-disciplinary applications of statistics and statistical concepts to materials science and the formulation of a research agenda leading to high-impact advances. An outgrowth of this collaboration was a workshop, *Statistics and Materials Science:*

Microstructure - Property - Performance Relations, which was held at NIST on July 26-28, 1993. It was attended by fifty-two participants from industry, government laboratories and universities. The principal findings were (i) crucial problems in materials science are inherently statistical, so that statistics is an enabling technology for progress in materials science; and (ii) fulfilling industrial needs and goals demands cross-disciplinary collaboration between materials and statistical scientists. More detailed findings and recommendations are contained in a report, *Statistics and Materials Science: Report of a Workshop*, by Alan F. Karr (Technical Report #14, National Institute of Statistical Sciences, Research Triangle Park, NC, January 1994).

National Renewable Energy Laboratory

Carbon films deposited by solar methods at the National Renewable Energy Laboratory (R. Pitts) were examined for diamond content by Raman spectroscopy (L. Robins).

National Research Institute for Metals (Japan)

R. G. Munro and J. Rumble (SRD) are collaborating with S. Nishijima, Y. Asada and K. Hoshimoto on development of a comprehensive materials property data base for High T_c Superconductors.

Naval Research Laboratory

S. Lawrence and B. Bender (NRL) are collaborating with J. Wallace on the thermochemical treatment of polymer-derived SiC fibers and the degradation mechanisms of these fibers during high temperature heat treatments. A joint publication is planned.

NIST (Mike Hill and Grady White) is collaborating with Dr. Sadananda at the Naval Research Laboratory investigating cyclic fatigue of piezoelectric material. Mechanical properties are investigated at NIST and TEM will be done at NRL.

Collaboration in a study of the role of crystalline irregularities on the performance on quartgz crystal resonators is being carried out by Bruce Steiner, NIST, Michael Bell, NRL, and Robert Whitlock, NRL.

Naval Surface Weapon Center (NSWC)

NIST (Winnie Wong-Ng) and I. Talmy of NSWC are in collaborating in the study of the phase diagram of barium and strontium feldspar solid solutions, $(Ba,Sr)Al_2Si_2O_8$. Revised phase diagrams and standard X-ray powder diffraction patterns were obtained based on these collaborations.

Tom Russell, Naval Surface Warfare Center (NSWC) has been working with NIST (Gasper J. Piermarini) collaborating on the study of energetic materials and Buckminsterfullerenes at high pressure.

A joint research project with D. R. Black has been developed to supply and characterize

copper single crystal substrates for use as substrates for heteroepitaxial growth of diamond films.

Norton Company

In one collaborative project V. Pujari and C. Willkens of Norton Company, and S. Malghan of NIST are studying the characteristics of agitation milled silicon nitride powders in aqueous environment. Norton Company has provided silicon nitride powder samples. Based on the results of first stage of collaboration, a second stage of research was initiated with an intent to compare the performance of agitation ball milling to large-scale processing by conventional methods.

Thermal conductivity measurements are important for characterizing diamond films. Interaction with Norton (K. Grey) involved learning to use the NIST (A. Feldman and H.P.R. Frederikse) photothermal radiometry facility for the purpose of setting up such a facility at Norton. We plan to collaborate in the analysis of the data generated at Norton.

Dr. Vimal Pujari is cooperating with S. M. Hsu on the effects of machining on tensile strength of silicon nitrides. Tensile bars were received from Norton and were subjected to chemical assisted machining. These bars are being tested.

Norton/TRW (R. Yeckley) has provided a Y_2O_3-containing silicon nitride to S. Wiederhorn and D. Cranmer for evaluation of creep and creep rupture, and changes in microstructure as a result of creep.

S. M. Hsu is working with Brian McEntire at Norton-TRW to jointly evaluate ceramic materials for valve seat insert application. The program is a joint program with the Gas Research Institute (GRI), Caterpillar, and Southwest Research Institute (SWRI). A Full-scale engine test is being conducted at SWRI to evaluate different materials for the valve seat inserts in a gas-fuelled Caterpillar 3500 series engine.

OPTEX Inc

NIST, (Winnie Wong-Ng) in collaboration with an ATP funded company OPTEX (of Rockville, Maryland), conducted X-ray diffraction studies of undoped and doped optical SrS thin films (for optical data storage) to characterize these films in order to correlate processing parameters.

Research Triangle Institute

A joint research project was developed with D. R. Black to study the microstructure of diamond substrates to be used for homoepitaxial growth of diamond films by chemical vapor deposition.

Rockwell International

A collaboration between NIST (A. Feldman) and Rockwell International (S. Holly) to

organize the Diamond Optics IV conference sponsored by the Society of Photo-Optical Instrumentation Engineers (SPIE).

Russian Academy of Sciences Institute of Solid State Physics

A collaborative program to elucidate the nature of disorder in oxide crystals has been initiated by Bruce Steiner, NIST, and Veniamin Shekhtman, Institute for Solid State Physics.

Russian Research Center for Standardization, Information and Certification of Materials

R. G. Munro and J. R. Rumble (SRD) are collaborating with A. D. Koslov to establish evaluated property data for selected oxide and carbide structural ceramics worldwide.

Rotem, Inc.

Collaboration in the characterization of sapphire substrates. (Bruce Steiner and Uri Laor, NIST, and Shlomo Biderman and Yezekiel Einav, Rotem)

Russian Academy of Science

Cooperative activities under the NIST-Russian Academy of Science Agreement have continued in the areas of tribology and materials science. Current emphasis is on a joint US-USSR book on tribology (A. W. Ruff and S. Jahanmir). Future benefits to NIST and the Division include exchange of tribology data, exchange of computer software for surface analysis, and future exchange of technical staff.

A collaborative program between the Russian Academy of Sciences and NIST Ceramics (D. Kaiser) and Metallurgy Divisions is underway to map flux distributions in high temperature superconductors by a magneto-optical technique.

Sanders Corporation

Collaboration on the crystal growth of barium titanate single crystals (Bruce Steiner, NIST, Mark Cronin-Golomb and Gerard Fogarty, Tufts University, and Tom Pollack, Sanders)

Schmidt Instruments

A collaborative research project was initiated with D. R. Black to grow heteroepitaxial diamond films and characterize their crystal perfection.

Southwest Research Institute

Dr. Richard Page of SRI is collaborating with S. Kruger (NIST) and G. Long (NIST) on the microstructure evolution of alumina during densification.

Smithsonian Institute

NIST (Winnie Wong-Ng) in collaboration with Y.S. Dai of the Smithsonian Institute has studied the twin structure of Ba-Ti-Zn-(F,O) as well as the characterization of Na-doped $Ba_2YCu_3O_{6+x}$ superconductors.

Trans-Tech, Inc.

NIST (C. Lindsay and R. Roth) and Trans-Tech, Inc. (T. Negas), collaborate on microwave dielectric materials processing, phase equilibria and crystal structure data for these materials. Measurement of electrical properties is a joint effort between NIST and Trans-Tech.

Ube Industries, Japan

Ube Industries (T. Yamada) has collaborated with S. Malghan by providing powder samples for studying the high energy agitation milling of silicon nitride powders. The specific interest lies in the development of an understanding of morphological and surface chemical changes taking place to the milled powders.

U. S. Army Research Laboratory

NIST (Lawrence Cook, Mark Vaudin, and C. K. Chiang) has collaborated with the U. S. Army Research Laboratory on measurements of ferroelectric and dielectric properties of $BaTiO_3$, PZT and $PbTiO_3$ thin films, prepared by pulsed laser deposition.

U.S. Bureau of Mines at Albany

The goal of this collaboration between N. Gokcen of U.S. Bureau of Mines and W. Wong-Ng of NIST is to investigate the effect of high oxygen pressure on the structural and superconducting properties of the superconductors, $Ba_2RCu_3O_{6+x}$ R=neodymium and yttrium, and $(Ca,Sr)CuO_2$.

Xsirius, Inc.

Collaboration in the characterization of sapphire substrates for high temperature superconducting devices. (Bruce Steiner and Uri Laor, NIST, and William Graham, President, Xsirius, Inc.)

ACADEMIA

Alabama A&M University

Collaboration on the crystal growth of triglycine sulfate in space and on the ground (Bruce Steiner, NIST, and Ravindra Lal and Ashok Batra, Alabama A&M)

University of Colorado/Joint Institute for Laboratory Astrophysics

Collaboration in the surface treatment and characterization of barium titanate single crystals and their photorefractive interactions with laser beams is underway by Bruce Steiner, NIST, Mark Cronin-Golomb and Gerard Fogarty, Tufts University, and Dana Anderson, University of Colorado/Joint Institute for Laboratory Astrophysics.

Auburn University

A collaboration between NIST (A. Feldman) and Auburn University (Y. Tzeng) to organize the First International Conference on the Applications of Diamond Films and Related Materials, ADC'91.

Boston University

L. Robins has collaborated with Boston University (S. Jin) to examine by cathodoluminescence spectroscopy the defect content of thin boron-doped diamond films grown by the electron cyclotron resonance microwave plasma assisted CVD method. The CL results were correlated with electrical and ESR measurements. This is part of a manuscript submitted for publication.

Clemson University

B. I. Lee is collaborating with S. Malghan on surface chemical characteristics of silicon nitride powders in aqueous environment in the presence of organic surface active agents.

Cleveland State University

Professor Stephen Duffy is collaborating with T.-J. Chuang in the area of continuum damage mechanics on continuous fiber reinforced ceramic composites for high-temperature applications.

Columbia University

P. Somasundaran has been collaborating with S. Malghan on a research project to study basic parameters affecting the preparation of dense suspensions of silicon nitride powder containing sintering aids.

Dartmouth College

Real-time imaging of dislocation motion in pure and doped ice is currently underway between Dave Black (NIST) and Dr. Fuping Liu of Dartmouth.

Drexel University

This is a joint program between Drexel University (M. Barsoum) and NIST (D. Cranmer) to investigate and control the fracture behavior of ceramic and glass matrix composites.

East China University of Chemical Technology

This is a joint effort to use finite-element techniques to analyze creep behavior of ceramic c-rings at elevated temperatures. ECUCT (D. Wu and Z-D Wang) is developing the finite element model for C-rings and a computational algorithm for creep and NIST (T.-J. Chuang) is providing a theoretical framework and experimental data to support the program.

Professor D. Wu and Dr. Z Wang are collaborating with T.-J. Chuang in the area of finite element method and numerical analysis for mechanical evaluation of advanced ceramics.

Florida State University

A collaborative study between Florida State University (J. Schwartz) and NIST (D. Kaiser, F. Gayle) is underway to correlate microstructure with microscopic flux flow during magnetization of $Bi_2Sr_2CaCu_2O_{8+x}$ superconducting tapes by means of a magneto-optical imaging technique.

Harvard University

Professor Gene Golovchenko of Harvard and Joe Woicik (NIST) are collaborating on standing-wave x ray and scanning tunneling microscopy studies of Bi on Si(111).

Howard University

Prof. George Walrafen, Chemistry Dept., Howard University and NIST, Gasper Piermarini. Long standing collaboration on study of materials at high pressures. Currently studying liquid state of H_2O in the superpressed state at elevated temperatures and pressures.

Iowa State University

Characterization of defects in icosahedral AlPdMn is being performed by Dave Black (NIST), Dr. Alan Goldman and Stefan Kycia of Iowa State.

Johns Hopkins University

Professor J. Kruger and L. Krebs are collaborating with G. G. Long, NIST, and C. Majkrazak (Reactor Division, NIST) on in situ polarized neutron reflectometry studies of the nature and structure of passive films.

Dan Shechtman of Johns Hopkins is collaborating with NIST (A. Feldman and E. Farabaugh) in the high resolution TEM analysis of CVD diamond nucleation and growth.

Illinois Institute of Technology

P. R. Jemian is collaborating with G. G. Long and S. Krueger (Reactor Division) on neutron and x-ray scattering by novel materials.

Lehigh University

This is a collaboration to determine the effect of microstructure on the fracture resistance of monolithic ceramic materials. The materials under study have been manufactured at Lehigh University (H. Chan, M. Harmer) and are being characterized at NIST (B. Lawn).

Massachusetts Institute of Technology

Collaboration in diffraction imaging on the crystal growth of barium titanate (Bruce Steiner, NIST, and Mark Garrett, MIT)

Interaction with R. Hallock and W. Rhine of MIT (W. Wong-Ng of NIST) was conducted to characterize the $BaTiO_3$ precursor material, $BaTi(O)(C_2O_4)_2 \cdot 5H_2O$ by x-ray diffraction method.

National Tsing Hua University

Professor S. Lee and Dr. J.-L. Chu are collaborating with T.-J. Chuang, NIST on creep life prediction.

Northwestern University

S. M. Hsu is collaborating with Prof. M. Fine on optimization of ceramic wear resistance by introducing compressive stress into the surface and interfaces. A previous study by Prof. Fine has demonstrated that introduction of a compressive surface layer increased the wear resistance of ceramic material significantly.

Professor Katherine T. Faber and several students at Northwestern University are collaborating with E. R. Fuller, Jr. on a research project focused on the understanding and control of materials which undergo process-zone phenomena around propagating cracks. These phenomena occur in materials which possess large thermal expansion anisotropy, or for multi-phase materials, thermal expansion mismatch, or in materials which undergo crystallographic, martensitic phase transformations. In all instances, lack of microstructural control, such as exaggerated grain growth, causes the phenomenon to occur spontaneously.

Profesor D.L. Johnson is collaborating with G. Long (NIST) and A. Allen (U. Md.) on microwave-assisted reaction-bonded silicon nitride.

Oklahoma State University

Collaborative research between OSU and NIST (R. Powell and D. Cranmer) is being conducted to investigate the properties of permanent, laser-induced refractive index gratings based on Eu-containing glasses. The end result of this effort will be a device for processing optical signals.

Pennsylvania State University

S. M. Hsu is collaborating with Profs. Duda, Klaus, Philips, and Christen on a variety of projects. Duda and Klaus are working on lubrication, development of lubricants for alternative fuels and ceramic lubrication. Philips is working on synthesis of nano-sized particles of ceramic materials using a microwave assisted plasma reactor. Christen is working on computer simulation of grain growth.

Purdue University

NIST (Mark Vaudin) has interacted with Prof. K. Bowman on the measurement of texture in tape-cast Al_2O_3 samples. Bowman has determined x-ray pole figures for the same samples on which we have measured texture by BEKP analysis and by x-ray powder diffraction.

Rensselaer Polytechnic Institute

Collaboration on the diffraction imaging of semiconducting multilayers in order to determine the genesis and influence of disorder on photonic device performance is being carried out by Bruce Steiner, NIST, Heribert Wiedemeier, RPI, and Krishna Rajan, RPI.

Rutgers University

S. C. Danforth (Rutgers) has provided S. Malghan (NIST) with nano-sized Si_3N_4 powder. The powder is processed at NIST using cryogenic compaction.

S. M. Hsu is collaborating with Profs. Niesz and Wachtman on microstructural design for wear resistance on silicon nitrides. Variation of grain size, shape and interface strength are being examined. The materials processed are evaluated both at NIST and at Rutgers.

H. Han is collaborating with G. G. Long (NIST) and S. Krueger (NiST/Radiation Reactor Division), A. Allen and H. Kerch in the study of nanophase powders and processing.

NIST (Linda Braun, Grady White, and Gasper Piermarini) has begun a collaborative effort with Roger Cannon to investigate toughening mechanisms in ceramics via micro-focus Raman spectroscopy measurements.

Grady White of NIST has been interacting with Steve Garofalini at Rutgers University investigating environmental effects on crack growth in silica.

Seoul National University

NIST (John E. Blendell) is collaborating with Doh-Yeon Kim of Seoul National University, Korea on the wetting of grain boundaries in Al_2O_3.

Stanford University

Professor William Spicer of Stanford is collaborating with Joe Woicik in the use of x-ray standing-wave studies, surface-EXAFS, and ultraviolet photoemission of metal/semiconductor interfaces and semiconductor surfaces.

State University of New York at Stony Brook

Collaboration on the observation of four wave mixing and related optical phenomena in non linear optical crystals (Bruce Steiner, NIST, and Mark Cronin-Golomb and Gerard Fogarty, Tufts)

Tufts University

Collaboration on the observation of four wave mixing and related optical phenomena in non linear optical crystals (Bruce Steiner, NIST, and Mark Cronin-Golomb and Gerard Fogarty, Tufts)

University of California at Berkeley

Professor Andrea M. Glaeser is collaborating with T.J. Chuang, NIST, on microdesign of interfacial defects for creep crack growth experiments.

University of California at Santa Barbara

Joint experiments between University of California (J. N. Israelachvili, P. McGuiggan) and NIST (R. Horn and D. Smith) are being conducted to investigate frictional properties of silica surfaces under dry conditions and with a variety of thin (< 10 nm) intervening liquid films.
University of Colorado/Joint Institute for Laboratory Astrophysics

Collaboration in the surface treatment of barium titanate single crystals (Bruce Steiner, NIST, Mark Cronin-Golomb and Gerard Fogarty, Tufts University, and Dana Anderson, U. Col.)

University of Dayton Research Institute

Using UDRI's x-ray photoelectron spectrometer (XPS) and Auger electron spectrometer (AES), T. Wittberg, UDRI, is conducting studies on surface structures and reactivities with P. S. Wang, NIST. A variety of powders and ceramic materials have been investigated and the results have been published.

University of Florida

B. Moudgil is studying the characterization techniques and structure of flocs in dense slurries with G. G. Long and S. G. Malghan. Primary emphasis is placed on interfacial, rheological, and scattering (neutron and x-ray) techniques.

University of Grenoble

NIST (Benjamin P. Burton) has been working with Prof. A. Pasturel, CNRS/University of Grenoble, to make first principles phase diagram calculations of BCC based ordering in Ni-Al-Ti and Fe-Be alloys.

University of Illinois

Prof. S. Danyluk is collaborating with S. M. Hsu on wear mechanisms of ceramic materials and the definition of surface quality in terms of strength as a result of machining damage.

University of Illinois and Rockwell Science Center

NIST (Grady White and Steve Freiman) has written a joint proposal with Dwight Viehland of the University of Illinois and Ratnaker Neurgaonkar of Rockwell Science Center to investigate mechanical and electronic properties of piezoelectric and electrostrictive materials for use in smart material applications.

University of Maryland

A collaborative study between the University of Maryland (A. Roytburd) and NIST (D. Kaiser, F. Gayle) involves theoretical aspects of the effect of twin boundary and grain boundary defects on flux flow during magnetization of high temperature superconductors.

L. Chang (U. Md.) is collaborating with E. Begley and C. Lindsay (NIST) on appropriate instructional techniques for a computer-based tutorial in phase diagram interpretation. U. Md. will also provide a testbed of students for evaluation of the tutorial.

Bai-Hao Chen and Bryan Eichgorn of UM are collaborators in the structural investigation of possible new superconductor related single crystal materials (with W. Wong-Ng, NIST). New members of a Ruddlesten-Popper series of compounds $Ba_{n+1}A_nS_{3n+1}$, where A = Hf and Zr have been successfully studied.

Investigators at NIST (Mike Hill, Grady White, and Steve Freiman) are collaborating with Isabelle Lloyd investigating mechanical and electrical effects of cyclic loading of PZT. Mike Hill is using the research as partial fulfillment of requirements for a PhD in materials science.

University of Michigan

John Gland (University of Michigan) and Dan Fischer (NIST) are collaborating on the study of hydrogenolysis of aniline on the Pt(111) surface.

University of Michigan

J. Schwank is carrying out specialized characterization of conductive ceramic powders by ESCA and Auger spectroscopy in collaboration with J. Ritter, NIST. These powders are

synthesized at NIST for NASA.

University of Pennsylvania

P. Davies of the University of Pennsylvania has been working with NIST (Robert S. Roth, Claudia J. Rawn, and Curtis G. Lindsay) on high-resolution transmission electron microscopic images of microwave dielectric materials.

University of Virginia

NIST (Mark D. Vaudin) and John Wert, University of Virginia, have been investigating the orientation of grains adjacent to a fracture surface in a brittle intermetallic (Al_3Ti) as part of a project to test a model of fracture in these materials.

University of Washington

Professor Larry Sorenson (U.of W.) and Joe Woicik (NIST) are using diffraction anomalous fine structure measurements to study strained semiconductor layers and 123 semiconductors.

Collaboration on strain relaxation in III-V photonic crystals is being carried out by Bruce Steiner, Joseph Woicik, and Joseph Pellegrino, NIST, and Larry Sorenson, University of Washington.

University of Western Ontario

A collaboration was initiated this year between H. H. Schloessin and R. A. Secco of the Geophysics Department and R. D. Spal, NIST, involving the study of geological samples by means of x-ray diffraction topography and the asymmetric Bragg diffraction microscope.

University of Wisconsin

V. Hackley, Water Chemistry Program, Civil Eng. Department at the University of Wisconsin is conducting joint research with NIST on the electrokinetic sonic amplitude (ESA) measurement technique for dispersion of powders. The results of this research are to be used for the application of ESA technique for on-line monitoring of ceramic slurry properties.

A joint activity is underway between the University of Wisconsin (S. Babcock, X. Cai, D. Larbalestier) and NIST (D. Kaiser) to characterize the microstructural, magnetic and electrical transport properties of single crystals and bicrystals of superconducting $YBa_2Cu_3O_{6+x}$.

University of Washington

David Castner, Buddy Ratner, and Dan Fischer (NIST) have used the polarization dependence of carbon and fluorine NEXAFS to understand the orientation of fluorocarbon groups and proteins on polymeric biomaterials used in medical implants. The orientation of surface species was shown to differ for various polymeric preparation techniques which also

correlated with protein film growth, an important consideration in bio compatibility of these materials.

FACILITIES

FACILITIES

POWDER CHARACTERIZATION AND PROCESSING

High Temperature X-ray Diffraction - J. P. Cline

The x-ray diffraction facility at NIST consists of a high temperature machine of theta-two theta geometry equipped with an incident beam monochrometer and a position sensitive proportional counter. The incident beam monochrometer removes the Kα2 radiation and results in diffraction profiles that are more sensitive to effects of sample character. The position sensitive detector allows for data collection at a rate two orders of magnitude faster than conventional detectors. The furnace is an enclosed high vacuum chamber capable of reaching 3000K, it is equipped with a mass flow controller for atmospheric control. This equipment is used for the study of high temperature phase equilibria, high temperature reaction kinetics, sintering of monolithic ceramics, and strain development during sintering of ceramic composites. Additional equipment consists of four automated and updated Philips diffractometers which are used for certification of standard reference materials (SRMs), studies on the effects of microabsorption and extinction, and the development of the Rietveld method for a conventional, sealed tube, X-ray diffraction equipment.

Electrokinetic Measurements - V. A. Hackley and S. G. Malghan

The Matec ESA-8000 system has the unique capability for measuring colloidal properties in dense slurries. The analytical capabilities of the ESA system include performance in the following modes: potentiometric titration, conductometric titration, time-series titration, and concentration series titration. In the selected mode, the equipment can monitor: electrokinetic sonic amplitude, zeta-potential, electrophoretic mobility, electrical conductivity, isoelectric point, surface charge density, and phase angle of the material with the specified experimental conditions.

Slurry Rheology - S. G. Malghan and V. A. Hackley

The RTI rheometer allows for viscosity as well as rheology characterization of ceramic slurries. Rheological measurements are more informative and flexible with respect to the various slurry properties: Newtonian, pseudoplastic, plastic, dilatant, and thixotropic. The modeling of these rheological properties as a function of sample treatment, surface chemical properties is paramount in developing and improving the slurry processing technology.

Physical Properties Characterization Laboratory - L. Lum, D. Minor, P. Pei and S. Malghan

The physical properties characterization laboratory is equipped with state-of-the-art techniques for the measurement of particle size distribution, specific surface area, specific gravity, tap density, and porosity. The particle size distribution is measured by three techniques -- gravity sedimentation by Sedigraph, centrifugal sedimentation by Joyce-Loeble, laser diffraction by Horiba LA-900. The range of particle size distribution covered by these techniques is 0.01

micron to 200 microns. The specific surface area determination is carried out by nitrogen adsorption and the BET method. The porosity of powders and ceramics is measured by mercury intrusion.

Colloidal Processing of Powders - S. Malghan, D. Minor and P. Pei

The focus of this laboratory is to develop data and understanding of non-oxide powders processing in aqueous environment. The laboratory is equipped with instruments and equipment for studying deagglomeration, dispersion, suspension stability, slurry casting, and green body microstructure evaluation.

Agitation Milling of Powders - D. Minor and S. Malghan

High energy agitation milling of silicon nitride powders is carried out with a minimum contamination by the use of a specially designed milling system. This milling device allows for the size reduction of silicon nitride powder by milling at high slurry densities in approximately 1/6th to 1/10th of the time required by the conventional tumbling ball mill. The mill is lined with silicon nitride and the media are made of silicon nitride materials. Hence, external sources of contamination can be minimized.

Nuclear Magnetic Resonance (NMR) - P. S. Wang

The solid state NMR facility includes a Bruker MSL-400 NMR system capable of studying almost all NMR active nuclei in the periodic table in both solid and liquid states as well as performing NMR imaging in proton and carbon-13 frequencies. Currently, the operation parameters for both states at proton, deuterium, carbon-13, and aluminum-27 have been defined and proved by documented NMR spectra of organic and inorganic molecules. The equipment has been tuned to Si-29, Cu-63, and Y-89.

Scanning Electron Microscope/Image Analysis (SEM) Facility - J. F. Kelly

This laboratory is equipped with an Amray 1830 digital scanning electron microscope with LaB_6 source and a Leitz optical microscope. The SEM is equipped with a solid state backscatter detector and an ultrathin window x-ray detector. A Kevex Delta V EDS x-ray analysis and image analysis system is interfaced to both the SEM and optical microscopes. Automated imaging capabilities enable rapid size and shape analysis of a variety of imaged features, including ceramic powder particles and second phase regions in composite structures. Fracture stages have been developed for real time observation and measurement of in-situ crack propagation in ceramic specimens. The addition of an interior mounted phosphore screen with video camera imaging provides the capability of imaging single grain electron backscatter diffraction patterns from bulk specimens. This permits the measurement of crystallographic orientation in ceramic specimens.

Thermal Analysis Facility - J. Wallace and J. Blendell

This facility includes equipment for measurement of behavior of ceramic materials in a wide

range of atmospheres and temperatures. The equipment is comprised of a computer-controlled differential pushrod dilatometer capable of measuring thermal expansion or sintering shrinkage in vacuum, inert, oxidizing or reducing conditions from room temperature to 1600°C. The atmosphere can be monitored using either a zirconia oxygen cell or an external mass spectrometer using its own associated computerized data acquisition system.

The second major piece of equipment is a simultaneous thermal analysis (STA) system which is capable of performing simultaneous thermogravimetric and differential thermal analysis from room temperature to 1700°C. Atmospheres can be varied from vacuum to single and mixtures of gases using a four channel mass flow controller. The STA is also connected to the mass spectrometer system and it's associated data acquisition system. The quadrapole mass spectrometer system has a capability of analyzing to 512 AMU.

Chemical Laboratory Facilities - J. J. Ritter

Chemical synthesis of powders is carried out in a well-equipped laboratory, which consists of controlled atmosphere glove boxes, preparative chemical vacuum systems, and a chemical flow reactor. A range of powders can be synthesized for exploratory purposes.

Ceramics Powders Processing Laboratory - J. Wallace and J. Blendell

A processing laboratory for processing and sintering well controlled ceramic powders has been assembled. This facility consists of: equipment for chemical powder synthesis routes; attrition mills; ball mill; jet mill; pressure slip caster; uniaxial presses; cold isostatic press; spray dryers; drying ovens; hot presses; air furnaces to 1700°C; controlled atmosphere furnaces with associated gas flow systems and oxygen sensors for temperatures to 1600°C; graphite furnace for temperatures to 2300°C and a hot isostatic press/gas pressure sintering furnace capable of 2300°C and 200 MPa using graphite elements and insulation.

Nano-Size Powders Processing - W. Chen and S. Malghan

This is a new facility which consists of equipment for powder handling in inert environment, compaction of nano-size powders, and sintering under environment control. The compaction equipment was designed to facilitate the application of wide range of pressures (up to 5 GPa), temperatures (cryogenic to 1000°C) and environments. The size of green ceramic produced in this system is 3.0 mm diameter.

SURFACE PROPERTIES

Wear Tests - S. M. Hsu and S. W. Ruff

A state-of-the-art friction and wear testing laboratory is available for the evaluation of materials under different applications and conditions. Contact geometries include pin-on-disk, cross cylinders, ball-on-flat, ball-on-balls, flat-on-flat, and ring-on-block. Various motions and

operating conditions are available to simulate many industrial applications. Environmental control includes temperature (room temperature to 1200°C), vacuum, and humidity.

Surface Analysis - S. M. Hsu, R. S. Gates, and S. W. Ruff

Many modern specialized instrumentation are available for the analysis of surface properties of materials. Mechanical property measurement include hot hardness tester, Vicker's indenter, nano-indentor, scratch test, and controlled depth micro-scratch test. Chemical property measurement include time-resolved micro-Raman spectroscopy, FTIR microscopic spectroscopy, GC-MS, SEM with EDX analysis, IR and UV spectroscopies with API compound identification files. A specially designed organo-metallic specification facility is also available to detect surface reaction products at ppm level. Access to conventional surface analysis such as XPS, ESCA, AUGER, etc are also available through external contract.

Hydrocarbon Oxidation Facility - S. M. Hsu

Various oxidation apparatus are available to study the oxidation and degradation mechanisms of hydrocarbon mixtures. These include DSC, TGA, a simultaneous TGA/DTA, a specially designed chemiluminescence apparatus, hot tube, panel coker, micro-oxidation, TFOUT, and other engine simulation instruments.

STM/AFM - S. M. Hsu

A Digital commercial scanning tunnelling microscope (STM) and atomic force microscope (AFM) is available to measure surface properties at atomic level.

Time-Resolved Micro-Raman - S. M. Hsu

This versatile facility consists of a pulsed ND-YAG laser, a CW Ar-ion laser, a triple monochromator, and a gated intensified diode array detector. This facility, therefore, provides a wide variety of Raman analysis techniques in both time-resolved and continuous operation modes, using either visible or ultra-violet excitation sources for either operation mode. In addition, either bulk macro-Raman or 5 μm resolution micro-Raman analysis is available.

MECHANICAL PROPERTIES

Surface Forces Laboratory - D. Smith

The surface forces laboratory consists of a semi-clean-room preparation facility and a crossed-cylinders surface force apparatus. The crossed-cylinder apparatus permits measurements of atomic-scale forces between surfaces. It can be operated with a variety of liquid or gaseous environments, thus allowing investigations of the effects of chemical changes on the forces between two surfaces. The apparatus includes several unique features that were developed and built by the surface forces group. First, sensitive custom electrometer circuits were built into the apparatus to allow in situ measurements of surface charges resulting from contact

electrification. Second, the apparatus has been modified to permit the sliding of one surface over the other under constant applied load.

Instrumented Indenter - D. Cranmer

This apparatus is designed to enhance our ability to measure the properties of the fiber/matrix interface in ceramic matrix composites. The instrumented indenter permits us to measure the force on and displacement of a fiber directly during loading and unloading. Previous methods for examining these properties could only measure the maximum applied load and inelastic displacement.

Analytical Electron Microscopy - B. Hockey

Several transmission and scanning electron microscopes are available for analysis of the changes in microstructure as a result of creep.

Glass Melting - D. Kauffman

Extensive glass melting and annealing facilities for production of melts up to 1600 °C are available. Batch sizes up to about 2.5 -3 kg can be produced using this equipment. Special facilities for melts containing heavy metals such as thallium and lead are also available.

Creep Apparatus -- R.F. Krause, Jr. and S.M. Wiederhorn

The creep measurements laboratory possesses 19 controlled-temperature furnaces (800 to 1700°C), 7 laser extensometers, 10 optical long-distance microscopic extensometers, 20 loading frames (14 pneumatically driven, 4 screw driven, and 2 direct weight). Among these loading frames 14 can be used in tension, 3 in tension or compression, 1 in flexure, and 1 as a sintering forge.

Hot-Pressing Apparatus -- R.F. Krause, Jr.

A graphite heating-element furnace (2300°C max) which be can operated in vacuum or an inert gas atmosphere is mounted in a hydraulic loading frame (0.5 MN max). Ceramic powders can be hot pressed in graphite dies (50, 75, 100, and 125 mm diam).

Nano-Indentation Facility - D.T. Smith

The Ceramics Division nano-indentation facility consists of a Nano Indenter II indentation machine, manufactured by Nano Instruments, Inc., and related computer and optical components. The indenter, under computer control, is capable of measuring loading-unloading curves with displacement resolution better than 0.1 nm and load resolution better than 200 nN. Nomarsi interference contrast (NIC) optics and translation stages with placement precision better than 1 μm permit the measurement of material properties such as hardness and Young's modulus in selected volumes as small as 10^{-17} m^3.

ELECTRONIC MATERIALS

Level 10 Clean Room - J. Blendell

A Level 10 Clean Room has been constructed for the processing of ceramics in a controlled environment where the presence of air low contaminants can seriously affect the final products properties. The room is provided with separated work stations to allow simultaneous conduct of experiments.

Thermal Wave Analysis Facility - A. Feldman and G. White

This facility is used for characterizations based on variations of thermal diffusivities. Equipped with both an Ar-ion and CO_2 laser, the facility permits analyses by infrared and Mirage methods. It is especially useful as a nondestructive method of detecting flaws in ceramics especially in near-surface regions.

Single Crystal X-ray Diffraction - W. Wong-Ng

Currently this research is primarily used to characterize single crystals in terms of crystal symmetry, lattice parameters and detailed structure.

OPTICAL MATERIALS

Optical Characterization - L. Robins and A. Feldman

Facilities include a Cary spectrophotometer for measuring optical transmittance in the spectral range 0.2 μm to 2.5 μm, optical spectrometers for measuring photoluminescence and Raman spectra, and an argon ion laser.

Magneto-Optical Imaging of High Temperature Superconductors - D. Kaiser, F. Gayle, A. Shapiro

The facility consists of a magneto-optical imaging system with attached video equipment. It is used to measure real-time flux distributions in high temperature superconductors as a function of temperature (7 -300 K) and applied magnetic field (0 to $\pm$ 65 mT).

Electro-optic Thin film Characterization - L. Rotter

The facility consists of a vibration isolated optical table, argon-ion and helium neon laser sources, polarizing components, lenses, optical stages, optical detectors, and electronic signal processing equipment for measuring the electro-optic coefficients and optical birefringence of thin ferro-electric films.

Metalorganic Chemical Vapor Deposition (MOCVD) System - D. Kaiser

A specialized system was constructed for the deposition of oxide thin films from metalorganic precursors. It has been used to deposit $BaTiO_3$ films on 1.5 cm x 1.5 cm substrates.

Diamond Film Deposition - E.N. Farabaugh and A. Feldman

Facilities consist of 3 hot filament CVD reactors and a microwave enhanced CVD reactor. The hot filament reactors can accommodate substrates up to 2.5 cm $\times$ 2.5 cm square. The microwave reactor can accommodate substrates up to 10 cm in diameter. The reactant gases are hydrogen, methane, oxygen, argon, and ethyl alcohol which contains boron of doping. Growth rates typically range from 0.1 to 0.6 μm/h.

MATERIALS MICROSTRUCTURE CHARACTERIZATION

Synchrotron Radiation Beamlines - G. G. Long

The Materials Microstructure Characterization Group operates two beamstations on the X23A port at the National Synchrotron Light Source at Brookhaven National Laboratory in New York. These two beamstations offer access to dedicated instrumentation for small-angle x-ray scattering, x-ray diffraction imaging (topography) and EXAFS.

Small-angle x-ray scattering can be carried out in the energy range from 5 to 11 keV. The minimum wavevector is 4 x 10^{-3} nm^{-1} and the wavelength resolution is $\Delta\lambda/\lambda = 10^{-4}$, nomalous small-angle scattering with excellent resolution. Diffraction imaging of single crystals and powders is carried out with monochromatic photons between 5 and 30 keV. An energy-tunable x-ray image magnifier enables imaging of microstructure down to less than 1 μm. EXAFS experiments are also performed over an energy range from 5 - 30 keV.

Small-angle scattering measurements on ceramic and metallurgical materials are being used to characterize the microstructure in the 2 nm to 1 μm size range as a function starting chemistry and processing parameters. Diffraction imaging is being used to study imperfections and strains in single crystals and powder compacts. EXAFS is being used to study the structure of strained semiconductor interfaces and metal multilayers. A combination of EXAFS and diffraction will provide a capability for site-specific local structure determination in crystals.

SANS - Ceramics Furnace - G. Long

The SANS-Ceramic furnace is a unique facility that is now coming together. This system will allow in-situ densification studies of ceramic powders and SANS application. The experimental system has been designed to carry out densification studies of oxide powders at temperatures up to 2000 °C. In addition, the furnace will be equipped with a dilatometer.

APPENDIX

National Institute of Standards and Technology

Organizational Chart

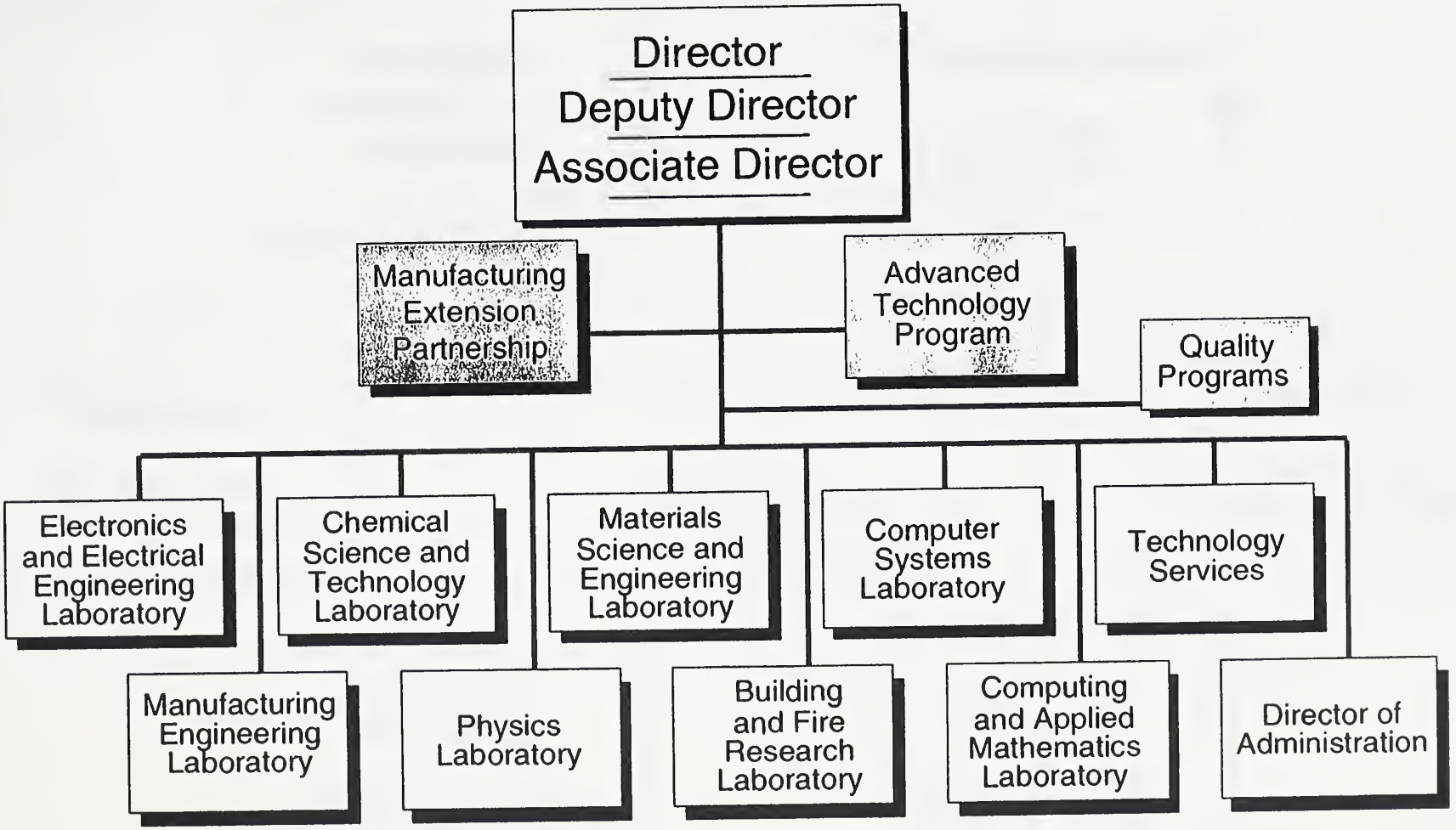

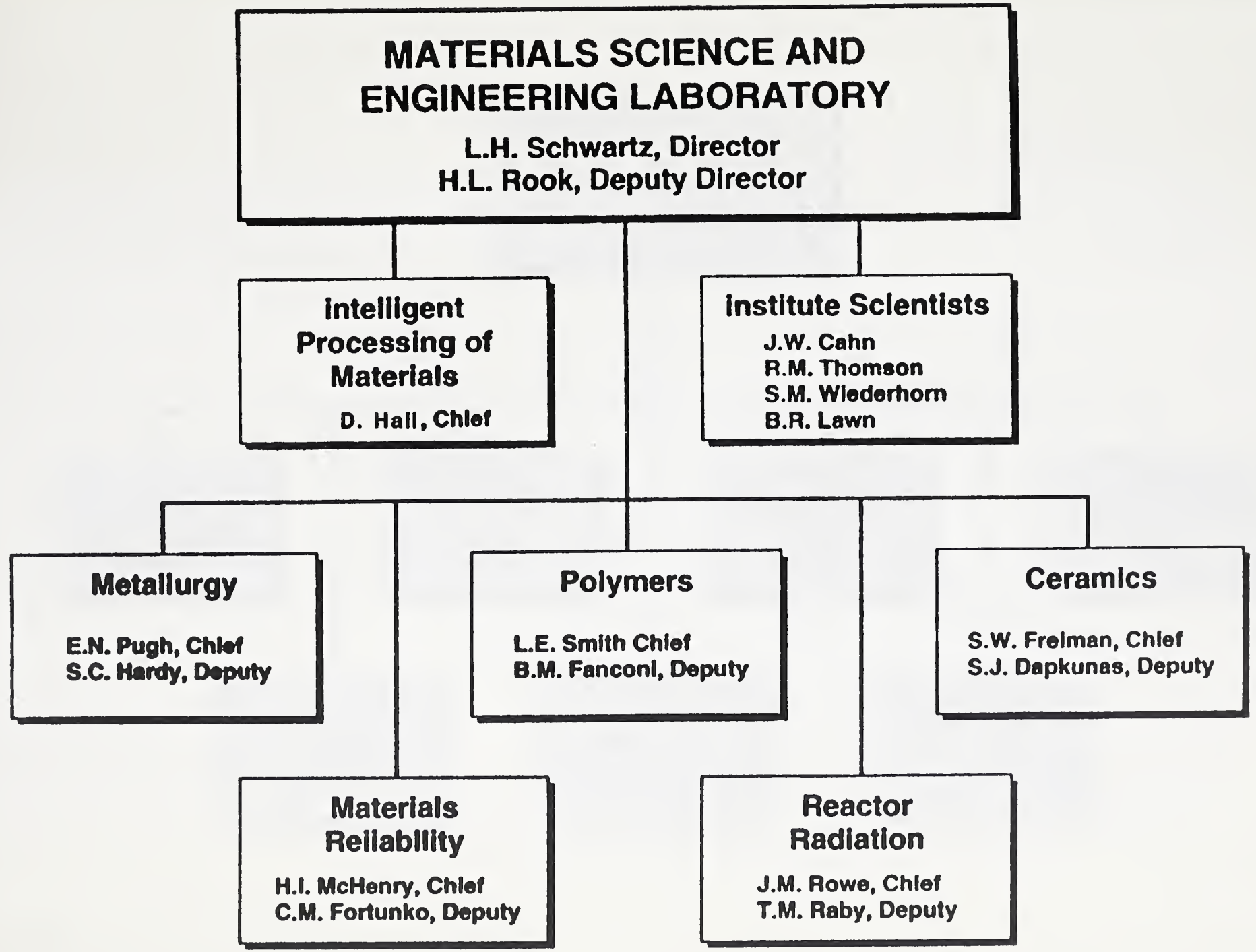
MATERIALS SCIENCE AND ENGINEERING LABORATORY
L.H. Schwartz, Director
H.L. Rook, Deputy Director
Intelligent Processing of Materials
D. Hall, Chief
Institute Scientists
J.W. Cahn
R.M. Thomson
S.M. Wiederhorn
B.R. Lawn
Metallurgy
E.N. Pugh, Chief
S.C. Hardy, Deputy
Polymers
L.E. Smith Chief
B.M. Fanconi, Deputy
Ceramics
S.W. Freiman, Chief
S.J. Dapkunas, Deputy
Materials Reliability
H.I. McHenry, Chief
C.M. Fortunko, Deputy
Reactor Radiation
J.M. Rowe, Chief
T.M. Raby, Deputy

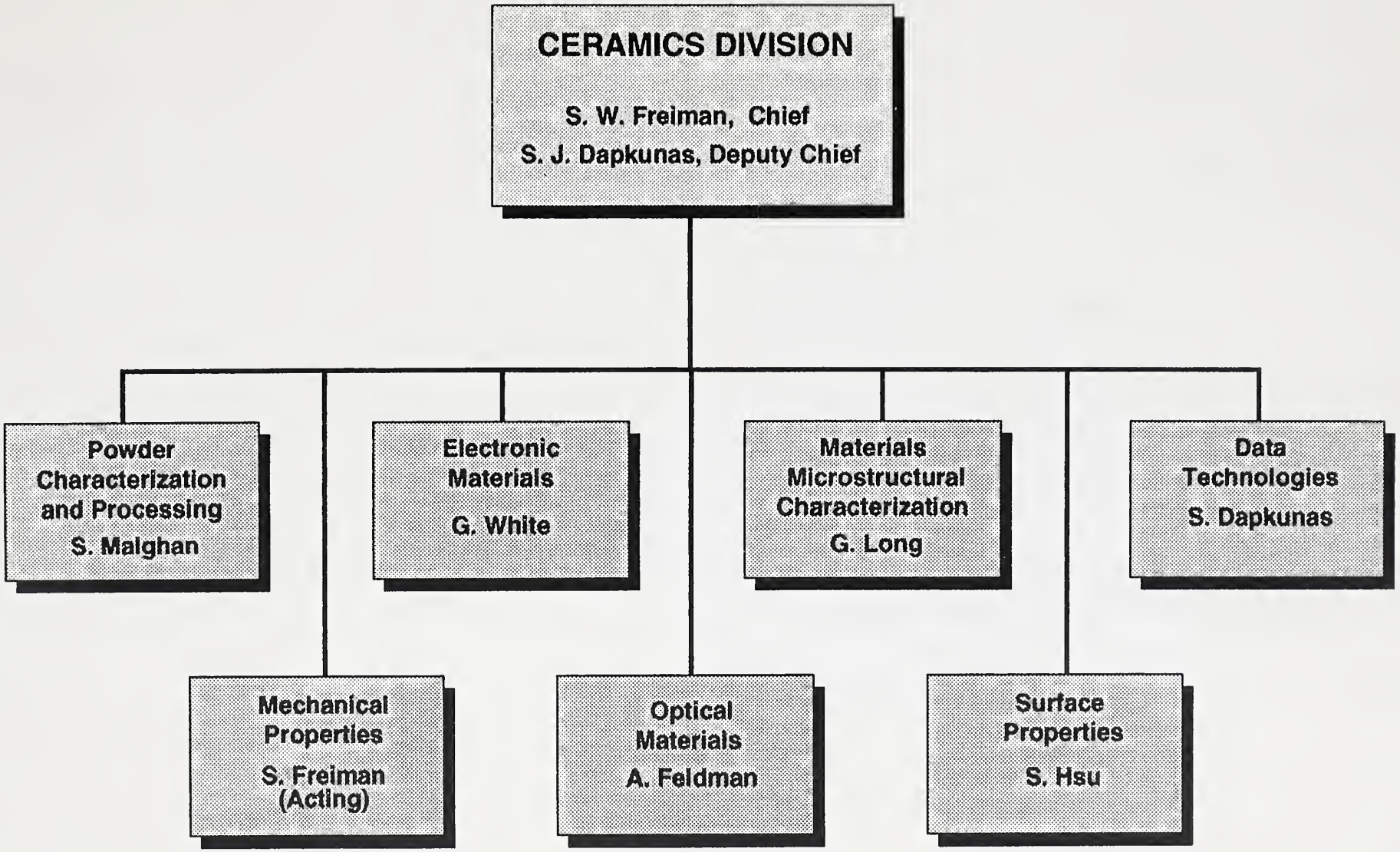
CERAMICS DIVISION
S. W. Freiman, Chief
S. J. Dapkunas, Deputy Chief
Powder Characterization and Processing
S. Malghan
Electronic Materials
G. White
Materials Microstructural Characterization
G. Long
Data Technologies
S. Dapkunas
Mechanical Properties
S. Freiman (Acting)
Optical Materials
A. Feldman
Surface Properties
S. Hsu